Modelling of the evolution of trace metal contents in urban agricultural soils

Xueqian Zhong

Université de Lorraine

École doctorale Sciences et Ingénierie des Ressources Naturelles

Laboratoire Sols et Environnement UMR 1120 UL-INRAE

Thèse

Présentée et soutenue publiquement pour l'obtention du titre de

DOCTEUR DE l'UNIVERSITE DE LORRAINE

Mention : Sciences Agronomiques

par **Xueqian ZHONG**

Sous la direction de **Thibault STERCKEMAN**

Modélisation des bilans et des flux de métaux en traces dans les sols sous agriculture urbaine

Soutenance publique prévue le 31 mai 2022

Membres du jury :

Directeur de thèse :	Thibault STERCKEMAN	Ingénieur de Recherche, INRAE
Co-Directeur de thèse :	Christophe SCHWARTZ	Professeur, Université de Lorraine
Président de jury :	Camille DUMAT	Professeure, INP-ENSAT, Toulouse
Rapporteurs :	Sabine HOUOT	Directrice de Recherche, INRAE
	Thierry LEBEAU	Professeur, Nantes Université, Nantes
Examinateurs :	Camille DUMAT	Professeure, INP-ENSAT, Toulouse
	Beatrice BECHET	Directrice de Recherche, MTE, Bouguenais
Membre invité :	Franck MAROT	Chef de projet, ADEME, Angers

Remerciements

Tout au long de mes études de doctorant et de la rédaction de cette thèse, j'ai reçu beaucoup de soutien et d'aide.

Je tiens tout d'abord à remercier mes encadrants, Dr. Thibault Sterckeman et Pr. Christophe Schwartz, dont l'expertise a été précieuse pour formuler les questions de recherches et la méthodologie de cette thèse. Vos commentaires perspicaces ont porté mon travail à un niveau supérieur. Je tiens également à vous remercier pour votre soutien, pour votre patience et pour toutes les opportunités qui m'ont été offertes au cours de cette thèse.

Je tiens également à remercier tous mes collègues du Laboratoire Sols et Environnement, qui s'accompagnent mutuellement dans ces moments de hauts et de bas émotionnels. Je n'aurais pas pu mener à bien cette thèse sans le soutien de mes amis, qui m'ont apporté des discussions stimulantes ainsi que d'heureuses distractions pour reposer mon esprit en dehors de mes recherches. Enfin, je tiens à remercier mes sœurs et mes parents qui se trouvent à 9000 km d'ici, ainsi que Carla Ghinassi du Sud. Vous êtes toujours là pour moi, comme un phare dans la mer, me guidant dans la bonne direction lorsque je me perdais.

Summary

Consumption of vegetables grown in a soil contaminated by trace metals and direct soil inhalation pose a risk to human health. In order to maintain the sustainability of urban gardens, predicting the evolution of metals in soils should allow to identify risks related to metal contamination of soil, and thus to apply practices to better preserve the functions and services provided by garden soils and target a more efficient rehabilitation of contaminated soils.

We used a mass balance model to simulate the evolution of soil metals under contrasted gardening practices over time. The mass balance was improved to make it more applicable to vegetable gardens by considering the regular and intensive use of organic waste amendments. Leaching and plant uptake are the main flows of metals loss in soils. We incorporate the RothC and VSD^+ models to simulate the changes in soil carbon and pH over time, respectively. Specific values of plant uptake factor for over 60 vegetable species have been collected from literature to simulate metal loss via plant uptake. Metal input flows are associated to chemical fertilizers, organic waste amendment, pesticides and atmospheric deposition. Soil tillage depth and crop rotation have also been considered in the model.

We predicted the evolution of soil metal (Cd, Cu, Pb and Zn) concentrations in 104 French vegetable gardens over the next 100 years. If current gardening practices are maintained, an increase in soil Cd (35% on average), Cu (183%), and Zn (27%) contents should occur after a century. Soil Pb concentration should not vary consistently. The model has also been used to simulate the historical and future trends of soil metal concentrations in the King's Vegetable Garden (Potager du Roi) in Versailles, which has accumulated more than 300 years of gardening practices since its creation in 1683. Simulated soil pH and organic matter by the integrated RothC and VSD^+ modules are very close to measured values, with variation less than 10%. Soil Zn contents have been well simulated comparing to measured values, with a variation range of 3% to 25% in different scenarios. Less accurate results were found in the historical trend simulations of Cd, Cu and Pb content in soils. In the future trend simulations, the soil metal contents will increase by 39% for Cd, 20% for Cu, 5% for Pb, and 32% for Zn for the next century, while the current gardening practices will be maintained in King's Vegetable Garden. Green waste compost contributes over 70% of the total input and output metal flows. Moreover, there would be a chronic over-exposure to Cd and Pb for people who would only consume vegetables grown in the King's Vegetable Garden in the future. According to the

results of the simulations, current gardening practices can lead to accumulation of metals in French vegetable garden soils. A standard for gardening practices should be developed to prevent/mitigate soil metal contamination in order to ensure food safety and to promote urban agriculture.

Résumé

La consommation de légumes cultivés dans un sol contaminé par des métaux et l'inhalation directe du sol représentent un risque pour la santé humaine. Afin de maintenir la durabilité des jardins urbains, la prédiction de l'évolution des métaux dans les sols devrait nous permettre d'identifier les risques liés à la contamination des sols par les métaux, et ainsi de mettre en place des pratiques permettant de mieux préserver les fonctions et les services rendus par les sols des jardins et de cibler une réhabilitation plus efficace des sols s'ils sont contaminés.

Nous avons utilisé un modèle de bilan de masse pour simuler l'évolution des métaux du sol sous les différentes pratiques de jardinage au cours du temps. Le modèle de bilan de masse a été amélioré pour le rendre applicable aux jardins potagers en considérant leur utilisation régulière et intensive d'amendements organiques. La lixiviation et le prélèvement par les plantes sont les principaux flux de perte de métaux dans les sols. Nous avons incorporé, respectivement, les modèles RothC et VSD^+ pour simuler les évolutions des teneurs en matière organique (MO) et du pH dans les sols. Des valeurs spécifiques de PUF (plant uptake factor) pour plus de 60 espèces végétales ont été recueillies dans la littérature pour simuler la perte de métaux par le prélèvement par les plantes. Les flux d'entrée de métaux ont été pris en compte dans le modèle de bilan de masse, en considérant les apports d'engrais chimiques, d'amendements organiques, de pesticides et les dépôts atmosphériques. La profondeur du travail du sol et la rotation des cultures ont également été prises en compte dans le modèle.

Nous avons prédit l'évolution des concentrations en métaux dans le sol de 104 jardins potagers français au cours des 100 prochaines années. Si les pratiques de jardinage actuelles sont maintenues, une augmentation des teneurs en Cd (35% en moyenne), Cu (183%) et Zn (27%) du sol devrait se produire après un siècle. La concentration de Pb dans le sol ne devrait pas varier de façon notable. Le modèle a également été utilisé pour simuler les tendances historiques et futures des concentrations en métaux du sol dans le Potager du Roi à Versailles, qui compte plus de 300 ans de pratiques de jardinage depuis sa création en 1683. Le pH du sol et la MO du sol simulés par les modules RothC et VSD^+ sont très proches des valeurs mesurées, avec une variation inférieure à 10%. Les teneurs en Zn des sols ont été bien simulées par rapport aux valeurs mesurées, avec un intervalle de variation de 3% à 25% dans les différents scénarios. Des résultats moins précis ont été trouvés dans les simulations de tendances historiques de la teneur en Cd, Cu et Pb dans les sols. Dans les simulations de tendances futures, les teneurs en métaux des sols du Potager du Roi augmenteront de 39 % pour le Cd, 20 % pour le Cu, 5 %

pour le Pb et 32 % pour le Zn dans un siècle, alors que les pratiques de jardinage actuelles seraient maintenues. Les composts de déchets verts contribuent à plus de 70 % du total des flux de métaux entrants et sortants. En outre, il existerait une surexposition alimentaire chronique au Cd et au Pb pour les personnes qui ne consommeraient que des légumes cultivés dans le Potager du Roi à l'avenir. D'après les résultats des simulations, les pratiques de jardinage actuelles peuvent entraîner une accumulation de métaux dans les sols des potagers français. Une norme relative aux pratiques de jardinage devrait être élaborée pour prévenir/atténuer la contamination des sols par les métaux afin de garantir la sécurité alimentaire et promouvoir les agricultures urbaines.

Sommaire

Summary i

Résumé iii

Sommaire 1

Liste des figures 3

Liste des tableaux 9

Glossaire 13

Chapitre 1 : Introduction générale 14

1 L'agriculture urbaine : concept, définition, typologie, ordre de grandeur et fonctionnalités 14

2 Enjeux de la contamination des métaux dans les sols de jardins potagers 24

3 Dynamique de métaux en traces (Cd, Cu, Pb, Zn) dans les sols 29

4 Modélisation du devenir des métaux dans les sols 36

5 Objectifs de la thèse 40

6 Questions scientifiques 40

7 Structure du mémoire 42

Chapitre 2 : Évaluation des tendances futures des teneurs en métaux en traces dans les sols des jardins urbains français 43

1 Introduction 44

2 Materials and methods 47

3 Results and discussion 87

4 Conclusions 109

5 Code Availability 110

Chapitre 3 : Amélioration du modèle actuel par l'ajout d'un module de simulation du pH du sol 111

1 Introduction 111

2 Materials and methods 112

3 Results and discussion 129

Chapitre 4 : Tendances historiques et futures des teneurs en métaux traces dans les sols du Potager du Roi (Versailles, France) 133

1 Introduction 134

2 Materials and methods 134

3 Results and discussion 154

4 Conclusions 166

Chapitre 5 : Discussion générale sur la modélisation du bilan de masse des métaux traces dans les sols des jardins urbains français 167

1 Valeur pratique du modèle de bilan de masse et comment l'adapter à d'autres études dans les sols agricoles 169

2 Impact des pratiques de jardinage sur l'accumulation des métaux dans le sol 171

3 La performance du modèle et l'incertitude liée à la simulation 172

4 Principales avancées liées à la thèse 173

5 Limitations 173

6 Perspectives 175

Conclusion générale 177

Références 179

Annexe 196

A1 Solubility of the four metals 196

A2 Benchmarking of RothC model 199

A3 Assessing the future trends of soil trace metal contents in French urban gardens 202

A4 Historical and future trends of soil trace metal contents in King's Vegetable Garden (Versailles, France) 205

Liste des figures

Figure 1. Les facteurs spatiaux, écologiques et socio-économiques définissant les différences entre l'agriculture urbaine et péri-urbaine, adapté d' Opitz et al. (2016)..... 16
Figure 2. Trois approches et leurs composants pour spécifier différents types de l'AUP, résumé du rapport de McEldowney et al. (2017) ; Mougeot (2001) 17
Figure 3. Typologies de l'agriculture urbaine en Europe, adapté de (Santo and Palmer, 2016) 18
Figure 4. Population par région : estimation, 1950-2015 ; prédiction, 2015-2100. (Source : "World Urbanization Prospects - Population Division - United Nations," 2017) 22
Figure 5. Populations urbaines et rurales du monde, 1950-2050, adapté de United unions (2018) 22
Figure 6. Voies d'exposition de l'homme aux métaux présents dans le sol, adapté de (DAMAS et al., 2018)..... 27
Figure 7. Représentation schématique des différents pools des métaux en traces dans le système du sol et de leurs interactions, adapté de Tack (2010) 29
Figure 8. Schéma de l'équilibre d'ions métalliques dans les sols, par ordre croissant de simplicité adapté de Degryse et al. (2009) 31
Figure 9. La gamme estimée des taux de dissociation des complexes métalliques dans les solutions du sol, adapté de Degryse et al. (2009)..... 32
Figure 10. Distribution des métaux lourds dans la phase solide et liquide, adapté de Fang et al. (2016b) 34
Figure 11. Distribution des métaux dans la phase liquide, adapté de Fang et al. (2016b)..... 35
Figure 12. Schéma de la dynamique des polluants métalliques dans l'écosystème des sols de jardins..... 37
Figure 13. Location of the 104 vegetable gardens in France 47
Figure 14. Location of EMEP-CCC monitoring stations in Europe and geographical coordinates of the six stations in France..... 51
Figure 15. Monthly average percolating water in mm simulated by model for the three cities 63
Figure 16. Structure of the RothC model, adapted from Coleman and Jenkinson. (1996)..... 70
Figure 17. Diagram of the calculation of the balance of DPM compartment after one month of degradation..... 71
Figure 18. Flow diagram leading to the calculation of accTSMD 72

Figure 19. Vegetables most planted in autumn/winter (a) and vegetables planted in spring and summer (b) for the three cities: Marseille, Nancy and Nantes; n is the number of surveys carried out (Joimel, 2015) 80
Figure 20. Relative variation presented as boxplots of metal content in garden surface soils by decade, for the CP scenario in three French metropolises M: Marseille (n = 36); NC: Nancy (n = 33); NT: Nantes (n = 35)..... 88
Figure 21. Evolution of the four metals soil concentration in the surface layer (0-20 cm) of 104 gardens, under the CP scenario. M: Marseille (n = 36); NC: Nancy (n = 33); NT: Nantes (n = 35)..... 90
Figure 22. Changes in topsoil metal content after a century for the 8 groups of gardens under CP scenario. Cinit: initial soil metal content; Ccent: soil metal content after one century of gardening practices. Paired Student's t test: p value: *value higher than 0.05; **value between 0.05 and 0.01; ***value lower than 0.01 91
Figure 23. Relative variation of soil Cu content presented as boxplots by decade, for three fungicide application doses (F-0.2: 20% of recommended dose; F-0.5: 50% of recommended dose; F-1: recommended dose) 94
Figure 24. Mean distribution of input and output flows of the four metals after a century for 104 garden soils under the CP scenario. In % of the sum of the absolute value of all the flows. Qatm: atmospheric deposition; Qfer: NPK fertilizers; Qorg: organic amendments; Qphy: plant protection products; Qlea: leaching; Qcrop: crop offtake 95
Figure 25. Mean distribution of input and output flows of the four metals after a century for 104 garden soils under the OA scenario. In % of the sum of the absolute value of all the flows... 96
Figure 26. Ranking of variables according to their normalized coefficients (SRC) in the multiple linear regression with the absolute variation of soil metal content after one century (VC_i). Description of acronyms: Density = p, Soil pH in 0.01 M CaCl2 = pH, Cation exchange capacity = CEC, Organic carbon content = SOC, Clay content = clay, Sand content = sand, Initial Cd(Cu, Pb, Zn) content = Cd(Cu, Pb, Zn)_init, Start(end) of cultivation = Cult_start(end), Metal content in bulk sampling precipitation = Catm, Metal content in chemical fertilizer = Cfer, Quantity of chemical fertilizer application = Mfer, Metal content in manure = Cmanu, Quantity of manure application = Mbiow, Annual irrigated water volume = Wirr, Cu brought by culture from fungicides = App_phy, Organic matter content of manure = OMmanu, Organic matter content of bio-waste compost = OMbiow, Yield per year or by crop = Y, Transfer factor of Cd(Cu, Pb, Zn) from soil to the plant = PUF_Cd(Cu, Pb, Zn). More details of these variables are presented in
Table 20. Parameters and variables tested for model sensitivity analysis 98

Figure 27. Evolution of soil metal concentrations in solution of in the dug layer (20 cm) of 104 gardens, under the CP scenario with constant pH. M: Marseille; NC: Nancy; NT: Nantes 99
Figure 28. Evolution of soil metal concentrations in solution of in the dug layer (20 cm) of 104 gardens, under the CP scenario with pH linearly increasing by one unit after a century. M: Marseille; NC: Nancy; NT: Nantes 100
Figure 29. Evolution of soil metal concentrations in solution of in the dug layer (20 cm) of 104 gardens, under the CP scenario with pH linearly decreasing by one unit after a century. M: Marseille; NC: Nancy; NT: Nantes 101
Figure 30. N processes in VSD^+, each number indicates the order of calculation, adapted from Bonten et al. (2016) 119
Figure 31. Average wet atmospheric depositions of nitrogen (NH_4 and NO_3), sulphate (SO_4), chloride (Cl) and base cations (K, Na, Ca, Mg) recorded from 17 monitoring stations in France, from 1978-2019 (main graphic); reduced graph shows values of NH_4, NO_3, SO_4, K, Ca, Mg with appropriate y axis scale. 124
Figure 32. Predicted changes in soil pH during the period of 1683-2021 under historical gardening practices in the KVG. Background colors denote different gardening practices: terreau application (white); grassland (black dot); NPK-type fertilizer and cow manure (grey); green waste compost (green) 130
Figure 33. Predicted changes in base saturation during the period of 1683-2021 under historical gardening practices in the KVG. Background colors denote different gardening practices: *terreau* application (white); grassland (black dot); NPK-type fertilizer and cow manure (grey); green waste compost (green) 130
Figure 34. Relationship between base saturation (BS) and H^+ in KVG's soils, as simulated with VSD+ 131
Figure 35. Acidity production simulated by VSD^+ for different gardening practices in KVG during the period of 1683-2021. NP: no practices; Terreau: horse manure compost input; NPK+Manure: NPK-type of fertilizer and cow manure input; GWC: green waste compost input. Method adapted from Zeng: Acidity production (N: net NO3 leaching plus net NH4 input; HCO3: net HCO3 leaching; BC: BC removal by crops; Other: net H, SO4, Cl and PO4 release (output minus input)) and Acidity consumption (Al: net Al leaching; BC: BC input minus BC uptake minus BC leaching) 132
Figure 36. Acidity consumption simulated by VSD^+ for different gardening practices in KVG during the period of 1683-2021. NP: no practices; Terreau: horse manure compost input; NPK+Manure: NPK-type of fertilizer and cow manure input; GWC: green waste compost input.

Method adapted from Zeng: Acidity production (N: net NO3 leaching plus net NH4 input; HCO3: net HCO3 leaching; BC: BC removal by crops; Other: net H, SO4, Cl and PO4 release (utput minus input)) and Acidity consumption (Al: net Al leaching; BC: BC input minus BC uptake minus BC leachin 132
Figure 37. Location of King's Vegetable Garden (1) and of Verrières forest (2). Maps are from Google maps and Géoportail 138
Figure 38. Soil sampling plan of 16 plots and 5 pedologic pits in King's Vegetable Garden 139
Figure 39. Soil profile observed during the sampling of the initial material in the Forêt de Vérrières 142
Figure 40. Determination of the four metal contents in the initial soil of King's Vegetable Garden by comparing measured values from the Verrières soil (supposed parent material) with measured values and simulated values from the Fe total content in the Great Square soil (mean of 16 plots sampled in 2021 144
Figure 41. Concentrations of Cd, Cu, Pb and Zn in different pits of KVG: driveway border(Pit 1), orchard plot-one use over time (Pit 2), Great Square (Pit 3), orchard/vegetable plot-two use over time (Pit 4), alternance of orchard/vegetable (Pit 5) 154
Figure 42. Principal component analysis of major and trace elements for Great Square soils. S1-S16: Soil samples of 0-20 cm layer collected from each of the 16 plots. 156
Figure 43. Evolution of the four metals soil concentration in the surface layer (0-20 cm) of the Great Square with different application rates of *terreau* 157
Figure 44. Annual distribution of input and output flows of the four metals during the period of 1683-2021, with 25% terreau application rate. In % of the sum of the absolute value of all flows. Qatm: atmospheric deposition; Qfer: NPK fertilizers; Qorg: organic amendments; Qlea: leaching; Qcrop: crop offtake 161
Figure 45. Relative variation of metal content in Great Square topsoil (0-20 cm) by decade 163
Figure 46. Mean distribution of input and output flows of the four metals during the period of 2021-2121 for Great Square topsoil (0-20 cm). In % of the sum of the absolute value of all the flows. Qatm: atmospheric deposition; Qfer: NPK fertilizers; Qorg: organic amendments; Qlea: leaching; Qcrop: crop offtake 163
Figure 47. Processus formalisés dans la modélisation du bilan de masse des métaux en traces dans les sols de jardins potagers 170

Figures dans l'Annexe

Figure A1. Comparison of measured values of metals concentrations in soil solution with predicted values from the selected regression models 198
Figure A2. Organic carbon content in the 5 compartments for the 3 versions of RothC during 2007-2016..... 200
Figure A3. Total organic carbon content in soil for the 3 versions of RothC during 2007-2016 200
Figure A4. Relative difference in simulated results between RothC-R and the other two versions 201
Figure A5. Evolution of the four metals soil concentration of in the dug layer (20 cm) of 104 gardens, under the CP scenario for 1000 years. M: Marseille; NC: Nancy; NT: Nantes 202
Figure A6. Evolution of soil organic carbon content of in the dug layer (20 cm) of 104 gardens, under the CP scenario. M: Marseille; NC: Nancy; NT: Nantes 203
Figure A7. Relative variation of soil Cu content presented as boxplots by decade, for three fungicide application doses (F-0.2: 20% of recommended dose; F-0.5: 50% of recommended dose; F-1: recommended dose) 204
Figure A7. Reconstructed bulk atmospheric deposition of the four metals during 1683-2021 in Versailles..... 205
Figure A8. Monthly average percolating water in mm simulated by model for the Great Square of soil..... 205
Figure A9. Pearson correlation coefficient among major and trace elements of KVG's topsoil 214
Figure A10. Evolution of topsoil organic carbon content in the surface layer (0-20 cm) of KVG with different application rates of terreau, simulated by RothC model during 1683-2021.... 216
Figure A11. Evolution of topsoil Cd content in the surface layer (0-20 cm) of KVG with different application rates of terreau and reducing 50% of atmospheric deposition (during 1900-2000)..... 217
Figure A12. Concentrations of phosphorus in different pits of KVG: alley interface (Pit 1), orchard plot-one use over time (Pit 2), vegetable plot-one use over time (Pit 3), orchard/vegetable plot-two use over time (Pit 4), alternance of orchard/vegetable (Pit 5) ... 217
Figure A13. Concentrations of As in different pits of KVG: alley interface (Pit 1), orchard plot-one use over time (Pit 2), vegetable plot-one use over time (Pit 3), orchard/vegetable plot-two use over time (Pit 4), alternance of orchard/vegetable (Pit 5)..... 218

Figure A14. Annual distribution of input and output flows of the four metals during the period of 1683-2021 with 50% terreau application rate. In % of the sum of the absolute value of all flows. Qatm: atmospheric deposition; Qfer: NPK fertilizers; Qorg: organic amendments; Qlea: leaching; Qcrop: crop offtake 219
Figure A15. Evolution of the four metals soil concentration in the surface layer (0-20 cm) of the Great Square under the 1000 scenarios 220
Figure A16. Measured (n = 16) and predicted (n = 1000) values of topsoil metal contents in the Great Square, in the left plot; frequency density of relative difference between predicted values and the average measured value, in the right plot 221
Figure A17. Evolution of the four metals concentration in soil solution in the surface layer (0-20 cm) of the Great Square for the next century 222
Figure A18. Frequency density of relative difference between predicted values and the average measured value of SOC 223
Figure A19. Evolution of the four metals soil concentration in the surface layer (0-20 cm) of the Great Square for the next century 223

Liste des tableaux

Tableau 1. Bénéfices et limitations liées aux services écosystémiques, adapté de Santo et Palmer (2016) 21
Table 2. Physicochemical properties of the garden soils (surface horizons: 0.2 m; n = 104) in the three metropolises, given as mean (range). 48
Table 3. Metal concentrations in bulk sampling precipitation in the three metropolises (corresponding stations) (monthly average values of the period 2017 to 2019 for Cd and Pb, and monthly values of the period 2014 to 2015 for Cu and Zn) 52
Table 4. Brands of fertilizer products mentioned several times in the surveys and their recommended doses for kitchen gardens. 54
Table 5. Characterization of the organic amendments. 54
Table 6. List of applicable fungicides to gardens in France (ITAB, 2020) 57
Table 7. Annual Cu brought per crop (kg/ha) by Cu fungicides for the studied species in three cities. 58
Table 8. Monthly climate data of Nancy city. Description of acronyms: Tem = monthly average temperature (℃), Pre = monthly average precipitation (mm), Eva_po = monthly potential evapotranspiration (mm), Pre1mm = number of wet days with precipitation more than 1mm, Sun = monthly average sunshine hours (hr), Tmx = monthly average maximum temperature (℃), Tmn = monthly average minimum temperature (℃) 62
Table 9. Monthly climate data of Marseille city 62
Table 10. Monthly climate data of Nantes city 63
Table 11. Sources of irrigation water of the three cities 64
Table 12. Equations of the tested models. 65
Table 13. Chemical characteristics of soils and solutions in percolates. Description of acronyms: Soil pH in water = pH, Organic carbon content = SOC, Clay content = clay, Cation exchange capacity = CEC, Total Cd (Cu, Pb, Zn) content in soil = Cd (Cu, Pb, Zn)_total 69
Table 14. Selected regression models for calculating the solution concentration of the four metals. Metal(S): concentration of dissolved metal (μg L^{-1}). Metal(T): total metal concentration (mg kg^{-1}). OM: Organic matter = 1.72OC. OC: organic carbon. 70
Table 15. Default allocation parameters in the RothC module, adapted from the RothC model version 73

Table 16. Average yields of vegetables per harvest in the Grand Est, Pays de la Loire and Provence-Alpes-Côte d'Azur regions, from professional growers, for the period 2000-2018 (Agreste database). *lack of data for artichoke in Grand Est, its value has been repla 77
Table 17. Plant uptake factors (PUF) of Cd, Cu, Pb and Zn for the harvested part of the vegetables, from the BAPPET database. n values are not provided for certain crops, because their PUF values were inferred from similar species. 78
Table 18. Succession of crops for the vegetable gardens of Nancy, Marseille and Nantes. 81
Table 19. Classification of the 104 gardens into 8 classes, according to the type and number of agricultural inputs 83
Table 20. Parameters and variables tested for model sensitivity analysis. 84
Table 21. Evolution of the four metals' soil content in the surface layer (0–20 cm) of 104 French vegetable gardens, according to two different scenarios. CP: current practices, OA: organic agriculture 89
Table 22. Estimated mean annual flows of the four metals in the surface layer (0-20 cm) of soil for 104 garden soils, under the CP scenario 104
Table 23. Monthly climate data of King's Vegetable Garden (Versailles). Description of acronyms: Tem = monthly average temperature (℃), Pre = monthly average precipitation (mm), Eva_po = monthly potential evapotranspiration (mm), Pre1mm = number of wet days with precipitation more than 1mm, Sun = monthly average sunshine hours (hr), Tmx = monthly average maximum temperature (℃), Tmn = monthly average minimum temperature (℃).. 123
Table 24. Characterization of fertilizers for soil pH modelling 125
Table 25. Values of used parameters for soil pH modelling in KVG 127
Table 26. Physicochemical properties of the KVG's soils, given as mean values for different horizons and initial soil (parent material). SOC: Soil organic carbon 140
Table 27. Pedo-transfer functions used to calculate the metal concentrations of initial soil ([Metal], in mg kg^{-1}) based on soil Al or Fe contents ([Al] or [Fe], in g kg^{-1}) (Sterckeman et al., 2006b) 142
Table 28. Historical bulk atmospheric deposition of four metals in King's Vegetable Garden. Each value represents an average annual deposition rate for the corresponding period 146
Table 29. Characteristics of the organic amendments applied in the Great Square of the King's Vegetable Garden. 148

Table 30. Data for simulating metal output from crop offtake: average yields of vegetables per harvest in Paris, from Agreste database; plant uptake factors (PUF) of Cd, Cu, Pb and Zn for the harvested part of the vegetables, from the BAPPET database 149
Table 31. Regression models for calculating the metal concentrations in solution concentration. Metal(S): concentration of dissolved metal (μg L^{-1}). Metal(T): total metal concentration (mg kg^{-1}). OM: Organic matter = 1.72*OC. OC: organic carbon. 152
Table 32. Threshold and guideline values for metals in agricultural soils..... 155
Table 33. Measured and simulated values of the four metals' soil content in the surface layer (0–20 cm) of the Great Square, according to different application rates of terreau..... 157

Tableaux dans l'Annexe

Table A1. Meta-data of investigated Kd models 196
Table A2. Input variables in RothC models 199
Table A3. Crop rotation and ploughing depth in King's Vegetable Garden from 1683 to 2021 206
Table A4. Independent variables tested for modelling uncertainty analysis. *lack of data, minimum and maximum values estimated from ±25% of average values 206
Table A5. Measured soil metal concentrations and initial metal concentrations estimated by pedo-transfer functions from soil Fe content. S1-S16: Soil samples of the first 20 cm collected from 16 vegetable plots; Symbol "C" indicates soil composites of deeper layers for the 16 vegetable plots (20-40 cm, 40-60 cm, 70-80 cm and 80-120 cm) 215
Table A6. Initial metal concentrations estimated by pedo-transfer functions from soil Fe content for garden soils (surface horizons: 0.2 m; n = 104) in the three metropolises: Marseille, Nancy and Nantes 215
Table A7. Total metal contents of the garden soils (surface horizons: 0.2 m; n = 104) in the three metropolises: Marseille, Nancy and Nantes 216
Table A8. Cumulated flows of the four metals in the ploughing soil layer of Great Square soil for different periods during 1683-2021. 218
Table A9. Number of predicted values within ± x% difference of the average measured value. Range: the range of absolute relative differences, in % 221

Glossaire

ADEME : Agence de l'Environnement et de la Maîtrise de l'Energie

ANC : Acid Neutralizing Capacity

ANR : Agence Nationale de la Recherche

ANSES : Agence Nationale de Sécurité Sanitaire de l'Alimentation

AURAN : Agence d'Urbanisme de la Région Nantaise

BAPPET : Base de données des teneurs en éléments traces métalliques de plantes potagères

COST (projet COST) : Coopération européenne en science et technologie

CNRS : Centre National de la Recherche Scientifique

CRPG : Centre de Recherches Pétrographiques et Géochimiques

EMEP : European Monitoring and Evaluation Program

EFSA : European Food Safety Authority

FAO : Food and Agriculture Organisation

KVG : King's Vegetable Garden

GWC : Green Waste Compost

INRAE : Institut National de Recherche pour l'Agriculture, l'Alimentation et l'Environnement

INSEE : Institut national de la statistique et des études économiques

ITAB : Institute of Organic Agriculture and Food

JASSUR : Jardins ASSociatifs Urbains et villes durables

PCA : Principal Component Analysis

PCC : Pearson Correlation Coefficient

RMSEP : Root Mean Square Error or Prediction

RothC : Rothamsted Carbon Model

SARM : Service d'Analyse des Roches et des Minéraux

SNHF : Société Nationale d'Horticulture de France

SOERE PRO : Observatoire de recherche en environnement sur les produits résiduaires organiques

SRC : Standardized Regression Coefficients

WRB : World Reference Base

Chapitre 1 : Introduction générale

1 L'agriculture urbaine : concept, définition, typologie, ordre de grandeur et fonctionnalités

1.1 Concept et définition de l'agriculture urbaine

Récemment, l'agriculture urbaine (AU) a ravivé l'intérêt du public, d'où la publication d'un large nombre de recherches scientifiques. Malgré l'existence de très nombreuses recherches multidisciplinaires, la définition de l'agriculture urbaine reste toujours non-standardisée. Depuis la fin du 20^{e} siècle, les définitions proposées se sont multipliées pour mieux comprendre la façon dont l'espace urbain s'implique dans la production agricole par une dimension intégrative, incluant les pratiques, l'espace, les acteurs et les fonctionnalités (Chalmandrier et al., 2017; FAO, 1999; La Rosa et al., 2014; Mougeot, 2001; Moustier and Fall, 2004; Nahmias and Le Caro, 2012; Pearson et al., 2010; Smit and Nasr, 1992).

La FAO (1999) a proposé une définition : « L'agriculture urbaine et périurbaine (AUP) se réfère aux pratiques agricoles dans les villes et autour des villes qui utilisent des ressources - terre, eau, énergie, main-d'œuvre - pouvant également servir à d'autres usages pour satisfaire les besoins de la population urbaine ». Autrement, Nahmias et Le Caro (2012) ont défini l'agriculture urbaine à partir des liens entre la ville et l'agriculture en terme de localisations, de fonctionnalités, de régulations et de diverses formes agricoles : « L'agriculture [urbaine est] pratiquée et [est] vécue dans une agglomération par des agriculteurs et des habitants aux échelles de la vie quotidienne et du territoire d'application de la régulation urbaine ». Une autre définition plus récente, proposée par Santo et Palmer (2016), énonce que « l'agriculture urbaine comprend la production de plantes alimentaires et non alimentaires, ainsi que l'élevage, dans des espaces urbains et périurbains ».

De plus, un autre argument différencie l'agriculture urbaine de l'agriculture péri-urbaine : certains auteurs préfèrent préciser la notion d'agriculture « péri-urbaine » au lieu de la notion globale « agriculture urbaine ». Certains scientifiques se focalisent sur les fermes ou les jardins localisés dans les centres-villes, et préfèrent utiliser la notion de l'AU au lieu de celle d'agriculture urbaine et péri-urbaine (AUP). Pour d'autres, l'agriculture péri-urbaine est une composante de l'AU. Par défaut, l'agriculture péri-urbaine (AP) est décrite comme l'agriculture dans la transition entre l'espace urbain et de l'espace rural. Ce dernier est caractérisé par une

faible densité de population et des infrastructures moins complexes par rapport à l'espace urbain. D'autre part, l'agriculture péri-urbaine ne peut pas être incluse à l'agriculture rurale en raison du fait qu'elle subit généralement les pressions économiques, sociales et environnementales du milieu urbain et bénéficie des avantages liés à la proximité de l'aire urbaine (par exemple les transports, les marchés de proximité, la conservation à l'état frais, etc.) (Piorr, 2011; Opitz et al., 2016). Depuis la fin du 20th siècle, la croissance urbaine progresse à une très grande vitesse dans les différentes régions du monde. La migration des campagnes vers la ville devient un phénomène commun à l'échelle globale. Appliquer seulement la localisation géographique pour différentier l'agriculture urbaine de l'agriculture péri-urbaine n'est plus adapté à ce jour. De plus, l'agriculture urbaine et péri-urbaine dépendent des services des villes, des planifications urbaines et de développement social économique urbain. Elle est normalement intégrée aux stratégies de développement urbain. Cependant, il existe encore des différences entre agricultures urbaine et rurale, qui ne sont cependant pas évidentes.

Opitz et al. (2016) ont proposé une analyse multifactorielle pour comprendre les similitudes et les différences entre l'agriculture urbaine et l'agriculture péri-urbaine selon leurs facteurs spatiaux, écologiques et sociaux-économiques (Figure 1).

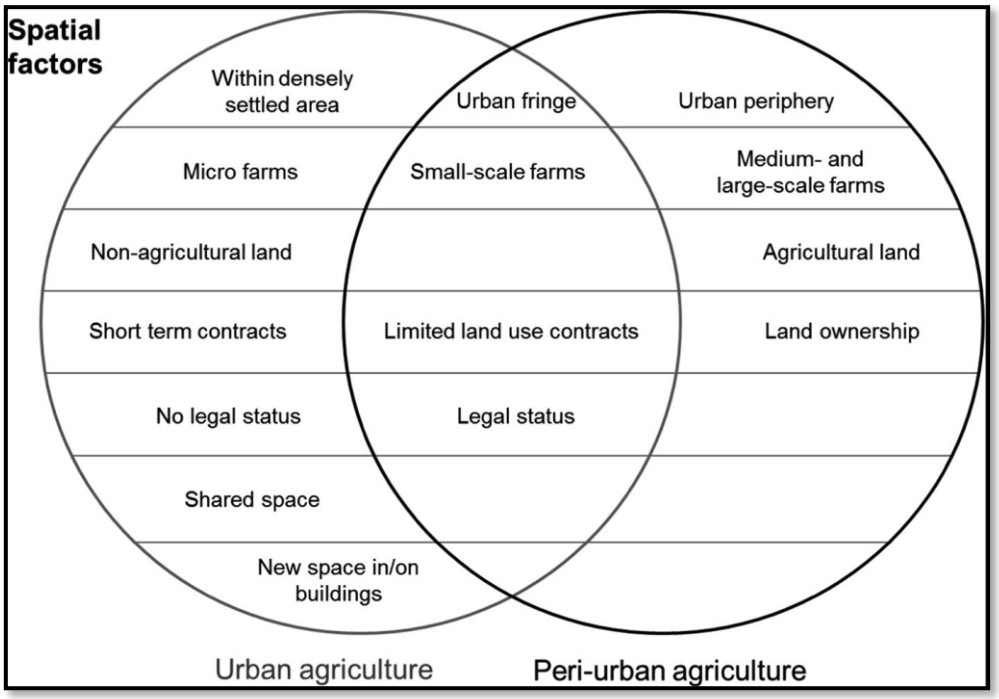

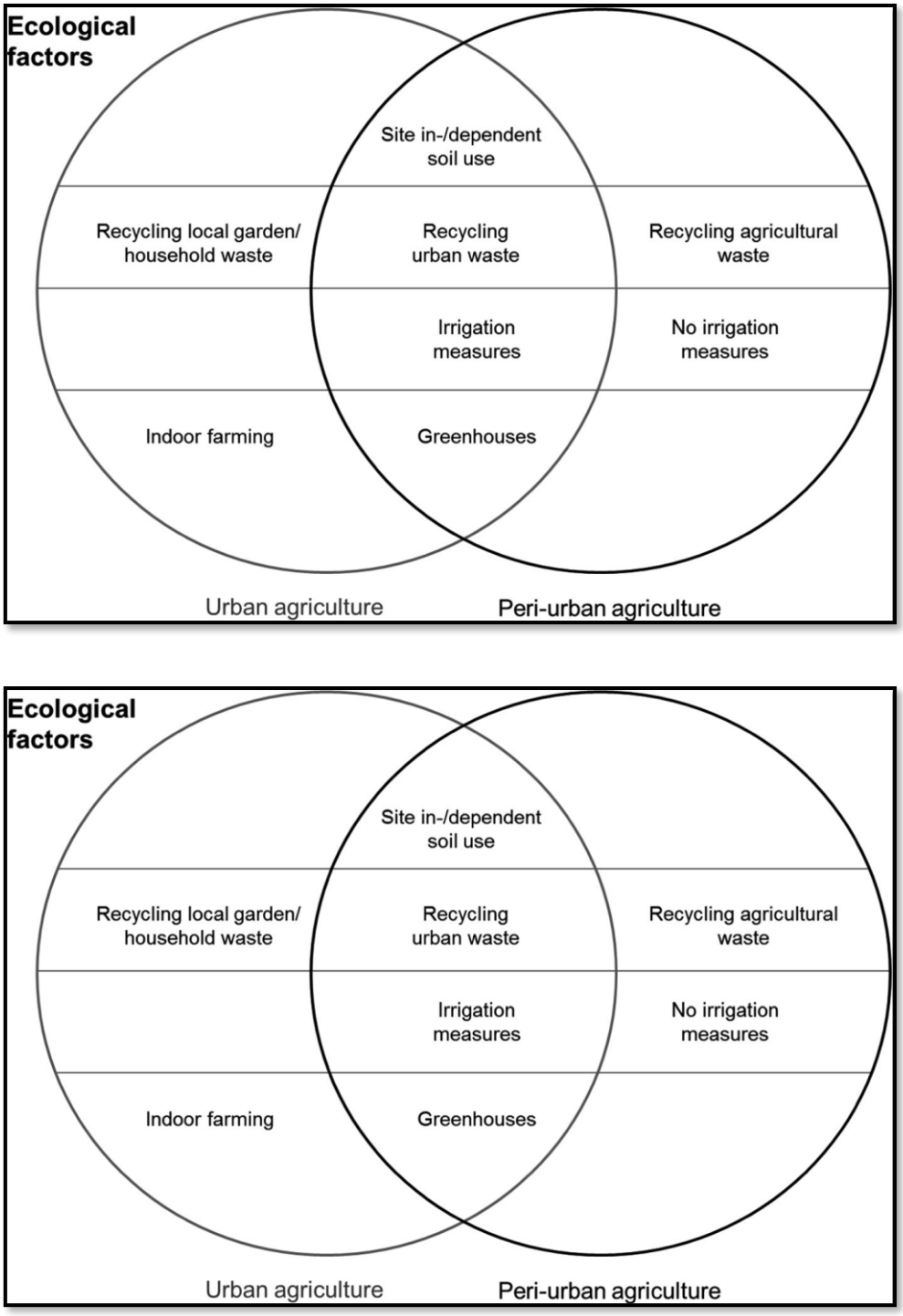

Figure 1. Les facteurs spatiaux, écologiques et socio-économiques définissant les différences entre l'agriculture urbaine et péri-urbaine, adapté d' Opitz et al. (2016)

Ils ont trouvé plus de différences que de similarités entre l'agriculture péri-urbaine et l'agriculture urbaine. D'après leur point de vue, l'agriculture péri-urbaine fournit principalement des produits agricoles et des produits annexes pour la ville, et répond aux besoins de la consommation de produits primaires urbains. L'agriculture urbaine est donc un service qui

répond à de nombreux besoins de la ville, notamment en ce qui concerne les fonctions productives, écologiques et socio-économiques. Aujourd'hui, l'agriculture péri-urbaine est généralement incluse dans la notion globale d'agriculture urbaine.

1.2 Typologie de l'agriculture urbaine

Pour la typologie de l'agriculture urbaine, on peut continuer à utiliser la dimension de la localisation pour faire des classements plus détaillés, par exemple en distinguant les terres des domiciles (ex. l'arrière-cour de maison), les terres communes (ex. les jardins familiaux de communauté), les terres privées (ex. les fermes urbaines), les terres publiques (ex. la ceinture verte ; le jardin collectif dans un parc) ou les terres semi-communes (ex. les jardins pédagogiques dans l'école).

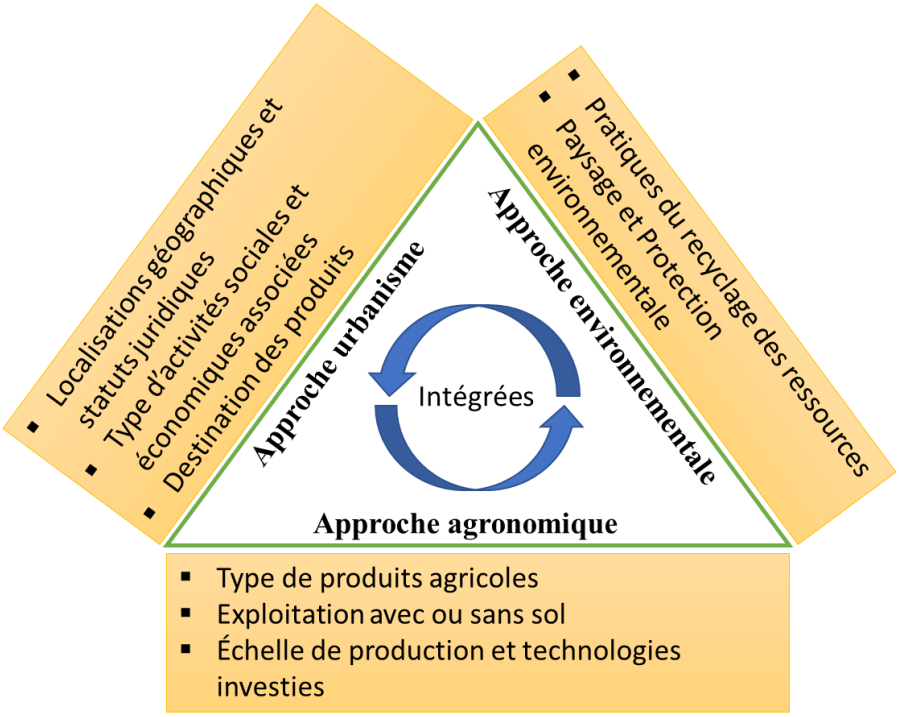

Figure 2. Trois approches et leurs composants pour spécifier différents types de l'AUP, résumé du rapport de McEldowney et al. (2017) ; Mougeot (2001)

Pour caractériser plus finement les différentes formes de l'AUP, on peut s'appuyer sur les différentes dimensions des approches urbanistique, agronomique et environnementale. Bien que ces différentes dimensions ne soient pas indépendantes, elles sont souvent combinées pour définir le type de l'agriculture urbaine (McEldowney et al., 2017; Mougeot, 2001) (Figure 2). Adapté de Santo et Palmer (2016), la Figure 3 présente une typologie de l'agriculture urbaine :

celle en milieu urbain désigne principalement des jardins et des micro-fermes, et celle en milieu péri-urbain, des fermes assimilées à celles de l'agriculture conventionnelle. Ces deux catégories peuvent encore être analysées en sous-catégories précises, par exemple en distinguant, l'agriculture industrielle (*e.g.,* Ferme verticale), l'aquaculture à petite échelle, les toitures végétalisées, les jardins potagers, les jardins pédagogiques, les jardins collectifs, les jardins privés, les espaces vertes, les serres etc.

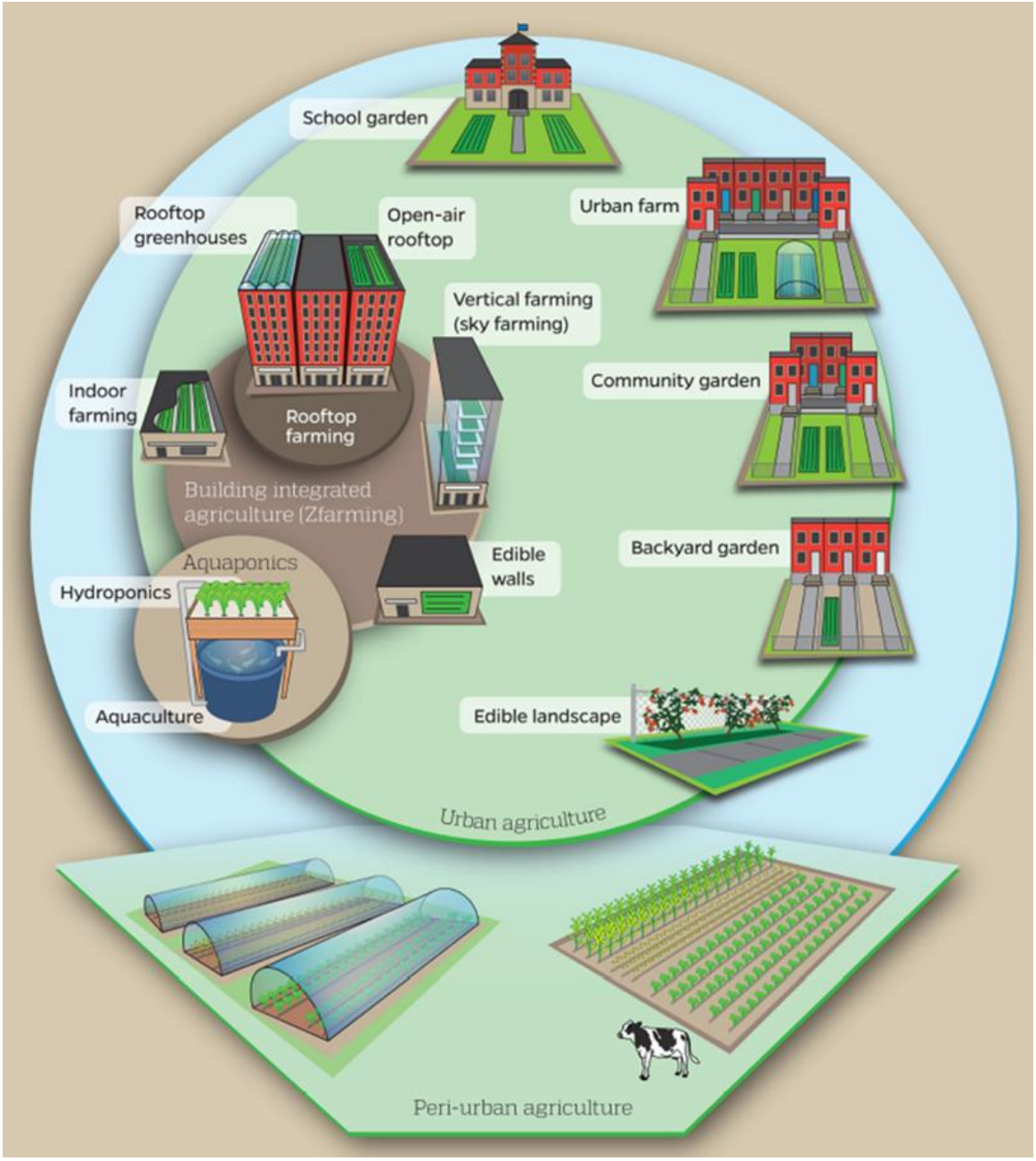

Figure 3. Typologies de l'agriculture urbaine en Europe, adapté de (Santo and Palmer, 2016)

1.3 L'agriculture urbaine en France : formes principales, ordre de grandeur

En France, ce sont les jardins qui représentent la forme majeure de l'agriculture urbaine (Chalmandrier et al. 2017). Le système cultural d'un jardin est principalement constitué d'horticulture (Schwartz, 2013a). Ainsi on peut y trouver un grand nombre de variétés d'occupations (différentes plantes, légumes, etc.). Les jardins potagers varient considérablement en termes de forme et de gestion (Cameron et al., 2012). Les jardins potagers prennent la forme de jardins familiaux, de jardins privés ainsi que de jardins partagés. Un jardin familial correspond à une parcelle de terrain pouvant être louée à une famille (ou un citoyen) afin qu'elle produise ses propres plantations (le plus souvent potagères). Un jardin partagé est un jardin collectif géré par un comité/une association d'habitants d'un quartier (ou une autorité locale) qui désirent jardiner ensemble. Chacun peut apporter sa contribution dans le choix des plantations, et doit en même temps respecter certaines règles collectives. Un jardin privé est réservé à l'usage exclusif d'un propriétaire. Il est le seul à pouvoir l'exploiter. En général, un jardin potager est un lieu de production d'aliments végétaux à partir de plantes herbacées (*e.g.,* légumes racines, feuilles, fruits).

Selon Agreste (2020a), les cultures maraîchères ou fruitières occupaient une surface totale de 165 890 ha de jardins familiaux en 2019 sans compter les jardins privés. Par exemple, à Nantes, sur 6570 hectares de la superficie communale, près de 2900 hectares publiques et privés sont sous couvert végétal, soit 45% de la superficie de la ville. Un quart du couvert végétal nantais est lié aux jardins privés de maisons individuelles, et $^{1}/_{10}$ est correspond aux jardins partagés de logements collectifs (AURAN, 2018). Aujourd'hui, l'agriculture urbaine est de plus en plus prise en considération. Pour répondre à une demande citoyenne forte, le nombre de jardins collectifs a augmenté de moins de 5 en 2002 à 119 en 2018 à Paris (Torres et al., 2018). Depuis une dizaine d'années, la ville de Marseille s'est engagée dans le développement de jardins collectifs et familiaux sur le territoire, comptant 52 jardins partagés et 10 autres en construction (au total, ils couvrent 4.5 hectares), et 12 jardins familiaux (soit 24 hectares du territoire marseillais) (France Urbaine, 2018). Le nombre de jardins urbains en France tend à augmenter au fil des ans, avec actuellement 33 initiatives développées par les 22 métropoles sur des stratégies alimentaires territoriales et des projets innovants dans le domaine de l'agriculture urbaine (France Urbaine, 2018). La situation actuelle en France laisse penser que le nombre de jardins potagers va augmenter à l'avenir.

1.4 Les fonctionnalités rendues par l'agriculture urbaine

L'agriculture urbaine est souvent inscrite dans la planification urbaine durable en tant que système alimentaire de territoire, mais elle y est également inscrite pour ses services économiques, sociaux, environnementaux, sanitaires, éducatifs et culturels (Bell et al., 2016; Pearson et al., 2010; Santo and Palmer, 2016; Smit and Nasr, 1992; Torres et al., 2018; Zasada, 2011). Cameron et al. (2012) ont fait un comparatif résumé pour examiner les preuves de la contribution des jardins privés à la fourniture de services écosystémiques, et pour comprendre comment la gestion des jardins peut influencer l'étendue de ces services. En général, un jardin urbain peut servir aux hommes en tant qu'espace naturel en ville pour se détendre et contribuer à la régulation de l'eau (*e.g.*, services d'atténuation des tempêtes ; réduction le risque d'inondation en augmentant l'infiltration dans le sol et en réduisant les ruissellements de surface). Il peut aussi servir à la prévention des îlots de chaleur locaux, et donc à réduire la consommation d'énergie. Il fournit des productions alimentaires aux citadins, et peut servir de site pédagogique pour enseigner aux enfants l'origine de leur nourriture. Il contribue également à la régulation climatique et à la fourniture de ressources et d'habitats pour la biodiversité dans la ville. Par exemple, la qualité biologique basée sur la présence de microarthropodes dans les sols de jardin potager est proche de celle des sols de forêt (Joimel, 2015). Le jardin permet également de stocker et valoriser les déchets organiques urbains.

Récemment, Santo et Palmer (2016) ont réalisé une synthèse de 165 articles sur l'agriculture urbaine dans laquelle ils résument les bénéfices et les limitations apportées par l'agriculture urbaine. Ils la divisent en 4 grandes catégories : les considérations socioculturelles ; les services écosystémiques ; les développements économiques ; la santé humaine et sécurité alimentaire. Par exemple, le Tableau 1, adapté de Santo and Palmer (2016), résume les bénéfices et les limitations liées aux services écosystémiques.

Cependant, de nombreuses études citées dans le résumé de Santo et Palmer (2016) utilisent des recherches exploratoires avec des méthodes qualitatives ; il y a rarement des études quantitatives sur les changements avant et après la mise en œuvre de projets agricoles urbains. De plus, il n'y a pas de recherches qui quantifient les intérêts ou les limitations à une grande échelle d'étude ou avec un échantillon important (McEldowney et al., 2017).

Tableau 1. Bénéfices et limitations liées aux services écosystémiques, adapté de Santo et Palmer (2016)

Reported Benefits	Reported Limitations
Local ecosystem services	
▪ Increased biodiversity, including provision of habitat for pollinators[8,73] ▪ Reduced air pollution through filtration of particulates by vegetation[67,68] ▪ Micro-climate regulation (e.g., reduction in the "urban heat island effect") through transpiration processes[66] ▪ Increased rainwater drainage, reducing the risk of flooding, ground water contamination, and depleted groundwater levels[99] ▪ Recycling of organic waste (e.g., through composting)[74]	▪ Soil management and amendment, irrigation, and fertilizer use practices by UA growers may not be ecologically sound[3,8]
Climate change mitigation	
▪ Potential reduction in greenhouse gas (GHG) emissions associated with food transportation, particularly when replacing typically air-freighted produce (e.g., greens, berries)[78] ▪ Carbon sequestration by vegetation and crops[77,78] ▪ Some technological UA operations may reduce the energy and resource inputs – and waste outputs – associated with food production[6,65,75,118] ▪ Urban growing maintains collective memory of food production and protects urban green spaces, upholding cities' capacity to produce food in times of crisis[76]	▪ May increase GHG emissions and water use if plants are grown in energy- or resource-intensive locations[13,75,85-88] ▪ Small-scale, fragmented UA may be less efficient in resource use and transport emissions than conventional agriculture[79] ▪ If UA becomes ubiquitous in cities, it may reduce population density, requiring more driving and GHG emissions than the current system[63,82]

1.5 Enjeux sur la sécurité alimentaire mondiale et le rôle de l'agriculture urbaine face à ce dilemme

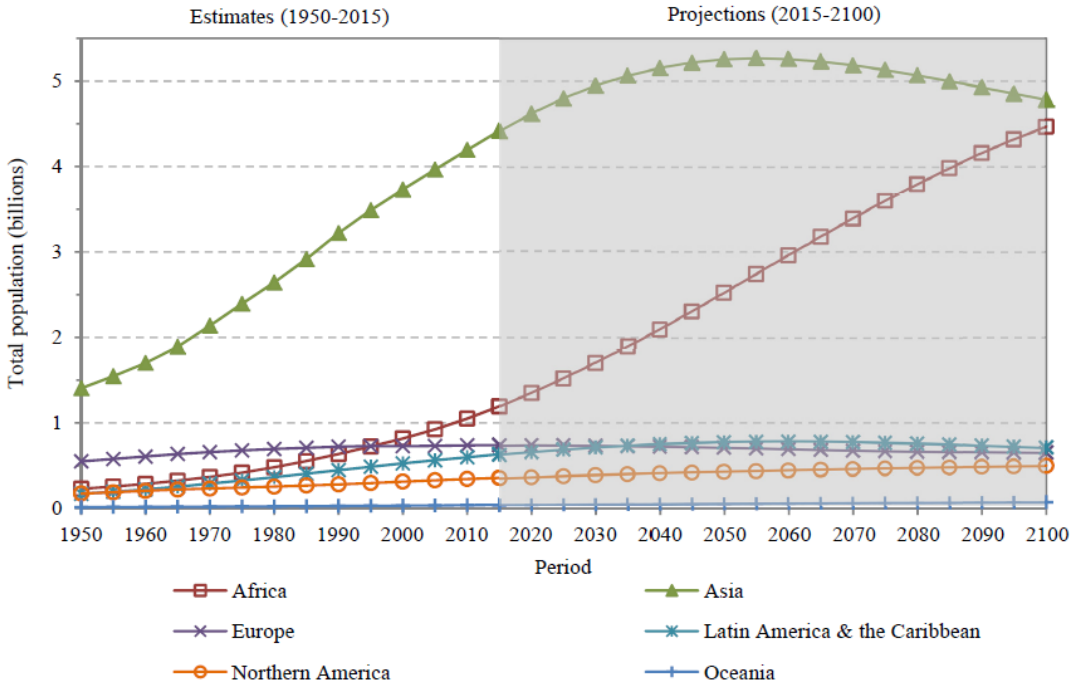

Figure 4. Population par région : estimation, 1950-2015 ; prédiction, 2015-2100. (Source : "World Urbanization Prospects - Population Division - United Nations," 2017)

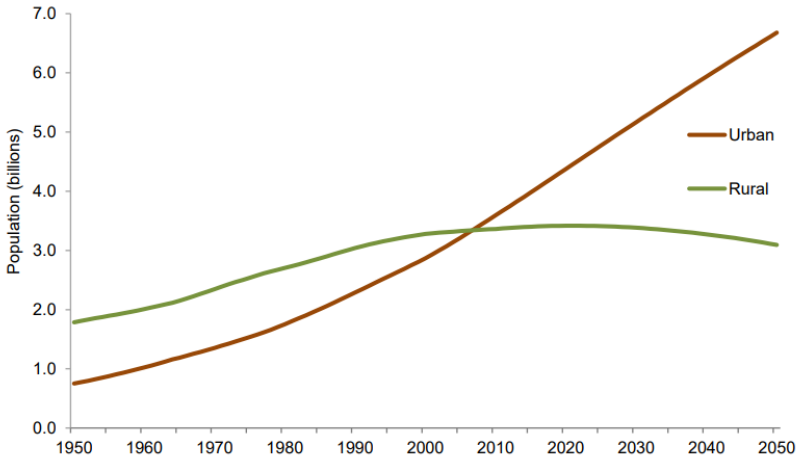

Figure 5. Populations urbaines et rurales du monde, 1950-2050, adapté de United unions (2018)

L'intérêt porté à l'agriculture urbaine n'est pas une nouvelle tendance. Elle avait autrefois été associée aux périodes de crise alimentaire, comme par exemple pendant les deux guerres mondiales. Dans le contexte des pays en développement, l'intérêt porté à l'agriculture urbaine concerne sa capacité à fournir des productions alimentaires (De Bon et al., 2010). La dernière

projection des Nations Unies sur la population à l'échelle mondiale en 2018 montre que la population mondiale estimée 7.8 milliards en 2018 va augmenter à 9.7 milliards en 2050 (United Nations, 2019) (Figure 4). En 2017, le nombre de personnes sous-alimentées atteint 821 millions, principalement dans les pays en voie de développement, soit environ une personne sur neuf dans le monde (FAO, 2018). De plus, 55 % de la population mondiale vit dans des zones urbaines. Cette proportion devrait passer à 68 % en 2050 (United unions, 2018) (Figure 4).

Pour nourrir cette population dans le futur, la FAO a annoncé que la production alimentaire mondiale doit augmenter de 60 % en 2050 pour l'ensemble des terres cultivées. Les terres arables disponibles dans l'UE diminuent en raison de l'augmentation de la sylviculture et de l'urbanisation. Nous sommes également confrontés à un grave problème de perte de nourriture. Un tiers de tous les légumes produits est gaspillé lors des étapes de transport et de distribution (FAO, 2019). Face à ce besoin, l'agriculture urbaine est l'un des moyens stratégiques contribuant à lutter contre l'insécurité alimentaire. La production alimentaire locale devient un projet intéressant pour ralentir l'impact négatif de l'insécurité alimentaire et de la crise économique (Miccoli et al. 2016; Tedesco et al. 2017; Martellozzo et al. 2014; Orsini et al. 2014, 2013; Galhena et al. 2013). La sécurité alimentaire est un autre problème mondial. Les aliments contaminés contiennent des bactéries, des virus ou des substances chimiques nocives, qui peuvent provoquer plus de 200 maladies. Chaque année, on estime que 600 millions de personnes, soit près d'une personne sur dix dans le monde, tombent malades après avoir consommé des aliments contaminés. Jusqu'à 420 000 personnes meurent chaque année à cause de problèmes liés à la sécurité alimentaire (WHO, 2020).

Dans le contexte Européen, l'intérêt actuel porté à l'agriculture urbaine concerne plutôt ses fonctionnalités socioculturelles et environnementales. Ceci est confirmé par la projection de 253 projets en Europe dans le cadre du projet COST (Coopération européenne en science et technologie). L'agriculture urbaine peut potentiellement fournir des bénéfices multidisciplinaires, mais non sans limitations. Généralement, deux enjeux sont associés au développement de l'agriculture urbaine : (1) le manque d'estimation du potentiel de produits alimentaires fournis par l'agriculture urbaine et (2) le risque potentiel sur la santé humaine lié à la consommation des aliments contaminés.

2 Enjeux de la contamination des métaux dans les sols de jardins potagers

2.1 Propriétés physicochimiques des sols de jardins potagers

Les sols de jardins potagers généralement font partie des sols urbains car ils sont des sols agricoles situés en milieux urbanisés (Schwartz, 2013a). Les sols urbains sont souvent fortement remaniés et caractérisés par une très forte hétérogénéité physico-chimique résultant en particulier des divers intrants de matériaux exogènes, technogéniques en mélange ou non avec des matériaux terreux, faisant apparaître des Technosols ou Anthrosols d'après WRB (World Reference Base for soil) (IUSS Working Group WRB, 2015). Ils peuvent être distingués au deuxième niveau de classification à l'aide des qualificatifs suivants : Hortic, Plaggic, Terric, Irragric, Anthraquic et Pretic, respectivement. Par conséquent, les sols de jardins potagers sont identifiés comme les Hortic-Anthrosols en raison d'une culture de longue durée et/ou intensive avec apports de matières organiques, irrigation, travail du sol.

Les propriétés physico-chimiques des sols de jardins potagers varient largement en fonction de leurs fond géochimiques, des anciennes occupations et pratiques agricoles. Le pH du sol dans les potagers urbains varie entre 3,4 et 8,6 (Bidar et al., 2020). Différentes pratiques de jardinage telles que le chaulage, la fertilisation organique, et même certains déchets de construction enfouis dans les sols des potagers peuvent entraîner une hétérogénéité du pH.

Ayant subi des pratiques culturales intenses et répétées, les sols des jardins potagers ont généralement des quantités élevées en matière organique, qui peuvent atteindre 10 % (Bidar et al., 2020). Ces valeurs sont plus haut que ceux observés dans les sols agricoles qui se situent en général entre 1 - 3% (Burghardt et al., 2018; Morel and Schwartz, 1999). Joimel et al. (2016) ont montré que la teneur moyenne en carbone organique mesuré dans les jardins potagers (2,62 %) est presque deux fois celle observée dans les sols agricoles (1,49 %) en France.

N (azote), P (phosphore), K (potassium) sont les éléments qui sont souvent pris en compte dans l'analyse des propriétés agricoles des sols. Leur teneurs dans les jardins potagers sont élevées en raison de l'application intensive d'engrais chimique (Burghardt et al., 2018; Joimel et al., 2021, 2016).

2.2 Présence de la contamination des métaux en traces des sols de jardins potagers : origine de métaux, ordre de grandeur

Comme tous les sols urbains, les sols de potagers peuvent être contaminés, car ils sont souvent localisés sur des sites précédemment urbanisés et affectés par les activités humaines (Douay et al., 2008a, 2008b; Joimel et al., 2016; Kachenko and Singh, 2006; Li et al., 2013; Wei and Yang, 2010). Les modes d'occupation et de gestion des sols de jardins sont souvent non-standardisés, contrairement aux systèmes agricoles conventionnels (Schwartz, 2013a).

L'origine de ces métaux en traces dans les sols de jardins est multiple. Ils peuvent provenir de de sources naturelles et de sources anthropiques. Les sources naturelles des métaux en traces sont l'activité volcanique et de l'altération des roches mères (Alloway, 2013a; Liu et al., 2013, 2015; Nriagu, 1989). Les sources anthropiques sont généralement des anciennes occupations des sols, des pollutions atmosphériques, des intrants pour la culture (les engrais chimiques, les amendements organiques, l'irrigation, les produits phytosanitaires, etc.) (Alloway, 2004, 2013a; Arora et al., 2008; Hernandez et al., 2003; Khan et al., 2017; Laidlaw et al., 2018; X. Li et al., 2001). Belon et al. (2012) ont étudié les sources d'entrée de métaux en traces dans les sols agricoles français. Les fumiers, les engrais minéraux et les pesticides sont les sources prédominantes des métaux en traces. En Europe, la proportion de Cd provenant des engrais phosphatés s'élevait à 74 % de la charge totale en Cd dans les sols arables (Chen et al., 2007). Weissengruber et al. (2018) montrent que les composts importent plus de métaux en traces dans les sols que les fertilisants chimiques et les digestats, et leurs contributions peut atteindre 10 fois celle des dépôts atmosphériques de Pb, Zn.

Douay et al. (2008a) ont étudié des sols de jardins potagers localisés près d'anciennes usines métallurgiques, et ont montré que ces sols sont fortement contaminés en métaux en traces (*e.g.*, Cd, Pb, Zn, Cu), et ce, des dizaines de fois plus que la concentration des métaux présente dans les sols agricoles de cette région. Récemment, Joimel et al. (2016) ont comparé les concentrations des métaux en traces dans les sols de potagers à ceux de différents systèmes selon un gradient d'anthropisation (forêt, prairie, agriculture conventionnelle, verger et vignoble, technosols). Ils ont remarqué que la teneur en métaux en traces est plus ou moins liée au niveau d'anthropisation des sols. Les sols de jardins (104 jardins potagers localisés séparément à Marseille, Nancy et Nantes) sont sur-fertilisés, riches en phosphore et en pollutions métalliques, particulièrement en Cu, Cu, Pb et Zn (Joimel et al., 2016).

Pour les sols agricoles, la distribution spatiale de métaux en traces varie fortement selon les régions en lien avec certaines activités agricoles (Belon et al., 2012). Pour les sols urbains, la distribution spatiale de métaux peut être très variable entre les quartiers d'une ville (Imperato et al., 2003). De plus, une forte variabilité sur la distribution de Pb peut être observée à l'échelle d'un même jardin collectif (Bechet et al., 2018). Douay et al. (2008a) ont montré que la distribution de métaux en traces dans les sols de jardins varie aussi en fonction de la profondeur du sol, qui est liée aux contributions des horizons profonds mélangés avec celui de surface lors du travail du sol.

2.3 Risques potentiels sur les fonctionnalités d'écosystème du sol et la santé humaine liés à la contamination de métaux en traces

Malgré les règlements établis pour limiter la contamination présente dans l'environnement, la contamination des sols de jardins urbains par les métaux reste toujours un problème. Dans le cadre de cette thèse, les quatre métaux ciblés sont cadmium (Cd), plomb (Pb), cuivre (Cu) et zinc (Zn). Ces métaux sont très documentés comme étant des polluants fréquents dans les sols et sont donc des indicateurs de la qualité d'un sol (Douay et al., 2008a).

Les métaux sont très persistants dans les sols où ils peuvent s'accumuler au fil du temps (Laidlaw et al., 2018; Tresch et al., 2018), être prélevés par les plantes vers la partie comestible, ou polluer les eaux souterraines par la lixiviation (Figure 6), et même influencer la biodiversité du sol (Joimel et al., 2018). Leitão et al. (2018) ont montré que les concentrations de métaux dans les sols et les eaux souterraines ont dépassé les valeurs recommandées dans certains jardins collectifs à Lisbonne. Des travaux ont prouvé que les légumes cultivés dans les sites très contaminés contiennent de fortes quantités en métaux en traces (Augustsson et al., 2018; Chen et al., 2015; Douay et al., 2008a, 2008b; Pelfrene et al., 2011). La consommation d'aliments produits à partir de terres contaminées et l'inhalation ou l'ingestion de sols contaminés, peuvent conduire à l'apport de polluants métalliques dans le corps humain (Figure 6). Il existe des systèmes de contrôle de la qualité pour les aliments commerciaux, mais pas pour les légumes cultivés à la maison (Augustsson et al., 2018).

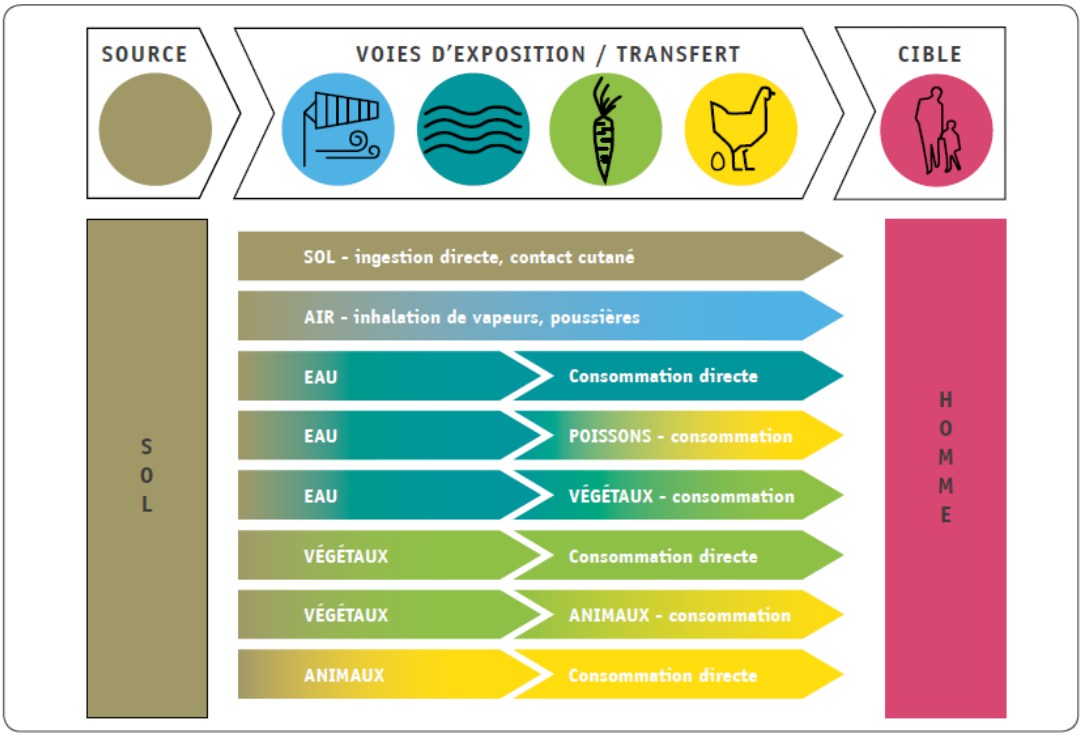

Figure 6. Voies d'exposition de l'homme aux métaux présents dans le sol, adapté de (DAMAS et al., 2018)

Le cuivre est un micronutriment essentiel nécessaire aux processus de transfert d'électrons. Il est un composant central de nombreuses enzymes (EFSA, 2015). Le zinc joue un rôle catalytique dans chacune des six classes d'enzymes, ainsi que des rôles biologiques incluent le contrôle/modulation de la transcription et de la traduction et la transduction du signal (EFSA, 2014). Le cuivre et le zinc ne sont pas facilement bioaccumulable, et leur toxicité pour l'homme est donc relativement faible. A haute concentration dans les sols, ils peuvent présenter une toxicité pour les plantes, les micro-organismes du sol et la faune du sol, affectant les fonctions écologiques du sol. L'excès du cuivre peut altérer des processus cellulaires, particulièrement bloquer le transport des électrons photosynthétiques, et inhiber la croissance des plantes (Fernandes and Henriques, 1991; Yruela, 2005). La toxicité du Zn chez les plantes est beaucoup plus faible que la carence en Zn, mais la toxicité du Zn peut également se produire dans les sols agricoles traités avec de grandes quantités de boues d'épuration, ou dans les sols urbains et périurbains présentant différentes sources de contamination de zinc, notamment ceux à faible pH du sol. Le seuil d'apparition des symptômes toxiques varie considérablement entre les espèces végétales et même au sein d'une même espèce. Par exemple, les cultures à feuilles sont sensibles à la toxicité du Zn, en particulier les épinards et les betteraves à sucre, en raison de leur forte capacité d'absorption du Zn (Broadley et al., 2007).

Le Cd et le Pb sont présentés dans l'environnement en raison d'activités anthropiques, par exemple l'ancienne utilisation du plomb dans les conduites d'eau, la peinture et l'essence. Sans utilité pour les organismes vivants, ils sont hautement toxiques et largement répandus, et ont notamment des impacts sur la santé humaine. L'exposition à long terme au cadmium produit des effets toxiques principalement sur les reins, mais aussi sur les os (EFSA, 2012a). La toxicité chronique du Pb est la plus préoccupante lorsqu'on considère les risques potentiels pour la santé humaine, en raison de sa longue demi-vie dans l'organisme. Le système nerveux central est le principal organe cible du saturnisme (EFSA, 2012b). D'après un programme national de biosurveillance en 2014-2016, il existe une imprégnation de la population française par différents métaux en traces. En particulier, 48% de la population adulte française âgée de 18 à 60 ans (N = 1716) présente une cadmiurie supérieure à 0,5 µg g^{-1} de créatinine dans les urines, proposée comme concentration critique pour un adulte de 60 ans en supposant que l'ingestion est la seule source d'exposition au Cd (Fillol et al., 2021a, 2021b). Les déterminants de l'exposition au Cd, Cu, Pb sont principalement d'ordre alimentaire. Pour les non-fumeurs, comme les enfants, la consommation de céréales est la principale source de Cd. Les aliments issus de l'agriculture biologique entraînent une imprégnation de la population par le Cu (Fillol et al., 2021a, 2021b).

2.4 Évaluation du niveau de contamination des sols par les métaux et du risque sanitaire associé

Différentes approches existent en Europe, et même dans le monde entier, pour définir les seuils associés aux concentrations maximales des métaux dans les sols. Les seuils et sont généralement déterminés en fonction de l'utilisation des sols, en tenant compte des voies de transmission des polluants aux personnes et des risques sanitaires qu'elles peuvent entraîner. Les normes des polluants sont établies sur la base des connaissances sur le polluant, des technologies de détection et quantification, des values de fond géochimique, ainsi que des coûts pour la remédiation. En fonction des différentes utilisations des valeurs de ces seuils dans les cadres réglementaires nationaux, elles représentent parfois des "valeurs de seuils", des "concentrations maximales tolérables", des "valeurs réglementaires" ou des "valeurs indicatives" (Antoniadis et al., 2017b; Dziubanek et al., 2015; Mathieu et al., 2008; Ministry of the Environment, Finland, 2007; Tóth et al., 2016). De ce fait, leurs valeurs varient fortement d'un pays à l'autre. Datant de 2006, la législation de l'Union européenne a fixé des seuils pour

lesquels les aliments peuvent être considérés comme sans danger, en fonction de leur contenu en cadmium, en plomb et en mercure (European Union, 2021a, 2021b, 2006). Encore aujourd'hui, les seuils pour la teneur en métaux dans les sols ne sont pas établis en France.

Malgré un très faible niveau de contamination métallique du sol, une exposition chronique peut entraîner des effets néfastes sur la santé humaine. Par conséquent, le calcul de l'exposition alimentaire chronique aux métaux est un bon moyen d'évaluer la sécurité alimentaire liée à la consommation des produits agricoles cultivés sur des terres contaminées par les métaux. Dans le contexte de la France, plus d'attention à la qualité des sols de jardins devrait être apportée pour assurer leurs fonctions et leur durabilité (Schwartz, 2013a). Ainsi, l'estimation de la qualité des sols ne doit pas seulement considérer les caractéristiques du sol liées à la fertilité, mais doit aussi inclure leur contamination.

3 Dynamique de métaux en traces (Cd, Cu, Pb, Zn) dans les sols

3.1 Cycle biogéochimique des métaux dans les sols de jardins

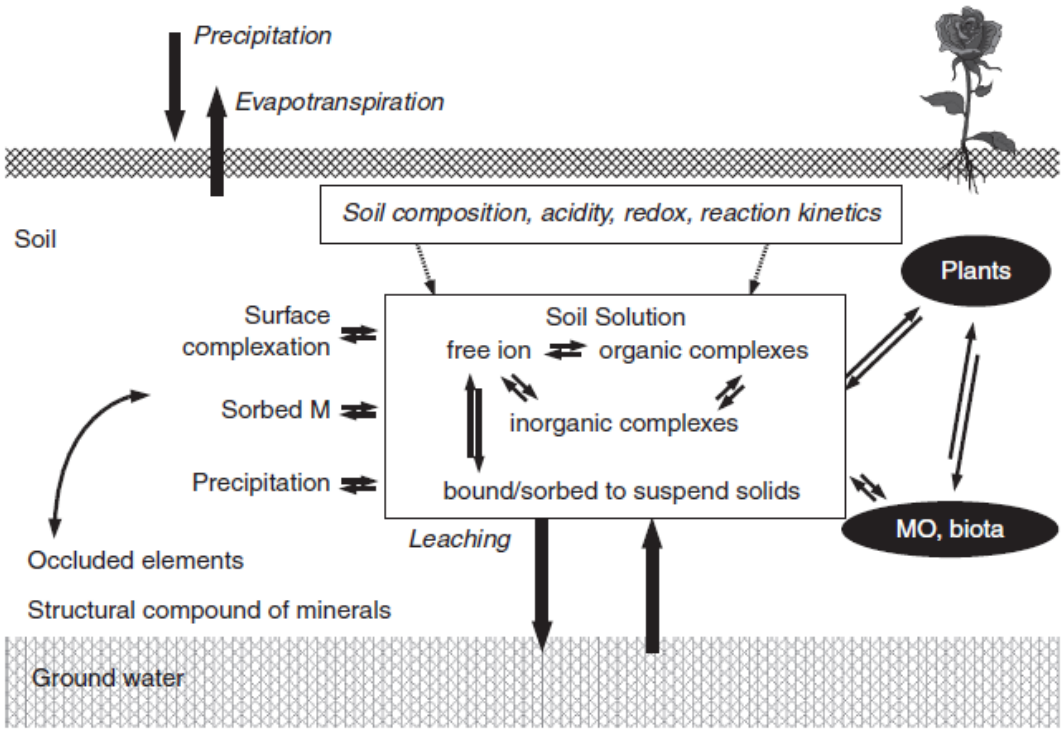

Figure 7. Représentation schématique des différents pools des métaux en traces dans le système du sol et de leurs interactions, adapté de Tack (2010)

Les métaux sont répartis dans différents compartiments du sol, où ils sont présents sous différentes formes chimiques et varient considérablement dans leur réactivité (Figure 7). La concentration des métaux en solution dans les sols non-contaminées est souvent de l'ordre du microgramme par litre. Les métaux en phase aqueuse et phase solide peuvent être présents sous leur forme ionique la plus simple, mais aussi sous formes de complexes inorganiques ou organiques, pouvant être résumées comme suit (Tack, 2010) :

- *Espèces dans la solution du sol :*

1. Des ions libres ;
2. Complexes inorganiques ;
3. Complexes organiques ;
4. Liaison aux colloïdes en suspension (argiles, matières organiques).

- *Espèces en phase solide du sol :*

1. Liés de manière échangeable à des surfaces chargées ;
2. Complexé ou occlus dans la matière organique ;
3. Adsorbé ou occlus dans des oxydes hydratés de fer et de manganèse ;
4. Adsorbé ou occlus dans les carbonates ;
5. Sous forme de précipités (carbonates, phosphates, sulfures) ;
6. Composant structurel dans les minéraux.

Outre les éléments sous leur véritable forme dissoute, la solution du sol contient également des matières colloïdales et de fines particules en suspension qui peuvent transporter une proportion importante des éléments traces présents dans la solution du sol. Le Cd et le Zn sont plus souvent trouvés sous forme d'ions libres, tandis que jusqu'à 90 % du Cu et du Pb sont associés à la fraction colloïdale (Tack, 2010).

Les colloïdes et les métaux en suspension jouent un rôle important dans la migration des métaux. Les processus physiques, chimiques et biologiques dans le sol déterminent la distribution, la mobilité et la biodisponibilité des métaux. Les échelles de temps sur lesquelles différents processus se produisent dans le sol peuvent aller de quelques nanosecondes à des siècles ou plus (Tack, 2010). Notamment, l'environnement du sol étant en constante évolution, par exemple par les changements de température et de teneur en eau, cela peut entraîner des modifications du pH et de l'état de réduction du sol. Les sols ne sont donc jamais en véritable équilibre chimique.

Degryse et al. (2009) ont effectué un résumé critique sur les principes, les méthodes de détection, les prévisions et les applications de la distribution des métaux (Cd, Co, Cu, Ni, Pb, Zn) entre les différentes phases dans les sols.

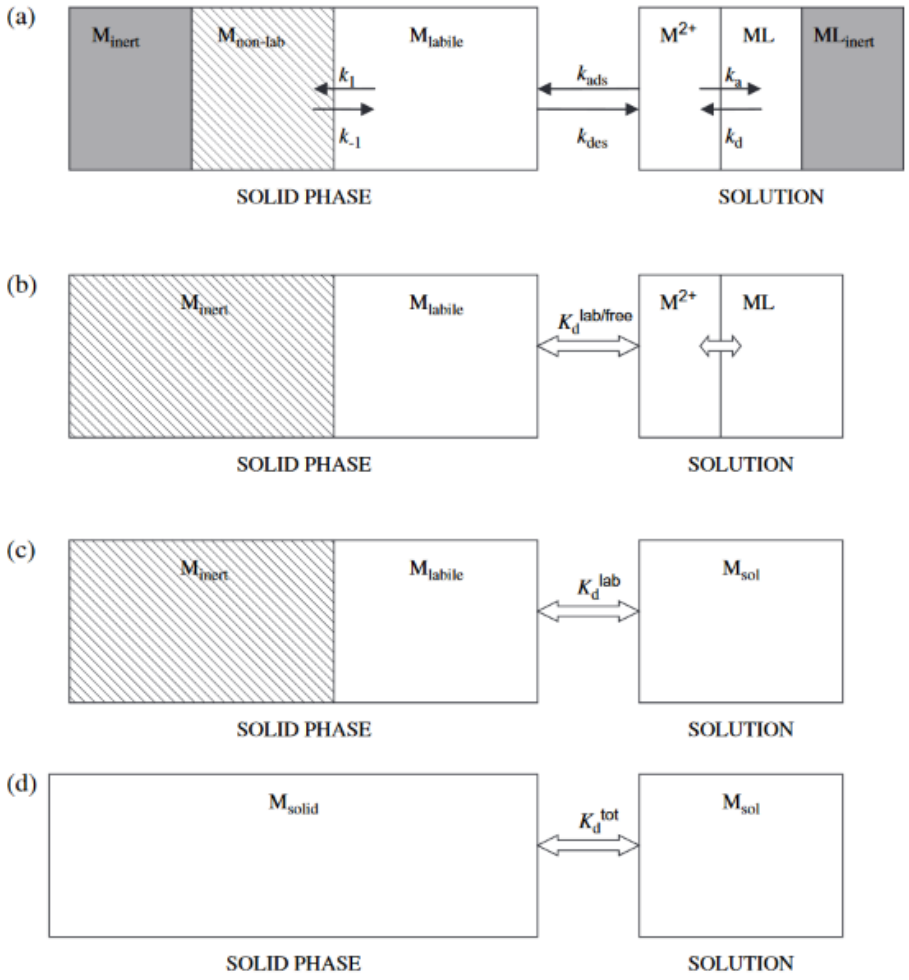

Figure 8. Schéma de l'équilibre d'ions métalliques dans les sols, par ordre croissant de simplicité adapté de Degryse et al. (2009)

Selon le schéma présenté dans la Figure 8 (a), les métaux dans le sol peuvent être associés à cinq phases : métaux inertes en phase solide ; métaux non-labile en phase solide ; métaux labile en phase solide ; métaux mobiles en solution ; métaux inertes en solution (Degryse et al., 2009). La phase inerte de métaux est celle de la fraction solide, qui ne réagit pas avec les autres constituants du sol. La phase non-labile de métaux peut exister dans les solides du sol, dans les solutions/suspensions liées à des ligands tels que l'acide humique/fulvique, ou dans des micro-/sous-microparticules. La phase labile de métaux représente l'ensemble de différentes formes chimiques de métaux qui sont impliqués dans les réactions réversibles. Lorsqu'il y a un changement de l'équilibre en solution, le phénomène d'hystérèse n'apparait pas dans cette

phase. L'adsorption et la désorption des ions métalliques sur la phase solide et la liaison et la dissociation des complexes métalliques en solution sont décrites comme des processus cinétiques utilisant des constantes de vitesse de premier ordre. Le passage du compartiment de métal labile au compartiment de métal non labile est donc un processus de réaction lent et réversible (Degryse et al., 2009).

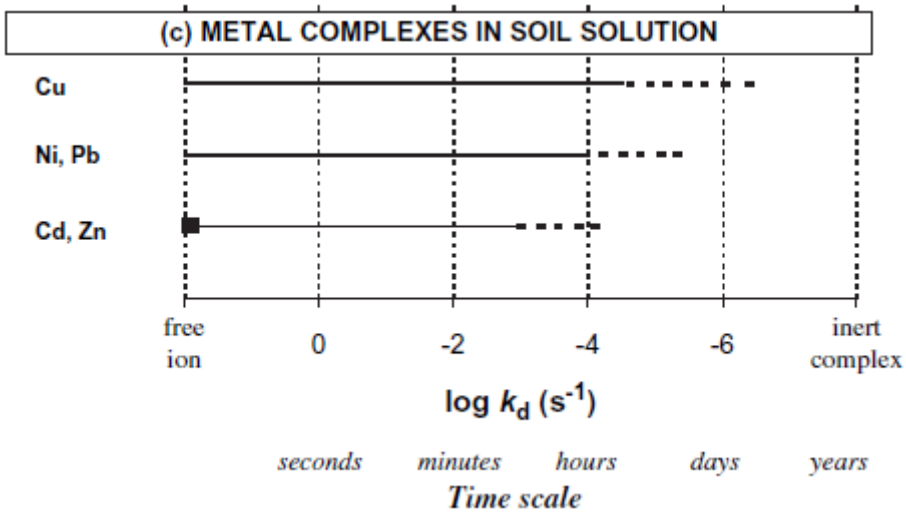

Figure 9. La gamme estimée des taux de dissociation des complexes métalliques dans les solutions du sol, adapté de Degryse et al. (2009)

Toutes les espèces métalliques en solution peuvent migrer. Dans le sol, la conversion des espèces des métaux est rapide par rapport à la lixiviation des métaux dans le sol (Figure 9). Par conséquent, les informations sur la spéciation du métal en solution ne sont pas strictement demandées pour les modèles de lixiviation du métal à long terme (Degryse et al., 2009).

3.2 Rôle des pratiques agronomiques sur la dynamique des métaux dans les sols de jardin potager

La dynamique des métaux dans les sols de jardin potager peut être influencée par les pratiques agricoles appliquées. Dans les sols de jardins, les pratiques agricoles (*e.g.*, amendement chimique ; apport de matière organique ; chaulage ; travail du sol) peuvent conduire à des changements des propriétés physico-chimiques et physiques des sols, puis influencer la mobilité et la biodisponibilité des métaux (Dube et al., 2001). Par exemple, Waterlot et al. (2017, 2011) ont trouvé que les amendements phosphatés peuvent efficacement immobiliser le Pb et Cd dans les sols de jardins contaminés. L'application intensive de N entraîne une acidification

du sol et augmente donc la mobilité et la biodisponibilité des métaux, mais l'ajout de grandes quantités de P entraîne une précipitation et réduit la perte de métaux par absorption par les plantes ou par lixiviation. L'ajout de grandes quantités de K peut augmenter absorption du Cd par les plantes en raison de la chloro-complexation du Cd^{2+} (McLaughlin et al., 2011).

L'apport de matières organiques est non seulement une source d'entrée pour les métaux, mais il joue aussi un rôle sur la sorption-désorption des métaux dans les sols, et donc, influence la spéciation chimique des métaux (Fang et al., 2016; Ren et al., 2015). Pareillement, l'apport de matières organiques peut modifier des caractéristiques physico-chimiques internes du sol. En outre, ce n'est pas seulement la quantité de matière organique dans les sols qui influence la sorption des métaux, mais aussi la typologie et la composition des matières organiques (Fest et al., 2008; Jalali and Latifi, 2018; Liu et al., 2018; Ren et al., 2015; Rosen and Chen, 2018). De plus, la majeure partie du métal en solution dans le sol est liée à la matière organique dissoute (DOM). En conséquence, les facteurs ayant un impact sur la solubilité de la matière organique affecteront également la solubilité du métal (McBride et al., 1997; Sauvé et al., 2000; Yang et al., 2018). Fang et al. (2018, 2017, 2016b) ont montré que l'ajout répété de compost augmente la teneur totale en MO du sol et la concentration en DOM. La plupart des métaux sont sous formes de complexes avec la matière organique particulaire, l'oxyde de fer ou les minéraux du sol à un pH neutre à alcalin ($6 < pH < 8$) (Figure 10) ; Cd, Cu, Pb et Zn liés à la DOM deviennent les espèces dominantes en phase liquide dans cette gamme de pH du sol (Figure 11). De ce fait, l'augmentation de la matière organique dissoute par l'application de compost accroit la mobilité du Cd (de manière équivalente pour le Cu et le Pb) via lixiviation.

Jalali et Latifi (2018) ont ainsi démontré que l'application de fumier et de résidus organiques dans les sols augmente le potentiel de lixiviation des métaux (Cd, Ni, Zn) en raison de l'augmentation de la concentration en DOM et du pH du sol. De plus, la composition des DOM, en particulier la fraction d'acide fulvique (FA), est un facteur crucial pour la spéciation chimique des métaux (Ren et al., 2015). En outre, Kochem Mallmann et al. (2014) ont montré que le travail du sol peut réduire les concentrations de métaux en traces dans les sols superficiels en augmentant leur transfert par les flux préférentiels vers les couches plus profondes. Richardson et al. (2016) ont démontré que les nutriments et les métaux peuvent rester dans le sol par la stabilisation à l'intérieur des résidus de vers de terre.

En conclusion, l'évolution des métaux en traces dans les sols est soumise à des processus dynamiques et interconnectés. Les pratiques agricoles peuvent non seulement ajouter des

métaux dans les sols, mais peuvent aussi changer les propriétés du sol, et jouent donc un rôle sur la dynamique des métaux.

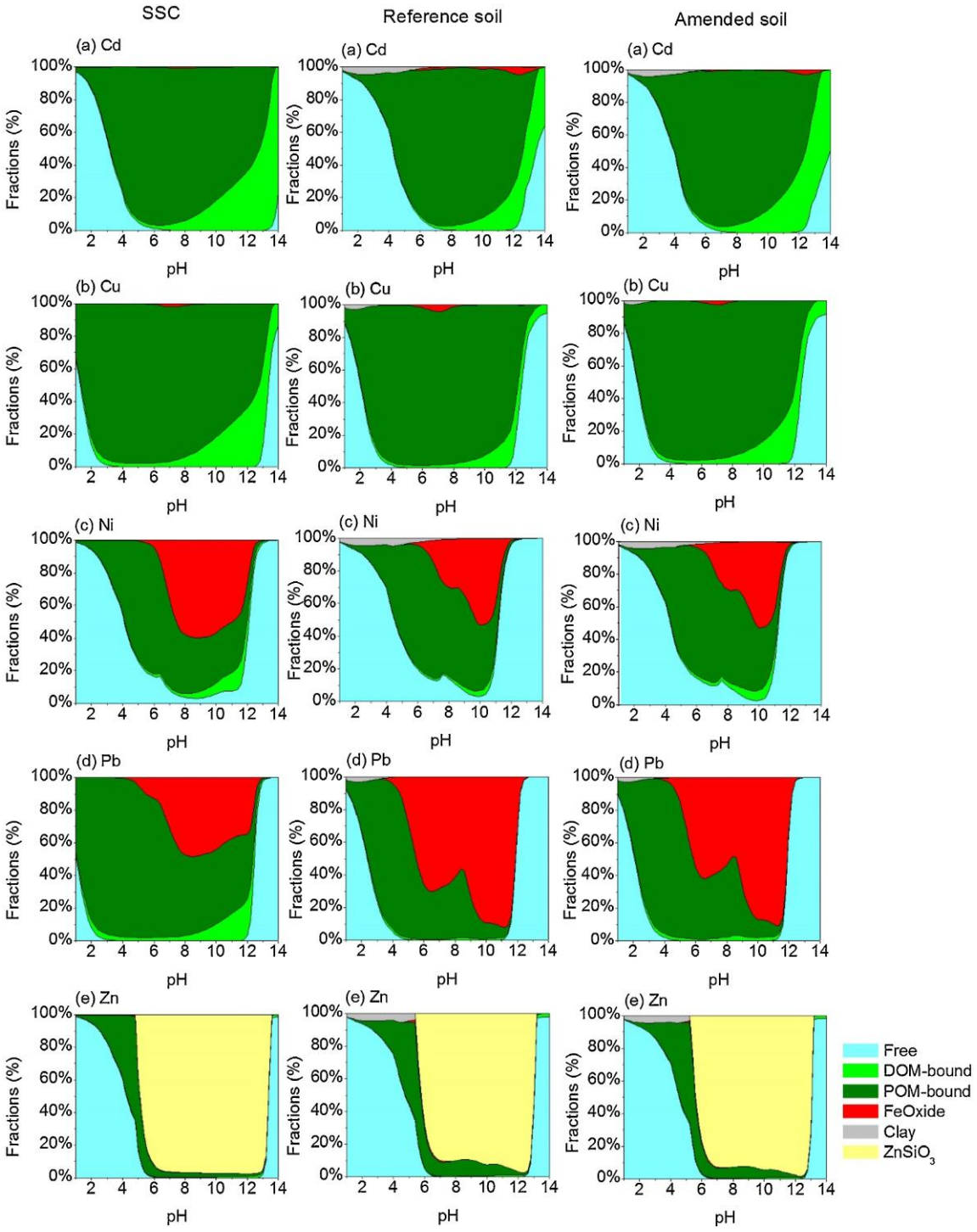

Figure 10. Distribution des métaux lourds dans la phase solide et liquide, adapté de Fang et al. (2016b)

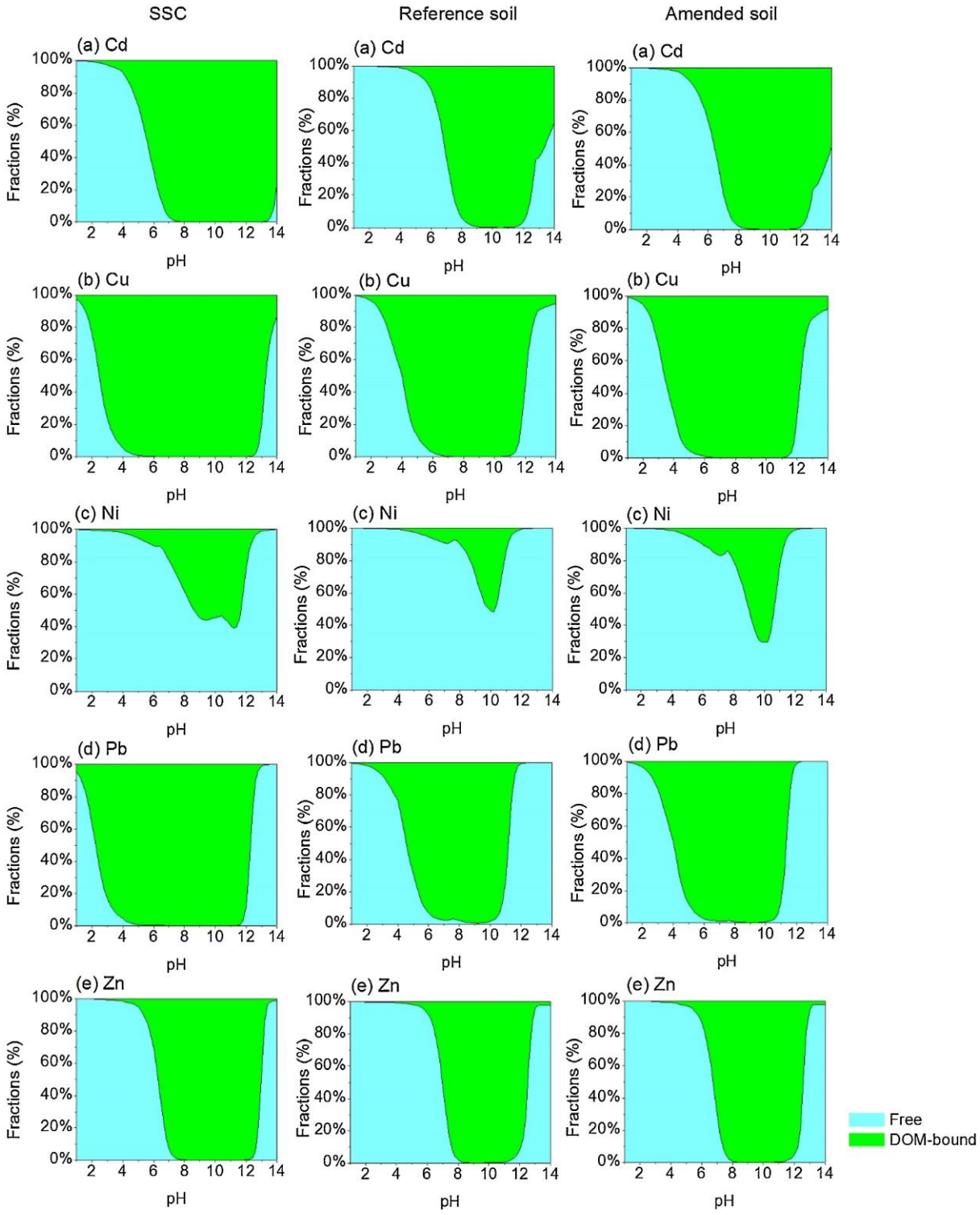

Figure 11. Distribution des métaux dans la phase liquide, adapté de Fang et al. (2016b)

4 Modélisation du devenir des métaux dans les sols

4.1 L'intérêt de modéliser le devenir des métaux en traces dans les sols de jardins potagers

En France, les sols de jardins présentent une contamination en métaux. Prédire le devenir des métaux en traces dans les sols au cours du temps nous permettra donc de mettre en évidence les risques potentiels liés à l'occupation et la gestion du sol. Cela permettra d'établir des recommandations de gestion du sol. Pour l'instant, il n'existe pas encore d'étude en France sur la prédiction du devenir des métaux dans les sols de jardins potagers au cours du temps, en considérant l'ensemble des flux de polluants métalliques.

4.2 Un regard global sur les modèles d'évolution des métaux en traces dans les sols de différents écosystèmes : avantages et inconvénients

Pour modéliser le devenir de la concentration de métaux dans les sols, des modèles de bilan de masse sont largement utilisés pour les sols agricoles (Baveye et al., 1999; Boekhold and Van der Zee, 1991; S. Chen et al., 2007; de Meeûs et al., 2002; de Vries and McLaughlin, 2013a; Doabi et al., 2016; Feng et al., 2018; Hu et al., 2013; Keller et al., 2001; McDowell and Gray, 2022; Moolenaar et al., 1998; Moolenaar and Lexmond, 1998; Mu et al., 2020; Oporto et al., 2012; Peng et al., 2017; Qian et al., 2018; Salmanzadeh et al., 2017; Shi et al., 2019; Six and Smolders, 2014; Sterckeman et al., 2018; Wang et al., 2021a; Yang et al., 2021). En général, les modèles existants de bilan de masse sont plutôt axés sur des processus, et se composent principalement de par les processus d'entrée et sortie des métaux, les processus d'adsorption de métaux dans le sol.

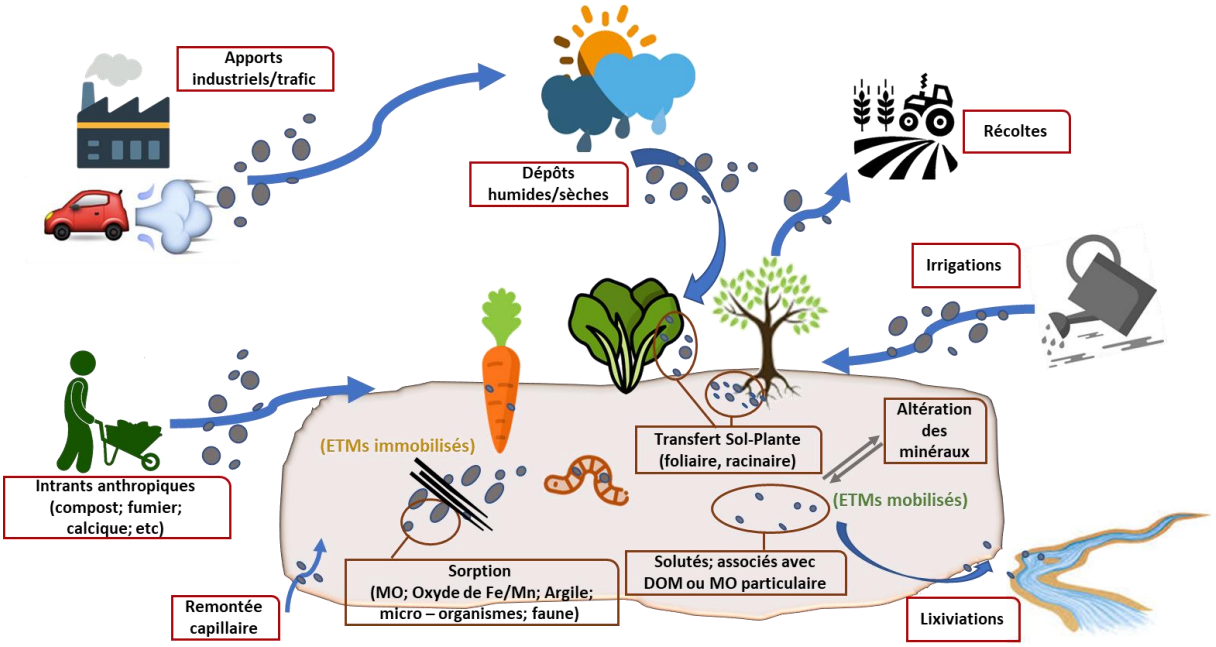

Figure 12. Schéma de la dynamique des polluants métalliques dans l'écosystème des sols de jardins

La Figure 12 est un schéma conceptuel de la dynamique des polluants métalliques dans l'écosystème des sols de jardins. Les métaux peuvent entrer dans le sol sous forme de dépôts atmosphériques ; ils peuvent aussi être apportés au sol par des intrants anthropiques ou par des ruissellements superficiels. Une fois que les métaux sont entrés dans les sols, ils entrent en interaction physico-chimique avec les constituants organiques et minéraux du sol. La partie de métaux qui sont absorbés/adsorbés par les minéraux/matières organiques ou par les micro-organismes, est considérée immobile. Au contraire, la partie des métaux dissous dans la phase aqueuse, ou associés avec la matière organique dissoute ou particulaire, est considérée mobile. Ces métaux peuvent être transférés vers la plante ou être drainés vers les eaux souterraines. Le principe des modèles du bilan de masse pour les sols cultivés est de calculer l'accumulation de métaux dans les sols à l'aide d'une différence entre l'entrée de métaux en surface du sol et la sortie de métaux par la récolte des plantes et la lixiviation. Si le calcul est un cycle par an, la teneur en métaux des sols dans l'année n+1 est égale à la teneur résiduelle de l'année n, plus la variation nette de métaux pendant l'année n+1. Pour simuler la dissolution des métaux, l'équation de Freundlich (Buchter et al., 1989) ou le coefficient de partage solide-soluté (Sauve et al., 2000a; Tack and Verloo, 1995) sont les plus utilisés. La perte de métaux par la lixiviation est souvent estimée en multipliant la concentration de métaux dissouts avec le volume d'eau lessivée au cours du temps (de Vries and McLaughlin, 2013a; Feng et al., 2018, 2018; Qian et al., 2018; Salmanzadeh et al., 2017; Shi et al., 2019; Six and Smolders, 2014; Sterckeman et al.,

2018). Pour le processus de prélèvement de métaux par les plantes, l'analyse directe sur la teneur en métaux dans les parties récoltées de plantes et le coefficient de transfert (*e.g.,* TC : [la teneur en métaux dans la partie de plantes récoltés] / [la teneur totale en métaux dans les sols]) sont les plus utilisés dans les modèles passés de bilan de masse pour calculer la perte des métaux par récolte des plantes.

Néanmoins, la formalisation mathématique de ces modèles n'est pas toujours la même, de même que celle des différents processus de la dynamique des métaux dans le sol (*e.g.,* prélèvement par plantes ; adsorption de métaux ; lixiviation). Les auteurs modifient les composants du modèle en fonction de l'objet d'étude, de son étendue et de la disponibilité des données. Boekhold and Van der Zee (1991) ont ajouté une fonction dans le modèle de bilan de masse pour prendre en compte la distribution spatiale du Cd à l'échelle du champ. Chen et al. (2007) ont développé un modèle qui considère l'interaction entre les processus physiques, chimiques et biologiques pour simuler les flux d'entrées et de sorties des métaux dans les sols agricoles. Les équations de chaque processus sont résolues simultanément pour calculer le bilan de masse. Ce type de modèle est souvent appliqué à l'échelle parcellaire car de nombreuses données sur les caractères du sol sont demandées. Moolenaar et al. (1998) ont couplé l'équation de Freundlich de deux espèces (pour simuler l'adsorption de Cu sur le SOC et DOC) avec le modèle du bilan de masse, afin d'étudier l'effet de la modification de la matière organique sur le devenir du cuivre dans les sols sableux. Récemment, Yang et al. (2021) ont couplé une fonction de transfert de type Freundlich pour l'absorption de Cd par le riz, et un modèle d'acidification du sol (VSD^{+}) dans un modèle du bilan de masse. Les concentrations de Cd simulées pour l'ensemble des sites étudiés étaient très proches des mesures sur le terrain, avec des différences entre -2,37 % et +1,29 %. Les composants du modèle peuvent souvent être modifiés par les auteurs en fonction de l'échelle d'étude et de la disponibilité des données (Keller et al., 2001). Dans les études à l'échelle globale (*e.g.,* régional ; national), les modèles sont souvent simplifiés en raison de contraintes d'accessibilité aux données. Une telle simplification des modèles perd certaines informations des conditions réelles de terrain, mais la simulation de pollution des sols au niveau régional et national est plus susceptible d'attirer l'attention des décideurs (Keller et al., 2001). La taille de l'écosystème des sols de jardin est restreinte par rapport à celle de l'agriculture conventionnelle. La modélisation du devenir des métaux dans les sols de jardins doit être basée à l'échelle parcellaire car on peut y trouver un grand nombre de variétés d'occupations.

4.3 Evaluation des modèles existants pour adapter à l'écosystème du sol de jardins potagers

Afin de simuler le devenir des métaux dans les sols de jardins au cours du temps, il reste à construire un modèle de bilan de masse adapté aux sols de jardins potagers en fonction des pratiques de jardinage.

La difficulté reste la validation du modèle. La validation du modèle de bilan de masse est réalisée à partir de simulations de concentrations des métaux actuelles couplées à des données antérieures (Oporto et al., 2012; Peng et al., 2017), ou à partir de la suivie de terrain (McDowell and Gray, 2022; Qian et al., 2018; Yang et al., 2021). La première nécessite de nombreuses recherches de données, et ceci dépend de l'accessibilité de ces données selon le site d'étude. La deuxième dépend du temps ou d'un grand nombre d'investissements.

Pour l'instant, ces modèles restent encore partiellement validés, particulièrement pour le transfert de métaux du sol à la plante et la lixiviation. Les espèces de métaux en traces absorbées par les plantes sont principalement : (1) ions libres, hydratées ; (2) paires d'ions inorganiques solubles ; (3) chélates organométalliques de faible poids moléculaire (Tack, 2010). Le coefficient de transfert sol-plante (TC) dépend des propriétés du sol (p. ex. pH, potentiel redox, argile, CEC, SOM), de l'espèce de la plante, de la partie de la plante concernée, et aussi de la nature et la quantité de métaux (Antoniadis et al., 2017a). C'est pourquoi estimer le facteur TC est encore un défi aujourd'hui. Yang et al. (2018) ont montré qu'il existe encore une grande incertitude sur les facteurs TC estimés simplement à partir des propriétés du sol. A cause de cela, le flux de métaux du sol à la plante, calculé à partir de la concentration totale de métaux et le coefficient de transfert (TC), présente des incertitudes. La modélisation du flux de métaux vers la plante dans les sols de jardins est difficilement réalisable puisque les types de plantes qui s'y trouvent ne sont pas souvent uniques. Les différentes plantes ont des capacités variables de prélèvement des métaux, en particulier si l'on considère les mécanismes d'absorption foliaire et racinaire (Dala-Paula et al., 2018; Sterckeman and Thomine, 2020).

Une autre grande incertitude est liée au processus de lixiviation. Sterckeman et al. (2018) ont observé que la perte de Cd par lixiviation a été surestimée dans un modèle de bilan de masse, dans lequel la lixiviation est estimée en multipliant la concentration de métaux solutés avec le volume d'eau lessivée au cours du temps. La lixiviation de métaux dépend de la phase soluble des métaux présents dans le sol. Cette phase soluble présente l'ensemble des spéciations chimiques des métaux mobiles (Figure 10 ; Figure 11). Comme présenté précédemment, la dynamique des métaux dans le sol est déterminée par les constituants du sol. Tous les

changements des constituants du sol impactent l'équilibre entre les métaux dans le sol, ainsi que les changements sur les propriétés physiques du sol (Kochem Mallmann et al., 2014). Il faut donc tenir compte de ces facteurs pour construire un modèle applicable aux jardins potagers.

5 Objectifs de la thèse

Dans le contexte du développement de l'agriculture urbaine, afin de maintenir la durabilité des jardins urbains, l'analyse des contaminations métalliques présentes sous l'actuelle occupation et gestion du sol est essentielle. En outre, la prédiction du devenir des métaux dans les sols devrait nous permettre d'identifier des risques potentiels liés aux contaminations métalliques du sol, et donc de mettre en place des pratiques pour mieux préserver les fonctions rendues par les sols de jardins. En conséquence, l'objectif de la thèse est de modéliser les flux des quatre métaux (Cd, Pb, Zn, Cu) dans les sols de jardins potagers, afin de prédire le devenir de la concentration de ces métaux dans les sols, ainsi que la part de métaux absorbée par les plantes, ou celle transférée vers les eaux souterraines en fonction du temps et des pratiques.

6 Questions scientifiques

La démarche scientifique envisagée pour la thèse est développée autour de différents questionnements scientifiques. Ella a donc été divisée en 4 questions scientifiques :

1ère question scientifique :

Peut-on améliorer le modèle du bilan de masse pour l'adapter aux sols de jardins potagers ?

- L'ajout de la dynamique du carbone organique dans le modèle peut-il servir à améliorer la prédiction du flux de métaux vers l'eau et les plantes ?
- L'ajout de la dynamique du pH de sol dans le modèle peut-il servir à améliorer la prédiction du flux de métaux vers l'eau ?
- Est-il possible de coupler un modèle du transfert de l'eau avec un modèle géochimique afin de mieux modéliser la perte des métaux par lixiviation ?

2ème question scientifique :

Est-il possible de prédire les flux et bilans globaux de métaux dans les sols de jardins potagers à l'échelle d'un siècle ?

- En fonction des pratiques de jardinage, quels seront les stocks de métaux des sols de jardins potagers au cours du temps ? Quelle est la contribution des pratiques de jardinage aux stocks de métaux des sols de jardins potagers ? En quelles quantités ?

3ème question scientifique :

Peut-on utiliser des données antérieures pour simuler la teneur actuelle en métaux en traces du sol, puis valider le modèle développé en comparant les résultats mesurés et les résultats simulés ?

4ème question scientifique :

Comment transcrire les résultats de modélisation en recommandations de pratiques de jardinage pour l'avenir ?

- A partir de la modélisation, peut-on obtenir des scénarios optimaux des pratiques de jardinage pour réduire l'exposition aux métaux, en tenant compte à la fois des besoins des sols en nutriments et des enjeux environnementaux (*e.g.*, stockage du carbone, recyclage du phosphate) ?
- Peut-on construire un guide de recommandations des bonnes pratiques de jardinage à utiliser (incluant le phyto-management) pour permettre une gestion durable du jardin et réduire la contamination métallique des sols ?

7 Structure du mémoire

- Dans le chapitre 2, nous présentons le développement d'un modèle de bilan de masse pour les jardins potagers et son application à 104 jardins potagers français. Nous avons ainsi simulé l'évolution des concentrations de Cd, Cu, Pb et Zn dans les sols de 104 jardins potagers pour le prochain siècle selon différent scénarios.
- Dans le chapitre 3, nous avons encore amélioré notre modèle de bilan de masse en y ajoutant un module de simulation du pH du sol. Ce module a été testé sur le sol du Grand Carré du Potager du Roi à Versailles.
- Dans le chapitre 4, nous présentons les résultats de simulations sur les tendances historiques et futures des concentrations en métaux du sol dans le Potager du Roi à Versailles, qui compte plus de 300 ans de pratiques de jardinage depuis sa création en 1683.
- Dans la discussion générale, nous discutons des questions scientifiques que nous avons soulevées, des limites de ce travail et des perspectives de recherches futures.

Chapitre 2 : Évaluation des tendances futures des teneurs en métaux en traces dans les sols des jardins urbains français

This chapter is published in Environmental Science and Pollution Research. The online version contains supplementary material available at: https://doi.org/10.1007/s11356-021-15679-4. In this chapter, we presented all details on our model construction processing, and application of the current model to simulate the evolution of trace metal contents in the soils of 104 French vegetable gardens.

The model is written in C^{++} with RStudio. All codes are available on request.

1 Introduction

In 2050, the United Nations project that world population will have increased to 9.7 billion and food security will be a huge global issue (United Nations, 2019). The available arable land in the EU is declining due to increased forestry and urbanization. To solve these problems, the FAO has predicted that current arable lands would need to improve their productivity by 60%, which would be difficult to attain. We are also currently facing a serious food loss problem. One-third of all produced vegetables is wasted during the transportation and distribution stages (FAO, 2019). Food safety is another global issue. Unsafe food contains harmful bacteria, viruses, or chemical substances, which can cause more than 200 diseases. Annually, an estimated 600 million, almost 1 in 10 people in the world fall ill after eating contaminated food. Up to 420 000 people die every year due to food safety issues (WHO, 2020). In this context, it is not surprising that urban agriculture (UA) has rekindled public interest, as it can potentially provide city people with local fresh vegetables. It is therefore often included in sustainable urban planning as a territorial food system, but is also being considered for its economic, social, environmental, health, educational and cultural services (Bell et al., 2016; Opitz et al., 2016; Pearson et al., 2010; Santo and Palmer, 2016; Smit and Nasr, 1992; Torres et al., 2018; Zasada, 2011).

In France, gardens are classified in two categories: allotment gardens and private gardens. Some areas of these gardens are used for growing vegetables or fruits, which represent the major form of urban agriculture in France (Chalmandrier et al., 2017). We call them vegetable gardens. According to Agreste (2020a), vegetable or fruit growing occupied a total area of 165,890 ha of allotment gardens in 2019 without counting private gardens. In response to strong citizen demand, the number of allotment gardens in Paris increased from less than 5 in 2002 to 119 in 2018 (Torres et al., 2018). Over the past ten years or so, Marseille, the second most populous city in France, has been committed to the development of allotment gardens in the territory, with 52 urban community gardens, 10 others under construction (covering a total of 4.5 hectares) and 12 allotment gardens (covering 24 hectares of Marseille's territory) (France Urbaine, 2018). The number of urban gardens in France is clearly increasing, if we refer to 33 initiatives currently under development by the 22 metropolises on territorial food strategies, as well as innovative projects in the field of urban agriculture (France Urbaine, 2018). The current situation in France suggests that the number of vegetable gardens will increase in the future.

Vegetable gardens provide food for city dwellers. They appear a promising way to respond to various needs. They can serve people as outdoor spaces to relax, while helping to regulate water and local climate. They are often educational sites to teach children about the origin of their food. They provide resources and habitats for the city's biodiversity (Santo and Palmer, 2016). In addition, vegetable gardens are used to store and recycle urban organic waste. However, one of the challenges associated with the development of vegetable gardens is the potential risk to human health from soil contamination, in particular by trace metals such as Cd, Cr, Cu, Hg, Pb or Zn (Alloway, 2004; Augustsson et al., 2018; Kachenko and Singh, 2006; Laidlaw et al., 2018; Pelfrene et al., 2012; Singh and Kumar, 2006). The origin of these trace metals in garden soils is multiple and can be natural or anthropogenic. Natural sources of trace metals are volcanic activity and alteration of source rocks (Alloway, 2013; Liu et al., 2015, 2013; Nriagu, 1989). Anthropogenic sources are generally the result of former land use, air pollution and artificial inputs to gardens (e.g., chemical fertilizers, organic/mineral amendments, irrigation, pesticides) (Alloway, 2013, 2004; Arora et al., 2008; Hernandez et al., 2003; Li et al., 2001).

In the same way as urban soils, garden soils can be contaminated because they are often located on previously urbanized sites and impacted by human activities (Douay et al., 2008a; Douay et al., 2008b; Joimel et al., 2016; Kachenko and Singh, 2006; Li et al., 2013; Wei and Yang, 2010). Because of exposure to urban pollution and the lack of restrictions on gardening practices, soil trace metal concentrations in vegetable gardens have frequently been observed above geochemical background levels (Joimel et al., 2016). There is an obvious link between these concentrations and intensive gardening practices. Recently, Joimel et al. (2016) compared trace metals concentrations in vegetable garden soils with other soils from different eco-systems (forest, meadow, conventional agriculture, orchards and vineyards, vegetable gardens and Technosols). They noted that trace metal content in soil increases with the intensity of anthropic land use. The soils from 104 vegetable gardens located in three French cities (Nancy, Marseille and Nantes) are over-fertilized, rich in phosphorus and contaminated by heavy metal pollution, particularly Cd, Cu, Pb and Zn (Joimel et al., 2016). Trace metals can be toxic to plants and also to humans exposed through direct soil inhalation or ingestion and consumption of contaminated vegetables (EFSA, 2012a). There are some systems of quality control for commercial foods but not for homegrown vegetables (Augustsson et al., 2018). Underground water could also be contaminated, while trace metals are leached from surface soil to deeper layers.

Belon et al. (2012) studied the sources of trace metal inputs into French agricultural soils. Manure, mineral fertilizers, and pesticides are the predominant sources of trace metals. Composts can import more trace metals into soils than chemical fertilizers and digestates and their contributions can reach 10 times that of atmospheric deposition of Pb and Zn (Weissengruber et al., 2018). The loss of metals from the soil is mainly related to leaching and transfer to harvested plant parts which are both dependent on metal speciation, resulting from many physicochemical reactions in soil (Degryse et al., 2009; Sauve et al., 2000a). These reactions vary from one metal to another, but in most cases a major part of the metal load is adsorbed onto the solid phase while the dissolved species represent a minor fraction. The intensity and the kinetics of metal sorption on the solid phase depend on the type and amount of sorbent which can be clay, organic matter and Al-, Fe-, Mn-hydroxides (Loganathan et al., 2012). In general, sorption is influenced by pH, ionic strength and organic or inorganic ligands in solution. Metals are present in solution as free ions and as complexes with inorganic and organic ligands.

To evaluate the impact associated with different gardening environments and practices in the long term, a mass balance model can be used to simulate the evolution of metal content in the garden soils. This model calculates the accumulation of metals from the difference between metal inputs and outputs in the soil layer under consideration, which to date has most often been a ploughed layer (de Vries and McLaughlin, 2013b; Feng et al., 2018; Shi et al., 2019; Six and Smolders, 2014; Sterckeman et al., 2018; Weissengruber et al., 2018). In France, even in Europe, there are no studies on the future evolution of trace metal in garden soils. We therefore based our analysis on a metal mass balance to predict the trend of Cd, Cu, Pb and Zn concentrations in the soils of 104 vegetable gardens from three French regional metropolises (Nancy, Nantes, Marseilles) as a function of time and practices. Different metal input flows, including atmospheric deposition, fertilizers, organic amendments, and crop protection products, were integrated in the model while the main metal output flows simulated were the transfer to harvested plant parts and leaching. The four metal mass balances were simulated according to current practices and according to a scenario based on organic farming practices. Some improvements to the model were made: (1) the RothC model for organic matter dynamics was added to better estimate the solid-solution metal partitioning; (2) a hydrological cycle model was also used to estimate metal loss by leaching. This chapter presents the trends in soil contents of the four metals for the next century.

2 Materials and methods

2.1 Study site

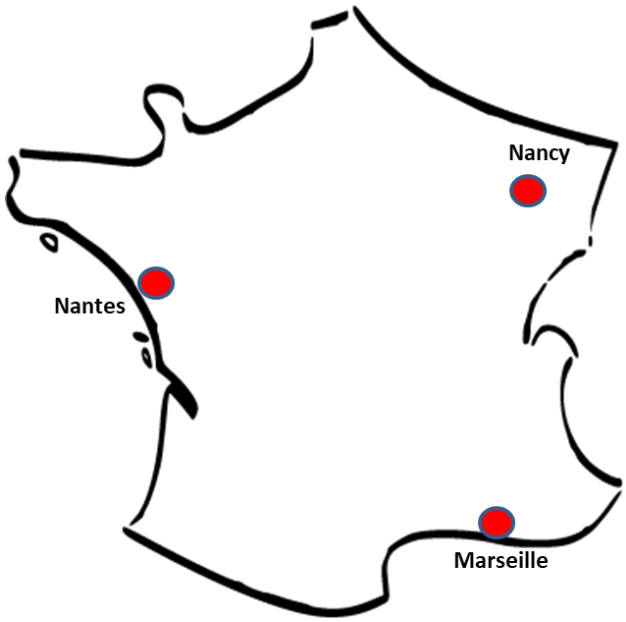

Figure 13. Location of the 104 vegetable gardens in France

The mass balance of four metals (Cd, Cu, Pb, Zn) were simulated for the soils of 104 urban vegetable gardens, located in three French metropolises, respectively Nancy, Nantes, and Marseille (Figure 13). These 104 vegetable gardens were studied as part of the ANR Jassur program (Joimel, 2015; Joimel et al., 2016). The 104 gardens were selected in order to represent French climate and associated cultivation habits: Marseille (south-east of France) for the Mediterranean climate, the metropolis of Nancy (north-east) for the semi-continental climate and Nantes (west) for the oceanic climate. These gardens are located in urban (urban pole or urban unit); in peri-urban (areas belonging to the urban area of a pole) or in rural (predominantly rural space), defined by the INSEE urban area zoning method. The types of land use around the garden are residential, industrial and mixed, as defined by using remote sensing images.

The first 20 cm of surface soils of 104 vegetable gardens were sampled. About 5 kg soil samples were air-dried, disaggregated and sieved at 2 mm. These samples were sent to the Soil Analysis Laboratory (LAS-INRAE, Arras, France) for soil physicochemical properties, presented in Table 2 (Joimel, 2015). In addition, a survey of gardening practices was conducted on these 104 gardens, so the different metal sources could be quantified (see below Section 2.2).

Table 2. Physicochemical properties of the garden soils (surface horizons: 0.2 m; n = 104) in the three metropolises, given as mean (range).

Metropolis	Number of gardens	pH ($CaCl_2$)	CEC (cmolc kg^{-1})	SOC (g kg^{-1})	Clay (%)	Sand (%)	Total metal contents in soils (mg kg^{-1})			
							Cd	Cu	Pb	Zn
Nancy	33	7.09 (6.35-7.49)	17.7 (7.40-34.9)	26.6 (9.79-52.0)	30.6 (11.4-72.6)	29.2 (3.9-60.1)	0.32 (0.11-0.55)	32.3 (19.0-51.2)	85.4 (33.9-397)	145 (65.5-254)
Marseille	36	7.36 (7.15-7.56)	15.6 (7.45-22.4)	37.7 (14.3-59.3)	17.8 (9.80-24.4)	25.0 (8-43.8)	0.90 (0.16-8.86)	86.7 (13.6-473)	151.1 (19.5-566)	354 (43.4-1020)
Nantes	35	6.81 (5.99-7.54)	8.35 (4.47-11.4)	19.8 (10.8-44.1)	10.8 (5.90-18.5)	64.5 (52.2-81.8)	0.18 (0.09-0.46)	49.2 (11.9-321)	56.9 (22.3-314)	92.1 (44.6-272)

2.2 Description and parameterization of the current model

2.2.1 Mass balance model

Gardening practices and soil data from each garden were used, as well as regional average data for climate. The same mean composition values were used for the input from fertilizers, amendments and pesticides, whatever the garden location, as well as the transfer factors for plant uptake. Based on the data from the 104 vegetable gardens, assuming that current gardening practices will be maintained, the concentration evolution of the four trace metals in the cultivated horizon of each garden was simulated for a century, with a monthly time-step.

The long-term changes in soil metal concentrations were calculated by the sum of the residual soil metal concentrations from previous month with the monthly difference between inputs and outputs. Trace metal element concentration at the end of month n in the horizon between 0 and z m is calculated by:

$$C_{i,soil,n} = C_{i,soil,n-1} + \Delta C_{i,soil,n} \quad (1)$$

$$\Delta C_{i,soil,n} = \frac{Q_{i,input,n} - Q_{i,output,n}}{\rho z} \quad (2)$$

where i represents the metal studied, $C_{i,soil,n}$ is the concentration of metal i in the soil at the end of month n (mg (kg DW)$^{-1}$); $C_{i,soil,n-1}$ is that of the previous month $n-1$ (mg (kg DW)$^{-1}$); $\Delta C_{i,soil,n}$ is the variation of metal concentration in month *n* (mg (kg DW)$^{-1}$); ρ is the soil dry density (kg DW m^{-3}); and z is the depth of the soil horizon (m).

$Q_{i,input,n}$ (mg m^{-2}) is obtained by summing metal flows provided by atmospheric deposition ($Q_{i,atm,n}$), NPK fertilizer applications ($Q_{i,fer,n}$), organic amendments ($Q_{i,org,n}$), plant protection product ($Q_{i,phy,n}$), liming ($Q_{i,lim,n}$), irrigation ($Q_{i,irr,n}$) and surface runoff flow ($Q_{i,fluin,n}$):

$$Q_{i,input,n} = Q_{i,atm,n} + Q_{i,fer,n} + Q_{i,org,n} + Q_{i,phy,n} + Q_{i,lim,n} + Q_{i,irr,n} + Q_{i,fluin,n} \quad (3)$$

Liming practice does not appear in the survey results. Consequently, we considered that the soils do not receive metal from calcic amendments. Irrigation sources are reclaimed rainfall, tap water and water points such as wells, fountains, streams, etc., showing very low metal concentrations. Contrarily to the practice in some developing countries as like in China (Shi et

al., 2019), wastewater is rarely used for irrigation in France. Therefore, metal inputs from irrigated water could be reasonably removed from the mass balance equation.

$Q_{i,output,n}$ (mg m^{-2}) is the sum of metal losses through leaching $Q_{i,lea,n}$ (mg m^{-2}), crop offtake $Q_{i,crop,n}$ (mg m^{-2}) and surface runoff ($Q_{i,fluout,n}$).

$$Q_{i,output,n} = Q_{i,lea,n} + Q_{i,crop,n} + Q_{i,fluout,n} \quad (4)$$

The gardens being located in flat terrains, surface runoff could be considered null for both input flow ($Q_{i,fluin,n}$) and output flow ($Q_{i,fluout,n}$).

2.2.2 Atmospheric deposition

Atmospheric deposition of metals is the sum of dry and wet deposition of metals. The monthly metal input due to atmospheric deposition was calculated according to

$$Q_{i,atm,n} = Pre_n \, C_{i,atm,n}/1000 \quad (5)$$

Pre_n being the precipitation in month n (mm = L m^{-2}), and $C_{i,atm,n}$ (µg L^{-1}) being the metal concentration in bulk sampling precipitation.

The monthly precipitation was provided by Meteo-France as normal values for the period 1981-2010. For $C_{i,atm,n}$, we used the EMEP database (https://www.emep.int/). The most recent monthly data of bulk sampler precipitation were collected for three monitoring stations in France, the Revin, Saint-Nazaire-le-Désert and Guipry stations for Nancy, Marseille, and Nantes, respectively (Figure 14). Since Inductively Coupled Plasma Mass Spectrometry (ICP-MS) has been chosen as the reference technique for heavy metal analysis within EMEP, this allows the determination of low metal concentrations in precipitation, which makes atmospheric deposition assessment more accurate. Comparing the measured bulk sampler precipitations of four metals in an urban residential area of Nantes in 2014, the data from the Guipry station can be larger or smaller than the data measured in the city, but within the same order of magnitude (Omrani et al., 2017). Therefore, we assumed that the measured data from these three monitoring stations are representative of bulk metal precipitation in the studied gardens located in peri-urban areas. The metal concentrations in bulk sampling precipitation are presented in the Table 3.

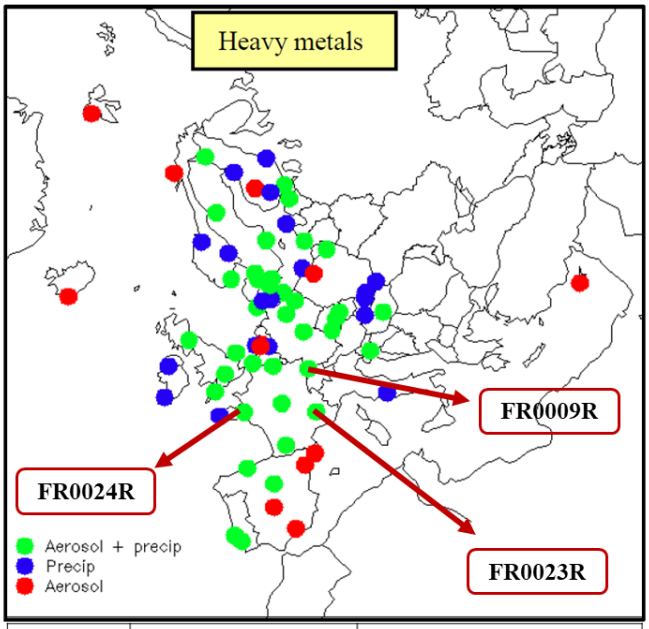

		Localisation	
Code	Station	Latitude	Longtitude
FR0009R	Revin	49 54 0 N	4 38 0 E
FR0013R	Peyrusse Vieille	43 37 0 N	0 11 0 E
FR0023R	Saint-Nazaire-le-Désert	44 34 10 N	5 16 44 E
FR0024R	Guipry	47 49 55 N	1 50 11 W
FR0025R	Verneuil	46 48 53 N	2 36 36 E
FR0090R	Porspoder	48 31 0 N	4 45 0 W

Figure 14. Location of EMEP-CCC monitoring stations in Europe and geographical coordinates of the six stations in France.

Table 3. Metal concentrations in bulk sampling precipitation in the three metropolises (corresponding stations) (monthly average values of the period 2017 to 2019 for Cd and Pb, and monthly values of the period 2014 to 2015 for Cu and Zn)

City	Period	Metal	Monthly value of metal concentration in bulk sampling precipitation (µg L^{-1})											
			Jan.	Feb.	Mar.	Apr.	May	Jun.	Jul.	Aug.	Sep.	Oct.	Nov.	Dec.
Nancy (Revin)	2017-2019	Cd	0.015	0.021	0.034	0.087	0.055	0.054	0.122	0.062	0.002	0.025	0.023	0.025
	2014-2015	Cu	0.500	4.000	4.100	1.860	0.500	4.840	1.280	0.984	1.650	0.500	1.080	2.290
	2014-2015	Pb	0.208	0.192	0.034	1.136	0.298	0.085	1.931	0.586	0.000	0.272	0.107	0.247
	2014-2015	Zn	3.130	1.000	66.110	5.140	3.250	26.290	8.410	19.960	13.660	1.990	8.480	19.840
Marseille (Saint-Nazaire-le-Désert)	2017-2019	Cd	0.029	0.035	0.034	0.099	0.017	0.059	0.013	0.039	0.039	0.164	0.026	0.023
	2014-2015	Cu	1.410	4.660	1.150	2.710	1.850	7.550	5.020	4.960	3.830	0.831	0.884	0.544
	2014-2015	Pb	0.467	0.093	0.181	4.285	0.039	1.553	0.077	0.730	0.438	0.549	0.626	0.116
	2014-2015	Zn	7.610	48.580	5.760	6.060	1.000	9.080	4.170	3.630	8.280	16.930	3.890	14.710
Nantes (Guipry)	2017-2019	Cd	0.005	0.039	0.032	0.058	0.030	0.021	0.013	0.014	0.034	0.019	0.023	0.004
	2014-2015	Cu	0.500	3.520	1.410	0.851	0.500	0.573	0.500	0.500	0.500	0.500	0.618	0.765
	2014-2015	Pb	0.112	0.000	0.399	1.840	0.244	0.547	0.115	0.117	0.107	0.048	1.294	0.027
	2014-2015	Zn	1.090	1.000	9.690	9.070	8.310	14.190	3.700	24.270	7.700	1.000	14.390	9.190

2.2.3 Inputs from NPK-type fertilizers

According to the survey of gardening practices (Joimel, 2015), on average, half of the gardeners in the three cities use fertilizers. Almost 100% of these consumers buy their fertilizers, mainly NPK-type fertilizers.

The inputs of metals from NPK-type fertilizers were calculated by multiplying the fertilizer's metal contents by the application rate:

$$Q_{i,fer,n} = C_{i,fer,n}\, M_{fer,n} \qquad (6)$$

$C_{i,fer,n}$ (mg (kg P_2O_5)$^{-1}$) being the concentration of metals in NPK-type fertilizers, and $M_{fer,n}$ (kg P_2O_5 m^{-2}) being the amount of fertilizer application in the month *n*.

The gardeners followed the manufacturer's recommended dose, which is indicated on the fertilizer package and $M_{fer,n}$ was calculated in the same way. Based on four commercial brands (Solabiol organic fertilizer, NPK Universal, Bochevo, Guano Marin) repeatedly cited in the surveys, an average P_2O_5 dose of 0.0077 kg P_2O_5 m^{-2} per application was estimated (Table 4). Generally, fertilizers are applied twice, during the periods from March to the end of May and from September to the end of October in vegetable gardens. The annual application rate is therefore 0.0154 kg P_2O_5 m^{-2} yr^{-1}, equivalent to 0.0067 kg P m^{-2} yr^{-1}, which is more than three times the average application rate on European field crops (0.002 kg P m^{-2} yr^{-1} on average) (Verbeeck et al., 2020).

Trace element concentrations in mineral P fertilizers used in Europe were studied by Verbeeck et al. (2020). A total of 414 samples of different fertilizers were collected from 25 European countries. The average contents of the four metals in phosphate fertilizers in France (n = 36) are: 8.79 mg Cd kg^{-1}; 24 mg Cu kg^{-1}; 3.8 mg Pb kg^{-1}; 472 mg Zn kg^{-1}. For the NPK type fertilizers (n = 9), the average contents of the four metals are: 2.36 (S.D. = 1.43) mg Cd kg^{-1}; 14.21 (S.D. = 17.40) mg Cu kg^{-1}; 4.88 (S.D. = 7.29) mg Pb kg^{-1}; 195.58 (S.D. = 198.89) mg Zn kg^{-1}. The % P_2O_5 in the samples ranged from 3 to 60%, with a mean of 21%. The mean concentrations of the four metals in NPK fertilizers relative to their P_2O_5 content were estimated as 11 mg Cd (kg P_2O_5)$^{-1}$, 68 mg Cu (kg P_2O_5)$^{-1}$, 23 mg Pb (kg P_2O_5)$^{-1}$, and 931 mg Zn (kg P_2O_5)$^{-1}$.

Table 4. Brands of fertilizer products mentioned several times in the surveys and their recommended doses for kitchen gardens

Product	Type	Dose	Dose in kg P_2O_5 m^{-2}
Solabiol engrais bio	NPK 4-6-10	Zucchini, Peas, Beans: 50 g m^{-2}. Leek, Lettuce, Cabbage, Strawberry, Asparagus, melon: 100 g m^{-2}. Potato, Carrot, Cauliflower, Eggplant, Pepper: 150 g m^{-2}	0.006 ± 0.003
NPK universal	NPK15-15-15	30 g m^{-2}	0.0045
Bochevo	NPK 3-2.5-3	200 to 700 g m^{-2}	0.0113 ± 0.006
Guano Marin	NPK 12-12-2.5	Green vegetables, Raw vegetables: 50 to 100 g m^{-2}	0.009 ± 0.003
Average			0.0077

2.2.4 Inputs from organic amendments

Organic amendments are spread on garden soils as organic fertilizers (bringing nutrients to the soil), as well as amendments (improving the physical and chemical properties of soil). The inputs of metals from organic amendments were calculated by multiplying their metal contents by their application rate:

$$Q_{i,org,n} = C_{i,org,n}\, M_{org,n} \qquad (7)$$

$C_{i,org,n}$ (mg (kg DW)$^{-1}$) being the concentration of metals in organic amendments, and $M_{org,n}$ (kg DW m^{-2}) being the amount of organic amendments application in the month *n*. The characterization of the organic amendments is presented in Table 5, based on two recent references (AROMIS, 2020; Houot et al., 2014; Weissengruber et al., 2018).

Table 5. Characterization of the organic amendments

			Metal content (mg (kg DW)$^{-1}$)				
Amendment	DW (%)	Organic C content in the fresh mass (%)	Cd	Cu	Pb	Zn	References
Cattle manure	20	8	0.3	23	3.2	133	Huout et al. (2014); AROMIS, (2020)
Bio-waste composts	62	29.3	0.4	41	28	150	Weissengruber et al. (2018)
French maximum content for compost spreading	-	-	3	300	180	600	Norme NFU-44051

In all scenarios, two types of organic amendments were used in all gardens: cattle manure and bio-waste composts. According to the garden practice survey, 64 gardeners out of 98 produce

their composts individually (in heaps or in composters), while 8 gardeners do collective composting. Most of the green waste are residues from the plants grown in the garden itself, mixed with the residues of external products (*e.g.*, purchased vegetal food) in individual and collective composting. Therefore, to estimate the input of metals from external sources, we multiplied by factor of 0.5 the input from bio-waste composts. According to the survey, the frequency of application of organic amendments is once a year, or once every two years.

However, it is difficult to quantify the rate of application of organic amendments because gardening practices can be very varied, although generally higher than recommended (Joimel et al., 2016). To meet the nutrient requirements of plants, the French national agency for the environment and energy management (ADEME), advises 3 to 5 kg FW m^{-2} $year^{-1}$ of domestic compost for plants with high requirements, 1 to 3 kg FW m^{-2} $year^{-1}$ for plants with medium needs (ADEME, 2019). Organic amendments are not necessary for vegetables with low needs, such as garlic, broad beans, green beans, turnip, onions, etc. The Canadian national reference recommends 12 to 14 g N m^{-2} yr^{-1} as organic amendments for plants with high needs and 9 to 11 g N m^{-2} yr^{-1} for vegetables with medium needs (Equiterre, 2009). Converting these amounts into kg FW m^{-2} $year^{-1}$, they are close to those recommended by ADEME. In all simulations, 1.8 kg FW m^{-2} $year^{-1}$ of manure and 1.3 kg FW m^{-2} $year^{-1}$ of domestic compost is applied for crops with high requirements and 1.5 kg FW m^{-2} $year^{-1}$ of manure and 0.8 kg FW m^{-2} $year^{-1}$ of domestic compost used for plants with medium requirements. Application of organic amendments occurs at the beginning of the year, depending on the spring/summer crop requirement.

2.2.5 Inputs from crop protection products

According to the survey, about half of the gardeners use crop protection products. Molluscicides (slug pellets), insecticides and fungicides (bactericides) are used extensively, at least once a year. Among these phytosanitary products applied in gardens, fungicides are an important source of Cu. Fungicides based on copper (II) hydroxide, copper (II) oxide, tribasic copper sulphate or copper sulphate are usually employed into garden (Table 6). The presence of other metals in crop protection products can be neglected. The metal input by fungicide was calculated by:

$$Q_{i,phy,n} = C_{i,phy,n}\, M_{phy,n} * 0.9 \qquad (8)$$

$C_{i,phy,n}$ (mg kg^{-1}) being the concentration of i = copper in fungicides, and $M_{phy,n}$ (kg m^{-2}) being the amount of fungicides applied in the month n.

In the simulations of Cu mass balance, different fungicide application rates were used, depending on the crop planted. Most gardeners follow the manufacturer's instructions for applying crop protection products to treat their gardens. Considering that practices in gardens are very similar to those in organic agriculture, the list of crop protection products used in organic agriculture in France, summarized by the Institute of Organic Agriculture and Food (ITAB, 2020), was used as a reference for fungicides application to gardens. We have summarized the per crop maximum dose for the all-cultivated species, according to the authorized uses of each brand name (information available on the E-Phy website: https://ephy.anses.fr/) (Table 6 and Table 7). The Cu dose sprayed on the crop does not immediately and entirely enter the soil, as part of it is intercepted by the foliage. Although after washing by rain or irrigation, there is always some Cu remaining on the surface of the harvested part of plants and consequently removed from Cu mass balance, we have therefore considered that 90% of the sprayed Cu enters the soil.

Table 6 summarizes the maximum annual, or per crop maximum dosages for the treatments of different diseases or pests targeted for different species (ITAB, 2020). In our simulations, only the concerned species, listed in the Table 7, received treatments (Cu fungicide) according to the specified doses.

Table 6. List of applicable fungicides to gardens in France (ITAB, 2020)

Active substance	Brand name	Targeted disease or pest	Species concerned	Application dose per year or per crop	Annually Cu brought or per crop (kg/ha)
Copper (II) hydroxide	NUFARM S.A (552,74 g copper compound /L)	Bacterial Diseases	Cherry tree, Nuts, Lettuce, Olive, Apple tree, Plum, Peach	7 L/ha	2.51
			Tomato, Vine	11 L/ha	3.95
		Mildew(s)	Potato	14 L/ha	5.03
			Tomato	3.5 L/ha	1.26
			Vine	4.3 L/ha	1.54
		Various illnesses*	Apple tree, Peach tree, Cherry tree, Peach tree, Olive tree, Seed carrier, PPAMC, Apple tree	9.8 L/ha	3.53
Copper (II) oxide	NORDOX 75 WG JARDIN (750 g copper compound /kg)	Bacterial Diseases	Tomato	5 kg/ha	3
			Celery, Nuts, Kiwi, Olive, Peach, Plum	6.7 kg/ha	4
			Artichoke, Celery, Chicory, Cabbage, Strawberry, Beans, Lettuce, Onion, Leek	10 kg/ha	6
		Mildew(s)	Artichoke, Cabbage, Leek	10 kg/ha	6
			Tomato	5 kg/ha	3
			Vine	6 kg/ha	3.6
		Various illnesses*	Carrot, Apple, Peach, Olive, Strawberry, Apple, Plum	11.7 kg/ha	7
Tribasic copper sulphate	CUPROXAT JARDIN (345 g copper compound /L)	Bacterial Diseases	Apple tree, Peach tree, Plum tree, Cherry tree	10.4 L/ha	1.44
			Nuts	12 L/ha	1.66
			Onion, Fresh Shelled Beans and Peas, Fresh Shelled Peas, Lettuce	16.8 L/ha	2.32
			Melon, Tomato	21.2 L/ha	2.93
		Mildew(s)	Vineyard, Rose, Indoor plants and balconies, Trees and shrubs, Flower growing and green plants	16 L/ha	2.2
			Onion, Cucumber, Lettuce	16.8 L/ha	2.32
			Vine	19.8 L/ha	2.73

			Melon, Tomato	21.2 L/ha	2.93
		Various illnesses*	Apple tree, Almond tree, Peach tree, Plum tree, Cherry tree, Hazelnut tree, Trees and shrubs, House and balcony plants, Citrus fruits, Chestnut tree	12.2 L/ha	1.68
Copper sulphate	BOUILLIE BORDELAISE EXPRESS; BOUILLIE BORDELAISE MACC 80 JARDINS; BOUILLIE BORDELAISE NOVAJARDIN; BOUILLIE BORDELAISE SUPER 20 K (20% copper /kg)	Bacterial Diseases	Melon	4 kg/ha	0.8
			Peach	6.25 kg/ha	1.25
			Bean	10 kg/ha	2
			Artichoke, Celery, Cabbage, Cabbage, Strawberry, Nuts, Lettuce, Olive, Peach, Apple, Plum	12.5 kg/ha	2.5
			Tomato	20 kg/ha	4
		Mildew(s)	Tomato	6.25 kg/ha	1.25
			Artichoke, Cabbage, Lettuce	12.5 kg/ha	2.5
			Vine	19.25 kg/ha	3.85
			Onion, Leek, Potato	25 kg/ha	5
		Various illnesses*	Carrot, Apple, Peach, Celery, Olive, Strawberry	16.45 kg/ha	3.29

Table 7. Annual Cu brought per crop (kg/ha) by Cu fungicides for the studied species in three cities

Crop	garlic	artichoke	eggplant	beet	chard	broccoli	carrot	celeriac rave	cabbage	pumpkin	cucumber	gherkin	squash	zucchini	shallot	spinach
Application dose	0	4.55	0	0	0	0	5.15	2.95	3.89	0	3.26	0	0	0	0	0

Crop	fennel	broad bean	green bean	lettuce	turnip	onion	pea	chili pepper	leek	bell pepper	potato	radish	black radish	escarole	tomato
Application dose	0	0	2.63	3.54	0	4.55	0	0	5.83	0	5.02	0	0	3.54	3.17

2.2.6 Soil adsorption and leaching

In the mass balance, leaching ($Q_{i,lea,n}$) is one of the two main metal outputs.

$$Q_{i,lea,n} = C_{i,solute,n-1} W_{percly,n} \quad (9)$$

$C_{i,solute,n}$ (mg L^{-1}) is the concentration of metals in soil solution of month n. $W_{percly,n}$ (mm) is the quantity of water percolating through the horizon (between 0 and z m), which was estimated by a hydrologic cycle model.

In this section, a detailed description shows how we simulate the percolating water with a hydrologic cycle adapted from SWAT model and MetHyd model, as well as a paired model of RothC model and Partition coefficient model for simulating the concentration of metals in soil solution.

❖ *Hydrologic cycle model for simulate percolating water in the soil layer*

The hydrologic cycle model is designed with reference to the SWAT model (Neitsch et al., 2011) and MetHyd model (Bonten et al., 2016). It can simulate daily evapotranspiration, soil moisture and percolating water in the soil layer, by using monthly average climatic data and soil texture data.

- Pre-processing climatic data and estimation of soil hydraulic variables

Temperature data for a given day (mean (T, °C), maximum (T_{mx}, °C) and minimum temperature (T_{mn}, °C)) are derived from monthly average temperature data by fitting a spline function. Daily precipitation data are estimated by randomly assigning wet and dry days within a month and then the precipitation amount on a wet day is set to the monthly value divided by the number of wet days. To estimate daily sunshine hours from monthly average sunshine hours, the percentage of sunshine on days with precipitation is set at twice the time of those days without precipitation.

The four soil hydraulic variables in fraction (soil density, soil water content at saturation (θ_s), field capacity (θ_f), wilting point (θ_w) and -1 bar ($\theta_{P=1\text{-bar}}$)) are needed. Soil density is calculated from SOC by the equation of Manrique and Jones. (1991).

$$\rho = 1.66 - 0.318 * \%OC^{1/2} \quad (10)$$

Soil water content at saturation θ_s is derived from a pedo-transfer equation (Wösten et al., 1999). The three other variables can be derived from the Mualem-van Genuchten equation by setting h = 200 (θ_f), h = 1000 (θ_w) and h = 15000 ($\theta_{P=1\text{-bar}}$), respectively (Genuchten, 1980).

$$\theta(h) = 0.01 + \frac{\theta_s - 0.01}{[1 + (ah)^{N_n}]^{(1-N_n)}} \quad (11)$$

where a and N_n are two parameters for the Mualem-van Genuchten equation, which can be derived with non-linear pedo-transfer functions given in Table 5 of Wösten et al. (1999).

- Snow melt and accumulation

If daily temperature T is below T_s (= –2.8ºC), all precipitation falls as snow, otherwise, if T is above T_r (= +1.8ºC) then all precipitation falls as rain. In the case when the daily temperature occurs in the interval between both phases, the amount of snow falling P_s (in mm of water per day) is calculated as (Rekolainen and Posch, 1993):

$$P_s = Pre * \min\left\{max\left\{0, \frac{T_r - T}{T_r - T_s}, 1\right\}\right\} \quad (12)$$

where Pre is the daily precipitation (in mm/day).

Snow falling P_s will be added into the existent snowpack S every day. The amount of melted snowpack Q_s (in mm/day) is simulated by a degree based model (Rekolainen and Posch, 1993):

$$Q_s = \min\left\{max\{0, f_0(T + 0.3), S\}\right\} \quad (13)$$

where f_0 is the melting factor (= 1.95 mm/K/day). The amount of water entering the soil is given as $W = Pre - P_s + Q_s$. If we have irrigation water, we can add it into the percolating water balance.

- Potential evapotranspiration

The potential evapotranspiration is calculated with the Hargreaves method which is used in the SWAT model.

$$PE = 0.0023H(T_{mx} - T_{mn})^{0.5}(T + 17.8)/\lambda \quad (14)$$

Where PE is the daily potential evapotranspiration (mm d^{-1}), H is the daily extra-terrestrial radiation (MJ m^{-2}) calculated with the equation 1:1.2.6 of Neitsch et al. (2011), λ is the latent heat of vaporization (MJ kg^{-1}),

$$H = 37.59\left[1 + 0.0335\cos\left(\frac{2\pi j}{365}\right)\right]\left[\frac{2\pi t}{24}\sin(\varphi)\sin(lat) + \cos(\varphi)\cos(lat)\sin\left(\frac{2\pi t}{24}\right)\right] \quad (15)$$

Where j is the given day, which is from 1 to 365, φ is the solar declination in radians (unit angle), lat is the geographic latitude in radians (unit angle), t_j is the time from noon to sunset (hour), here assuming t = 0 at noon.

$$t_j = \frac{12}{\pi} arccos[-\tan(lat)\tan(\varphi)] \quad (16)$$

If the argument of *arccos* >1, then there is polar night, t_j = 0; if the argument is < -1, there is midnight sun, t_j = 12.

The latent heat of vaporization (MJ kg^{-1}) calculated with the equation of Harrison. (1963),

$$\lambda = 2.501 - 2.361 \times 10^{-3} T \quad (17)$$

- Actual evapotranspiration

The actual evapotranspiration (AE) is estimated as the lowest level of the water supply in soil layer for evapotranspiration (W_s) and the demand as the potential evapotranspiration (Bonten et al., 2016; Cowan, 1965; Molz et al., 1968). If we assume t = 0 at noon, then the day length is equal to $2t_j$.

$$AE = \min\left\{2t_j * W_s, max\{0, PE\}\right\} \quad (18)$$

- Soil moisture and percolating water

Soil moisture is simulated by estimating the soil water content. Soil moisture in each day j is estimated as

$$S_{m,j} = \max\left\{0, S_{m,j-1} + W - AE\right\} \quad (19)$$

We have assumed that all the gardens are located on flat land with no slope, water runoff is neglected in all simulations. If $S_{m,j}$ (mm) is greater than the soil water content at saturation, the excess part percolates, and $S_{m,j+1}$ equals to the soil water content at saturation after the day j; if $S_{m,j}$ (mm) is greater than the soil water content at field capacity, the excess part also percolates, but $S_{m,j+1}$ equals to the soil water content at field capacity after the day j.

The soil moisture is initialized with the water content at field capacity for the beginning of simulations. The climate data of the three cities are presented in Table 8, Table 9, Table 10. The precipitation, potential evapotranspiration and temperature data are monthly normal from the period 1981-2010, retrieved from the public data of Météo France.

Table 8. Monthly climate data of Nancy city. Description of acronyms: Tem = monthly average temperature (℃), Pre = monthly average precipitation (mm), Eva_po = monthly potential evapotranspiration (mm), Pre1mm = number of wet days with precipitation more than 1mm, Sun = monthly average sunshine hours (hr), Tmx = monthly average maximum temperature (℃), Tmn = monthly average minimum temperature (℃)

Site	Month	Tem	Pre	Eva_po	Pre1mm	Sun	Tmx	Tmn
NC	Jan	1.9	65.4	11.1	11.2	55.9	4.6	-0.8
NC	Feb	2.9	55.3	20.1	9.5	79.7	6.4	-0.7
NC	Mar	6.5	59.5	47.1	10.6	129.1	10.9	2
NC	Apr	9.5	49.3	78.5	9.3	173.9	14.8	4.1
NC	May	13.8	67.6	111.1	11	199.1	19.2	8.4
NC	Jun	17.2	69.2	134.2	9.9	220.9	22.6	11.7
NC	Jul	19.4	62.4	140.6	9.6	229.1	25.1	13.7
NC	Aug	18.95	63	114	9.2	213.7	24.7	13.2
NC	Sep	15.2	64.7	67	9.2	162.8	20.3	10.1
NC	Oct	10.95	73.8	32.6	11.4	104.8	15.1	6.8
NC	Nov	5.85	65.9	12.7	11.6	51.7	8.9	2.8
NC	Dec	2.9	79	9.2	11.8	44.3	5.4	0.4

Table 9. Monthly climate data of Marseille city

Site	Month	Tem	Pre	Eva_po	Pre1mm	Sun	Tmx	Tmn
M	Jan	7.15	48	28.8	5.3	145.1	11.4	2.9
M	Feb	8.05	31.4	45.6	4.5	173.7	12.5	3.6
M	Mar	11	30.4	88.8	3.9	238.7	15.8	6.2
M	Apr	13.85	54	123.7	6.1	244.5	18.6	9.1
M	May	18	41.1	168.6	4.5	292.9	22.9	13.1
M	Jun	21.85	24.5	201	3	333.4	27.1	16.6
M	Jul	24.8	9.2	225.1	1.3	369.1	30.2	19.4
M	Aug	24.35	31	189.5	2.7	327.4	29.7	19
M	Sep	20.6	77.1	122.7	4.5	258.6	25.5	15.7
M	Oct	16.65	67.2	71.8	6.1	187.1	20.9	12.4
M	Nov	11.15	55.7	37.1	5.9	152.5	15.1	7.2
M	Dec	7.95	45.8	29.3	5.5	134.9	11.9	4

Table 10. Monthly climate data of Nantes city

Site	Month	Tem	Pre	Eva_po	Pre1mm	Sun	Tmx	Tmn
NT	Jan	6.05	86.4	12.5	12.3	73.2	9	3.1
NT	Feb	6.4	69	24.4	10	97.3	9.9	2.9
NT	Mar	8.9	60.9	54.8	10.1	141.3	13	4.8
NT	Apr	10.95	61.4	84.1	10.1	169.8	15.5	6.4
NT	May	14.55	66.2	120.1	10.9	189	19.2	9.9
NT	Jun	17.65	43.4	142.2	7.2	206.5	22.7	12.6
NT	Jul	19.6	45.9	145.5	6.9	213.7	24.8	14.4
NT	Aug	19.6	44.1	125.6	6.6	226.8	25	14.2
NT	Sep	17	62.9	81.1	8	193.8	22.1	11.9
NT	Oct	13.45	92.8	41.8	11.8	118.2	17.5	9.4
NT	Nov	9.05	89.7	15.2	12.2	85.8	12.4	5.7
NT	Dec	6.35	96.8	10.1	13	76.1	9.3	3.4

Briefly, from average monthly temperature, precipitation, number of wet days and from four soil hydraulic variables (soil water content at saturation, field capacity, wilting point and -1.0 bar), daily percolating water was estimated and used to calculate the monthly percolating water. The monthly average flows of percolating water in the three cities are presented in the Figure 15. We simulated on average 41 (S.D. = 4) mm/year percolating water in the surface soil from 0 to 20 cm for gardens located in Marseille, 188 (S.D. = 23) mm/year for gardens located in Nancy, and 276 (S.D. = 6.5) mm/year for gardens located in Nantes.

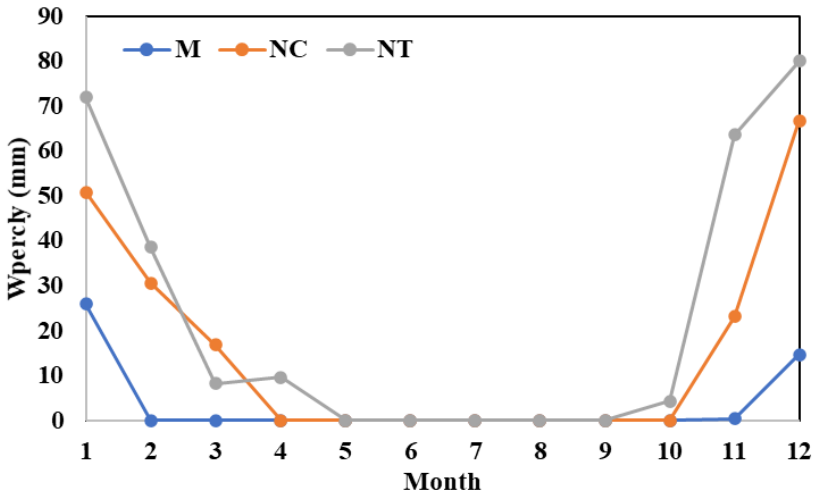

Figure 15. Monthly average percolating water in mm simulated by model for the three cities

Besides, according to the survey on garden practices in these 104 gardens, the sources of irrigation water are harvested rainwater, tap water and water points such as wells, fountains,

streams, etc. The percentage observed varies from one source to another, depending on the city studied (Table 11).

Table 11. Sources of irrigation water of the three cities

Source d'irrigation	Grand Nancy	Marseille	Nantes
d'un puits, forage, fontaine, cours d'eau	**50%**	**17%**	**21%**
de pluie	**57%**	**6%**	**52%**
du robinet	**7%**	**83%**	**70%**
Total	**28**	**36**	**33**

❖ *Calculation of the concentration of the four metals (Cd, Cu, Pb, Zn) in soil solutions*

The solubility of the metal is quantified by a partition coefficient ($K_{d,i}$), which represents the distribution of an element between the solid phase and the aqueous phase. It can be estimated with the physico-chemical properties of soils. We used a typology of models proposed by Sauvé et al. (2000) and additional criteria to pre-select different prediction models for the four metals (meta-data of these models presented in the Annexe, Table A1):

- Models based on the Freundlich isotherm, $K_{d,i}$ or competitive adsorption,
- Models relating the total metal content $\{M\}_{Total}$ (non-labile content) to the metal content in solution $[M]_{Solution}$,
- Soil physic-chemical properties close to those of gardens (e.g., excluding soils with extreme pH or heavily polluted),
- Availability of model parameters.

According to these criteria, we chose 17 models for Cd, 14 models for Cu, 13 models for Pb and 9 models for Zn.

To calculate $C_{i,solute,n}$ for Cd and Cu, we used two models based on competitive adsorption in our simulations:

$$\log\left(1000C_{i,solute,n}\right) = a + b * pH + c * logC_{i,solid,n-1} + d * log\left(OM_{n-1}(\%)\right) \quad (20)$$

$K_{d,i}$, the partition coefficient of metal, between the solid phase of metal and the solute fraction of the metal is applied for Pb and Zn:

$$C_{i,solute,n} = \frac{C_{i,solid,n-1}}{K_{d,i,n}} \quad (21)$$

$C_{i,solid,n-1}$ (mg (kg DW)$^{-1}$) is the fraction of metal i on the soil solid phase, estimated as the total metal content of the soil at the beginning of month n. $K_{d,i,n}$ factor is deduced from the physic-chemical properties of the soil:

$$logK_{d,i,n-1} = a + b\,pH + c\,log\left(OC_{n-1}(\%)\right) + d\,log(CEC) + e\,log\left(DOC_{n-1}(\%)\right) + f\,log\left(OM_{n-1}(\%)\right) \quad (22)$$

All metal partitioning models were pre-selected from the literature (Table 12) and assessed against experimental data (Table 13), i.e., concentrations of the metal in solutions percolating from agricultural soils which are sampled in the field. For each element, the models which simulated metal concentrations closest to those in solutions collected from the field experiments were selected. Apart from metal contents and soil organic carbon, all other soil parameters were considered as being the same all along the simulation time. As soil organic carbon could vary due to gardening practices, the RothC model (Coleman and Jenkinson, 1996) was used to simulate the variation of this parameter. The equations of these models are presented in Table 12.

Table 12. Equations of the tested models

Metal	Code	Equation	n	R^2	Reference
Cd	Cd1	log K_d = -0.738 + 0.529 pH($CaCl_2$)	78	0.72	Christensen, (1989)
	Cd2	log K_d = -0.582 + 0.478 pH(water)	136	0.858	Lee et al. (1996)
	Cd3	log K_{om} = 0.996 + 0.491 pH(water)	136	0.928	Lee et al. (1996)
	Cd4	log K_p = 0.28 + 0.48 pH($CaCl_2$)	18	0.74	Janssen et al. (1997)
	Cd5	log Cd(S) = 3.62 - 0.50 pH(water) + 0.96 log Cd(T) - 0.45 log OM	31	0.934	McBride et al. (1997)
	Cd6	Log K_p = -1.20 + 0.34 pH + 1.26 log CEC	100	0.76	Römkens and Salomons, (1998)
	Cd7	log K_d = -0.65 + 0.48 pH + 0.82 log %OC	751	0.613	Sauve et al. (2000a)
	Cd8	log Cd(S) = 3.42 - 0.47 pH +1.08 log Cd(T) - 0.81 log %OC	751	0.884	Sauve et al. (2000a)
	Cd9	log Cd(S) = 3.23 - 0.54 pH(KNO_3) + 0.77 log Cd(T)	64	0.759	Sauve et al. (2000b)
	Cd10	log K_d = -0.23 + 0.54 pH(KNO_3) - 0.23 log Cd(T)	64	0.763	Sauve et al. (2000b)
	Cd11	log K_d = -1.52 + 0.59 pH(KNO_3) + 0.82 log Cd(T)	40	0.696	Luo et al. (2006)
	Cd12	log K_d = -1.04 + 0.55 pH + 0.70 log %OC	123	0.72	Degryse et al. (2009)
	Cd13	log K_p = 2.35 + 0.114 pH(water)	150		Sheppard, (2011)
	Cd14	log K_d = 2.58 + 0.325 pH(water) - 0.431 log DOC + 0.383 log CEC	74	0.91	Ivezic et al. (2012)
	Cd15	log K_d = -0.94 + 0.54 pH($CaCl_2$) + 0.79 log %OC	151	0.71	Six and Smolders, (2014)
	Cd16	log S = 1.773 + 0.736log C	11		Buchter et al. (1989)

	Cd17	log Cd(S) = 0.742 + 0.741 log Cd(T) - 0.926 log K_f	41	0.71	Lamb et al. (2016)
Cu	Cu1	log S = 2.501 + 0.755log C	11		Buchter et al. (1989)
	Cu2	log K_p = 0.68+ 0.33 pH($CaCl_2$)	20	0.54	Janssen et al. (1997)
	Cu3	log K_p = 0.89+ 0.88 log Feox	20	0.66	Janssen et al. (1997)
	Cu4	log Cu(S) = 0.699 - 0.11 pH(water)+0.86 log Cu(T)	70	0.877	McBride et al. (1997)
	Cu5	log Cu(S) = -0.05 + 0.76 logCu(T)	31	0.862	McBride et al. (1997)
	Cu6	log K_p = 1.22 + 0.10 pH + 0.68 log CEC	100	0.49	Römkens and Salomons, (1998)
	Cu7	log K_d = 1.75 + 0.21 pH + 0.51 log %OC	353	0.419	Sauve et al. (2000a)
	Cu8	log Cu(S) = 1.37 - 0.21 pH + 0.93 log Cu(T) - 0.21 log %OC	353	0.611	Sauve et al. (2000a)
	Cu9	log K_d = 0.70 + 1.04 log Cu(T) - 0.91 log %OC	40	0.728	Luo et al. (2006)
	Cu10	log K_d = 0.45 + 0.34 pH + 0.65 log %OC	128	0.44	Degryse et al. (2009)
	Cu11	log Cu(S) = -2.259- 0.058 pH(water) + 0.594 log Cu(T) + 0.091 log %OM	87	0.732	Unamuno et al. (2009)
	Cu12	log K_d = 2.384 + 0.466 log Cu(T)	87	0.612	Unamuno et al. (2009)
	Cu13	log K_p = 2.47 + 0.0656 pH(water) + 0.00726 %clay	205		Sheppard, (2011)
	Cu14	log K_d = 3.98 - 0.596 log DOC + 0.205 log CEC + 0.483 log %OM	74	0.5	Ivezic et al. (2012)
Pb	Pb1	log K_d = 0.157 + 0.473 pH(water)	156	0.788	Lee et al. (1998)
	Pb2	log K_{om} = 1.436 + 0.508 pH(water)	156	0.933	Lee et al. (1998)
	Pb3	log K_p = 2.06 + 0.35 pH($CaCl_2$)	19	0.65	Janssen et al. (1997)
	Pb4	log K_p = 1.98+ 0.24 pH + 0.40 log Feox	19	0.71	Janssen et al. (1997)
	Pb5	log Pb(S) = - 0.34 - 0.15 pH(water) + 0.61 log OM	31	0.605	McBride et al. (1997)
	Pb6	log K_d = 1.19 + 0.37 pH + 0.44 log Pb(T)	204	0.562	Sauve et al. (2000a)
	Pb7	log Pb(S) = 1.81 - 0.37 pH + 0.56 log Pb(T)	204	0.347	Sauve et al. (2000a)
	Pb8	log K_d = 1.32 + 0.40 pH + 0.50 log %OC	78	0.66	Degryse et al. (2009)
	Pb9	log Pb(S) = 3.219- 0.56 pH(water) + 1.250 log Pb(T) - 2.977 log %clay	87	0.853	Unamuno et al. (2009)
	Pb10	log K_d = -3.22 + 0.51 pH - 0.250 log Pb(T) + 2.98 log %clay	87	0.835	Unamuno et al. (2009)
	Pb11	log K_p = 1.96 + 0.276 pH(water) + 0.294 log %OC	362		Sheppard, (2011)
	Pb12	log K_d = 1.92 + 0.378 pH(water) + 0.561 log %OM	74	0.63	Ivezic et al. (2012)
	Pb13	log S = 3.528 + 1.485log C	11		Buchter et al. (1989)
Zn	Zn1	log S = 1.68 + 0.739 log C	11		Buchter et al. (1989)
	Zn2	log K_p = -0.65 + 0.61 pH($CaCl_2$)	20	0.85	Janssen et al. (1997)
	Zn3	log Zn(S) = 4.44 - 0.71 pH(water) + 0.68 log Zn(T)	31	0.859	McBride et al. (1997)
	Zn4	log K_p = -1.50 + 0.56 pH + 0.68 log CEC	100	0.83	Römkens and Salomons, (1998)
	Zn5	log K_d = -1.34 + 0.60 pH + 0.21 log Zn(T)	298	0.573	Sauve et al. (2000a)
	Zn6	log Zn(S) = 3.68 - 0.55 pH +0.94 log Zn(T) - 0.34 log %OC	212	0.618	Sauve et al. (2000a)
	Zn7	log K_d = -2.46 + 0.62 pH(KNO_3) + 0.69 log Zn(T)	40	0.728	Luo et al. (2006)
	Zn8	log K_d = -1.77 + 0.66 pH + 0.79 log %OC	143	0.72	Degryse et al. (2009)
	Zn9	log K_d = 0.349 + 0.541 pH(water) + 0.209 log %OM	74	0.87	Ivezic et al. (2012)

*The meanings of the symbols in these equations are marked in the list below:

- S: metal on the solid phase of the soil (mg kg^{-1})
- C: metal in solution (mg L^{-1})
- K_d: ratio between the concentration of metal on the solid phase and the concentration of metal in the extract (L kg^{-1})
- K_p: ratio between the concentration of metal on the solid phase and the concentration of metal in the water of the soil pores (L kg^{-1})
- $K_{om} = K_d * \frac{100}{\%OM}$, (ven Oepen et al. 1991) (L kg^{-1})
- Metal(S): concentration of dissolved metal (µg L^{-1})
- Metal(T): total metal concentration (mg kg^{-1})
- % OM: soil organic matter content (mass %)
- OM: teneur en matière organique dans le sol (g kg^{-1})
- % OC: soil organic carbon content (mass %)
- % clay: soil clay content (mass %)
- CEC: cation exchange capacity (cmolc kg^{-1})
- Feox: Fe content (mmol kg^{-1})
- DOC: Dissolved organic carbon (mg L^{-1})

To evaluate these models, we collected three sets of independent experimental data, namely Cd, Cu, Pb and Zn contents in draining water in low contaminated agricultural soils, and the physic-chemical properties of these soils:

(1) A dataset for Cd, Cu and Zn in Swedish cultivated soils, which presents analyses of the physic-chemical properties of the soil at depths of 0-25, 25-55 and 55-85 cm from 4 experimental plots (3 plots under organic fertilization, 1 plot under the conventional system) for 5 years (1998-2002). Soil water samples were collected by porous candles at depths of 20, 50 and 80 cm and analysed for metals, pH and DOC (Bengtsson et al., 2006).

(2) Two sets of data for Cd, Cu, Pb and Zn in French cultivated soils from the SOERE PRO network (https://www6.inrae.fr/valor-pro/SOERE-PRO-Presentation-de-l-observatoire). First, we benefited from the results of three treatments from the QualiAgro trial (Cambier et al., 2019, 2014; Filipovic et al., 2016). These plots were amended with different urban composts to evaluate their long-term effects on soil and drainage water composition, and on their concentrations of metallic contaminants. Soil analyses were carried out in 2011-2013 at different horizons: 0-28, 28-35, 35-50 and 50-90 cm. Each plot was equipped with two lysimeters to collect percolating water at depths of 45 and 100 cm. We also used data from the experimental plots of the PRO'spective project in Colmar. These data were acquired using the same principle as those from the QualiAgro trial. Soil analysis data and metal concentrations in percolates at a depth of 45 cm were taken from 6 plots. A summary of the selected data is presented in Table 13.

Using the above data, we calculated the concentrations of metals in solution and compared them to the measured concentrations. A first statistical analysis was to compare the distribution of the ratios between the simulated values and the observed values.

$$Ratio_{average} = (\sum_{i}^{n} value_{simulated_i}/value_{measured_i})/n$$

We looked for models providing the ratio closest to 1. Considering the potential risks of metals in soil on human health, in case of models with similar performances, we favoured the one that underestimated the solubility of the metal, i.e., underestimating the metal's leaching output.

In addition, to evaluate the predictive capability of the models, *RMSEP* (Root Mean Square Error of Prediction) values were also calculated for each model:

$$RMSEP = \sqrt{\frac{\sum_{i=1}^{n}(value_{measured_i} - value_{simulated_i})^2}{n}}$$

The model has better prediction capacity when the *RMSEP* value is lower.

Finally, Table 14 presents the selected regression models which have been used in our simulations for four metals. In the Figure A1, we presented the comparison between the measured values of metals concentrations in soil solution with the predicted values from the four selected regression models.

Table 13. Chemical characteristics of soils and solutions in percolates. Description of acronyms: Soil pH in water = pH, Organic carbon content = SOC, Clay content = clay, Cation exchange capacity = CEC, Total Cd (Cu, Pb, Zn) content in soil = Cd (Cu, Pb, Zn)_total

Experiment	Plot	Lysimeter	pH	SOC	clay	CEC	Fe_total	Cd_total	Cu_total	Zn_total	Pb_total	DOC	Cd_solution	Cu_solution	Zn_solution	Pb_solution
				%	%	cmol/L	g/kg	mg/kg	mg/kg	mg/kg	mg/kg	mg/L	µg/L	µg/L	µg/L	µg/L
Beng	I (Org)	20	6.00	1.60	4.00	-	-	0.11	9.60	43.00	-	39.00	0.10	49.00	19.00	-
Beng	I (Org)	50	6.30	0.40	2.00	-	-	0.03	7.20	23.00	-	22.00	0.04	20.00	5.00	-
Beng	I (Org)	80	6.60	0.10	2.00	-	-	0.03	7.40	19.00	-	23.00	0.08	25.00	5.00	-
Beng	II (Org)	20	6.20	2.70	4.00	-	-	0.11	9.50	35.00	-	46.00	0.15	31.00	9.00	-
Beng	II (Org)	50	5.20	0.80	7.00	-	-	0.03	10.00	25.00	-	8.00	0.18	30.00	18.00	-
Beng	III (Conv)	20	6.50	5.30	18.00	-	-	0.11	20.00	35.00	-	33.00	0.05	19.00	5.00	-
Beng	III (Conv)	50	4.60	1.50	18.00	-	-	0.03	16.00	30.00	-	13.00	0.05	18.00	5.00	-
Beng	IV (Org)	20	5.70	4.60	20.00	-	-	0.10	21.00	42.00	-	44.00	0.05	27.00	5.00	-
Beng	IV (Org)	50	4.60	2.20	20.00	-	-	0.03	18.00	34.00	-	13.00	0.10	15.00	15.00	-
QualiAgro	SGW	45	7.15	0.48	21.60	9.91	23.60	0.12	11.07	51.20	17.90	14.20	0.21	8.03	10.49	-
QualiAgro	SGW	100	7.58	0.12	29.40	14.25	29.50	0.11	13.53	60.20	18.10	10.60	0.03	2.27	11.53	0.12
QualiAgro	MSW	45	7.63	0.48	19.80	10.03	23.40	0.13	11.37	56.60	19.30	14.20	0.08	6.63	3.94	-
QualiAgro	MSW	100	7.27	0.12	29.60	14.76	33.80	0.12	15.78	66.80	19.60	10.60	0.03	2.15	3.57	0.12
QualiAgro	CTR	45	7.03	0.44	20.50	8.28	23.20	0.11	10.55	48.30	17.70	14.20	0.08	3.70	6.08	-
QualiAgro	CTR	100	7.64	0.17	30.10	10.75	29.70	0.10	12.90	60.10	17.20	10.60	0.03	1.93	3.96	0.12
PROspective	BOUE_N	45	8.49	0.81	23.30	14.30	21.58	0.17	17.50	52.40	17.28	-	0.04	5.88	10.88	0.73
PROspective	DVB_N	45	8.48	0.78	23.30	15.18	22.33	0.18	18.08	53.93	17.98	-	0.06	8.60	12.18	0.71
PROspective	BIO_N	45	8.53	0.84	23.30	14.85	21.80	0.19	17.63	53.23	17.88	-	0.03	5.46	10.49	0.62
PROspective	FUM_N	45	8.53	0.83	23.30	15.03	21.80	0.18	17.63	53.33	17.65	-	0.04	7.41	9.34	0.58
PROspective	FUMC_N	45	8.52	0.83	23.30	15.40	22.58	0.18	18.70	55.45	19.08	-	0.05	8.34	12.58	0.80
PROspective	TEM_N	45	8.50	0.83	23.30	14.90	21.95	0.19	17.80	56.48	18.75	-	0.05	6.98	9.81	0.61

Table 14. Selected regression models for calculating the solution concentration of the four metals. Metal(S): concentration of dissolved metal (µg L^{-1}). Metal(T): total metal concentration (mg kg^{-1}). OM: Organic matter = 1.72OC. OC: organic carbon

Metal	Model equation	Based on data from
Cd	log Cd(S) = 3.62 - 0.50 pH + 0.96 log Cd(T) - 0.45 log OM ($g\ kg^{-1}$)	McBride et al. (1997)
Cu	log Cu(S) = 1.37 - 0.21 pH + 0.93 log Cu(T) – 0.21 log %OC	Sauve et al. (2000a)
Pb	log K_d = 1.32 + 0.40 pH + 0.50 log %OC	Degryse et al. (2009)
Zn	log K_d = 0.349 + 0.541 pH + 0.209 log %OM	Ivezic et al. (2012)

❖ *Simulation of the change of soil organic carbon by the RothC model*

Soil organic carbon is used to calculate the solution concentration of the four metals in all regression models of Table 14. In French urban gardens, soil organic carbon content changes significantly resulting to the use of organic amendments. In order to take into account the impact of this change on soil metal availability, we coupled an organic carbon dynamic model (RothC) to the trace metal mass balance model. It has been validated by different field experiments. There's only 11 variables and parameters requested by RothC model which makes it easy to apply into different conditions. In this subsection, we present the main equation of RothC model. Figure 16 presents a conceptual model of soil carbon dynamics in non-waterlogged arable land as formalized in the RothC model. Figure 17 presents a flow chart on the calculation of a compartment balance after one month of degradation (e.g., DPM).

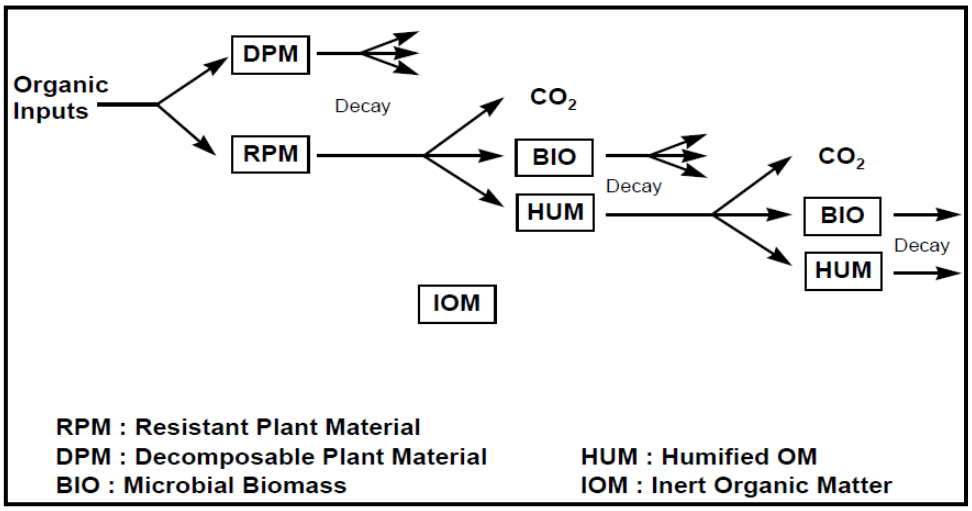

Figure 16. Structure of the RothC model, adapted from Coleman and Jenkinson. (1996)

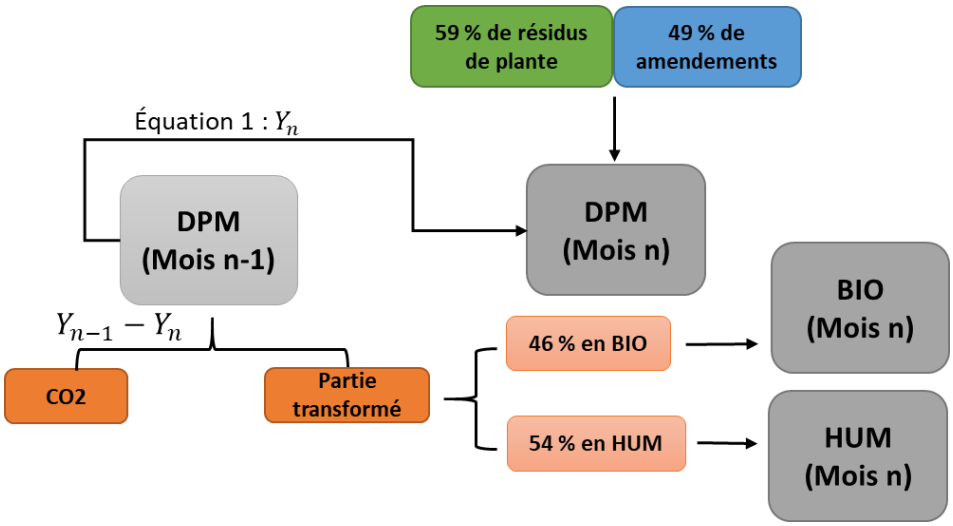

Figure 17. Diagram of the calculation of the balance of DPM compartment after one month of degradation

In the RothC model, soil organic carbon (SOC) is divided into four compartments: DPM (Decomposable Plant Material); RPM (Resistant Plant Material); BIO (Microbial Biomass); HUM (Humified organic Matter); IOM (Inert Organic Matter). Each compartment decomposes according to first order kinetics with its own degradation rate. The IOM compartment is resistant to decomposition. The principle of the RothC model is to take into account the effects of soil type, temperature, moisture content and vegetation cover on the organic carbon (OC) turnover process of each compartment. The degradation of each compartment is therefore calculated by:

$$C_n = C_{n-1} e^{-abckt} \qquad (23)$$

where C_n is the amount of OC in a compartment at the end of month *n* (t C ha^{-1}); C_{n-1} is the initial amount of OC in a compartment at the end of the previous month *n-1* (t C ha-1); *a* is a decay factor of OC as a function of temperature ; *b* is a factor of OC decomposition as a function of moisture; *c* is a factor of OC decomposition as a function of vegetation cover; *k* is a constant of the decomposition rate for each compartment; *t* is the time step (t = 1/12, in years).

The temperature factor a is calculated according to:

$$a = \frac{47.91}{1 + e^{\left(\frac{106{,}06}{Tem + 18.27}\right)}} \qquad (24)$$

where *Tem* is the monthly air temperature (° C).

The moisture factor *b* is calculated from *maxTSMD* (*maximum topsoil moisture deficit*) and *accTSMD* (*accumulated topsoil moisture deficit*):

$$maxTSMD = z(-(20 + 1.3\,clay - 0.01\,clay^2))/0.23 \quad (25)$$

where *z* is the thickness of the soil (m); *clay* is the clay content of the soil (% by mass).

When the ground is bare,

$$maxTSMD.real = maxTSMD/1.8 \quad (26)$$

When the ground is covered by vegetation,

$$maxTSMD.real = maxTSMD \quad (27)$$

$$Defi_n = Pre_n - ETP_n \quad (28)$$

$$accTSMD.pro = accTSMD_{n-1} + Defi_n \quad (29)$$

where ETP_n is the potential evapotranspiration in month *n* (mm); $accTSMD_{n-1}$ is the *accTSMD* value in month *n-1*. To calculate *accTSMD*, we follow a flow chart shown in Figure 18.

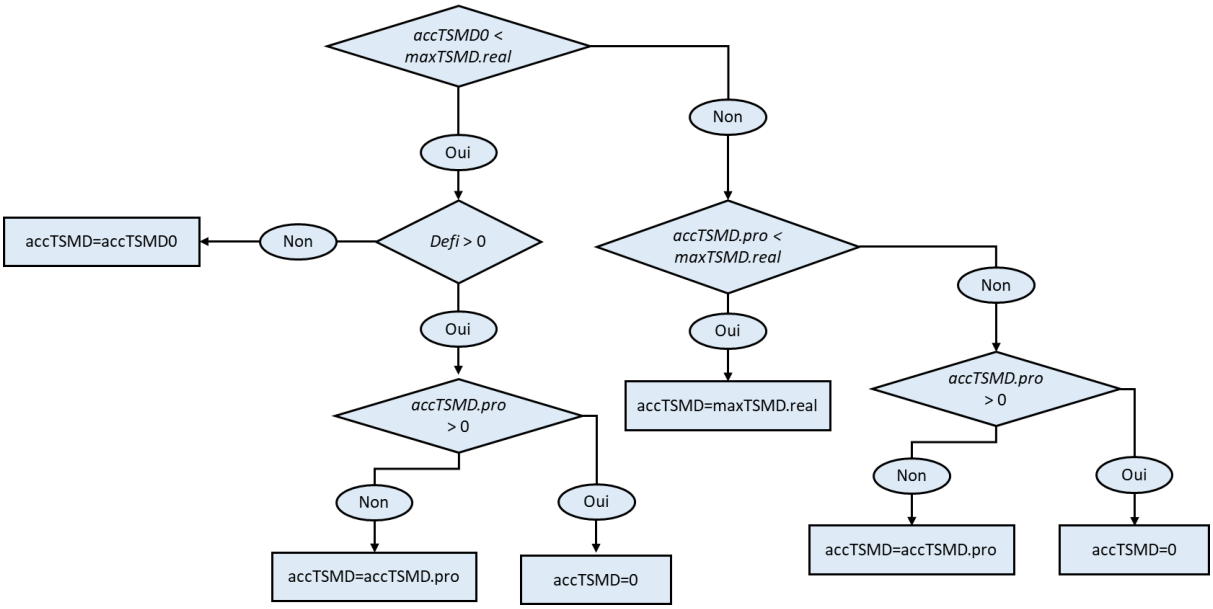

Figure 18. Flow diagram leading to the calculation of accTSMD

With regard to the vegetation cover factor *c*,

If the ground is vegetated, $c = 0.6$;

otherwise, $c = 1$

The decomposition rate constant *k* (S.D.) is given for each organic carbon compartment:

$$kDPM = 10\ ;\ kRPM = 0.3\ ; kBIO = 0.66\ ;\ kHUM = 0.02$$

RatioC (S.D.) is the distribution between the organic carbon lost in gaseous form and that remaining in the soil following decomposition:

$$RatioC = \frac{CO_2}{BIO + HUM} \quad (30)$$

$$RatioC = 1.67\ (1.85 + 1.60\ exp(-0.0786\ clay)) \quad (31)$$

LostCO2 (S.D.), the proportion of loss of mineralized organic carbon to CO_2 is calculated by:

$$LostCO2 = \frac{RatioC}{1 + RatioC} \quad (32)$$

RemainC (S.D.), the proportion of organic carbon reformed as BIO + HUM is calculated by:

$$RemainC = \frac{1}{1 + RatioC} \quad (33)$$

The proportions of organic carbon (% by mass), distributed in the different compartments according to the organic matter added to the soil, are given in Table 15. These are default values.

Table 15. Default allocation parameters in the RothC module, adapted from the RothC model version

Plant input		Amendment input				Degradation		
DPM	RPM	DPM	RPM	BIO	HUM	BIO	HUM	CO2
59%	41%	49%	49%	0%	2%	46%	54%	[calculated]

By default, plant residues are allocated 59% to DPM and 41% to RPM. Organic amendments are distributed 49% in DPM, 49% in RPM, and 2% in HUM. 46% of the total proportion of reworked carbon (*RemainC*) is transformed into BIO, and 54% is transformed into HUM. The default values presented in Table 15 can be redefined according to different exogenous organic matter contributed to the soil (Dechow et al., 2019; Li et al., 2016; Mondini et al., 2017). In our current model, we use the default values for amended organic matters in French urban gardens.

The input organic carbon of the different compartments can be calculated by:

$$accDPM_n = 0.59\ Resi_n + 0.49\ Amend_n \quad (34)$$

$$accRPM_n = 0.41\ Resi_n + 0.49\ Amend_n \quad (35)$$

$$accBIO_n = 0 \quad (36)$$

$$accHUM_n = 0.02\ Amend \quad (37)$$

$$accIOM_n = 0 \quad (38)$$

where $accDPM_n, accRPM_n, accBIO_n, accHUM_n, accIOM_n$ (t C ha^{-1}) represent an increase in OC in each compartment in month n from external sources; $Resi_n$ is the amount of organic carbon contributed by plant residues (t C ha^{-1}); $Amend_n$ is the amount of organic carbon contributed by organic amendments (t C ha^{-1}).

$Resi_n$ is calculated by using the portion of plants remaining above and below the soil, based on the formulas used by Farina et al. (2018):

$$C_{pla,tot} = C_{pla,res} + C_{pla,r} + C_{pla,e} + C_{pla,w} \quad (39)$$

$$C_{pla,res} = \frac{C_{pla,Y}}{HI} - C_{pla,Y} \quad (40)$$

$$C_{pla,r} = C_{pla,Y}/(HI * R:S) \quad (41)$$

$$C_{pla,e} = 0.09\ \frac{C_{pla,Y}}{HI} \quad (42)$$

$$C_{pla,w} = 0.07\ \frac{C_{pla,Y}}{HI} \quad (43)$$

$$C_{pla,Y} = 0.45\ YR_{pla,dw} \quad (44)$$

where total plant-derived organic carbons equal the sum of C inputs from plant residues above ground ($C_{pla,res}$) (kg C m^{-2}), root residues ($C_{pla,r}$) (kg C m^{-2}), root exudates ($C_{pla,e}$) (kg C m^{-2}), weeds ($C_{pla,w}$) (kg C m^{-2}). These different organic carbon input fluxes are calculated from plant yield (*Y*), harvest index (*HI*), root-to-shoot ratio (*R : S*) (0.3 for all crops). We estimate that all dry residues contain 45% organic carbon (Farina et al., 2018; Skjemstad et al., 2004). *Y* (kg FW $m^{-2}\ harvest^{-1}$) is the fresh mass harvested from plants. $R_{pla,dw}$ (S.D.) is the ratio of dry mass to fresh mass in the harvested part of plant, estimated by (1- $W_{pla,dw}$) for vegetables. The values of plant's water content ($W_{pla,dw}$) are given by the ANSES Nutritional Composition of Foods Table (https://ciqual.anses.fr/), presented in Table 16. More details are presented in the following section 2.2.7.

Similarly, $Amend_n$ can be calculated by:

$$Amend_n = M_{org,n} * \%DW * \%OM * 10 \quad (45)$$

where $M_{org,n}$ (kg FW m^{-2}) is the application of amendments to fresh mass; $\%DW$ (S.D.) is the ratio of dry mass to fresh mass in %, estimated to be 38% (21%-56%) for manures, 57% (36%-75%) for green waste composts, and 62% (38%-95%) for domestic waste (biowaste) composts. The organic carbon contents of the total dry mass, $\%OM$ (S.D.), are estimated to be: 41% (37%-44%) for manures; 27% (17%-48%) for green waste composts; 24% (16%-35%) for household waste composts (Houot et al., 2014).

The amounts of organic carbon in the different compartments at the end of the month can be calculated as follows:

$$C_{DPM,n} = C_{DPM,n-1}\, e^{-abck_{DPM}t} + accDPM_n \quad (46)$$

$$C_{RPM,n} = C_{RPM,n-1}\, e^{-abck_{RPM}t} + accRPM_n \quad (47)$$

$$\begin{aligned} C_{BIO,n} = {} & C_{BIO,n-1}\, e^{-abck_{BIO}t} + accBIO_n \\ & + 0{,}46\, RemainC\, [\left(C_{DPM,n-1} - C_{DPM,n-1}\, e^{-abck_{DPM}t}\right) \\ & + \left(C_{RPM,n-1} - C_{RPM,n-1}\, e^{-abck_{RPM}t}\right) \\ & + \left(C_{BIO,n-1} - C_{BIO,n-1}\, e^{-abck_{BIO}t}\right) \\ & + \left(C_{HUM,n-1} - C_{HUM,n-1}\, e^{-abck_{HUM}t}\right)] \end{aligned} \quad (48)$$

$$\begin{aligned} C_{HUM,n} = {} & C_{HUM,0}\, e^{-abck_{HUM}t} + accHUM_n \\ & + 0{,}54\, RemainC\, [\left(C_{DPM,n-1} - C_{DPM,n-1}\, e^{-abck_{DPM}t}\right) \\ & + \left(C_{RPM,n-1} - C_{RPM,n-1}\, e^{-abck_{RPM}t}\right) \\ & + \left(C_{BIO,n-1} - C_{BIO,n-1}\, e^{-abck_{BIO}t}\right) \\ & + \left(C_{HUM,n-1} - C_{HUM,n-1}\, e^{-abck_{HUM}t}\right)] \end{aligned} \quad (49)$$

$$C_{SOC,n} = C_{DPM,n} + C_{RPM,n} + C_{BIO,n} + C_{HUM,n} + C_{IOM,n} \quad (50)$$

where $C_{DPM,n}$, $C_{RPM,n}$, $C_{BIO,n}$ and $C_{HUM,n}$ are the amounts of organic carbon in the different compartments at the end of month n (t C ha^{-1}); $C_{SOC,n}$ is the total organic carbon content at the end of month n (t C ha^{-1}).

The initial organic carbon content in the 5 compartments can be calculated based on the total organic carbon content of the soil: 2% of total carbon for the DPM and BIO compartments, 14% for the RPM compartment; 73% for the HUM compartment; and 9% for the IOM compartment (Zimmermann, 2007).

The RothC model was reconstructed on R for integrating into the mass balance model. In addition, we applied the Benchmarking method to validate the RothC model reconstructed in R by comparing it with an Excel version of RothC and also the software version of RothC (version 26.3). The results of the comparison among these models are presented in the Annexe, section A2.

2.2.7 Crop offtake

Output of metals by harvested plant is estimated by

$$Q_{crop,n} = PUF\ Y\ (1 - W_{pla})\ C_{i,solid,n-1} \quad (51)$$

$$PUF = \frac{C_{i,crop}}{C_{i,solid}} \quad (52)$$

where Y is the vegetable yield per harvest (kg FW m^{-2} $harvest^{-1}$); W_{pla} is the moisture fraction in the harvested plant part (dimensionless).

PUF (plant uptake factor, dimensionless) is calculated as the ratio between the metal concentration in the harvested plant part ($C_{i,crop}$, mg $(kg\ DW)^{-1}$) and that in the soil ($C_{i,solid}$, mg $(kg\ DW)^{-1}$). The *PUF* values were calculated for each vegetable harvested part with the BAPPET database (ADEME, 2012). This database has been built up from documentary sources (e.g., scientific articles and reports). To construct the *PUF* values of metals to the harvested part of the vegetables, we selected the data according to the following criteria: (1) vegetables planted in urban ecosystems; (2) the metal concentrations measured after washing; (3) metal concentrations in the dry matter of the harvested part; (4) soil metal concentrations measured after total and nearly total (*e.g.*, aqua regia) extraction. For each plant species, a mean *PUF* value was calculated by excluding the 5% extreme values (

Table 17).

Vegetable yields of French professional vegetable growers are reported by the Ministry of Agriculture, Agrifood, and Forestry (Agreste, 2020b). From its annual agriculture statistics, we obtained the yields per harvest of each crop in three regions: Grand Est region for Nancy, Pays de la Loire region for Nantes and Provence-Alpes-Côte d'Azur region for Marseille (Table 16).

Marie. (2019) reported an observed vegetable yield of 2 kg per m^2 in vegetable gardens less than 60 m^2, and of 1.2 kg per m^2 for those more than 60 m^2 in three French cities (Rennes, Caen and Alençon). Pourias et al. (2015) reported an average vegetable yield of 1.2 kg per m^2 in 14 allotment and shared gardens with an average surface area of 158 m^2, located in Parisian region. Besides, in the study of McDougall et al., (2019), small urban plots with a median area of 10.8 m^2 result in high yields than professional farms in the adjacent cities of Sydney and Wollongong, New South Wales, Australia. These studies show that smaller vegetable garden leads to higher plant density, thus results to higher yields. Regarding to 104 gardens of this study, the average size of a garden is variable, from small plots (100 m^2), medium-sized plots (close to 200 m^2) to large plots (300 to 500 m^2). Moreover, the average regrouped yields of the studied vegetables from Table 16 range between 3.05 and 3.31 kg per m^2 in three studied cities. Yields from vegetable gardens were estimated at 50% of those of professional growers.

Table 16. Average yields of vegetables per harvest in the Grand Est, Pays de la Loire and Provence-Alpes-Côte d'Azur regions, from professional growers, for the period 2000-2018 (Agreste database). *lack of data for artichoke in Grand Est, its value has been repla

		Yield (kg FW m^{-2} $harvest^{-1}$)		
Crop	**Water content**	**Grand Est**	**Pays de la Loire**	**Provence-Alpes-Côte d'Azur**
garlic	0.9	0.80	0.97	1.07
artichoke	0.849	0.51*	0.51	0.51
eggplant	0.929	4.75	5.49	4.19
beet	0.867	3.29	2.27	2.22
chard	0.954	2.62	3.15	4.53
broccoli	0.889	0.90	0.64	1.62
carrot	0.896	2.57	3.14	3.74
celeriac rave	0.886	4.37	3.15	2.19
cabbage	0.918	6.75	2.87	2.11
pumpkin	0.916	3.86	2.16	4.72
cucumber	0.96	17.00	19.44	10.16
gherkin	0.9	2.37	1.39	0.83
squash	0.923	3.99	0.91	3.33
zucchini	0.947	3.50	2.88	6.83
shallot	0.796	1.52	2.22	1.64
spinach	0.916	1.40	1.39	1.93
fennel	0.92	2.75*	2.75*	2.75*
broad bean	0.768	0.70	0.62	0.86
green bean	0.904	0.86	0.61	1.02
lettuce	0.953	2.09	2.10	3.57
turnip	0.919	1.77	2.84	2.08
onion	0.896	4.52	2.45	2.07
pea	0.792	0.62	0.64	0.57

chilli pepper	0.879	5.76	5.45	3.70
leek	0.876	2.59	3.55	3.18
bell pepper	0.921	5.76	5.45	3.70
potato	0.79	4.68	2.82	2.94
radish	0.959	1.31	1.52	1.53
black radish	0.936	3.29	2.27	2.22
escarole	0.934	2.75	3.32	3.32
tomato	0.941	9.98	14.41	9.31

Table 17. Plant uptake factors (PUF) of Cd, Cu, Pb and Zn for the harvested part of the vegetables, from the BAPPET database. n values are not provided for certain crops, because their PUF values were inferred from similar species

Crop	Cd		Cu		Pb		Zn	
	PUF	n	PUF	n	PUF	n	PUF	n
Garlic	0.7716		0.1407		0.0278		0.2802	
Artichoke	0.2355		0.2270		0.0095	3	0.1107	2
Eggplant	0.7183	6	0.3663	5	0.3846	13	0.4319	4
Beet	0.1225	12	0.5140	1	0.0045	15	0.6445	2
Chard	1.0921	9	0.1466	7	0.1169	12	0.2137	9
Broccoli	0.6897	5	0.8235	1	0.1417	3	0.5240	
Carrot	0.2546	166	0.2071	64	0.0072	163	0.1709	92
Celeriac rave	0.9074	4	0.3082	6	0.0653	10	0.2655	6
Cabbage	0.3436	36	0.0893	25	0.0232	36	0.2043	31
Pumpkin	0.0675		0.1229		0.0352		0.0223	
Cucumber	0.0675	5	0.1229	6	0.0352	7	0.0223	5
Gherkin	0.0675		0.1229		0.0352		0.0223	
Squash	0.6550	1	0.1229		0.0076	1	0.2857	1
Zucchini	0.6550	1	0.1229		0.0076	1	0.2857	1
Shallot	0.4672		0.1400		0.0148		0.1936	
Spinach	1.1833	44	0.3657	46	0.0189	46	1.2366	40
Fennel	0.4456		0.6341		0.0531		0.6127	
Broad bean	0.1249	3	0.3191	1	0.0113	3	0.1929	2
Green bean	0.0257	111	0.1523	35	0.0022	125	0.1911	57
Lettuce	1.3984	242	0.2270	97	0.0161	192	0.3497	128
Turnip	1.6221	1	0.2430		0.0072	1	0.1327	1
Onion	0.7716	20	0.1407	19	0.0278	17	0.2802	18
Pea	0.0909	18	0.2671	18	0.0092	18	0.3912	18
Chili pepper	0.2693		0.5102		0.7336		0.5910	
Leek	0.1628	80	0.1392	9	0.0019	81	0.1070	34
Bell pepper	0.2693	5	0.5102	1	0.7336	1	0.5910	1
Potato	0.0912	164	0.2886	43	0.0014	162	0.0736	101
Radish	0.3529	159	0.2430	40	0.0148	170	0.2522	83
Black radish	0.3529		0.2430		0.0148		0.2522	
Escarole	1.3984		0.2270		0.0161		0.3497	
Tomato	0.1695	113	0.2873	39	0.0034	106	0.1176	64

The crop rotation was also considered in our simulations. According to the surveys in the 104 gardens, more than 95% of gardeners rotate vegetable plantings for their gardens. The main reason for crop rotation, according to the respondents, is to let the soil rest to preserve soil fertility. Therefore, we took a classic example of rotation to build a 100-year scenario. We based on the rotation proposed by the Société Nationale d'Horticulture de France (SNHF) (https://www.jardiner-autrement.fr/la-rotation-des-cultures-au-potager/) and chose the following succession type: leaf/fruit/root.

The 100-year successions were based on the frequency of planting during the autumn/winter and spring/summer period obtained from the survey of Joimel. (2015) (Figure 19), For a given city, we first considered the spring crops which are the most numerous in all gardens.

The frequency of each crop (F_i^{SC}) across all gardens of a given metropolis was determined by:

$$F_i^{SC} = \frac{n_i}{N^{SC}}$$

$$N^{SC} = \sum_{i=1}^{I} n_i$$

n_i is the number of gardens in which a spring crop *i* is cultivated. It was then considered that the frequency of growing a crop in a bed in a garden was the same as the frequency of this crop in all the gardens of the metropolis. This led to the establishment of an identical and average succession per bed in each garden. F_i^{SC} made it possible to distribute the spring crops over 100 years, in the most homogeneous way possible, by trying to respect the leaf/fruit/root succession. The number of each crop (c_i^{SC}) over 100 years is

$$c_i^{SC} = 100 F_i^{SC}$$

Depending on the spring crop duration, an autumn crop could be planted after the spring crop if it is allowed. The installation of an autumn crop has been identified and counted (C^{AC}). The frequency of each autumn crop (F_j^{AC}) was determined for all gardens:

$$F_j^{AC} = \frac{n_j}{N^{AC}}$$

$$N^{AC} = \sum_{j=1}^{J} n_j$$

The number of occurrences of each autumn crop for the century was determined:

$$c_i^{AC} = C^{AC} F_i^{AC}$$

Then the autumn crops were placed after the spring crops, considering the practice. Crops present in less than 10% of the gardens were eliminated, as well as those that are not grown in beds (herbs). Some nearby crops have been grouped together, such as pumpkin. A detailed crop rotation for each of the three cities is given in the Table 18.

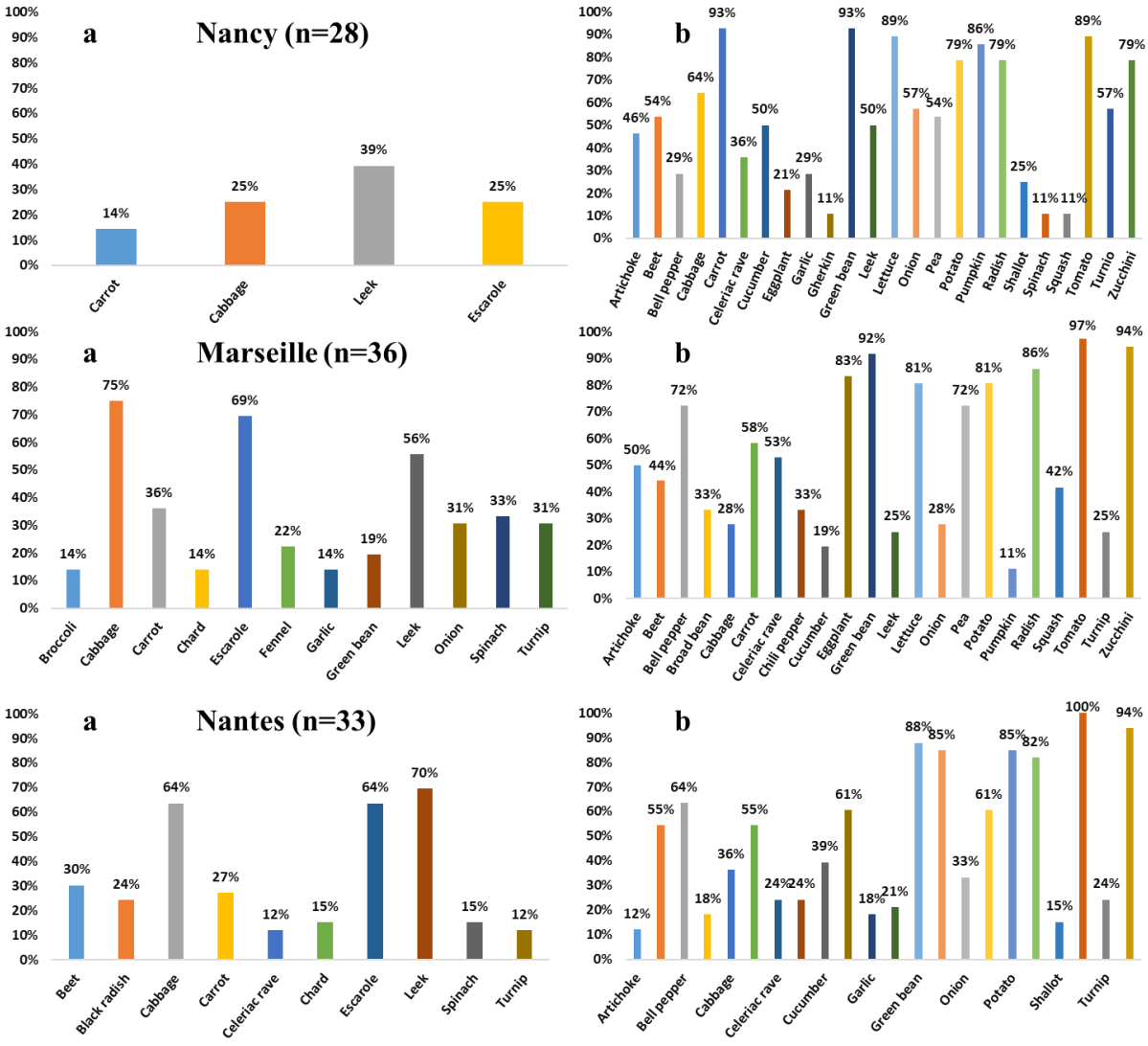

Figure 19. Vegetables most planted in autumn/winter (a) and vegetables planted in spring and summer (b) for the three cities: Marseille, Nancy and Nantes; n is the number of surveys carried out (Joimel, 2015)

Table 18. Succession of crops for the vegetable gardens of Nancy, Marseille and Nantes

City	Nancy		Marseille		Nantes	
Year	Spring/summer	Autumn/winter	Spring/summer	Autumn/winter	Spring/summer	Autumn/winter
1	spinach	carrot	cabbage		broad bean	turnip
2	squash		onion		gherkin	
3	eggplant		turnip	escarole	turnip	escarole
4	garlic		artichoke		onion	
5	artichoke		artichoke		carrot	
6	artichoke		artichoke		pea	spinach
7	artichoke		leek		eggplant	
8	pea	leek	cucumber		lettuce	cabbage
9	cucumber		carrot	escarole	potato	
10	leek		squash		tomato	
11	carrot	cabbage	tomato		radish	carrot
12	green bean	escarole	green bean	spinach	shallot	
13	tomato		zucchini		bell pepper	
14	Lettuce	leek	radish	onion	celeriac rave	
15	pumpkin		eggplant		garlic	
16	zucchini		potato		carrot	
17	potato		lettuce	garlic	lettuce	leek
18	radish	cabbage	pea	carrot	zucchini	
19	cabbage		beet		green bean	black radish
20	turnip	leek	bell pepper		tomato	
21	onion		celeriac rave		potato	
22	beet		tomato		eggplant	
23	bell pepper		green bean	turnip	beet	
24	celeriac rave		zucchini		cabbage	
25	green bean	escarole	radish	fennel	cucumber	
26	carrot	leek	eggplant		bell pepper	
27	tomato		potato		lettuce	leek
28	Lettuce	carrot	lettuce	cabbage	zucchini	
29	pumpkin		carrot	pea	green bean	cabbage
30	radish	cabbage	broad bean	chard	tomato	
31	leek		pea	escarole	potato	
32	cabbage		bell pepper		radish	celeriac rave
33	zucchini		green bean	leek	beet	
34	potato		tomato		chili pepper	
35	shallot		beet		cucumber	
36	carrot	leek	zucchini		celeriac rave	
37	green bean	escarole	chili pepper		pea	chard
38	tomato		radish	cabbage	zucchini	
39	Lettuce	cabbage	eggplant		green bean	cabbage
40	pumpkin		potato		tomato	
41	turnip	carrot	lettuce	cabbage	potato	

42	onion		celeriac rave		radish	carrot
43	beet		tomato		bell pepper	
44	pea	escarole	carrot	escarole	carrot	
45	cucumber		green bean	spinach	onion	
46	zucchini		zucchini		cucumber	
47	potato		pea	leek	lettuce	leek
48	radish	leek	bell pepper		zucchini	
49	celeriac rave		squash		green bean	cabbage
50	gherkin		radish	onion	tomato	
51	carrot	escarole	eggplant		potato	
52	green bean	cabbage	potato		eggplant	
53	tomato		lettuce	pea	pea	spinach
54	Lettuce	carrot	broad bean	broccoli	cabbage	
55	pumpkin		tomato		gherkin	
56	cabbage		green bean	leek	carrot	
57	turnip	leek	beet		lettuce	leek
58	onion		zucchini		zucchini	
59	beet		celeriac rave		green bean	black radish
60	pea	cabbage	pea	carrot	tomato	
61	cucumber		bell pepper		potato	
62	leek		radish	fennel	radish	carrot
63	carrot	escarole	eggplant		eggplant	
64	green bean	leek	potato		beet	
65	tomato		lettuce	cabbage	garlic	
66	Lettuce	cabbage	tomato		turnip	escarole
67	pumpkin		green bean	turnip	lettuce	leek
68	zucchini		zucchini		zucchini	
69	potato		carrot	pea	green bean	cabbage
70	radish	leek	chili pepper		tomato	
71	cabbage		pumpkin		radish	beet
72	celeriac rave		pea	spinach	bell pepper	
73	pea	leek	broad bean	carrot	pea	cabbage
74	cucumber		squash		carrot	
75	leek		bell pepper		cucumber	
76	carrot	escarole	cucumber		eggplant	
77	green bean	leek	tomato		lettuce	escarole
78	tomato		green bean	leek	zucchini	
79	Lettuce	cabbage	zucchini		green bean	escarole
80	pumpkin		radish	onion	tomato	
81	zucchini		eggplant		potato	
82	potato		potato		radish	beet
83	radish	escarole	lettuce	cabbage	bell pepper	
84	cabbage		celeriac rave		beet	
85	turnip	leek	green bean	turnip	cabbage	
86	onion		leek		onion	

87	beet		beet		lettuce	leek
88	eggplant		tomato		zucchini	
89	carrot	cabbage	carrot	escarole	green bean	escarole
90	green bean	leek	zucchini		tomato	
91	tomato		pea	leek	potato	
92	lettuce	escarole	bell pepper		radish	beet
93	pumpkin		cabbage		bell pepper	
94	zucchini		onion		pea	escarole
95	potato		turnip	escarole	beet	
96	radish	leek	chili pepper		chili pepper	
97	garlic		radish	cabbage	artichoke	
98	bell pepper		eggplant		artichoke	
99	shallot		potato		artichoke	
100	spinach	carrot	lettuce	cabbage	carrot	

2.2.8 Simulation scenarios

The mass balance of Cd, Cu, Pb and Zn in topsoil was simulated in each garden for the next 100 years from 2012, distinguishing the three metropolises, according to two scenarios:

Current practice scenario (CP): The initial input sources and the gardening practices as presented above do not change in the future. In this scenario, to assess the effect of gardening practices, the 104 gardens were classified into 8 classes, depending on the type and number of agricultural inputs (Table 19).

Table 19. Classification of the 104 gardens into 8 classes, according to the type and number of agricultural inputs

Garden class	Number of gardens (*n*)	Type and combination of agricultural inputs
GC1	6	No agricultural input
GC2	2	Fertilizers only
GC3	17	Organic amendments only
GC4	4	Crop protection products only
GC5	16	Fertilizers and organic amendments
GC6	4	Fertilizers and crop protection products
GC7	15	Organic amendments and crop protection products
GC8	40	Fertilizers, organic amendments, and crop protection products

Organic agriculture scenario (OA): No NPK fertilizers are applied to soil. Only organic amendments are applied for fertilization and crop protection products (Cu) could be used. The

application doses of amendments are the same as the CP scenario in which these amendments meet the requirements of different crops for nutrients.

2.3 Sensitivity analysis and uncertainty assessment

A global sensitivity analysis was performed using R software to evaluate the impact of the main parameters and input variables on the prediction of the absolute variation of metals in the soil after 100 years (VC_i).

$$VC_i = C_{i,soil,t=100} - C_{i,soil,t=0} \quad (53)$$

This global sensitivity analysis was performed using the SRC (Standardized Regression Coefficients) method (Faivre et al., 2013). This method is usually used to identify the effect of each independent variable on the dependent variable (VC_i) through a multiple linear regression. The higher the value of the standardized regression coefficient of a variable, the stronger its effect on the model output.

The variation range of each independent variable is presented in Table 20. Each of them was randomly sampled using a uniform distribution in the variation range, to create a sample of 20 000 simulation cases. VC_i was calculated for each of these 20 000 cases and regressed with the corresponding independent variables, to calculate the SRCs used to rank the variables.

Table 20. Parameters and variables tested for model sensitivity analysis

Parameter	Description	Unit	Min	Max	Reference
Soil parameters					
ρ	Density	kg m^{-3}	1000	1500	Posch et al. (2005)
pH	Soil pH in 0.01 M $CaCl_2$		5.5	8	Joimel, (2015)
CEC	Cation exchange capacity	cmolc kg^{-1}	4	40	Joimel, (2015)
SOC	Organic carbon content	g kg^{-1}	5	60	Joimel, (2015)
clay	Clay content	%	5	80	Joimel, (2015)
sand	Sand content	%	3	Min (100-clay, 85)	Joimel, (2015)
Cd_init	Initial Cd content	mg kg^{-1}	0.05	10	Joimel, (2015))
Cu_init	Initial Cu content	mg kg^{-1}	10	500	Joimel, (2015)
Pb_init	Initial Pb content	mg kg^{-1}	15	600	Joimel, (2015)
Zn_init	Initial Zn content	mg kg^{-1}	40	1100	Joimel, (2015)
Parameters related to applied practices					
Cult_start	Start of cultivation	month	3	4	
Cult_end	End of cultivation	month	10	11	

Catm	Metal content in bulk sampling precipitation				
	Cd	ug L^{-1}	0.02	0.2	EMEP
	Cu	ug L^{-1}	0.25	10	EMEP
	Pb	ug L^{-1}	0.15	3	EMEP
	Zn	ug L^{-1}	2.5	25	EMEP
Cfer	Metal content in chemical fertilizer				
	Cd	mg P_2O_5 kg^{-1}	3	25	Verbeeck et al. (2020)
	Cu	mg P_2O_5 kg^{-1}	10	250	Verbeeck et al. (2020)
	Pb	mg P_2O_5 kg^{-1}	10	116	Verbeeck et al. (2020)
	Zn	mg P_2O_5 kg^{-1}	135	3000	Verbeeck et al. (2020)
Mfer	Quantity of chemical fertilizer application	kg P_2O_5 m^{-2}	0	0.045	Estimated dosage based on the more frequent products mentioned in the survey of Joimel, (2015)
Cmanu	Metal content in manure				
	Cd	mg (kg DW)$^{-1}$	0.2	3	Houot et al. (2014); French standard: NF U 44-051
	Cu	mg (kg DW)$^{-1}$	15	300	Houot et al. (2014); French standard: NF U 44-051
	Pb	mg (kg DW)$^{-1}$	0.1	50	Houot et al. (2014); AROMIS, (2020)
	Zn	mg (kg DW)$^{-1}$	40	600	Houot et al. (2014); French standard: NF U 44-051
Mmanu	Quantity of manure application	kg FW m^{-2}	0	3	ADEME, (2019); Equiterre, (2009)
Cbiow	Metal content in bio-waste compost				
	Cd	mg (kg DW)$^{-1}$	0.3	3	Houot et al. (2014); French standard: NF U 44-051
	Cu	mg (kg DW)$^{-1}$	35	300	Houot et al. (2014); French standard: NF U 44-051
	Pb	mg (kg DW)$^{-1}$	40	180	Houot et al. (2014); French standard: NF U 44-051
	Zn	mg (kg DW)$^{-1}$	150	600	Houot et al. (2014); French standard: NF U 44-051
Mbiow	Quantity of bio-waste compost application	kg FW m^{-2}	0	3	ADEME, (2019); Equiterre, (2009)
Wirr	Annual irrigated water volume	L m^{-2}	0	400	
App_phy	Cu brought by culture from fungicides	mg m^{-2}	0	700	ITAB, (2020)
OMmanu	Organic matter content of manure	kg (kg FW)$^{-1}$	0.1	0.4	Houot et al. (2014)
OMbiow	Organic matter content of bio-waste compost	kg (kg FW)$^{-1}$	0.1	0.4	Houot et al. (2014)

Climatic parameters

Tem	Monthly temperature	°C	fixed	fixed	Météo France
Pre	Monthly rainfall	mm	fixed	fixed	Météo France
Eva_po	Potential evapotranspiration	mm	fixed	fixed	Météo France

Wpercly	Monthly percolating water	mm	fixed	fixed	Simulated by the model
		Vegetation			
Y	Yield per year or by crop	kg FW m^{-2}	0.3	21.7	Agreste database
PUF_Cd	Transfer factor of Cd from soil to the plant	S.D.	0.026	1.4	BAPPET database
PUF_Cu	Transfer factor of Cu from soil to the plant	S.D.	0.09	0.63	BAPPET database
PUF_Pb	Transfer factor of Pb from soil to the plant	S.D.	0.0014	0.3846	BAPPET database
PUF_Zn	Transfer factor of Zn from soil to the plant	S.D.	0.0223	1.2366	BAPPET database

3 Results and discussion

3.1 Future trends of the Cd, Cu, Pb, Zn contents in the vegetable garden soils

Figure 20 shows the relative changes in soil metal content by decade for the CP scenario in the three French metropolises. Table 21 shows the relative evolution of metal content in garden soils under CP and OA scenarios. On average, the concentrations of the four metals in soil increase over time, at a rate which depends on the metropolis. In the CP scenario, soil Cd content should increase by 8.0% after 20 years and 37.3% after 100 years for the gardens located in Nancy, while in Marseille, it should increase by 3.6% after 20 years and 17.4% after 100 years. For the gardens in Nantes, Cd content should increase up to 15.2% after 20 years and 84.3% after a century. The highest Cd relative change occurs in Nantes, which is due to their lowest initial Cd concentrations in soils, while net flux of Cd entering garden soils are close in the three cities (0.39, 0.34 and 0.33 mg m^{-2} yr^{-1} for Nancy, Nantes and Marseille respectively).

Soil Cu content would increase strongly in the garden soils of Nancy (by about 102% after 20 years and 503% after 100 years). In Marseille, the Cu relative change would be lower (about 9.7% after 20 years and 46.7% after 100 years), because the average initial Cu content of Marseille garden soils is double that in the other cities. Garden soils in Nantes should have an intermediate increase of Cu contamination (about 29.6% after 20 years and 154.8% after 100 years).

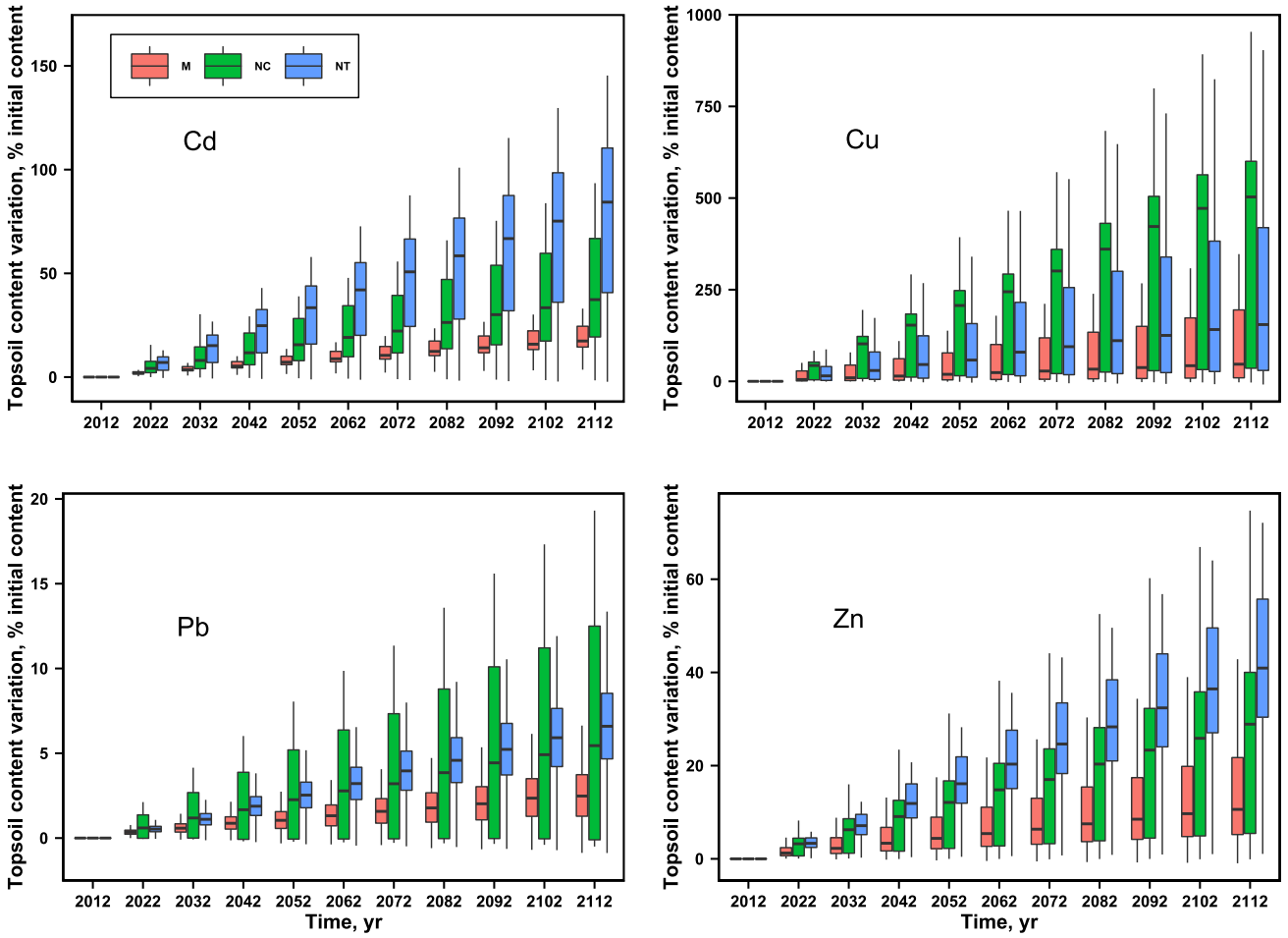

Figure 20. Relative variation presented as boxplots of metal content in garden surface soils by decade, for the CP scenario in three French metropolises M: Marseille (n = 36); NC: Nancy (n = 33); NT: Nantes (n = 35)

Table 21. Evolution of the four metals' soil content in the surface layer (0–20 cm) of 104 French vegetable gardens, according to two different scenarios. CP: current practices, OA: organic agriculture

Scenario	Nancy (n = 33)			Marseille (n = 36)			Nantes (n = 35)		
	Initial content, mg kg^{-1}	Variation, %		Initial content, mg kg^{-1}	Variation, %		Initial content, mg kg^{-1}	Variation, %	
		20 years	100 years		20 years	100 years		20 years	100 years
Cadmium (Cd)									
CP	0.35	8.02	37.3	0.59	3.62	17.4	0.15	15.2	84.3
OA	0.35	6.29	28.6	0.59	2.57	12.2	0.15	7.96	48.7
Copper (Cu)									
CP	33.4	102	503	69.2	9.69	46.7	33.9	29.6	155
OA	33.4	102	504	69.2	9.1	43.8	33.9	29.4	154
Lead (Pb)									
CP	73.1	1.18	5.45	125	0.58	2.48	41.7	1.11	6.59
OA	73.1	1.15	5.28	125	0.58	2.47	41.7	1.09	6.59
Zinc (Zn)									
CP	151	6.25	28.9	349	2.26	10.6	80.8	7.12	40.9
OA	151	6.11	28	349	1.88	8.75	80.8	6.4	38

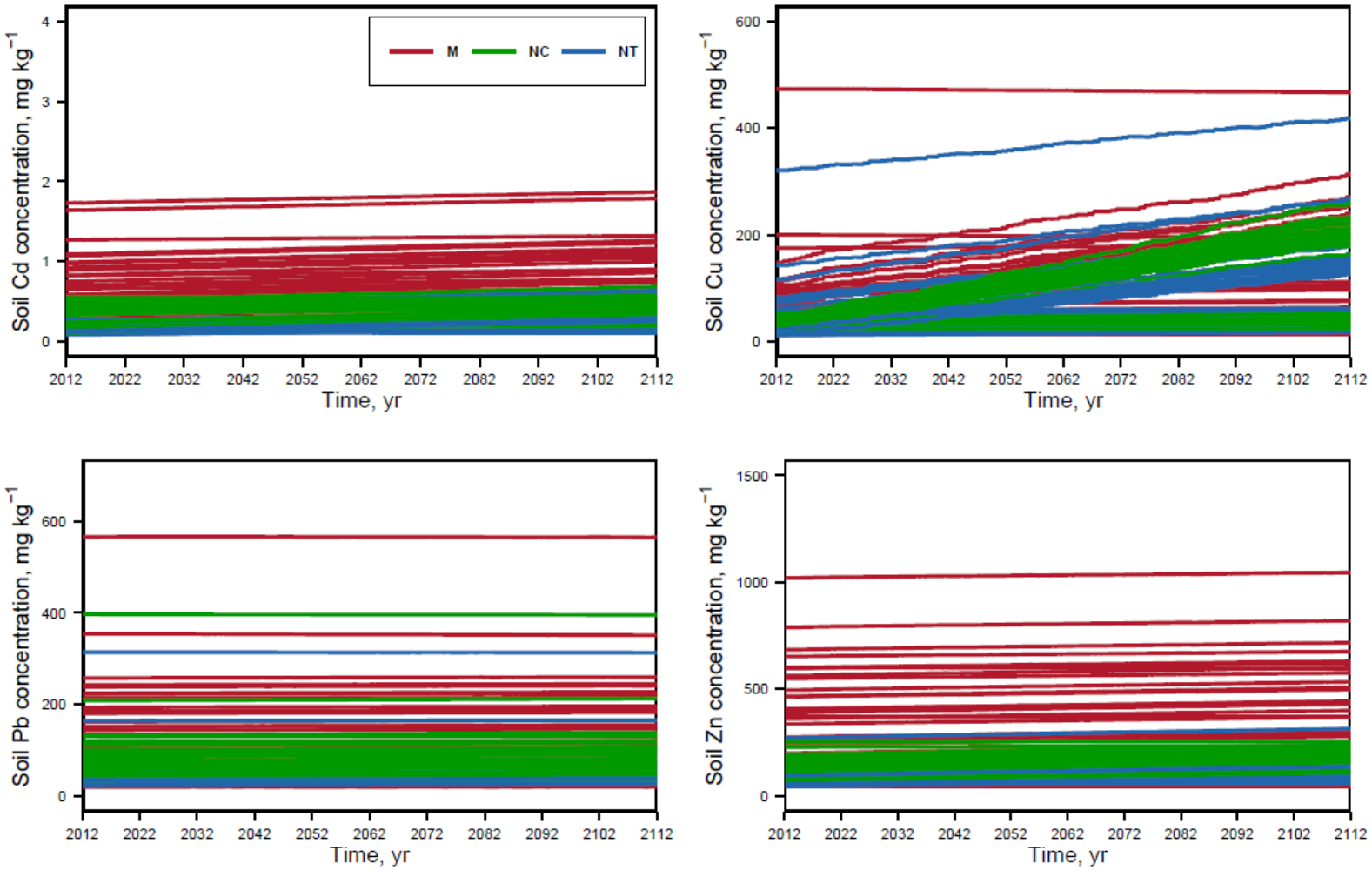

Figure 21. Evolution of the four metals soil concentration in the surface layer (0-20 cm) of 104 gardens, under the CP scenario. M: Marseille (n = 36); NC: Nancy (n = 33); NT: Nantes (n = 35)

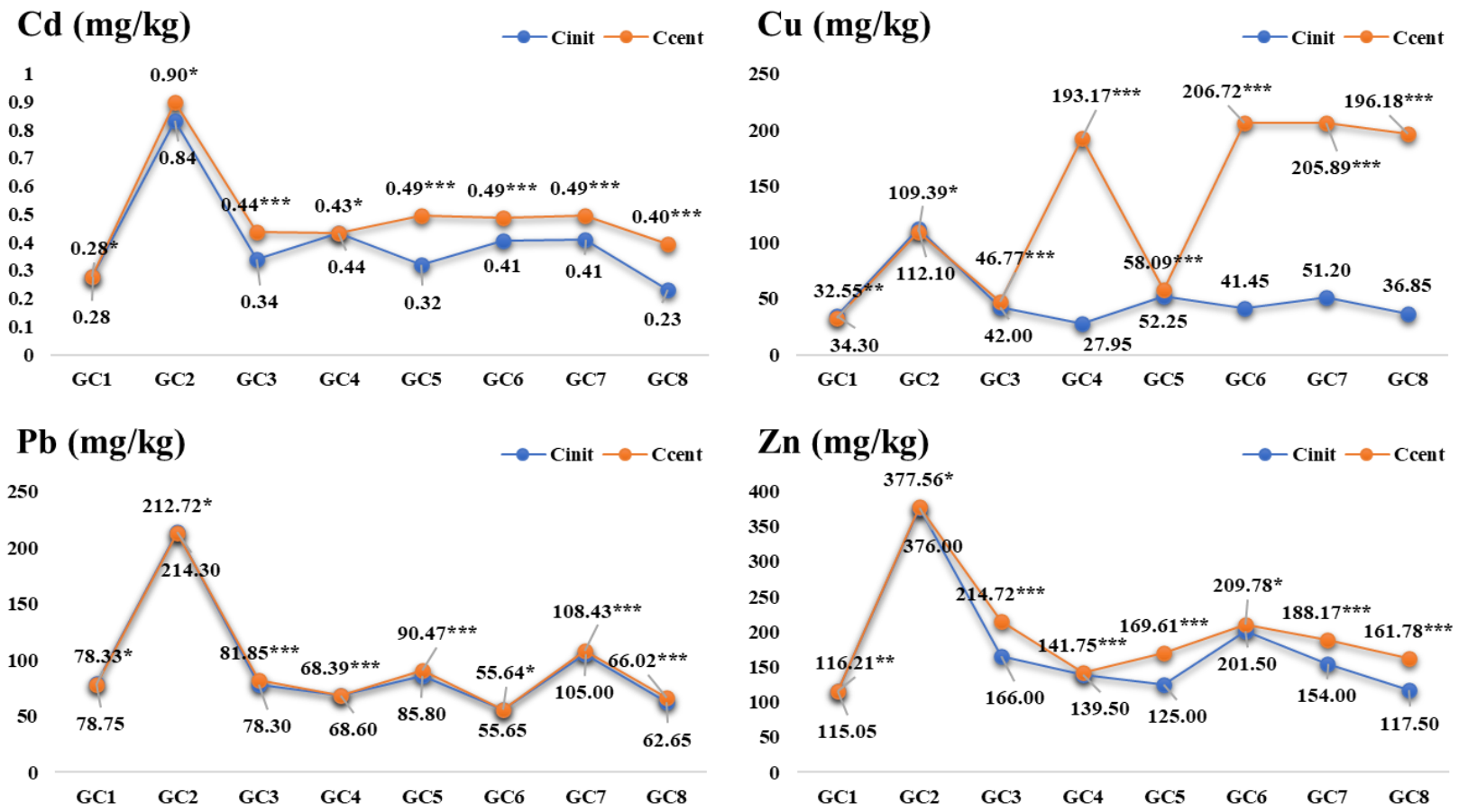

Figure 22. Changes in topsoil metal content after a century for the 8 groups of gardens under CP scenario. Cinit: initial soil metal content; Ccent: soil metal content after one century of gardening practices. Paired Student's t test: p value: *value higher than 0.05; **value between 0.05 and 0.01; ***value lower than 0.01

Simulations showed a small variation in soil Pb content (0.6% - 1.2%) after 20 years in the three cities, which will be difficult to detect. After a century, the soil Pb content should increase slightly, by 2.5% in Marseille, 5.5% in Nancy and 6.6% in Nantes. This is partly due to the initial Pb concentration in the garden soils (Table 2), which is abnormally high due to previous contamination. Indeed, lead levels in the soils of the three metropolises are much higher than in magmatic rocks (3 to 3.5 mg kg^{-1}), sedimentary rocks (5.7 to 10 mg kg^{-1}) (Bechet et al., 2018), upper continental crust (20 mg kg^{-1}) (Taylor and McLennan, 1995) or deep soil horizons (16.2 mg kg^{-1}) (Sterckeman et al., 2006a). The soil Pb enrichment is due to anthropogenic activities, mainly previous industrial land use, paint with white lead, atmospheric deposition of Pb from gasoline, etc. (Alloway, 2004). Indeed, as mentioned by Joimel et al. (2016), there is virtually no difference in soil Pb content in forests, meadows, agricultural land and vineyards and therefore, the initial Pb contamination of the garden soils is probably not due to cultivation practices but the result of other entry routes, via Atmospheric fallout, Particles of paint, Previous use of the site, etc (Alloway, 2004).

The model predicts that soil zinc content would increase by about 6.3% after 20 years and 28.9% after 100 years in Nancy, about 2.3% after 20 years and 10.6% after 100 years in Marseille, and about 7.1% after 20 years and 40.9% after 100 years in Nantes. Alternatively, if the gardeners adopted the organic farming practices, simulated in the OA scenario, i.e., chemical fertilizers are no longer applied to the soil but replaced by organic amendments to meet plant nutrient requirements, there would be a slight reduction in soil Cd enrichment compared to the CP scenario by 5.3% in Marseille, 9.6% in Nancy, and 16.1% in Nantes. In the cases of Cu, Pb and Zn, the results of CP and OA scenarios are very close. That means that adopting organic farming practices will not reduce the accumulation of these three metals in vegetable garden soils.

Figure 21 shows the concentration curves of the four metals in the soils of 104 gardens, under the CP scenario. In general, Marseille has the highest initial concentration of heavy metals contamination, followed by Nancy and Nantes. From the results of predicting changes in soil metal content, following the same order of magnitude of metal input and output flows in these 104 gardens, the higher the initial metal content of the soil, the smaller the relative change.

For Cd, Pb, and Zn, although their initial soil metal contents are very different, the trends in soil metal concentration (slope) are very similar in most of the gardens, the curves being almost linear whatever the metropolis. However, this not the case for Cu, for which some garden soils show a significant increase in Cu concentration, while others have a quasi-stationary content. A simulation for 1000 years, presented in Supplementary Material at Figure A5. Evolution of

the four metals soil concentration of in the dug layer (20 cm) of 104 gardens, under the CP scenario for 1000 years. M: Marseille; NC: Nancy; NT: Nantes, shows that the Cd, Cu and Zn content in soil will not reach a plateau should current gardening practices continue, because the metal inputs will always be much higher than the outputs. That means that regarding trace metal accumulation, the soil is far from a stationary regime corresponding equality between outputs and inputs. In the case of Pb, the soil content shows little or no change over 1000 years.

To better understand the effect of gardening practices on the evolution of soil metal concentrations, the 104 gardens were divided into eight classes of CP scenario ("Simulation scenarios"). Figure 22 shows a comparison of soil metal contents at the initial state and after a century in these eight classes (Table 19). There are few vegetable gardens without any agricultural input (GC1, n = 6), or with only chemical fertilizers (GC2, n = 2) or crop protection products (GC4, n = 4). Using organic amendments is very common in French vegetable gardens (GC3, GC5, GC7 and GC8, n = 88). In the two groups of garden soils using no crop protection products and no organic amendments (GC1, GC2, n = 8), there was no variation in any trace metal. The use of organic amendments or chemical fertilizers increases soil Cd content (GC3, GC5, GC6, GC7 and GC8).

Concerning Cu, in the two classes (GC3, GC5, n = 33) with no Cu fungicide but with organic amendments, soil Cu content increased by 11.4% and 10.1% respectively. On the contrary, in the other groups of gardens (GC4, GC6, GC7, GC8, n = 63) where Cu fungicides were applied, soil Cu concentrations tended to increase more markedly, in average by 3 to 6 times after a century. We may have overestimated the Cu input by fungicides because we assumed that the application rate of crop protection products equals the maximum recommended dose. However, a reduction in Cu fungicide application would slow down the accumulation of Cu in the garden topsoil, although soil Cu content will still increase, on average by 94% in a century even if we reduce the application rate by 50% in our simulations (Figure 23Figure).

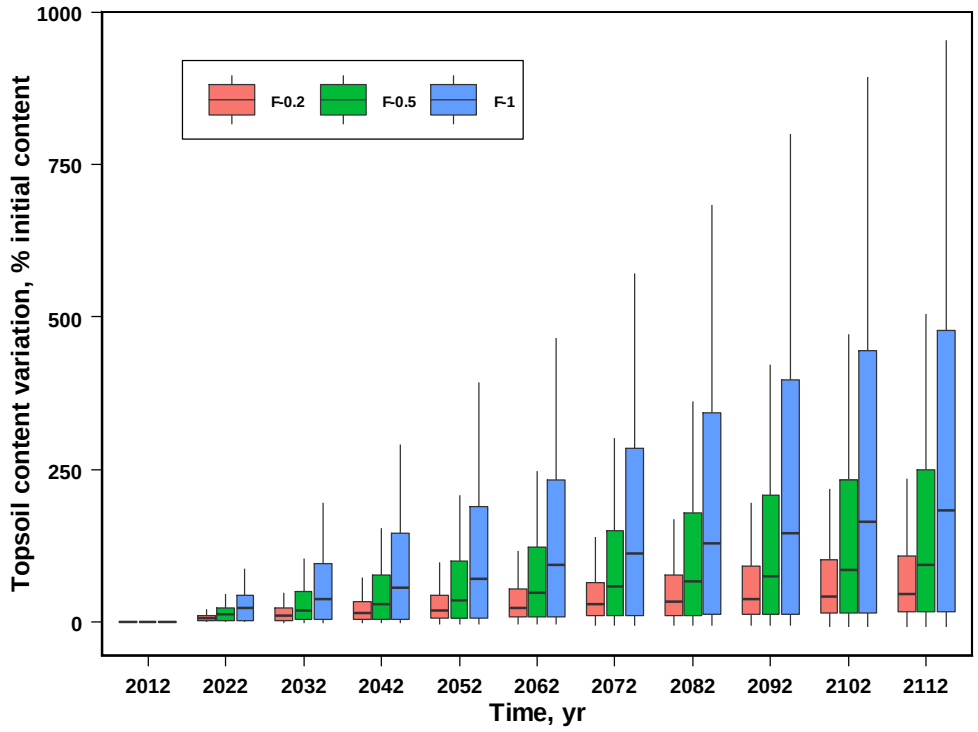

Figure 23. Relative variation of soil Cu content presented as boxplots by decade, for three fungicide application doses (F-0.2: 20% of recommended dose; F-0.5: 50% of recommended dose; F-1: recommended dose)

Several studies also found large variability and high values for soil Cu concentrations in urban allotments which are due to the use of copper-based fungicides (Bretzel et al., 2016; López et al., 2019). Bretzel et al., (2018) reported a significant accumulation of Cu in soil from 2012 (64.8 mg kg^{-1} in average) to 2017 (86.5 mg kg^{-1} in average) in the 72 urban allotments (Bretzel et al., 2016), resulting by improper use of anti-fungal treatments. A complete cessation of Cu fungicide use, as in GC3 and GC5 gardens would not suppress the increase in soil Cu content.

Soil accumulation of Pb does not seem to be affected by gardening practices, as it does not vary and remains very low whatever the garden class (Figure 22). Maintaining current gardening practices will not have any visible effect on soil Pb contamination. Zinc will accumulate significantly over time in the soils of classes GC3, GC5, GC7 and GC8 and not in the other classes, which makes organic amendments the major source of Zn accumulation in garden soils. Practicing organic farming in vegetable gardens is a mainstream trend which should also lead to increased Cd and Zn contamination in soils (Figure 22).

3.2 Input and output flows of the four trace metals

The mean distribution of the four metal flows after a century for 104 garden soils under the CP scenario is shown in Figure 24. The proportion of each flow is calculated relatively to the sum of all inflows and outflows.

For Cd, the distribution of the different input flows follows the order: Qorg (46.4%) > Qfer (25.3%) > Qatm (11.7%). For Cu, atmospheric deposition and chemical fertilizer contribute only 3.6% to the total input and output streams. Most Cu inputs are due to organic amendments (25.7%) and above all to Cu fungicides (54.9%). Pb is largely contributed by organic amendments (66.1%), followed by atmospheric deposition (6.4%) and chemical fertilizers (3.0%). The distribution of Zn flows is close to that of Pb, in the order: Qorg (62.6%) > Qatm (13.2%) > Qfer (9.4%). For Pb and Zn, these proportions are almost identical to those found in field agriculture at the national level in France by Belon et al. (2012): for Pb: Qorg (64.3%) > Qatm (32.6%) > Qfer (1.1%); for Zn: Qorg (82.1%) > Qatm (11.1%) > Qfer (4.6%).

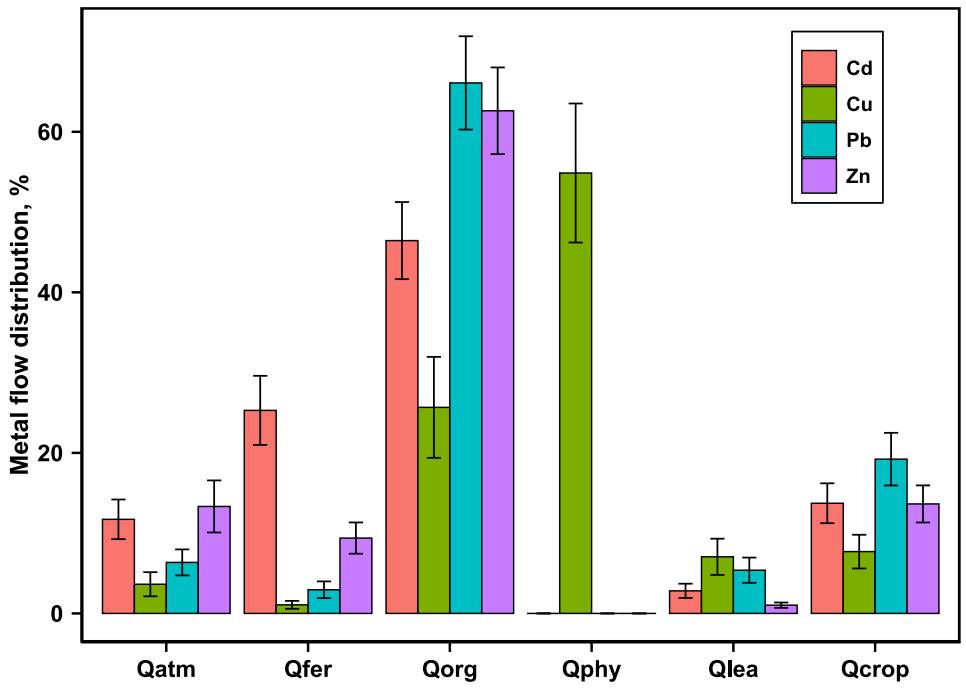

Figure 24. Mean distribution of input and output flows of the four metals after a century for 104 garden soils under the CP scenario. In % of the sum of the absolute value of all the flows. Qatm: atmospheric deposition; Qfer: NPK fertilizers; Qorg: organic amendments; Qphy: plant protection products; Qlea: leaching; Qcrop: crop offtake

However, the distributions of Cd are different in garden soils to those in field crops, where the major source is P fertilizer (Six and Smolders, 2014; Sterckeman et al., 2018). Hu et al. (2013)

also reported that organic fertilizers and atmospheric deposition are the major input flows of four metals to vegetable farm, which largely exceed output flow by vegetable harvesting thus would lead to an important accumulation of these metals in soil.

Leaching and crop offtake are the two output flows in the metal mass balance of garden soils. Metal leaching losses as a percentage of the total input and output flows are very low: Cd (2.8%), Cu (7.1%), Pb (5.4%) and Zn (1.0%). In addition, the quantity removed from soil by harvested plant parts represent 13.7% of Cd total flows, 7.7% for Cu, 19.2% for Pb and 13.6% for Zn. All output flows are much lower than the input flows, which explains the general accumulation tendency of the four trace metals in soils.

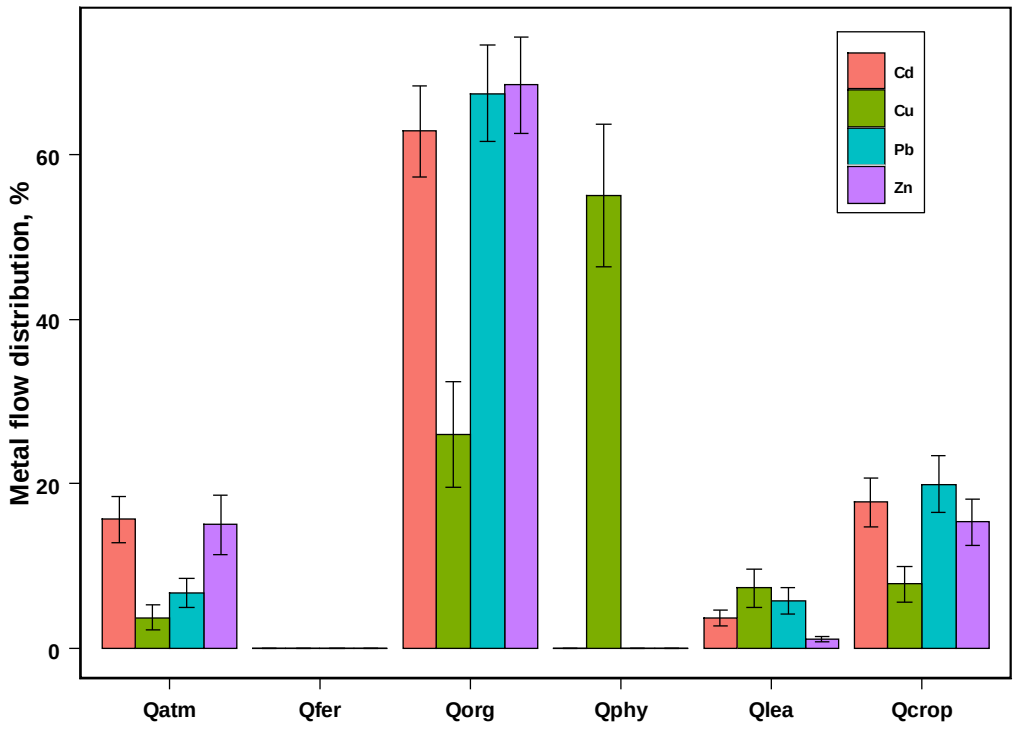

Figure 25. Mean distribution of input and output flows of the four metals after a century for 104 garden soils under the OA scenario. In % of the sum of the absolute value of all the flows

For the OA scenario, there is no metal input flows from chemical fertilizers and the other input flows are same as the CP scenario (Figure 25). The distribution of metal flows of the OA scenario is slightly different from that of the CP scenario. Metal leaching losses are also low and close to those of the CP scenario: Cd (3.7%), Cu (7.4%), Pb (5.8%) and Zn (1.1%). Outputs with harvest represent 17.8% of Cd flows, 7.8% of Cu flows, 20.0% of Pb flows and 15.4% of Zn flows.

3.3 Sensitivity analysis

The global sensitivity analysis ranked the model variables according to their contribution to the variation of total metal content in soils after 100 years (VC_i) (Figure 26). For the four metals, the variables related to input flows have a greater effect on the evolution of soil metal contents. In the case of Cd, the factors which more positively affect the evolution of soil metal content are the total application of fertilizers and their Cd contents, the amounts of amended biowaste compost or manure amendment as well as their Cd contents. This can be explained as follows: the higher the inputs due to organic amendments and fertilizer, the greater the increase in soil Cd.

The initial soil Cd content, the *PUF* and the yield have a negative effect on the Cd accumulation in soil. The initial soil content strongly affects VC_i negatively because Cd leaching and removal by vegetables are proportional to this (Eqs. 9, 10 and 13), while Cd offtake is also proportional to *PUF* and yield (Eq. 13). For Cu, the noticeable positive factors are the amounts of applied fungicide and biowaste compost and their Cu contents. The amount and Cu content of the fertilizer and manure also have a positive effect on Cu accumulation in the soil, while initial soil Cu content, yield and *PUF* have a negative effect. For Pb, it is the amount and composition of applied biowaste compost which the most positively affects the soil content evolution, followed by amount and composition of fertilizer. Initial soil Pb content, *PUF* and yield have the main negative effects on VC_{Pb}. The evolution of soil Zn content is positively affected by the mass and Zn content of the fertilizer and by the mass and Zn content of biowaste compost, followed by the mass and Zn content of the manure amendment, while yield, *PUF* and initial soil Zn content have negative influences. For all the elements, the soil bulk density (ρ) has a negative effect on the soil content evolution, because the denser the soil, the lower $\Delta C_{i,soil,n}$ (Eq. 2).

The values of these influential variables (e.g., initial metal content, different input flows) are initially fixed and do not change during the simulation. This is the reason why the evolution of soil metal concentrations is almost linear (Figure 21). Variables related to the metal output flows (e.g., *PUF*, *Y*) have a secondary impact on the variation of metals. The physicochemical properties of soils, such as soil pH or organic C seem to have a lesser effect on the evolution of metal content in soils. This is consequence of the low portion of metals in solution estimated by the partition coefficient models, which means that the leaching flow is too small to strongly influence the mass balance of metals.

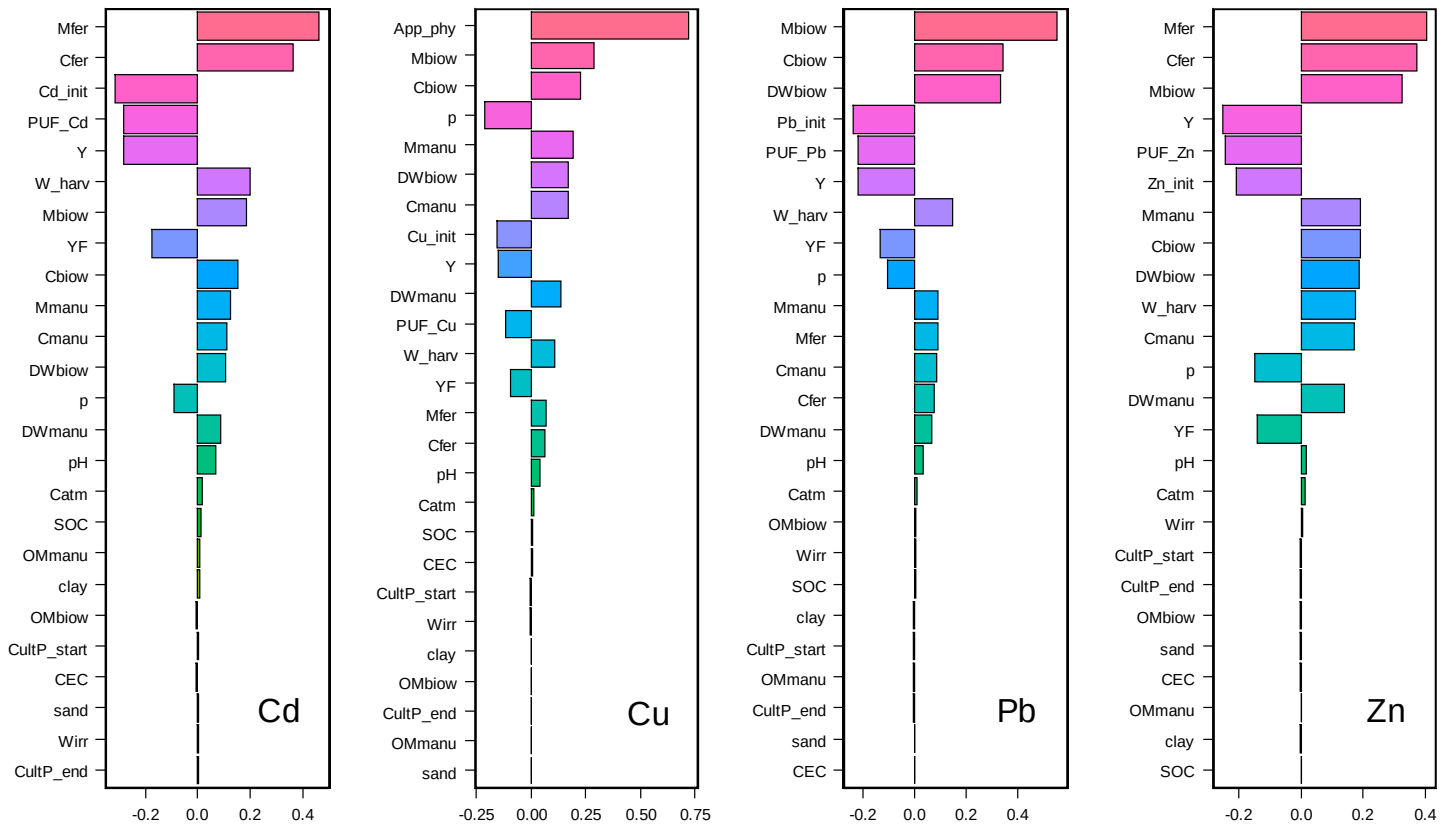

Figure 26. Ranking of variables according to their normalized coefficients (SRC) in the multiple linear regression with the absolute variation of soil metal content after one century (VC_i). Description of acronyms: Density = p, Soil pH in 0.01 M CaCl2 = pH, Cation exchange capacity = CEC, Organic carbon content = SOC, Clay content = clay, Sand content = sand, Initial Cd(Cu, Pb, Zn) content = Cd(Cu, Pb, Zn)_init, Start(end) of cultivation = Cult_start(end), Metal content in bulk sampling precipitation = Catm, Metal content in chemical fertilizer = Cfer, Quantity of chemical fertilizer application = Mfer, Metal content in manure = Cmanu, Quantity of manure application = Mbiow, Annual irrigated water volume = Wirr, Cu brought by culture from fungicides = App_phy, Organic matter content of manure = OMmanu, Organic matter content of bio-waste compost = OMbiow, Yield per year or by crop = Y, Transfer factor of Cd(Cu, Pb, Zn) from soil to the plant = PUF_Cd(Cu, Pb, Zn). More details of these variables are presented in Table 20. Parameters and variables tested for model sensitivity analysis

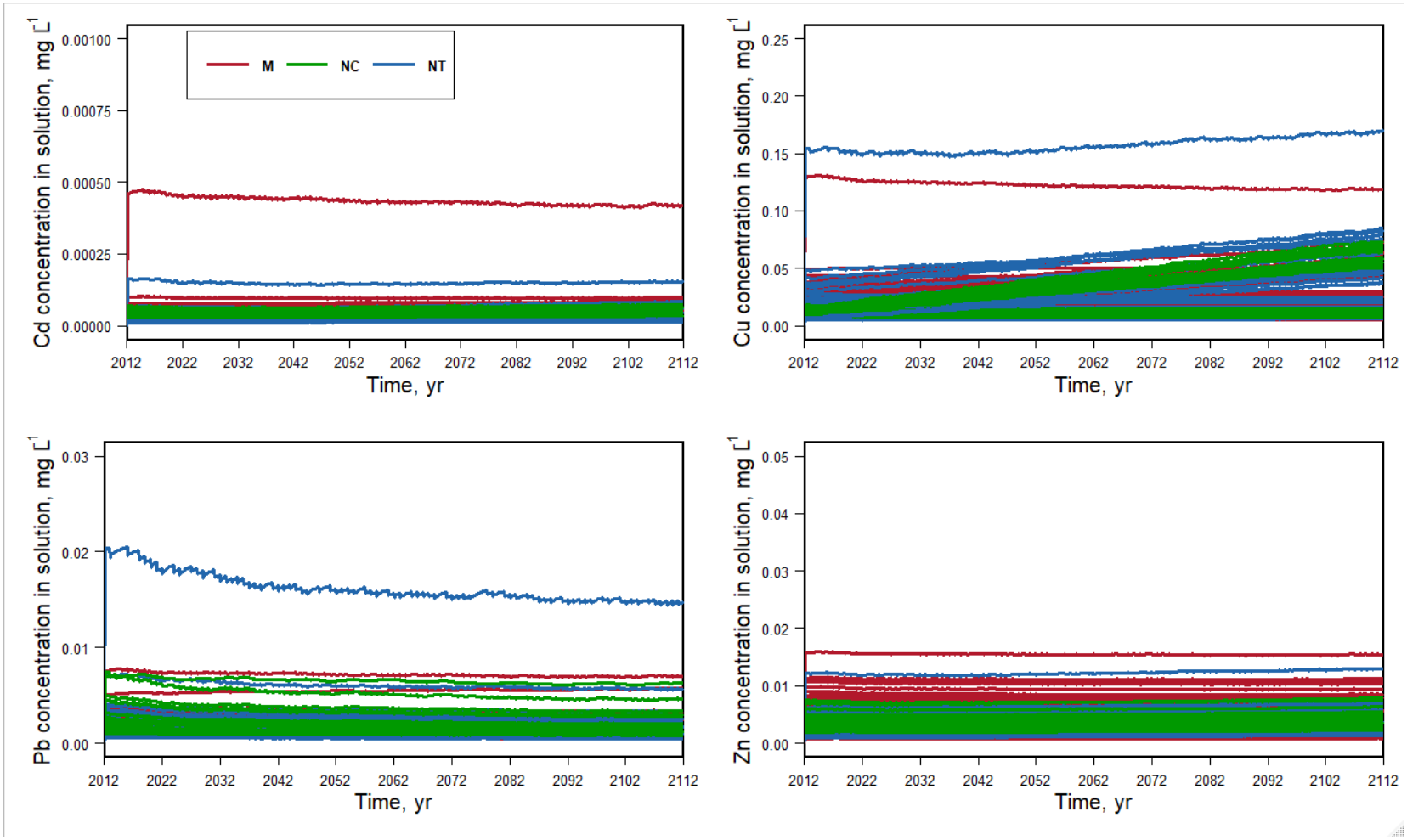

Figure 27. Evolution of soil metal concentrations in solution of in the dug layer (20 cm) of 104 gardens, under the CP scenario with constant pH. M: Marseille; NC: Nancy; NT: Nantes

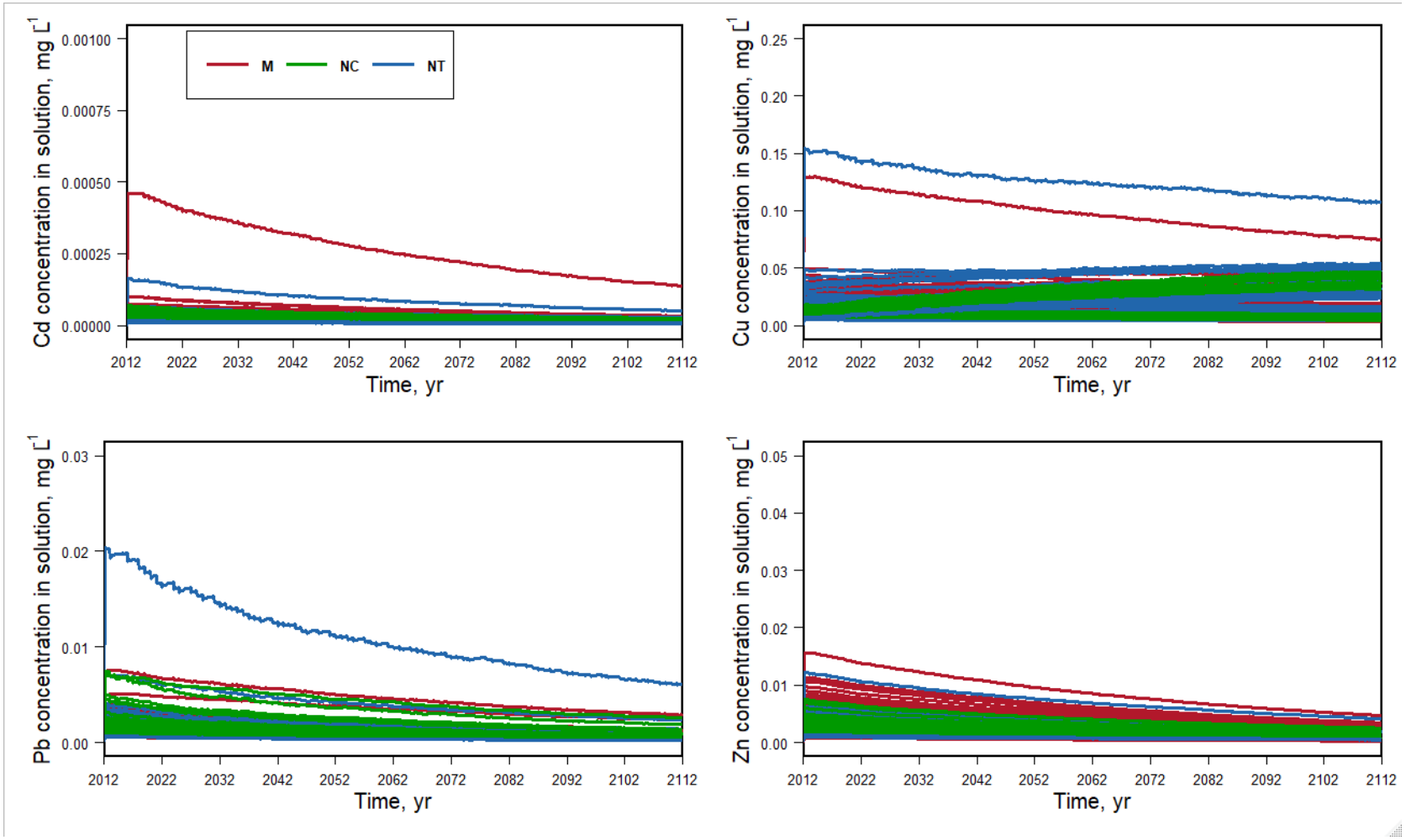

Figure 28. Evolution of soil metal concentrations in solution of in the dug layer (20 cm) of 104 gardens, under the CP scenario with pH linearly increasing by one unit after a century. M: Marseille; NC: Nancy; NT: Nantes

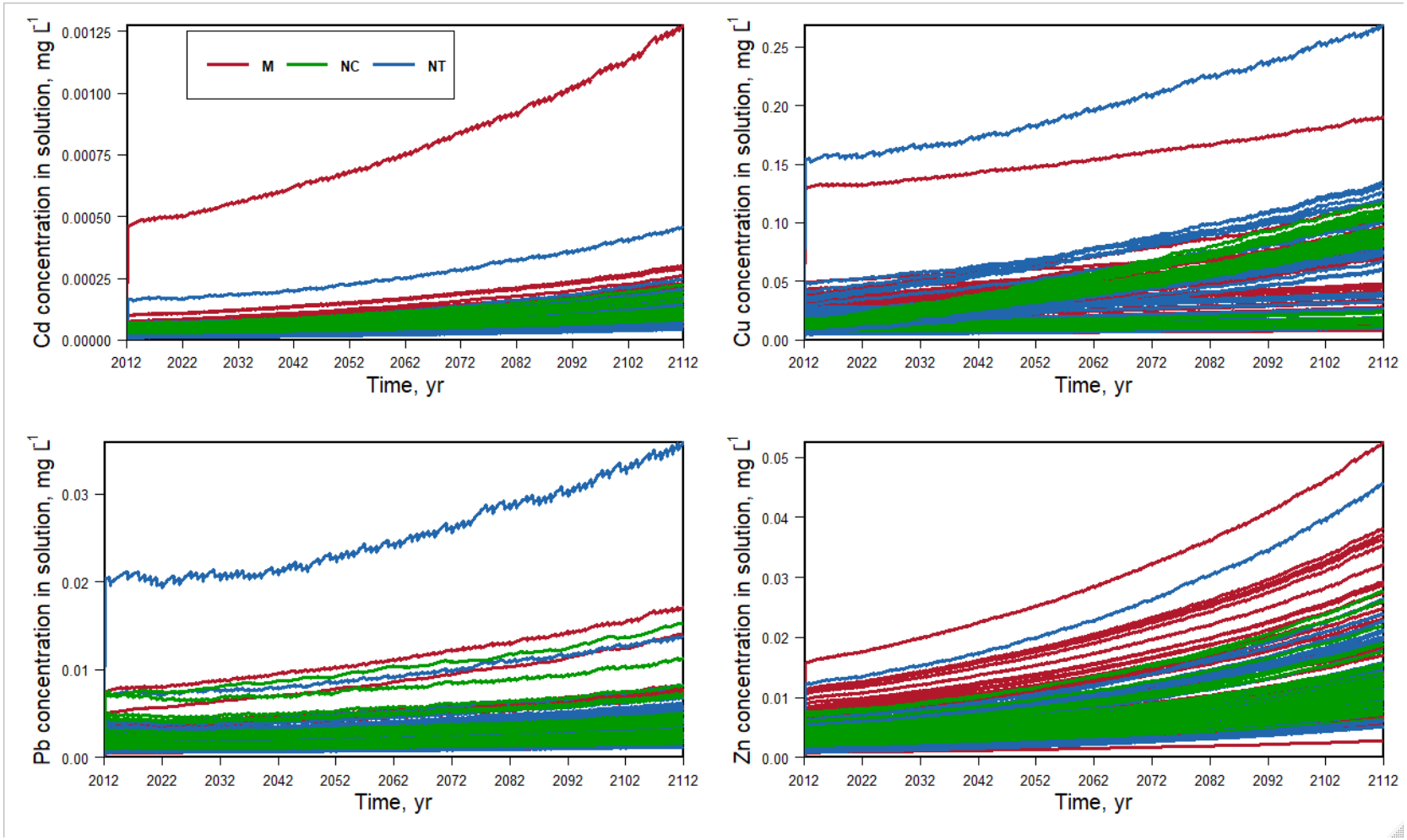

Figure 29. Evolution of soil metal concentrations in solution of in the dug layer (20 cm) of 104 gardens, under the CP scenario with pH linearly decreasing by one unit after a century. M: Marseille; NC: Nancy; NT: Nantes

3.4 Evolution of metal availability

Concentrations of Cd, Cu, Pb and Zn in garden soils should increase in the future, whatever the gardening practices. This raises the question of the evolution of their ecotoxicity. One way to assess this, is to estimate their concentration in the soil solution over time, since this drives the impact of metals on soil organisms (Lin et al., 2016; Liu et al., 2014; Slaveykova and Wilkinson, 2005). The models presented in Table 14 permit an estimation of the evolution of the trace metals in solution, using the total metal content, the pH and the organic carbon content as input variables. The evolution of total metal and organic carbon is simulated in our mass balance model. We projected 3 scenarios about the soil pH change, by alternatively considering constant pH, linear increasing pH by one unit and decreasing pH by one unit over a century and deduced the evolution of the concentrations of four metals in solution.

Cd, Pb and Zn solubility is almost constant when the pH does not change over a century, although the total metal content in soil increases (Figure 27). This is due the increase in organic matter (Figure A6) which enhances the sorption of the metal on the soil solid phase. Paradoxically, the contribution of organic matter which is largely at the origin of the enrichment of soils in metals, would at the same time be a mean of limiting their harmful effects. However, the increase in soil organic carbon is not sufficient to restrain the solubility of Cu in the gardens where Cu fungicides are applied (Figure 27). Cu solubility always increases over time due to Cu fungicide application. Alternatively, when compared to constant pH, the solubility of the four metals decreases by 0.4 to 0.7 times after a century when pH increases by one unit (Figure 28) or increases 0.6 to 2.5 times after a century when pH decreases by one unit (Figure 29). This indicates that an estimation of the evolution of the pH would be useful when predicting the ecotoxicity of the metals. The next version of our model should therefore include a pH evolution module. What could also be done to ameliorate such an approach would be to measure the trace metal concentration in the poral water of the 104 gardens, together with other soil variables (such as pH and organic C) in order to derive more specific functions for the prediction of the trace metal availability. Moreover, a liming practice in vegetable garden soils may be useful in maintaining the pH at its initial level or even to increase it by around half of unit, particularly in soils with a pH below 7.

3.5 Comparison with other mass balances

In Table 22, we compared the mean annual flows of the four metals estimated in the soils of the 104 gardens for the CP scenario with the estimated values in field crops (Belon et al., 2012; Six et Smolders, 2014; Sterckeman et al., 2018) and in a peri-urban vegetable farm located in Nanjing, China (Hu et al., 2013).

The input flow of Cd through chemical fertilizer application estimated in our study is 0.105 mg m^{-2} yr^{-1}, which is higher than the value estimated by Six et Smolders (2014). Among the different studies, Six et Smolders (2014) estimated the lowest value of Cd input by chemical fertilizer. This difference is due to the lower application of phosphate fertilizer at the European level, with an average application of 22 kg P_2O_5 ha^{-1} on arable land (21 kg P_2O_5 ha^{-1} on cereals and 45 kg P_2O_5 ha^{-1} on potatoes). In France, average phosphate application rates are 20 kg P_2O_5 ha^{-1} on wheat and 53 kg P_2O_5 ha^{-1} on potatoes (Sterckeman et al., 2018). In the 104 French vegetable gardens, NPK-type fertilizers are commonly used. We estimated an average application of 0.0154 kg P_2O_5 m^{-2} yr^{-1}, i.e., 154 kg P_2O_5 ha^{-1} yr^{-1} as NPK type fertilizers in the gardens. This is 7.7 times more than the application rate used on wheat. Belon et al. (2012) found a fertilizer Cd input closer to ours and lower than Sterckeman et al. (2018) as they counted 29,554,440 ha of the occupied agricultural area at the national level of France, which includes meadows, orchards and vineyards. Phosphate fertilizer application rates on these permanent crops could be lower than on annual crops (Sterckeman et al., 2018).

Table 22. Estimated mean annual flows of the four metals in the surface layer (0-20 cm) of soil for 104 garden soils, under the CP scenario

Reference	Input flow						Output flow			Balance
	Qatm	Qfer	Qlim	Qorg	Qphy	Total	Qcrop	Qlea	Total	
	Cd (mg m^{-2} yr^{-1})									
This study	0.027	0.105	0	0.173	0	0.305	0.032	0.006	0.037	0.267
Belon et al. (2012), France	0.025	0.102	0	0.056	0	0.183	n.d.	n.d.	n.d.	n.d.
Six and Smolders, (2014), Europe	0.035	0.079	0	0.006	0	0.129	0.020	0.256	0.276	-0.147
Sterckeman et al. (2018), France	0.020	0.142	0	0.025	0	0.189	0.093	0.028	0.139	0.050
Hu et al. (2013), China	0.530	0.013	0	0.662	0	1.21	0.160	0	0.160	1.05
	Cu (mg m^{-2} yr^{-1})									
This study	2.54	0.648	0	15.8	187	206	4.98	4.60	9.58	196
Belon et al. (2012), France	0.817	0.314	0.314	9.46	5.57	16.5	n.d.	n.d.	n.d.	n.d.
Hu et al. (2013), China	20.9	1.23	0	136	0	158	8.60	0	8.60	150
	Pb (mg m^{-2} yr^{-1})									
This study	0.862	0.219	0	7.73	0	8.82	1.27	0.247	1.51	7.30
Belon et al. (2012), France	0.769	0.027	0.045	1.52	0	2.36	n.d.	n.d.	n.d.	n.d.
Hu et al. (2013), China	31.1	0.767	0	23.8	0	55.6	2.49	0	2.49	53.2
	Zn (mg m^{-2} yr^{-1})									
This study	11.48	8.88	0	69.8	0	90.1	8.70	0.586	9.28	80.9
Belon et al. (2012), France	5.69	2.35	0.392	42.2	1.18	51.8	n.d.	n.d.	n.d.	n.d.
Hu et al. (2013), China	74.6	5.54	0	431	0	511	54.6	0	54.6	457

Note that the Cd input flow through chemical fertilizer estimated in 104 gardens is the mean of 62 gardens with chemical fertilizer application and 42 gardens without. The input flow of Cd through chemical fertilizer application estimated in our study is 0.17 mg m^{-2} yr^{-1} for these 62 gardens, which is the highest among the four studies.

The average contents of the four metals in NPK-type fertilizers (n = 9, France) in unit mg (kg P_2O_5)$^{-1}$ are: 11 mg Cd (kg P_2O_5)$^{-1}$; 68 mg Cu (kg P_2O_5)$^{-1}$; 23 mg Pb (kg P_2O_5)$^{-1}$; 931 mg Zn (kg P_2O_5)$^{-1}$ (Verbeeck et al., 2020). The average Cd content of NPK-type fertilizers is almost four times less than that used by Sterckeman et al. (2018) (51 mg Cd (kg P_2O_5)$^{-1}$) and three times less than that used by Six et Smolders (2014) (40 mg Cd (kg P_2O_5)$^{-1}$). All the differences on fertilizer application rate and Cd content in these fertilizers lead to the moderate metal input flow from chemical fertilizer in our simulations among the four studies. For the other metals (Cu, Pb and Zn), our estimated input flows by chemical fertilizer are much higher than those given by Belon et al. (2012) due to their high application rates in vegetable gardens.

In the CP scenario, we simulated two types of organic amendments for all soils: cattle manure and bio-waste composts, respecting the recommended doses. The application rate of organic amendments is excessive in garden soils where chemical fertilizers have been already added to meet plant nutrient requirements, but it is a common phenomenon that vegetable gardens are usually over-fertilized due to lack of restrictions (Joimel et al., 2021, 2016). Organic amendment inputs in gardens are much higher than in field crops, where manure application dose is three times of that used in field crops and bio-waste compost application dose is 40 times more than that used in field crops (Sterckeman et al., 2018). This may explain why our estimates of metal input flows from organic amendments are higher than those of other studies. Much higher metals input from organic amendments found in the peri-urban vegetable farm resulted from their higher application rate (Hu et al., 2013).

Michaud et al. (2020) studied the accumulation of trace elements in cultivated soils by applying urban composts or cattle manure from 1998 to 2015 as part of the QualiAgro program. By applying 1.4 kg FW m^{-2} yr^{-1} of bio-waste compost, they estimated the input flows of metals through organic amendments with 0.74 mg Cd m^{-2} yr^{-1}; 64 mg Cu m^{-2} yr^{-1}; 94 mg Pb m^{-2} yr^{-1}; 249 mg Zn m^{-2} yr^{-1}. These values are much higher than the values simulated in our study because more amendment is applied into their experiment fields comparing to into the 104 gardens. Moreover, the bio-waste compost in Michaud et al. (2020) contains more metals than that in the present study, to which in addition, a recycling factor of 0.5 was applied.

The atmospheric depositions of Cd and Pb estimated in our study is very close to the estimated values from other studies. The estimated atmospheric depositions of Cu and Zn in our study are respectively three times and twice the flows estimated by Belon et al. (2012). By comparing the monitored atmospheric deposition at the different dates of the last few years in the three stations concerned (Table 3), there is a high interannual variability in metal concentrations of bulk sampling precipitation. This explains the variation in atmospheric deposition flow in the four studies of Table 22 because these authors used data from different monitored years. Atmospheric deposition of metal in the studied site of Hu et al. (2013) can reach to 10 times that our study.

For crop protection products, we consider that there is no input flow for Cd, Pb and Zn. However, fungicides, usually made of Cu compounds, are widely used in vegetable gardens (*n* = 63). We have grouped together all fungicides authorized for use in gardens in France, according to their active ingredients (Table 6; Table 7). We estimated up to 187 mg Cu m^{-2} yr^{-1} introduced into the soils of the 104 gardens. This amount is much higher than that estimated with the application of pesticides in field crops (Belon et al., 2012). This can be explained by the fact that Cu salts are rarely used in field crops where fungicides are now most often based on organic compounds.

Six and Smolders (2014) mentioned that Cd leaching is the determining flow for the mass balance of Cd: 0.256 mg Cd m^{-2} yr^{-1} by leaching versus 0.129 mg Cd m^{-2} yr^{-1} by total input flows. This value is considerably higher than the values measured in percolating solutions (Bengtsson et al., 2006; Cambier et al., 2019, 2014; Filipovic et al., 2016). Sterckeman et al. (2018) modified the leaching model of Six et Smolders (2014) by dividing by 12 the metal output calculated for leaching. The latter authors estimated an outflow of 0.028 mg Cd m^{-2} yr^{-1} by leaching. Bengtsson et al. (2006) estimated the loss of Cd through percolation and runoff is up to 0.035 mg Cd m^{-2} yr^{-1}. The results of our simulations are smaller than theirs.

Recently, Cambier et al. (2019, 2014) and Filipovic et al. (2016) have published data from QualiAgro experimental plots at Feucherolles, near Paris, which is part of the French national SOERE-PRO network. These plots were amended with different urban composts to evaluate their long-term effects on soil and drainage water composition and on their concentrations of metallic contaminants. Each plot is equipped with two lysimeters to collect percolating water at 45 and 100 cm depths. The leaching Cd ranged from 0.011 to 0.014 mg Cd m^{-2} yr^{-1} and the leaching Cu ranged from 0.31 to 0.77 mg Cu m^{-2} yr^{-1} (Filipovic et al., 2016). The estimated leaching flow of Cd in our study is very close to the measured Cd concentration in percolating

water in QualiAgro experimental plots, but the estimated leaching flow of Cu in our study is much higher than that measured in this experiment.

Michaud et al. (2020) sampled percolates in the lysimeters of the QualiAgro plots at 45 cm depth in 2013/2014 and 2014/2015. They found that metal outputs through leaching and plant harvesting were generally very low. The metal losses by leaching were measured as 0.01 mg Cd m^{-2} yr^{-1}, 1.37 mg Cu m^{-2} yr^{-1}, 0.01 mg Pb m^{-2} yr^{-1} and 0.95 mg Zn m^{-2} yr^{-1}. The Cu, Pb leaching simulated in our study is more than these values measured by Michaud et al. (2020), while the leaching of Cd, Zn was less in our study. Comparing metal output by leaching levels deduced with those from other studies is always full of uncertainty. Indeed, soil differences, as well as different climatic conditions in different locations, can affect metal leaching. Different agricultural settings could also influence the metal solubility in soil. It is consequently difficult to determine the accuracy of simulation results by comparing our results with other studies.

A better metal leaching model should be developed, which would consider the impact of agricultural practices on soil physicochemical properties, such as soil pH or dissolved organic matter. These soil factors directly influence the solubility of metals and the plant metal uptake (Huang et al., 2020; Sterckeman and Thomine, 2020). Soil preferential pathways for water transfer should also be formalized in the metal leaching modelling, as well as the changes in the dominant soil factors over time. It is also necessary to carry out a larger verification of the metal leaching modelling at the field scale. To date, there are very few data available on metal concentrations in percolating water from vegetable gardens in Europe or elsewhere in the world, to compare with the model predictions. Field measurements should therefore be carried out to fill this gap.

Finally, the metal output flow by plant harvesting varied quite strongly from one species to another. In the study of Hu et al. (2013), simulated metal crop uptake is several times more than our for the four metals, because of their higher intensive vegetable production system. The average loss of Cd by vegetable harvesting in garden soils is 0.032 mg m^{-2} yr^{-1}. This value is of the same order of magnitude as estimated by Sterckeman et al. (2018) and Six et Smolders (2014). The average loss of Zn by vegetable harvesting in garden soils is 8.7 mg m^{-2} yr^{-1}. Michaud et al. (2020) found that the Zn output flow from grain harvest and wheat crop residues was 18.2 mg Zn m^{-2} yr^{-1}. Both Cd and Zn output flow by harvested plants from the above studies are very close to the value estimated by our model, considering that garden vegetable yield has been assessed as being half that of professional vegetable growers. Michaud et al. (2020) found that the Cu output flow from plant harvesting was 2.816 mg Cu m^{-2} yr^{-1}, which is almost half

of the value estimated by our model. This is probably due to the addition of Cu fungicides which made Cu accumulate in the soil, and thus the metal output by plant harvesting increases as estimated by plant uptake factor. The uptake of heavy metals by plants is a complex and dynamic process influenced by various soil and plant factors. Estimating metal output by harvested plants as a percentage of the total metal content of soil is certainly a too simplistic and incorrect method. A more mechanical root absorption model should be integrated into our mass balance model to better simulate output flow by crop offtake (Lin et al., 2016).

4 Conclusions

The soils of 104 French vegetable gardens generally have high metal contents compared to soils under field crops. Mass balance modelling suggests that if current gardening practices in the 104 gardens continue, the soil metal contents will increase from 17.4% to 84.3% for Cd, from 46.7% to 503.1% for Cu, from 2.5% to 6.6% for Pb and from 10.6% to 40.9% for Zn. This increase is mainly due to Cu fungicides in the case of Cu, and to organic amendments and secondarily to chemical fertilizers in the case of Cd, Pb and Zn.

Organic farming would result in similar changes in soil metal contents as current practices. It could slightly decrease the rate of Cd accumulation in soils, as this metal is brought in by chemical fertilizers. However, as the application of organic amendments has the greatest impact on the accumulation of the four metals and as Cu fungicides are used in organic gardening, this practice would not significantly reduce the metal accumulation over the medium or long-term. The use of copper-based products as fungicides is a significant issue with respect to Cu contamination of soils.

More precautions should be taken for the use of organic amendments in vegetable garden soils. These amendments should contain less metals and be applied at a rate corresponding to the soil and plant requirements. However, organic amendments will always contain trace metals and our results suggest that recycling of organic matter in soils to replace chemical fertilizers and store carbon will cause an enrichment of the topsoil with potentially toxic elements. It is also the application of organic amendments in the past decades which could partly explain the relatively high trace metal concentrations generally measured in vegetable gardens.

Organic amendments are also responsible for the increase in soil organic matter, which in turn should enhance the sorption of the trace metals on the soil solid phase, maintaining their concentrations in soil solution at relatively unchanged levels, although their total contents increase over time. Alternatively, the solubility of the four metals decreases significantly after a century when supposing that pH increases by one unit. A liming practice should be a feasible way to prevent an increase in the trace metal mobility and phytoavailability. Estimation of pH variation should be considered in a future mass balance model. Moreover, further investigations into the ecotoxicity of metals in French garden soils are to be carried out.

However, the current forecasts still suffer from many uncertainties, due for instance to the values taken for the amount and composition of fertilizers and amendments over time, or to the

leaching and plant offtake formalisms and parameters. These forecasts can only reveal trends and potential risks about soil metal accumulation under common gardening practices. Simulations of leaching and crop offtake are based on simplistic models, which could be improved in the future by more mechanistical models and by considering the evolution of dominant soil physicochemical properties.

5 Code Availability

Scripts using the R programming language are provided to process simulation of the change on soil metal content as function of time, make analysis of model sensitivity and produce figures. All codes are available from the corresponding author upon request.

Chapitre 3 : Amélioration du modèle actuel par l'ajout d'un module de simulation du pH du sol

1 Introduction

Soil pH is a dominant factor of soil metal solubility, as our previous K_d are functions of soil pH. However, soil pH has been set to a fixed value which does not change with time in our current mass balance model. Actually, soil pH can not only be significantly altered by atmospheric fallout, but also by anthropogenic activities such as farming practices. In French urban vegetable gardens, different chemical and organic fertilizers are applied to improve soil fertility, often due to very intensive practices. They contain a considerable amount of nitrogen and base cations (*BC*). Nitrogen transformation and *BC* uptake and release processes can lead to a significant change on soil element balance and thus alter soil pH (Xu et al., 2020; Zeng et al., 2017; Zhu et al., 2018b, 2018a). Furthermore, the change in soil pH can lead to the change in soil metal solubility, which consecutively results in different metal losses through leaching as simulated in our model. The Very Simple Dynamic model, called VSD^+ model, has been successfully used into different cropping systems to simulate the change of soil pH over time (Bonten et al., 2016; Posch and Reinds, 2009; Xu et al., 2020; Zeng et al., 2017; Zhu et al., 2018b, 2018a). The VSD^+ model is a single-layer model based on charge and mass balances of element in soil solution, together with different rate-limited reactions (*e.g.*, growth uptake, N mineralization and immobilization, nitrification and denitrification as well as silicate weathering) and equilibrium reactions (e.g., dissociation of bicarbonate, cation exchange, dissolution of Al hydroxides, adsorption-desorption of S and P), to compute changes in soil and soil solution chemistry, in particular focusing on changes in exchangeable base cations and soil pH (Bonten et al., 2016; Zeng et al., 2017). In this chapter, we present the feature of the adapted VSD^+ model, which consists in the main equations, parameterization, and input data. Some mathematic expressions have been changed to recode VSD^+ model into R programming language. In order to keep the connectivity of the description of the feature of this model for readers, we have fully presented the model even by repeating those main formulations which can be found in the VSD^+ software and related published articles. Furthermore, we have applied this model to simulate the changes in soil pH in the King's Vegetable Garden over the past 300 years, with the aim of identifying the impacts of historical gardening practices on soil acidification and assessing the prediction accuracy of the model.

2 Materials and methods

2.1 Process formalizing of the VSD$^+$ model

2.1.1 Charge balance equation in soil solution

In the VSD$^+$ model, the H^+ is calculated from the charge balance equation.

$$[H^+] = [SO_4^{2-}] + [NO_3^-] + [H_2PO_4^-] + [Cl^-] + [HCO_3^-] \quad (54)$$
$$+[RCOO^-] - [BC^{2+}] - [Na^+] - [Al^{3+}] - [NH_4^+]$$

$$[BC^{2+}] = [Ca^{2+}] + [Mg^{2+}] + [K^+] \quad (55)$$

where SO_4^{2-} stands for sulphate, NO_3^- for nitrate, $H_2PO_4^-$ for phosphate, Cl^- for chloride, HCO_3^- for bicarbonate, $RCOO^-$ for organic anions. *BC* for base cations (which denotes the sum of Ca^{2+}, Mg^{2+} and K^+, and K^+ is treated as divalent ion), Na^+ for sodium, Al^{3+} for aluminum, and NH_4^+ for ammonium. All concentrations are expressed in moles of charges in soil volume (Eq m^{-3}), i.e., the molar concentration of an ion multiplied by its charge.

The principle of the VSD$^+$ model is to solve the charge balance equation for H^+. Changes in the different element contents are computed from equilibrium processes and their masse balances over time, with a yearly time step. In response to our trace metal masse balance of which has a monthly time step, we sum up all influxes and outfluxes of different elements of one year, then launch the model in December to calculate the concentration of H^+ (equivalent to soil pH).

2.1.2 Equilibrium equations

The dissolution of Al hydroxides is calculated by:

$$[Al^{3+}] = K_{Alox}[H^+]^3 \quad (56)$$

where K_{Alox} is the dissolution constant. Here, we use the well-known gibbsite equilibrium constant.

The dissolution of HCO_3^- is calculated by:

$$[HCO_3^-] = \frac{K_1 K_H p_{CO_2}}{[H^+]} \quad (57)$$

where K_1 is the first dissociation constant, K_H is Henry's constant and p_{CO_2} (atm) is the partial pressure of CO_2 in the soil solution. Both constants are computed as a function of temperature (*Tem*) (Harned and Davis, 1943):

$$K_1 = 10^{\left(-\left(\frac{3404.71}{(Tem+273.15)}+0.032786\left((Tem+273.15)-14.8435\right)\right)\right)} \quad (58)$$

$$K_H = K_{H\_ref} exp^{\left(2400\left(\frac{1}{(Tem+273.15)}-\frac{1}{298.15}\right)\right)} \quad (59)$$

where K_{H_ref} = 0.034 is the Henry's constant for CO_2 at 298.15 K.

For non-calcareous soils, the exchange of H^+ against BC^{2+} is the most important buffer mechanism. In VSD$^+$ model, exchange between the solid phase and solution phase of Al^{3+}, H^+ and BC^{2+} are simulated by Gapon exchange model:

$$\frac{E_{\mathrm{Al}}}{E_{BC}} = K_{AlBC}\frac{[\mathrm{Al}]^{1/3}}{[BC]^{1/2}} \quad (60)$$

$$\frac{E_{\mathrm{H}}}{E_{BC}} = K_{HBC}\frac{[\mathrm{H}]}{[BC]^{1/2}} \quad (61)$$

where E_X is the equivalent fraction of ion X (Al^{3+}, BC^{2+}, H^+) at the exchange complex, K_{AlBC} is the selectivity constant for Al-BC exchange, and K_{HBC} is the selectivity constant for H-*BC* exchange.

As the exchange complex only comprises for H, Al and BC, mass balance requires that:

$$E_{BC} + E_{\mathrm{Al}} + E_{\mathrm{H}} = 1 \quad (62)$$

The values of cation exchange constant (K_{Alox}, K_{AlBC} and K_{HBC}) have been derived into average values from soil texture on Vries and Posch. (2003). The unit conversion of the three constants are also presented on Vries and Posch (2003).

If the soil is calcareous soil, cation exchange is not simulated as the variation in BC is dominated by that of Ca^{2+} which is controlled by the dissolution of Ca-carbonates. It is modelled by:

$$[\mathrm{Ca}^{2+}] = \frac{K_{carb}[\mathrm{H}^+]}{[\mathrm{HCO}_3^-]} \quad (63)$$

with K_{carb} (mol L^{-1}) is the temperature-dependent equilibrium constant,

$$K_{carb} = 10^{1.849}\exp\left[-\frac{\Delta H}{R}\left(\frac{1}{T}-\frac{1}{T_0}\right)\right] \quad (64)$$

Here, T is the temperature (in K), ΔH=22600 kJ mol^{-1}, R is the universal gas constant (= 8.314), T_0=298 K. To convert K_{carb} to Eq m^{-3}, the above equation is multiplied by 2000.

The dissociation of dissolved organic carbon can be modelled by:

$$[RCOO^-] = \frac{m * DOC * K_{org}}{K_{org} + [\mathrm{H}^+]} \quad (65)$$

where *DOC* is the concentration of dissolved organic carbon (in mol C m^{-3}), m is the charge density of functional groups (in mol (mol C)$^{-1}$) which is set to 0.12. K_{org} is the dissociation constant (in mol L^{-1}) which can be calculated by:

$$K_{org} = 10^{-(0.96+0.9pH-0.039pH^2)} \quad (66)$$

If the concentration of organic acids (m*DOC) is missing, no organic anions are modelled in VSD$^+$.

The VSD$^+$ model has been extended to simulate the effects of long-term mineral or organic fertilization in both calcareous and non-calcareous soils by Zeng et al. (2017). As a consequence, the S and P cycles have been included into VSD$^+$ model, where their equilibrium between dissolved and adsorbed in the soil-water interface is calculated by a Langmuir isotherm by:

$$X_{ad} = \frac{X_{max}X_{dis}}{X_{1/2} + X_{dis}} \quad (67)$$

X: SO_4, H_2PO_4

where X_{ad} (mEq kg^{-1}) is the amount of adsorbed SO_4^{2-} or $H_2PO_4^-$; X_{max} (mEq kg^{-1}) is maximum adsorption capacity of the soil; X_{dis} (mEq L^{-1}) is the dissolved SO_4^{2-} and $H_2PO_4^-$ and $X_{1/2}$ (mEq L^{-1}) is the half-saturation constant.

The mineral or organic fertilizers are considered to be dissolved within a year, implying that the non-adsorbed ions will get into the mass balance with the input from atmospheric deposition. Here, we denote X_{fer} (Eq m^{-2} yr^{-1}) as the total input of S or P from fertilization, then we have:

$$X_{fer} = X_{dis} + X_{ad} \quad (68)$$

2.1.3 Mass balance equations

The mass balances of cations (BC^{2+}, Na^+, NH_4^+) and anions (SO_4^{2-}, $H_2PO_4^-$, NO_3^-, Cl^-) are computed by:

$$\frac{d}{dt}X_{tot} = X_{in} - p_s[X] \quad (69)$$

for $X = BC^{2+}$, Na^+, NH_4^+, SO_4^{2-}, $H_2PO_4^-$, NO_3^-, Cl^-

where X_{tot} (Eq m^{-2}) denotes the total amount of above-mentioned cations and anions in the soil, X_{in} (Eq m^{-2} yr^{-1}) is the net influx of these ions (the sum of all inputs from atmospheric deposition as well as the uptake and release fluxes in the soil), and p_s (m yr^{-1}) is the precipitation surplus (equivalent to percolating water simulated in the hydrologic cycle model) in the thickness of the simulated soil layer. There is no mass balance for H^+, Al^{3+}, HCO_3^- and organic acids since their supply is considered as unlimited.

2.1.4 Input fluxes

The input fluxes for different anions are given by:

$$SO_{4in} = SO_{4dep} + SO_{4dis} \quad (70)$$

$$H_2PO_{4in} = H_2PO_{4dis} \quad (71)$$

$$Cl_{in} = Cl_{dep} \quad (72)$$

where X_{dep} (Eq m^{-2} yr^{-1}) is the deposition of the *X* element in ionic form, here the subscript *dep* denotes the total (dry + wet) atmospheric fallout; X_{dis} (Eq m^{-2}) is the dissolved SO_4^{2-} and $H_2PO_4^-$ in soil solution.

The input flux of ammonium (in Eq m^{-2} yr^{-1}) is modelled as atmospheric deposition plus N mineralization (N_{mi}, in Eq m^{-2} yr^{-1}) minus ammonium plant removal minus nitrification (subscript *nit*, in Eq m^{-2} yr^{-1}):

$$NH_{4in} = NH_{3dep} + N_{mi} - NH_{4rem} - NH_{4nit} \quad (73)$$

The input flux of nitrate (in Eq m^{-2} yr^{-1}) is modelled as deposition (subscript *dep*, in Eq m^{-2} yr^{-1}) plus nitrification (subscript *nit*, in Eq m^{-2} yr^{-1}) minus nitrate plant removal (subscript *rem*, in Eq m^{-2} yr-1) minus denitrification (subscript *denit*, in Eq m^{-2} yr^{-1}):

$$NO_{3in} = \mathrm{NO}_{xdep} + NH_{4nit} - NO_{3rem} - NO_{3denit} \qquad (74)$$

The N processes are dependent on the turnover of different organic carbon pools. In VSD^+ model, the turnover of *SOC* is computed by RothC model. A detailed description of N processes is given further in Section 2.1.7, N processes.

The input fluxes for base cations are computed as deposition plus fertilization (subscript *fer*, in Eq m^{-2} yr^{-1}) plus weathering (subscript *we*, in Eq m^{-3} yr^{-1}) minus net plant uptake

$$Y_{in} = \max\{Y_{dep} + Y_{fer} + z * Y_{we} - Y_{rem},\ p_s[Y_{min}]\} \qquad (75)$$

$$with\ Y = \mathrm{Ca}, \mathrm{Mg}, \mathrm{K}$$

Where $[Y_{min}]$ (Eq m^{-3}) is a given minimum concentration in soil solution. If its value is missing, $[Y_{min}]$ is set to 0. Consequently, $BC_{in} = Ca_{in} + Mg_{in} + K_{in}$.

For sodium, the input flux is given as the sum of deposition and weathering:

$$Na_{in} = Na_{dep} + z * Na_{we} \qquad (76)$$

2.1.5 Solution method for H^+ in the charge balance

In order to obtain $[\mathrm{H}^+]$, we need to denote the charge balance equation into a function of $[\mathrm{H}^+]$.

For $X = \mathrm{SO}_4^{2-}$, NO_3^-, NH_4^+, Na^+, Cl^-, $\mathrm{H_2PO_4^-}$, their concentrations in the end of year *n* are computed by discretizing the mass balance equation, which can be solved as:

$$[X]_n = \frac{\theta z[X]_{n-1} + [X]_{in}}{\theta z + p_{s,n}} \qquad (77)$$

where θ (S.D.) is the soil moisture of the layer of the first z m; p_s (m yr^{-1}) is the annual precipitation surplus.

The concentrations of Al^{3+}, HCO_3^-, and RCOO^- are computed from equilibrium equations with $[\mathrm{H}^+]$.

From the charge balance equation, the amount of the total base cations can be denoted as:

$$[BC^{2+}] = [SO_4^{2-}] + [NO_3^-] + [H_2PO_4^-] + [Cl^-] + [HCO_3^-] \quad (78)$$

$$+[RCOO^-] - [Na^+] - [Al^{3+}] - [NH_4^+] - [H^+] = G([H^+])$$

where the concentration of base cations is computed as a function of $[H^+]$.

The change in base saturation is computed as:

$$E_{BC,n} = a * (b - [BC]_n) \quad (79)$$

with

$$a = \frac{\theta z + p_s}{p_s CEC} \quad and \quad b = \frac{1}{a} E_{BC,n-1} + \frac{\theta z [BC]_{n-1} + [BC]_{n-1}}{\theta z + p_s} \quad (80)$$

Here parameters a and b for year n are computed from soil moisture variables and parameters of base cations from previous year.

Using the Gapon exchange, we can reduce the above equations to yield a single non-linear equation of $[H^+]$:

$$E_{BC,n} \left(\frac{K_{AlBC} {K_{Alox}}^{1/3} [H^+]_n + K_{HBC} [H^+]_n}{\left(G([H^+]_n)\right)^{1/2}} + 1 \right) = 1 \quad (81)$$

Finally, we obtain a non-linear equation with only unknown variable $[H^+]_n$, which can be solved by a simple bisection algorithm. In our model, we set a seed value of 1 10^{-7} to compute the value of $[H^+]_n$ with a precision of 1 10^{-7}.

Once $[H^+]$ is solved, the concentrations of BC^{2+}, Al^{3+}, HCO_3^-, and $RCOO^-$ can be derived and be used as the initial values for next time step to cycle through the calculations.

2.1.6 Model initialization

To launch simulations with the VSD$^+$ model, all the time-dependent variables need to be known. Initial conditions of the following variables are also required:

a. The initial concentrations of $[SO_4^{2-}]_0$, $[NO_3^-]_0$, $[NH_4^+]_0$, $[BC^{2+}]_0$, $[Na^+]_0$, $[Cl^-]_0$
b. The initial base saturation: $E_{BC,0}$
c. The initial amount of C pools in RothC model (presented previously).

To estimate the initial concentrations of different ions, we assume that these ions are in equilibrium state, in which the net input of ion is compensated by the loss via water leaching, therefore:

$$[X]_0 = \frac{X_{in,0}}{p_{s,0}} \qquad (82)$$

for *X* = *SO₄*, *NO₃*, *NH₄*, *Na*, *Cl*, *BC*,

where $X_{in,0}$ denotes the input of *X* ion at the beginning of simulation, besides we assume that atmospheric deposition is the single input into soil.

If the value of soil $E_{BC,0}$ is known, the initial concentration of $[BC]_0$ can be calculated by Gapon exchange:

$$[BC]_0 = \left(\frac{E_{BC,0}\left(K_{AlBC}[\mathrm{Al^{3+}}]_0^{\frac{1}{3}} + K_{HBC}[\mathrm{H^+}]_0\right)}{1 - E_{BC,0}} \right)^2 \qquad (83)$$

Here, the values of $[\mathrm{Al^{3+}}]_0$ and $[\mathrm{H^+}]_0$ are unknown. $\mathrm{Al^{3+}}$ denotes as a function of $\mathrm{H^+}$ (equation 56), thus $[BC]_0$ can be also obtained by numerically solving the single non-linear equation of $[\mathrm{H^+}]$.

2.1.7 N processes

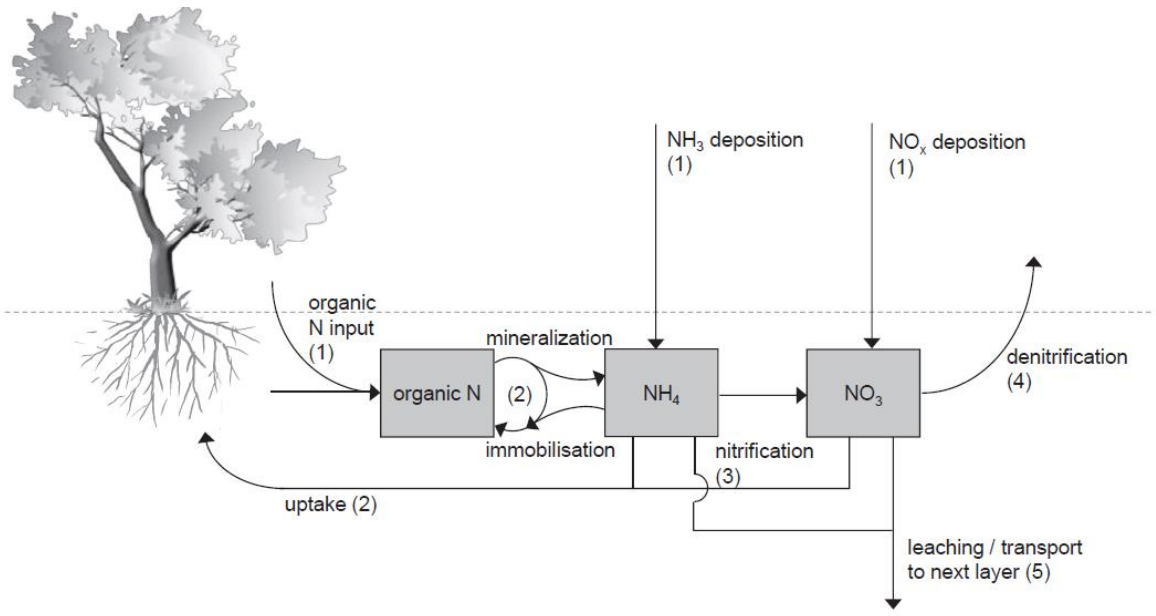

Figure 30. N processes in VSD$^+$, each number indicates the order of calculation, adapted from Bonten et al. (2016)

The N processes is sequentially computed in VSD$^+$ as illustrated in Figure 30. We will describe the calculation of annual net input of the ammonium and nitrate pools, by following these processes.

❖ *Organic N input*

In RothC model, vegetable residues can be deduced for a specific vegetation with its harvest index. The total organic N entering into soil is the sum of the influxes from plant residues (N_{lf}, in g m^{-2} yr^{-1}) and organic amendments (N_{org}, in g m^{-2} yr^{-1}).

$$N_{org} = CN_{org} * M_{org} * \%DW \quad (84)$$

$$N_{lf} = Resi * 100 * \frac{0.03}{0.45} \quad (85)$$

where CN_{org} (g kg^{-1}) is the content on N of amendments in dry mass; $M_{org,n}$ (kg FW m^{-2} yr^{-1}) is the application of amendments to fresh mass; $\%DW$ (S.D.) is the ratio of dry mass to fresh mass in %; $Resi_n$ is the amount of organic carbon contributed by vegetable residues (t C ha^{-1} yr^{-1}), here we multiple 100 for the unit conversion; For N litterfall flux, we assign 30 g N kg^{-1} in vegetable residues (Zhu et al., 2018a), with 45% C in vegetable residues, so C/N of vegetables is 0.03/0.45 = 15. We set this value as default for vegetables.

❖ *N removal by plants*

Our model uses a different approach to calculate the N loss via plant removal than the original model. We adapted the method of Zhu et al. (2018a), where N crop removal (N_{rem}, in g m^{-2}) is calculated as the sum of N content in harvested parts and crop residues:

$$N_{rem} = Y * \left(N_{RH} + R_{pla,dw} * N_{RR} * (1 - f_{CR})\right) \quad (86)$$

N_{RH} (g FW kg^{-1}) and N_{RR} (g DW kg^{-1}) denote the concentration of N in the removal harvested parts and crop residues, respectively; Y (kg FW m^{-2} $harvest^{-1}$) is the fresh mass harvested from plants. $R_{pla,dw}$ (S.D.) is the ratio of dry mass to fresh mass in the harvested part of plant,

estimated by (1- $W_{pla,dw}$) for vegetables; f_{CR} (S.D.) is the fraction of plant residues returned to cropland.

Crop removals for other ions (e.g., P, K, Ca, Mg, Na, S) are also simulated by using the same method. Values for different crops for the above parameters can be found in the Supplementary materials, Table A5 of Zhu et al. (2018a).

❖ *N mineralization and immobilization*

The N mineralization and immobilization are dependent on the turnover of C pools simulated by the RothC model. The net mineralization of N is calculated by the sum of changes of N in the five C pools:

$$N_{mi.Y,n} = \frac{C_{net,Y,n} * 100}{CN_{Y,n} * 14} - N_{im.Y,n-1} \quad (87)$$

$$N_{mi.IOM} = 0 \quad (88)$$

with (*Y = DPM, RPM, BIO, HUM),*

where $N_{mi.Y,n}$ (g m^{-2} yr^{-1}) is the net N mineralization of *Y* pool for year *n*; $N_{im.Y,n-1}$ (g m^{-2} yr^{-1}) is the N immobilization of *Y* pool for year *n-1*; $C_{net,Y,n}$ (t C ha^{-1} yr^{-1}) is the input of organic carbon from plant residues to *Y* pool during the year *n*, here we multiple 100 to convert the unit from t C ha^{-1} to g m^{-2}; $CN_{Y,n}$ (S.D.) is the C/N ratio of *Y* pool for year *n*. Following the C turnover, the N mineralization of IOM pool is neglected.

The immobilization of N for different C pools is calculated by:

$$N_{im.Y,n} = \frac{C_{Y,n} * 100}{CN_{Y,n} * 14} - \frac{C_{Y,n-1} * 100}{CN_{Y,n-1} * 14} \quad (89)$$

with (*Y = DPM, RPM, BIO, HUM, IOM),*

where $C_{Y,n}$ (t C ha^{-1}) is the amount of organic carbon in the *Y* pool for year n; $C_{Y,n-1}$ (t C ha^{-1}) is the amount of organic carbon in the *Y* pool for year $n-1$; $CN_{Y,n-1}$ (S.D.) is the C/N ratio of *Y* pool for year *n-1*. We multiply by 100 to convert the unit from t C ha^{-1} to g m^{-2}.

If the soil is under vegetation cover, the transfer of N to HUM pool is reduced until sufficient of N is available for uptake. N_{upeff} (S.D.) is the fraction of available N that plants can take up,

with value between 0.9–1.0, here we use the default value (0.92) of VSD^{+} for all vegetations. Therefore, $N_{im,HUM}$ can be computed by the following conditional equation:

$$If \left(N_{dep} - N_{im,tot} - \frac{N_{rem}}{N_{upeff}} \right) < 0 \qquad (90)$$

$$then,$$

$$N_{im.HUM} = max\left(\begin{pmatrix} N_{im.HUM} + N_{dep} - N_{im,tot} \\ - \frac{N_{rem}}{N_{upeff}} \end{pmatrix}, 0 \right)$$

Where N_{dep} (g m^{-2} yr^{-1}) is the atmospheric deposition of nitrogen, which is the sum of NH_3 and NO_x deposition; N_{rem} (g m^{-2} yr^{-1}) is the nitrogen uptake (only in nitrate form) by vegetation removal.

The C/N ratios of the five SOC compartments are determined differently. For the RPM, BIO and IOM pools, we use fixed C/N ratio values: 100 for RPM, 8.5 for BIO and 10 for IOM. For DPM, the C/N ratio in the end of year *n* is calculated from the N content of plant residues:

$$CN_{DPM,n} = \frac{\left(C_{DPM,n} + C_{net,DPM,n}\right) * 100}{\frac{C_{DPM,n-1} * 100}{CN_{DPM,n-1}} + N_{org} + N_{lf} - \frac{C_{net,RPM,n} * 100}{CN_{RPM}}} \qquad (91)$$

where $C_{DPM,n}$ (t C ha^{-1}) is the amount of organic carbon in the DPM pool at the end of year n; $C_{net,DPM,n}$ (t C ha^{-1})is the input of organic carbon from plant residues to *DPM* pool during the year n; $C_{net,RPM,n}$ (t C ha^{-1}) is the input of organic carbon from plant residues to *RPM* pool during the year n; CN_{RPM} is the C/N ratio for RPM pool.

For HUM, the C/N ratio is initialized by the total amount of N in soil and the C/N ratios of the other C pools:

$$CN_{HUM,n} = \frac{C_{HUM,n-1}}{\frac{C_{SOC,n-1}}{CN_{init}} - \left(\begin{matrix} \frac{C_{DPM,n-1}}{CN_{DPM,n-1}} + \frac{C_{RPM,n-1}}{CN_{RPM}} + \frac{C_{BIO,n-1}}{CN_{BIO}} \\ + \frac{C_{IOM,n-1}}{CN_{IOM}} \end{matrix} \right)} \qquad (92)$$

where $C_{SOC,n-1}$ (t C ha^{-1}) is the total amount of organic carbon in soil at the end of year *n-1*; CN_{init} (S.D.) is the initial C/N ratio of soil.

The biological N fixation is neglected for all vegetables in our model, denoting N_{fix} = 0. For all fluxes of N, all equations are divided by 14 to convert the unit g N m^{-2} to Eq N m^{-2} respectively.

❖ *N nitrification and denitrification*

The NH_4 nitrification follows the order of calculation presented in Figure 30:

$$NH_{4nit} = min\begin{pmatrix}\left(NH_{3dep} + N_{mi,tot} - NH_{4rem}\right) * k_{nit}, \\ NH_{3dep} + N_{mi,tot} - NH_{4,rem}\end{pmatrix} \quad (93)$$

Similarly, the NO_3 denitrification is calculated as:

$$NO_{3denit} = max\left(\left(NO_{xdep} - NO_{3rem} + NH_{4nit}\right) * k_{denit}, 0\right) \quad (94)$$

with k_{nit} and k_{denit} (yr^{-1}) are the first order rate constants for nitrification and denitrification at given pH:

$$k_{nit} = k_{nit,max} * rf_{nit} * \frac{1}{1 + exp^{(4*(2.75-pH))}} \quad (95)$$

$$k_{denit} = k_{denit,max} * rf_{denit} * \frac{1}{1 + exp^{(2.5*(5-pH))}} \quad (96)$$

where $k_{nit,max}$ and $k_{denit,max}$ (yr^{-1}) are the maximum nitrification and denitrification rates, setting their default values as 4; rf_{nit} and rf_{denit} (S.D.) are the reduction factors for nitrification and denitrification depending on temperature and soil moisture. The reduction factors are pre-calculated by using daily or monthly average values of temperature and soil moisture in our hydrologic cycle model. The detailed calculation can be found in the supplementary material, equations M12-M19 of Bonten et al. (2016).

2.2 Data collection for pH modelling in the King's Vegetable Garden

2.2.1 Site descriptions and soil characteristics

The King's Vegetable Garden (KVG) is located in an urban area, next to the Palace of Versailles (France), created between 1678 and 1683 by Jean-Baptiste de La Quintinie. Sixteen plots in the centre of KVG are used to grow vegetables since its construction. During the last 300 years,

large amounts of organic matters, such as compost of horse manure, cattle manure and green waste compost, have been amended into these plots to gradually build up a productive soil. For this study, we focus on the impacts of organic matters management on soil acidification and the validation of VSD^+ in the KVG. Table 23 shows climate conditions of the site. The measured current soil characteristics of the 16 plots are presented in Table 26 of Chapter 4. Initial data of soil characteristics was derived from the parental materials of KVG soils. More details about site information can be found in the Chapter 4, section Materials and Methods.

Table 23. Monthly climate data of King's Vegetable Garden (Versailles). Description of acronyms: Tem = monthly average temperature (℃), Pre = monthly average precipitation (mm), Eva_po = monthly potential evapotranspiration (mm), Pre1mm = number of wet days with precipitation more than 1mm, Sun = monthly average sunshine hours (hr), Tmx = monthly average maximum temperature (℃), Tmn = monthly average minimum temperature (℃)

Site	Month	Tem	Pre	Eva_po	Pre1mm	Sun	Tmx	Tmn
KVG	Jan	3.8	58.2	11	11.1	61.8	6.3	1.3
KVG	Feb	4.3	49.0	19.3	10.0	76.5	7.4	1.3
KVG	Mar	7.5	52.5	48.8	10.8	127.3	11.3	3.6
KVG	Apr	10.0	54.4	80.1	9.7	164.6	14.6	5.5
KVG	May	13.8	63.1	112	10.5	195.3	18.5	9.1
KVG	Jun	16.9	53.6	129.7	8.6	209.3	21.7	12.0
KVG	Jul	19.2	62.4	136.8	8.2	216.4	24.3	14.0
KVG	Aug	19.0	54.0	119.0	7.6	209.9	24.2	13.8
KVG	Sep	15.7	51.7	71.3	8.2	167.0	20.4	11.0
KVG	Oct	11.8	67.6	35.6	9.5	112.1	15.6	8.1
KVG	Nov	7.1	55.8	12.6	10.0	64.9	10.0	4.2
KVG	Dec	4.3	64.2	8.8	11.3	51.5	6.6	2.0

Data collection for pH modelling is a challenging mission since the starting point of simulation dates back to 1683. Some parameters have to be indirectly deduced by existing available data. High tolerance has to be given to the accuracy of deduced parameters. Data-collection for model initialization and specifically parameters related to element influxes are presented in detail below.

2.2.2 Atmospheric deposition and minerals' weathering

Atmospheric deposition data for different elements was collected from a European Monitoring and Evaluation Program (EMEP) at national scale of total of 17 monitoring stations, during the period of 1978-2019. Only wet deposition data are available from these stations, shown in Figure 31. We can observe that the atmospheric deposition of all elements decreases sharply

from 1978 to 1990. The atmospheric deposition of these elements tends to a lower and stable phase since 1990. As we do not have access to data on the atmospheric deposition of each element for the period from 1683 to 1978, we have assumed that their values are at a low level similar to the average value for the period from 1990 to 2019. For initializing the model, we therefore used the average values of the period from 1990-2019. To convert wet deposition to bulk deposition for all elements, we referred to the bulk:wet deposition ratios used at Rothamsted Research (UK) by Xu et al. (2020). Bulk deposition values were estimated by multiplying wet deposition with 2.2 for NH_4^+, 4.35 for NO_3^-, and 2 for Ca^{2+}, Cl^-, Mg^{2+}, K^+, Na^+, SO_4^{2-}. Average annual bulk depositions of different elements are shown in Table 25.

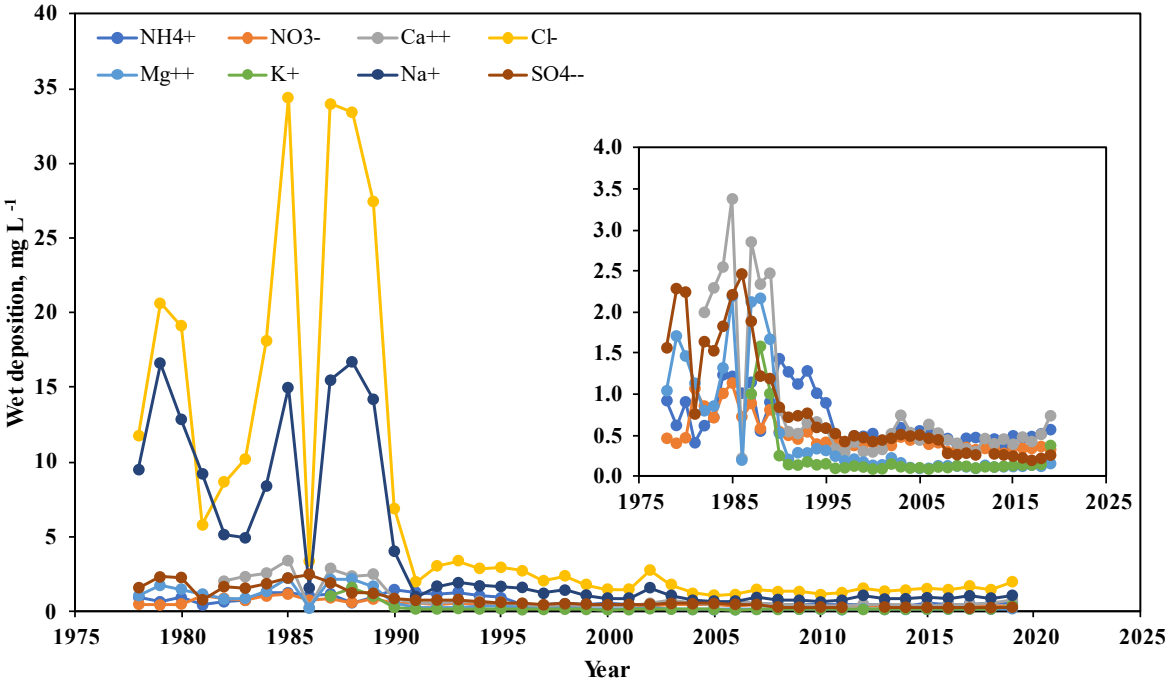

Figure 31. Average wet atmospheric depositions of nitrogen (NH_4 and NO_3), sulphate (SO_4), chloride (Cl) and base cations (K, Na, Ca, Mg) recorded from 17 monitoring stations in France, from 1978-2019 (main graphic); reduced graph shows values of NH_4, NO_3, SO_4, K, Ca, Mg with appropriate y axis scale.

Many studies have been done to estimate the weathering rate of silicate minerals under field conditions. In Sverdrup and Warfvinge (1988), the base cation fluxes from mineral weathering were estimated to 0.1-0.3 kEq ha^{-1} yr^{-1} for agricultural soils. Duan et al. (2002) have also estimated the base cation fluxes from weathering rate for different type soils sampled from different regions of China. We have compared the total element contents of TiO, CaO, MgO, K_2O, N_2O in KVG's soils and its parental soil with those studied in Duan et al. (2002). We assumed that the weathering rate in KVG's soils equal to brown forest soil, derived to around

0.25 kEq ha^{-1} yr^{-1} by using different methods in the study of Duan et al. (2002). Hence, we have chosen an average value regarding to the two references, with a weathering rate of 0.225 kEq ha^{-1} yr^{-1} for base cation fluxes. More details are presented in Chapter 4 about how the parental soil of KVG's soils has been determined.

Individual Ca, Mg, K, Na fluxes from weathering can be also derived by using the regression equations in Ouimet and Duchesne. (2005), respectively. Total BC fluxes from weathering are obtained by multiplying Ca flux by 0.362 (R^2=0.81), Mg flux by 0.235 (R^2=0.86), K flux by 0.158 (R^2=0.71), Na flux by 0.245 (R^2=0.42). The fluxes from soil mineral weathering for the four elements are shown in Table 25.

2.2.3 Input by fertilization and removal by crops

From the establishment of the King's Vegetable Garden (1683) until the end of the 20th century, only compost made from horse manure (called *terreau*) and cow manure were applied to the soil to improve its fertility. The use of chemical fertilizers in the King's Garden started in 1950 and was stopped completely in 2000. Since 2000, soil is regularly amended with compost. The quantity of elements added with the fertilizer can be calculated fertilizer composition and the annual amount of fertilizer used. More details about fertilization management can be found in Chapter 4, sections 2.2.4-2.2.5. Concentrations of different elements (e.g., N, P, K, Ca, Mg, Na, S) in cow manure, green waste compost, NPK type fertilizer, *terreau* are presented in Table 24.

Table 24. Characterization of fertilizers for soil pH modelling

Fertilizer	DW (%)	Element contents (g (kg DW)$^{-1}$)							
		N	P	K	Ca	Mg	Na	S	Reference
Cattle manure	20	28.5	6.50	28.5	31.8	7.00	0	0	Houot et al. (2014)
Green waste composts	62	14.0	2.62	11.6	55.7	4.22	0	0	Houot et al. (2014)
Terreau	41	12.7	3.94	16.0	21.1	4.22	0	0	Doligez and Leveau (2007)
NPK fertilizer 3-6-9	100	34.9	69.8	103	14.0	2.85	3	105	Verbeeck et al. (2020)

The removal of different elements (*e.g.*, N, P, K, Ca, Mg, Na, S) was calculated by multiplying the dry matter yields of harvest parts (grain, stem) and crop residues with element concentrations in these parts. Crop rotation has also been considered in simulation (see more in

Chapter 4). Relative parameters are presented in Table 25, as well as the fixed soil parameters and model parameters for different element turnover processes.

Table 25. Values of used parameters for soil pH modelling in KVG

Parameter	Description	Unit	Value	Data sources
Input fluxes				
X_{dep}	Deposition of SO_2	eq m^{-2} yr^{-1}	0.021	EMEP[a]
	Deposition of NO_X	eq m^{-2} yr^{-1}	0.062	EMEP
	Deposition of NH_3	eq m^{-2} yr^{-1}	0.11	EMEP
	Deposition of Ca	eq m^{-2} yr^{-1}	0.015	EMEP
	Deposition of Mg	eq m^{-2} yr^{-1}	0.015	EMEP
	Deposition of K	eq m^{-2} yr^{-1}	0.016	EMEP
	Deposition of Na	eq m^{-2} yr^{-1}	0.035	EMEP
	Deposition of Cl	eq m^{-2} yr^{-1}	0.057	EMEP
X_{we}	Weathering rate of Ca	eq m^{-2} yr^{-1}	0.0081	Duan et al. (2002); Ouimet and Duchesne. (2005); Sverdrup and Warfvinge. (1988)
	Weathering rate of Mg	eq m^{-2} yr^{-1}	0.0053	
	Weathering rate of K	eq m^{-2} yr^{-1}	0.0036	
	Weathering rate of Na	eq m^{-2} yr^{-1}	0.0055	
X_{fer}	Annual element (N, P, K, Ca, Mg, Na, S) input from fertilization	eq m^{-2} yr^{-1}	Calculated[b]	Doligez and Leveau (2007); Houot et al. (2014); Verbeeck et al. (2020)
Output fluxes				
X_{rem}	Annual element (N, K, Ca, Mg, P) removal from soil by crop harvest	eq m^{-2} yr^{-1}	Calculated	Zhu et al. (2018a)
Soil properties				
z	Thickness of the ploughing soil layer	m	0.65, 0.35, 0.25, 0.2	Historical gardening practices
p_{CO2}	Partial pressure of CO_2 in the soil solution	atm	0.0004	Bonten et al. (2015)
ρ	Average bulk density of the soil	g cm^{-3}	Calculated	MetHyd model

clay	Clay content of the soil	%	26.1	Measured[c]
CEC	Cation exchange capacity	meq kg^{-1}	119	Measured
$E_{BC,0}$	Initial base saturation	–	0.396	Measured
$Cpool_0$	Initial amount of C in topsoil (per unit area)	g m^{-2}	Calculated	Zimmermann (2007)
CN_{init}	Initial C:N ratio in topsoil	g g^{-1}	11.6	Measured
Model parameters				
$k_{nit,max}$	Maximum nitrification rate	yr^{-1}	4	EMEP
$k_{denit,max}$	Maximum denitrification rate	yr^{-1}	4	EMEP
rf_{nit}	Reduction factor for nitrification	-	Calculated	MetHyd model
rf_{denit}	Reduction factor for denitrification	-	Calculated	MetHyd model
$H_2PO_{4,max}$	Maximum P adsorption capacity	meq kg^{-1}	35	Xu et al. (2020)
$H_2PO_{4,1/2}$	Constant of half-saturation adsorption	meq L^{-1}	0.2	Xu et al. (2020)
$SO_{4,max}$	Maximum S adsorption capacity	meq kg^{-1}	1.4	Xu et al. (2020)
$SO_{4,1/2}$	Constant of half-saturation adsorption	meq L^{-1}	0.2	Xu et al. (2020)
lgK_{AlBC}	log_{10} of selectivity constant for Al-Bc exchange	-	0	Vries and Posch (2003)
lgK_{HBC}	log_{10} of selectivity constant for H-Bc exchange	-	3.2	Vries and Posch (2003)
lgK_{Alox}	log_{10} of gibbsite equilibrium constant	-	8	Vries and Posch (2003)

[a] European Monitoring and Evaluation Program.

[b] denotes parameters calculated in model, especially for those which change depending on annual gardening practices.

[c] denotes parameters measured from soil samples.

3 Results and discussion

3.1 Evaluating simulated soil pH with measured values

We applied an improved version of the VSD^+ model to simulate soil pH changes in KVG since its creation. The initial soil pH value was extrapolated from the measure on parent soil, which is equal to 4.96. The current pH value of soils in KVG, which has an average value of 7.46, was obtained by analysis of collected soil samples from 16 vegetable plots of KVG.

Initial soil pH in VSD^+ was simulated from deposition and weathering data. The mass balances of all elements are considered to be equilibrium, meaning that all inputs of elements equal to output by leaching. It was estimated to 4.72, which is slightly lower than the measured value from parental soil (4.96). Shown in Figure 32, different trends in soil pH have occurred for different periods. Over 300 years of continuous soil use, soil pH has significantly increased from 4.72 to 7.46. The simulated present-day soil pH (7.46) is consistent with the measured value. This indicates that VSD^+ was able to reconstruct both trends and values of soil pH, in response to different historical fertilization managements in KVG.

3.2 Main drivers of soil pH changing in KVG during the period of 1683-2021

To identity main drivers which result to soil pH altering, we divided the trend of soil pH into 4 stages according to the differences in gardening practices.

During 1683-1690, sharp increases of soil pH were observed along with an application rate of 6.66 to 39.96 kg DW m^{-2} yr^{-1} of *terreau* to soil every year (Figure 32). Subsequently, from 1690 to 1712, soil pH value was at a steady point and base saturation (BS) has basically reached to its saturation value (Figure 32; Figure 33). For the period of 1710-1723, those plots were left fallow and soil pH dropped by more than one unit. It came back to the previous steady point once gardening activities returned to KVG. Another significant change occurred during the period of 1920-2000, while *terreau* started to be replaced by NPK-type mineral fertilizer and cow manure. During this period, annual use of NPK-type fertilizer caused a reduction of soil pH. Contrarily, application of cow manures every 3 years repeatedly increased the pH. That can explain why a fluctuation of pH occurred during this period. From 2000 to 2021, green waste compost (GWC) replaced NPK-type fertilizer and cow manure in KVG. During this period, 6 kg FW m^{-2} of crop residues compost were applied in the plots with squash, cucumber and

tomato, considered as vegetables with high nutrient requirements. Additionally, purchased GWC was also applied on the seedlings of carrot, mesclun, beet and turnip, at a rate of 36 kg FW m^{-2}. Due to plant rotation, soil pH dropped down while no GWC was applied, and once GWC was added, soil pH raised rapidly and BS reached its saturation state. This is confirmed by our observation in which measured BS is infinitely close to 1 for the topsoil samples collected in 2021.

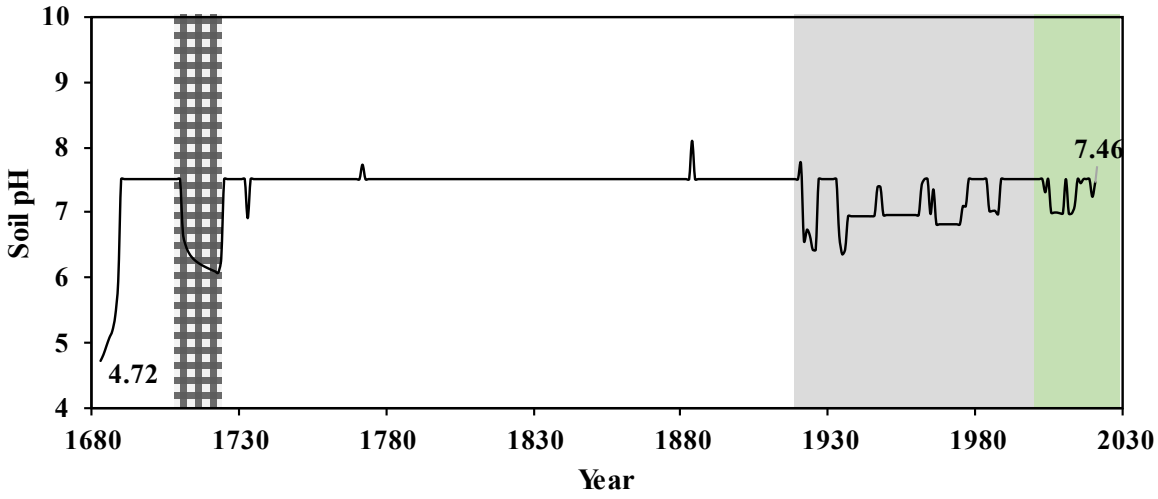

Figure 32. Predicted changes in soil pH during the period of 1683-2021 under historical gardening practices in the KVG. Background colors denote different gardening practices: terreau application (white); grassland (black dot); NPK-type fertilizer and cow manure (grey); green waste compost (green)

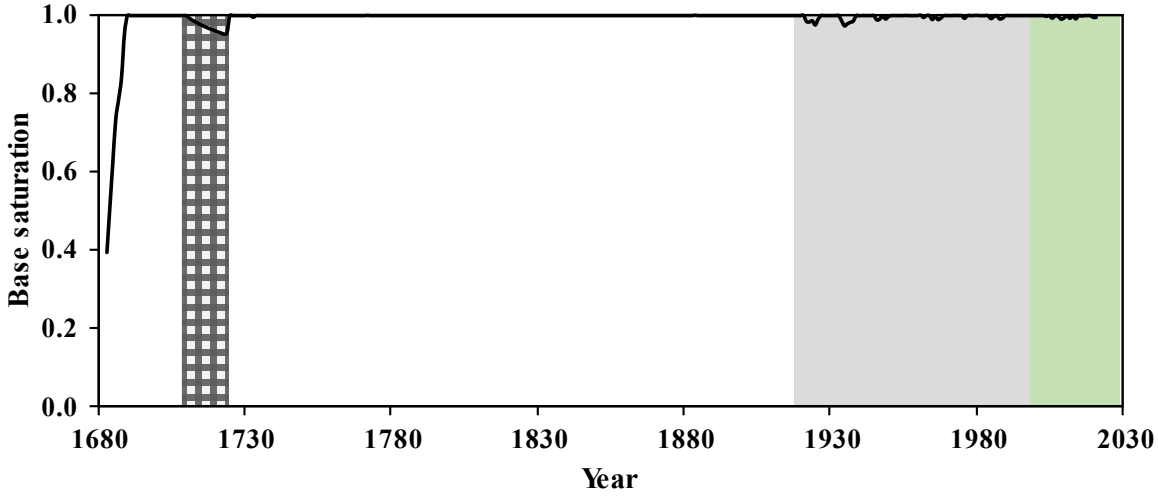

Figure 33. Predicted changes in base saturation during the period of 1683-2021 under historical gardening practices in the KVG. Background colors denote different gardening practices: *terreau* application (white); grassland (black dot); NPK-type fertilizer and cow manure (grey); green waste compost (green)

In Figure 34, we observed that simulated BS shows a linear relationship with H^+ as reported previously by Xu et al. (2020) from long-term liming experiments. A small change in base saturation can lead to a unit change in soil pH when it reaches above 90%, observed during the period of 1930 to 2021 in KVG. At this time, the base saturation of soil began to reach a saturation value. Soil pH no longer increased with the addition of organic fertilizers.

Figure 35 and Figure 36 show the acidity budgets for different gardening practices in KVG during the period of 1683-2021. Most of the acidity production came from N transformation, and followed by BC uptake by crops. Long-term addition of *terreau* and GWC with large amounts led to decrease of soil acid neutralizing capacity (ANC), which is a measure of the ability of water to neutralize acid inputs. The ANC consumption of each treatment was actually dominated by net BC^{2+} input, resulting in Al^{3+} immobilization and meanwhile raising soil pH. For the fallow period, the decrease of soil pH (net H^+ production) was due to BC^{2+} leaching (with negative net BC^{2+} balance). For the period of NPK-Manure treatment, the effects of NPK-type fertilizer and cow manure on soil pH altering compensated for each other. These results are generally consistent with previous studies that soil pH declines with the use of chemical fertilizer (because of N transformation) and increases with liming or organic amendment (because of BC^{2+} input) (Xu et al., 2020; Zeng et al., 2017; Zhu et al., 2018a).

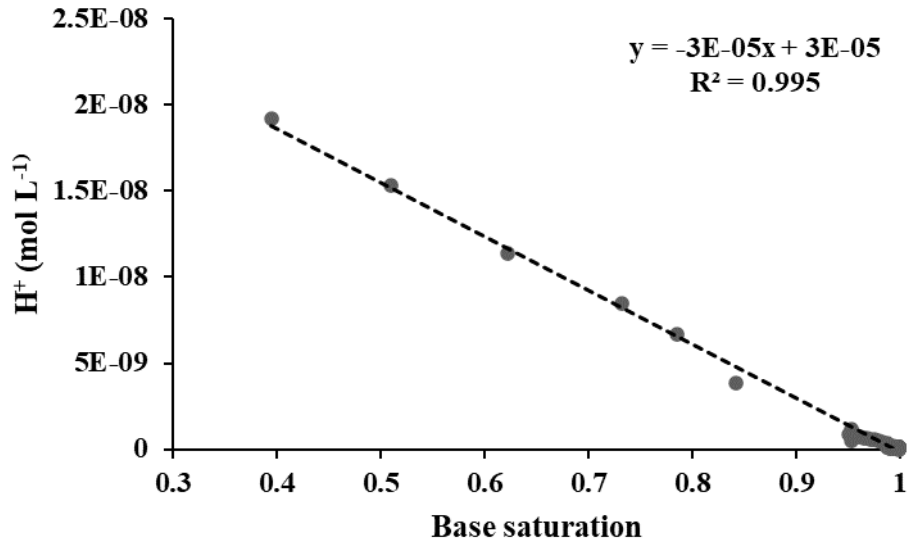

Figure 34. Relationship between base saturation (BS) and H^+ in KVG's soils, as simulated with VSD+.

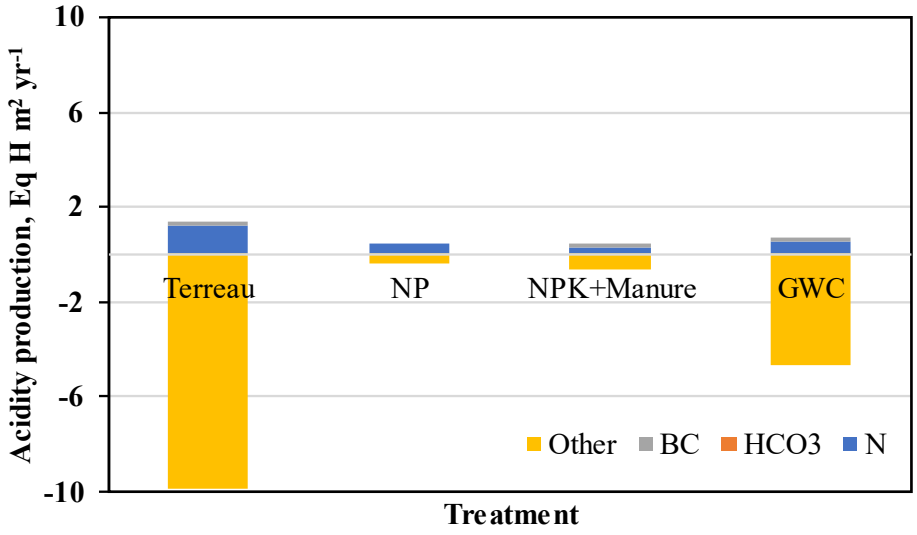

Figure 35. Acidity production simulated by VSD$^+$ for different gardening practices in KVG during the period of 1683-2021. NP: no practices; Terreau: horse manure compost input; NPK+Manure: NPK-type of fertilizer and cow manure input; GWC: green waste compost input. Method adapted from Zeng: Acidity production (N: net NO3 leaching plus net NH4 input; HCO3: net HCO3 leaching; BC: BC removal by crops; Other: net H, SO4, Cl and PO4 release (output minus input)) and Acidity consumption (Al: net Al leaching; BC: BC input minus BC uptake minus BC leaching)

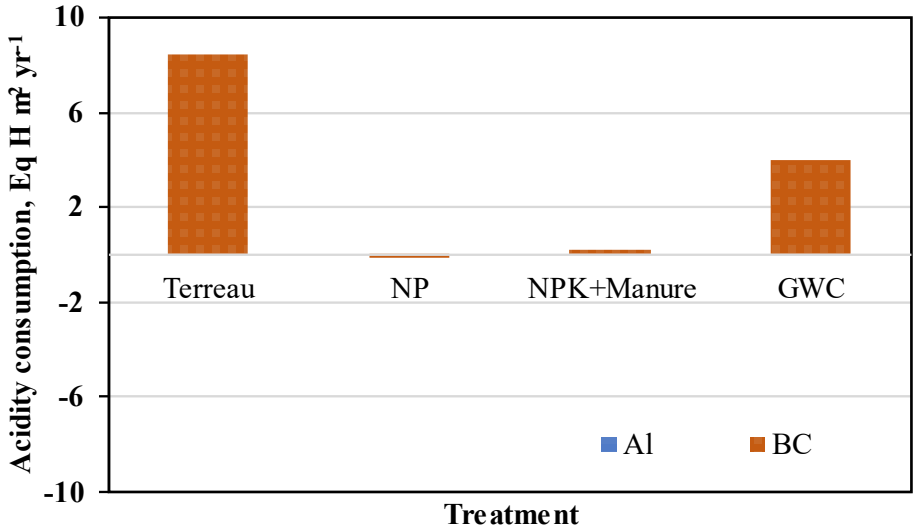

Figure 36. Acidity consumption simulated by VSD$^+$ for different gardening practices in KVG during the period of 1683-2021. NP: no practices; Terreau: horse manure compost input; NPK+Manure: NPK-type of fertilizer and cow manure input; GWC: green waste compost input. Method adapted from Zeng: Acidity production (N: net NO3 leaching plus net NH4 input; HCO3: net HCO3 leaching; BC: BC removal by crops; Other: net H, SO4, Cl and PO4 release (utput minus input)) and Acidity consumption (Al: net Al leaching; BC: BC input minus BC uptake minus BC leachin

Chapitre 4 : Tendances historiques et futures des teneurs en métaux traces dans les sols du Potager du Roi (Versailles, France)

The King's Vegetable Garden (Potager du Roi) in Versailles, which has more than 300 years of gardening practices since its creation in 1683, has been chosen in this study in order to test a mass balance model using historical fluxes, against the current trace metal contents. We have collected historical data on gardening practices and trace metal fluxes from 1683 to 2021, including different metal input flows such as atmospheric deposition, fertilizers, organic amendments, as well as crop rotation and ploughing depth. Parent material has been identified and analysed for obtaining the initial soil physicochemical properties of King's Garden soils in 1683. Current soil physicochemical properties were achieved by soil analysis in 2021. This work studies the accuracy of our model on modelling the long-term evolution of soil trace metal contents (Cd, Cu, Pb and Zn) since the creation of the site. We have also predicted the future trends of these trace metal contents by considering no changes on the current gardening practices and the environmental conditions (*e.g.*, climate, atmospheric fallout) for the next century.

This chapter will be submitted to an international peer reviewed journal.

1 Introduction

Vegetable gardens, the major form of urban agriculture in France, show a significant development since the last 20 years (Zhong et al., 2021). In response to citizen demand, more and more allotment gardens are springing up in different metropolises (France Urbaine, 2018; Torres et al., 2018). These vegetable gardens appear a promising way to improve food security and different eco-system services, such as regulation of water cycle and local climate, biodiversity or social connection (Santo and Palmer, 2016).

Trace metal concentrations in urban garden soils are often above the geochemical background values and the contents in soils from different eco-systems (forest, meadow, conventional agriculture) (Joimel et al., 2016). As other urban soils, garden soils can be polluted by trace metals, such as Cd, Cu, Pb and Zn (Douay et al., 2008b, 2008a; Joimel et al., 2016; Kachenko and Singh, 2006; Li et al., 2013; Schwartz, 2013a, 2013b; Wei and Yang, 2010) which originate from different sources, such as alteration of soil parent material, former land use, weathering of technogenic materials, deposition of volcanic, industrial and urban emissions into the atmosphere, and agricultural inputs (Alloway, 2013b, 2004; Arora et al., 2008; Bidar et al., 2020; Hernandez et al., 2003; Li et al., 2013; Li et al., 2001; Nriagu, 1989). These metals can be absorbed by plant roots and translocated to their edible parts, leading to an overexposure of their consumers (Fillol et al., 2021a; Oleko et al., 2021). A national biomonitoring program in 2014-2016 shows that there is an impregnation of the French population (including children) by different heavy metals. Particularly, 48% of the French adult population aged from 18 to 60 (N = 1716) has a cadmiuria greater than 0.5 µg g^{-1} of creatinine in urine, proposed as the critical concentration for a 60 years old adult while assuming that ingestion is the only source of cadmium exposure (Fillol et al., 2021a, 2021b). The determinants of exposure of Cd, Cu, Pb are mainly dietary. For non-smokers, such as children, the consumption of cereals is the main source of Cd. Moreover, foods from organic agriculture result to the impregnation of population by Cu (Fillol et al., 2021a, 2021b). Manure, mineral fertilizers and pesticides were found the most important sources of trace metals input in agricultural soils (Belon et al., 2012). In addition, organic amendments, such as compost, can import more than 10 times of Pb and Zn into soils than of atmospheric deposition (Weissengruber et al., 2018). These organic wastes are often used in vegetable gardens to store carbon and recycle organic wastes, recovering soil fertility as recommended by organic farming. Due to the lack of restriction, improper gardening practices, such as over-fertilization with organic amendments and P fertilizers, or excessive fungicide application can lead to an irreversible soil contamination with trace metals (Joimel et

al., 2021; Zhong et al., 2021). In order to ensure the sustainability of urban agriculture, it is important to evaluate the effect of gardening practices on trace metal content in soils, on the medium (decade) and on the long (century) term.

Modelling mass balance of trace metal fluxes in soil is a tool which has been used to predict the evolution of the soil metal contents on the long term and to determine its most influent factors. This method was used to estimate evolution of Cd in agricultural soils at the country or continent scale, under various scenarios (de Vries and McLaughlin, 2013b; Six and Smolders, 2014; Sterckeman et al., 2019, 2018; Yang et al., 2021). Mass balances were also simulated in vegetable garden soils, currently for Cd, Cu, Pb and Zn in France (Zhong et al., 2021). However, these modellings could not be validated as their outputs, typically the future trace metal content in soil after the coming decades or century, could not be measured. Their predictions were therefore uncertain, resulting on that of the numerous input variables of the model. One way to assess the validity of such modelling is to simulate past metal fluxes and to compare the resulting metal concentrations to current values in the studied soil layers. However, it is difficult to obtain data concerning initial soil conditions and historical cultivation practices to feed a mass balance modelling of the past fluxes, particularly over the whole previous century. It is probably the reason why there is few studies dealing with validation of long term simulation of soil metal evolution. Yang et al. (2021) deduced historical and future trends of Cd content in rice soils in China based on long-term regional investigation of cadmium input and output pathways in field scale. By coupling a Freundlich-type transfer function for plant uptake and a soil acidification model (VSD^{+}) (Bonten et al., 2016), their simulated Cd values were very close to field measurements, with the differences being -2.37% and +1.29%. Another study is from McDowell and Gray (2022), in which the change in topsoil Cd for the last few decades has been well simulated in three long-term grazed pasture trials in New Zealand, by using a mass balance model.

At the end of the 17^{th} century, Louis XIV commissioned Jean-Baptiste de La Quintinie to create a kitchen garden of 9 ha next to his palace in Versailles (France). Since 1683, the central part of this garden (denotes “The Great Square”, with a total surface around 1.4 ha) has been used to produce vegetables. The ways about how its vegetation plots were constructed and cultivated along the past three centuries are relatively well documented. Under this context, it appeared as an exceptional opportunity to assess the accuracy of mass balance modelling, by reconstituting the past fluxes of Cd, Cu, Pb and Zn in the topsoil and comparing the model simulated results to the current measured metal contents.

2 Materials and methods

2.1 Study site: brief history

The King's Vegetable Garden (KVG) is located in an urban area, next to the Palace of Versailles (France) (Figure 37). It was created between 1678 and 1683 by Jean-Baptiste de La Quintinie (La Quintinie, 1690) to supply the table of king Louis XIV with fruits and vegetables. Today, the garden is multifunctional: it is open to the public for visits and houses the National School of Landscape Architecture. Fruits and vegetables produced in the garden are sold to the citizens. Since 1683, the central part of KVG, namely the Great Square, representing 1.4 ha divided into 16 plots (shown inside of red frame of Figure 37) has been used to produce vegetables, with some interruptions. From 1715 (death of Louis XIV) to 1723, the Great Square became a grassy fallow. After the revolution, from 1793 to 1798, the use of the Great Square is vague, as the KVG was rented to a weapons factory and the agricultural society and intended for several uses including firearms testing and gardening. From 1798 to 1806, it would have been used to grow medicinal plants while between 1806 and 1815, it was a nursery and a vegetable garden. It is not known if the Great Square was cultivated during the second world war.

2.2 Soil characterization

Identifying initial materials used during the construction of the KVG soil was achieved through a historical and geological investigations. Well documented information since its construction and its historical evolution can be drawn from several manuscripts since the 17th century, in particular de La Quintinie's writings (La Quintinie, 1690). The KVG was built between 1678 and 1683, from a marshy meadow which depression was filled by successive additions of soil materials. A layer of 3 to 4 meters of sandy material (from recent alluvions and Fontainebleau sands of the Rupelian) excavated during the digging of the "Swiss Water Coin" (Figure 37) was first deposited. A second layer of soil material of unknown thickness from the hill of Satory, located near the site, was then overlaid to raise the soil above the water table and make it more fertile (La Quintinie, 1690). The geological map and the soil analyses indicated that the latter material corresponded to loess, typical from the plates of the Parisian region. The soil of the Great Square can be classified as Hortic-Anthrosols due to long-term and/or intensive cultivation, such as organic matter inputs, irrigation, tillage (IUSS Working Group WRB, 2015).

In March 2021, 16 individual samples homogeneously spread in each of the 16 plots have been collected, and well mixed to make a composite sample to represent soil sample of the surface layer (0-20 cm). Additionally, soil from 3 layers (0-20 cm, 20-40 cm and 40-60 cm) were also sampled in the centre of each of the 16 plots, with a hand corer. A subsample of the 20-40 cm and 40-60 cm layer was mixed in order to produce composite samples of these layers, representing the Great Square. These depths cover the different soil tillage depths during its history. Moreover, in three randomly chosen plots (plot 2, 7 and 15 shown in Figure 38), soils were sampled with an auger up to a 120 cm depth, in order to complete the pedological description and to be used as a supplement to samples of parent material (see below) to estimate the pedogeochemical background for trace metals (Baize and Sterckeman, 2001). Soil samples were air-dried, disaggregated and sieved at 2 mm. They were analysed by the Soil Analysis Laboratory of INRAE in Arras (France) for soil agro-pedological characterisation using ISO/AFNOR standardised methods. Trace and major element total contents were determined by the CNRS analytical research facility (SARM, CRPG, Nancy, France) by ICP-MS after alkaline fusion. Their characteristics are presented in Table 26.

Moreover, soil samples have been collected from 5 pedological pits located in different plots in the KVG (Figure 38). These plots were used for different purposes in the past: driveway border (Pit 1), orchard plot-one use over time (Pit 2), vegetable plot-one use over time (Pit 3, in the Great Square), orchard/vegetable plot-two use over time (Pit 4), alternance of orchard/vegetable (Pit 5). Soil characteristics have also been determined for the profiles of these 5 pits by the Soil Analysis Laboratory of INRAE in Arras (France).

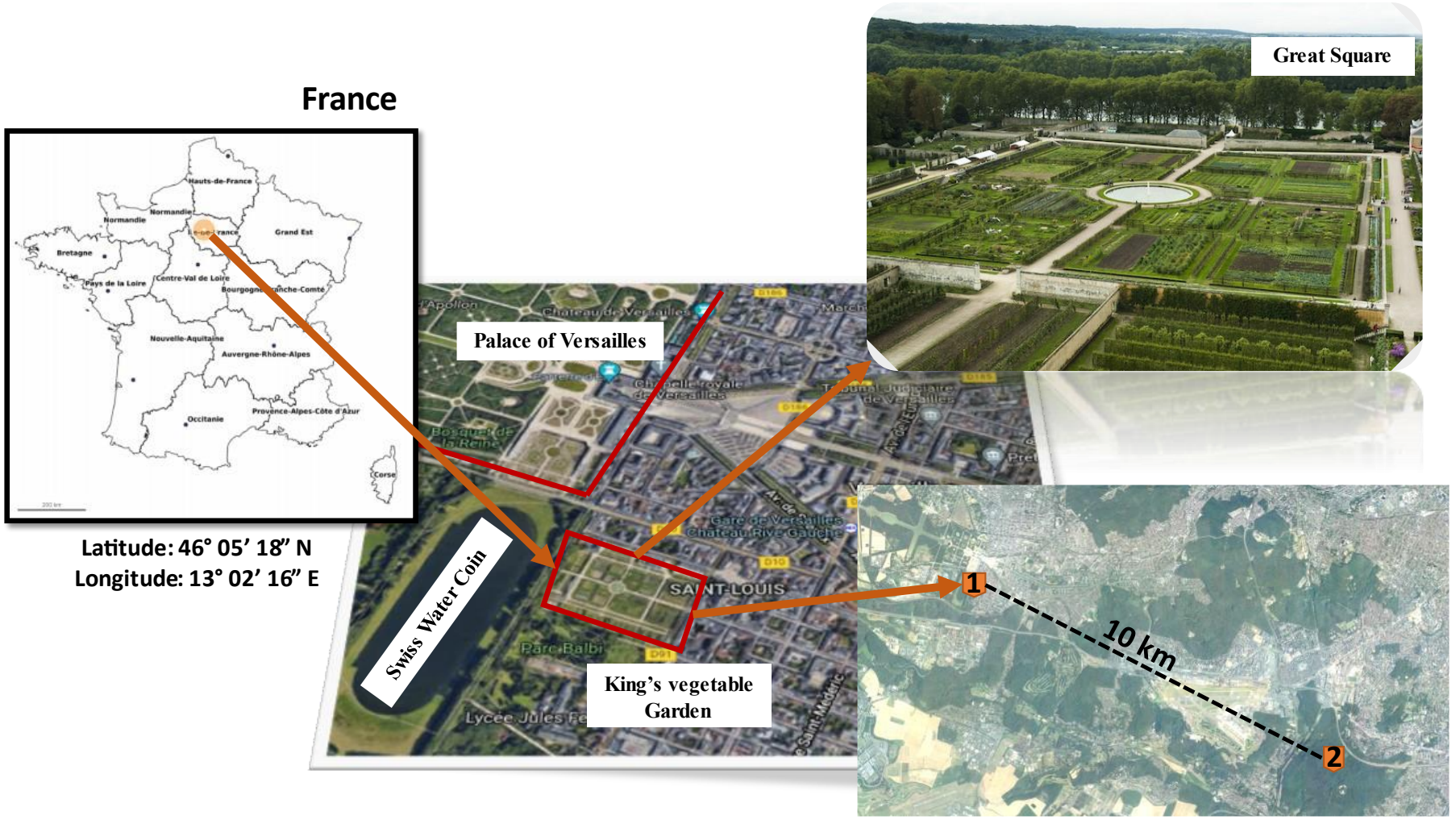

Figure 37. Location of King's Vegetable Garden (1) and of Verrières forest (2). Maps are from Google maps and Géoportail

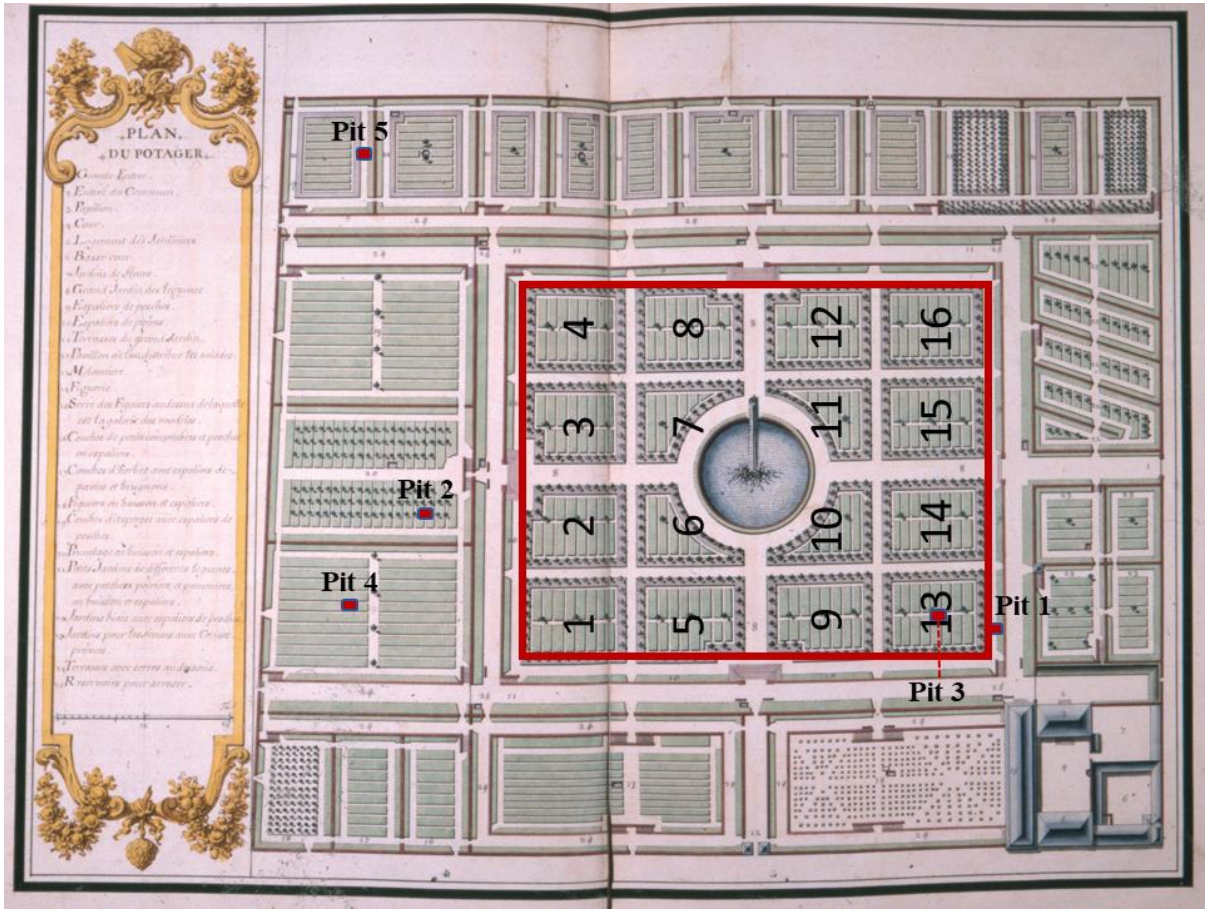

Figure 38. Soil sampling plan of 16 plots and 5 pedologic pits in King's Vegetable Garden

Table 26. Physicochemical properties of the KVG's soils, given as mean values for different horizons and initial soil (parent material). SOC: Soil organic carbon

Sampling depth	pH (water)	CEC (cmolc kg^{-1})	SOC (g kg^{-1})	Clay (%)	Silt (%)	Sand (%)	Total Al (g kg^{-1})	Total Fe (g kg^{-1})	Total metal contents in soils (mg kg^{-1})			
									Cd	Cu	Pb	Zn
0-20 cm	7.46	19.4	38.0	18.4	38.1	43.5	30.5	17.1	0.340	55.4	189	159
20-40 cm	7.45	16.9	23.3	19.4	41.4	39.2	33.0	19.3	0.277	48.0	223	114
40-60 cm	7.49	15.6	11.6	23.9	53.6	22.5	41.3	22.4	0.191	34.8	73.8	75.4
70-80 cm	7.46	13.3	6.83	21.9	62.3	15.8	42.3	22.1	0.158	22.4	49.9	56.8
80-120 cm	7.46	15.2	3.00	27.7	63.6	8.70	51.6	29.3	0.148	18.2	24.0	56.9
Initial soil	4.95	11.9	4.08	26.1	70.3	3.6	NA	NA	0.083	8.05	11.5	35.1

2.3 Predicting current soil metal contents

2.3.1 Mass balance model

We used the mass balance model previously developed for French vegetable garden soils (Zhong et al., 2021). The long-term evolution of soil metal content was calculated by summing the initial soil metal content with the monthly net metal input:

$$C_{i,soil,n} = C_{i,soil,n-1} + \Delta C_{i,soil,n} \quad (97)$$

$$\Delta C_{i,soil,n} = \frac{Q_{i,input,n} - Q_{i,output,n}}{\rho z} \quad (98)$$

where i represents the metal studied, $C_{i,soil,n}$ is the concentration of metal i in the soil at the end of month n (mg (kg DW)$^{-1}$) ; $C_{i,soil,n-1}$ is that of the previous month $n-1$ (mg (kg DW)$^{-1}$) ; $\Delta C_{i,soil,n}$ is the variation of metal concentration in month n (mg (kg DW)$^{-1}$) ; ρ is the soil dry density (kg DW m^{-3}) ; and z is the soil ploughing depth (m) presented in Table A3.

Plant protection product such as Cu-based fungicides, mineral amendments and wastewaters were not applied in the Great Square, thus being neglected in mass balance. The site being flat, surface runoff could be neglected for both input and output from each square. $Q_{i,input,n}$ (mg m^{-2}) is therefore obtained by summing metal flows provided by bulk atmospheric deposition ($Q_{i,atm,n}$), NPK fertilizer applications ($Q_{i,fer,n}$), organic amendments ($Q_{i,org,n}$):

$$Q_{i,input,n} = Q_{i,atm,n} + Q_{i,fer,n} + Q_{i,org,n} \quad (99)$$

$Q_{i,output,n}$ (mg m^{-2}) is the sum of metal losses through leaching $Q_{i,lea,n}$ (mg m^{-2}) and crop offtake $Q_{i,crop,n}$ (mg m^{-2}).

$$Q_{i,output,n} = Q_{i,lea,n} + Q_{i,crop,n} \quad (100)$$

The mass balance model was run to simulate the current soil metal concentrations (*i.e.*, in year 2021) based on historical data for initial conditions, atmospheric deposition and gardening practices. Forecast on future trends of soil metal contents were established for the next century.

2.3.2 Initial physicochemical properties of the soil

Initial soil physicochemical properties were needed to for the starting point of simulation in mass balance. Sampling of loess from Satory plateau was impossible because of its urbanization and occupation by a military zone. The plateau loess was therefore sampled about 10 km from the KVG, in the Verrières forest (Coordinates: 48.76018, 2.24465), through a pedological pit (Figure 37). Soil samples were taken from 4 horizons (0-5 cm, 5-12 cm, 12-40 cm, >40 cm) excluding the litter, and analysed by Soil Analysis Laboratory of INRAE in Arras (France) (Table 26). The carbon content and the pH in 12-40 cm of the Verrières soil were used as initial values for the Great Square soil.

Figure 39. Soil profile observed during the sampling of the initial material in the Forêt de Vérrières

Table 27. Pedo-transfer functions used to calculate the metal concentrations of initial soil ([Metal], in mg kg^{-1}) based on soil Al or Fe contents ([Al] or [Fe], in g kg^{-1}) (Sterckeman et al., 2006b)

Metal	R_{Al} = [Metal]/[Al]	R_{Fe} = [Metal]/[Fe]
Cd	0.0027	0.0049
Cu	0.27	0.47
Pb	0.39	0.67
Zn	1.16	2.05

To determine the initial trace metal contents (Cd, Cu, Pb and Zn), three methods were used and compared: 1) the contents in the Verrières soil, 2) the content of the deepest horizon (-100 cm) of the Great Square soil; and 3) the concentration estimated from the pedo-geochemical ratio of the trace metal to Fe (R_{Fe}) or Al (R_{Al}) content in sedimentary materials (Sterckeman et al.,

2006b). In this latter method, multiplying the current total Al or Fe content of the soil by the corresponding ratio (Table 27) gives the pedogeochemical initial trace metal content of the soil.

The initial content calculated by using R_{Fe} and R_{Al} were similar, as well as the initial content estimated by the three methods (Figure 40). For each of the four trace metals, the current total content in the deep horizon of the soil is very close to that in the Verrières soil and to that estimated using R_{Fe} and R_{Al}. The contents in the deep horizon were retained, because they corresponded the to the Fe and Al contents and considered free of contamination from the topsoil. The initial characteristics of Great Square soil used for simulation are also presented in Table 26.

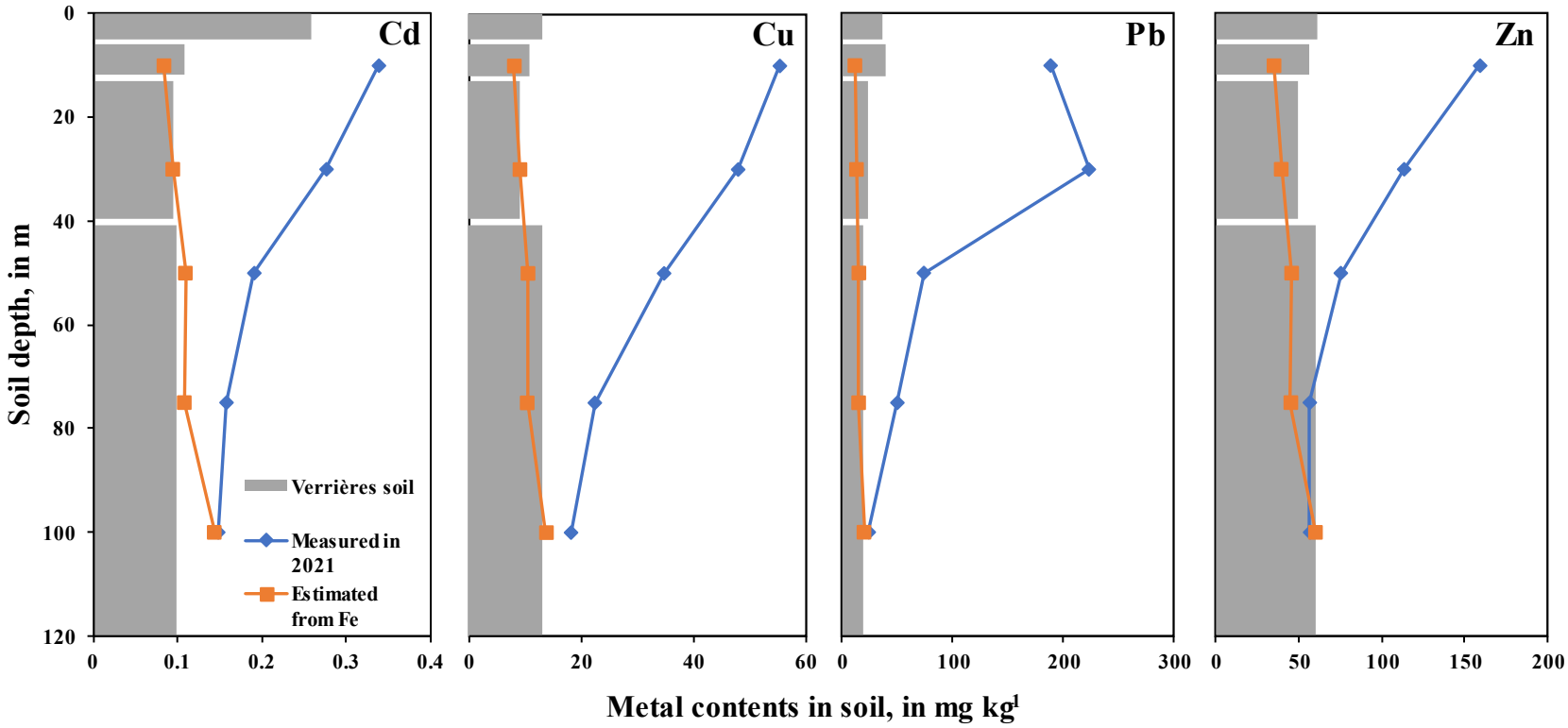

Figure 40. Determination of the four metal contents in the initial soil of King's Vegetable Garden by comparing measured values from the Verrières soil (supposed parent material) with measured values and simulated values from the Fe total content in the Great Square soil (mean of 16 plots sampled in 2021

2.3.3 Atmospheric deposition

Different approaches and datasets were used to reconstruct bulk atmospheric deposition of the four metals from 1683 to 2021 (Figure A8). Table 28 presents the average values for different periods, from 1683 to 2021. For the period before 1900, we referenced the deduced values of atmospheric deposition of four metals from the sampled peat bogs in three mountain areas located in Belgium and France (Allan et al., 2013; Elbaz-Poulichet et al., 2020; Mariet et al., 2018). Atmospheric deposition of each period (1683-1700, 1700-1800 and 1800-1900) was recorded in each specific layer of peat bog's profile (Hansson et al., 2015).

Secondly, during the period of 1900-2000, we referred to measured data from different monitoring sites in Parisian region. Baize and Bourgeois. (2005) estimated the average annual atmospheric depositions of Cd, Pb and Zn in Versailles from 1938 to 1999. Juste and Tauzin (1986) reported the averages values for Cd, Pb and Zn during 1929-1984. Azimi et al. (2005) measured the atmospheric deposition flux of the four metals for three periods (from 1994 to 1997, 1999-2000 and 2001-2002) in Créteil, Chatou and Paris.

Thirdly, for the period of 2000-2021, we used the dataset of metal concentrations in moss from a French national project (Biomonitoring of Metallic Atmospheric Fallout by Mosses, BRAMM). Metal concentrations in moss have been measured every 4 years from 1996, in more than 400 sampling sites across France territory. Datasets from 1996 to 2016 have been collected to obtain the average values of metal concentrations in moss for the period of 2000-2021 (BRAMM, 2018, 2013). A linear equation was used to calculate bulk atmospheric deposition from metal concentrations in moss (Rühling and Tyler, 2001).

$$\log(C_{Moss}) = 1.045 * \log(BD) + 0.568 \quad (R^2 = 0.996) \qquad (101)$$

where C_{Moss} is the concentration of metal in moss ($\mathrm{mg\ (kg\ DW)^{-1}}$); BD is the annual bulk atmospheric deposition of metal ($\mathrm{mg\ m^{-2}\ yr^{-1}}$).

Table 28. Historical bulk atmospheric deposition of four metals in King's Vegetable Garden. Each value represents an average annual deposition rate for the corresponding period

Period	Atmospheric deposition (mg m^{-2} yr^{-1})				Reference
	Cd	Cu	Pb	Zn	
1683-1700	0.002	0.375	1.65	2.00	Allan et al., 2013; Elbaz-Poulichet et al., 2020;
1700-1800	0.005	0.400	2.70	5.00	Mariet et al., 2018
1800-1900	0.010	1.00	6.05	15.0	
1900-2000	0.480	7.06	73.0	69.7	Azimi et al., 2005; Baize and Bourgeois, 2005; Juste and Tauzin, 1986
2000-2021	0.051	1.55	1.32	7.99	BRAMM, 2018, 2013; Hansson et al., 2015

2.3.4 Inputs from NPK fertilizers

Chemical fertilizers appeared in agriculture in the beginning of the 20th Century (Boulaine, 2006, 1995a, 1995b). However, from the memory of the senior gardeners of the site, they have been applied in the Great Square since *ca* 1950, and further abandoned due to converting the gardening practices into complete organic farming since 2000. Similar to other French vegetable gardens, NPK-type fertilizers have been used during the periods from March to the end of May and from September to the end of October (Zhong et al., 2021). The annual application rate is estimated on average 0.034 kg m^{-2} yr^{-1} from 1950 to 2000. Trace metal concentrations in French commercial NPK fertilizers (n = 9) were provided from the study of Verbeeck et al., (2020). The average concentrations of the four metals are: 2.36 (S.D. = 1.43) mg Cd kg^{-1}; 14.21 (S.D. = 17.40) mg Cu kg^{-1}; 4.88 (S.D. = 7.29) mg Pb kg^{-1}; 195.58 (S.D. = 198.89) mg Zn kg^{-1}.

2.3.5 Inputs from organic amendments

Historical books on gardening practices (La Quintinie, 1690; Le Gentil, 1705; Moreau and Daverne, 1845) enabled to reconstruct the origin and the application rate of organic amendments for different periods before the 20th century. In the Great Square of the KVG (as well as in aristocratic and market gardening), the only fertiliser applied for this period was the so-called "*terreau*", that is a sort of compost of horse manure. This manure was mainly

composed of wheat straw, as the horses' litter was renewed nearly every one or two days. The horse litter was used to build numerous warm beds at the end of November or beginning of December. These warm beds, located elsewhere than in the Great Square, were used for the production of vegetables and strawberries until April. At the end of their use, the beds were dismantled and the litter, which was more or less composted, was used as *terreau* to amend the soil of the Great Square. According to historical records, organic amendments were added to the soil after each sowing from approximately 1683 to 1920 (after the first world war). La Quintinie (1690) recommended to apply a *terreau* layer of 2 inches (5.4 cm) on the soil after sowing, while Le Gentil (1705) recommends only a 1-inch (2.707 cm) layer. We estimated a 1.5-inch layer, with a bulk density of 400 kg FW m^{-3}, and a dry matter content of 41% (in mass)(Doligez and Leveau, 2007), which corresponds to 6.6 kg DW m^{-2} of *terreau*. The annual application rate therefore depends on the annual number of sowings. It varies between 6.66 and 39.96 kg DW m^{-2} yr^{-1}, which is very high and should provide the soil with high amounts of organic matter and plant nutrients. However, in reality, such a high application rate of more than 200 years in a row is not very realistic, and that's without considering the accessibility of *terreau* in this amount. Instead choosing the single input amount, we have simulated 4 scenarios with different application rates of *terreau* during this period: 25%, 50%, 75% and 100% of above-mentioned quantity, respectively.

To estimate the metal contents in the *terreau* (Table 29), we used the composition of horse manure containing mostly straw (France Galop et al., 2013). The reduction in dry mass during composting was estimated 47% after 120 days (Paillat et al., 2005).

From our recordings, we know that between 1990 and 2000, there were inputs of cattle manure, every four years, in autumn. The manure was brought at a rate of 100 to 300 kg FW per 100 m^2 (i.e., on average 2 kg FW m^{-2}), on a roughly worked soil surface, before ploughing. Information on the gardening practices from 1920 to 1990 is scarce. Therefore, we considered that the organic amendments application for this period was similar to that between 1990 and 2000, because it is classical in agriculture and gardening.

From 2000 to 2021, cattle manure was replaced by compost as organic amendments. Since 2000, all crop residues are collected and composted (for 1 to 1.5 years) instead of being thrown away as they were before. During this period, 6 kg FW m^{-2} of crop residues compost were applied in the plots with squash, cucumber and tomato, considered as vegetables with high nutrient requirements. Green waste compost purchased from outside the KVG was applied on the

seedlings of carrot, mesclun, beet and turnip, at a rate of 36 kg FW m^{-2}. The compositions of cattle manure and composts are presented in Table 29.

Table 29. Characteristics of the organic amendments applied in the Great Square of the King's Vegetable Garden

Amendments	DW (%)	OC content in the fresh mass (%)	Metal contents (mg $(kg\ DW)^{-1}$)				
			Cd	Cu	Pb	Zn	Reference
Cattle manure	20	8.0	0.3	23.0	3	133	AROMIS, 2020; Houot et al., 2014
Green waste composts	62	29.3	0.4	41.0	28	150	Weissengruber et al., 2018
Terreau	41	15.2	0.06	8.15	1.52	20.8	France Galop et al., 2008

2.3.6 Crop rotation

For the 18th and 19th centuries (1683-1920), the list of cultivated species was deduced from three documents: the books from de La Quintinie (1690) and Moreau & Daverne (1845), and from one archive document (Anonymous, 1759). The latter also gives the digging depth together with the surface areas dedicated to the vegetable species in the Great Square. The percentage of the surface occupied by a vegetable was considered equal to the frequency of the vegetable cultivation in a century. Depending on the spring crop duration, an autumn crop could be planted after the spring crop if it is allowed (Zhong et al., 2021). The documents also give indications on the successions or on the number of certain crops per year.

During the period of 1987-2020, the type and frequency of vegetables grown were recorded for the 16 plots. Since the varieties of vegetables grown in the 20th and 21st centuries are similar, this dataset was therefore used to build up the crop rotation during the period of 1920-2021. A grassland was simulated for the period 1710-1723 as well as medicinal plant cultivation from 1799 to 1806. The vegetable production was considered to continue during the troubled periods of 1793 to 1798 and the second world war, because of a need for foods. The crop rotation and ploughing depth from 1683 to 2021 is presented in *Table A3*.

2.3.7 Crop offtake

The crop offtake was calculated as follows:

$$Q_{crop,n} = PUF \ \frac{Y}{HI}(1 - W_{pla}) \ C_{i,solid,n-1} \quad (102)$$

$$PUF = \frac{C_{i,crop}}{C_{i,solid}} \quad (103)$$

where Y is the vegetable yield (edible part) per harvest (kg FW m^{-2} $harvest^{-1}$); HI is the harvest index calculated as the ratio between edible vegetable yield and total above-ground biomass (dimensionless); W_{pla} is the moisture fraction in the harvested plant part (dimensionless); $C_{i,crop}$ and $C_{i,solid}$ are the trace metal contents in harvested part and in soil (mg kg^{-1} DW), respectively.

Mean vegetable yields for Paris area were taken from agricultural statistics of Ministry of Agriculture, Agrifood, and Forestry (Agreste, 2020b). Before 2000, crop residues were collected and discarded out of the KVG. For this period, the harvest index was set to 1 for root plants, and to 0.49 for other vegetables (Farina et al., 2018). The second value is very close to that reported for the remaining fraction of the biomass in European Union (442 Mt or 46%) (Camia et al., 2018). From 2000, the crop residues were composted. The harvest index was fixed to 1 and the metal inputs from these composts were not considered in the mass balance, contrarily to those of the purchased composts.

PUF (plant uptake factor, dimensionless) is the ratio between the metal concentration in that edible part of plant and soil metal concentration. The *PUF* values were calculated for each vegetable with the BAPPET database by using the previous data selection criteria (ADEME, 2012; Zhong et al., 2021). Table 30 represents all data concerning metal output from crop offtake.

Table 30. Data for simulating metal output from crop offtake: average yields of vegetables per harvest in Paris, from Agreste database; plant uptake factors (PUF) of Cd, Cu, Pb and Zn for the harvested part of the vegetables, from the BAPPET database

Crop	Water content	Yield (kg FW m^{-2} $harvest^{-1}$)	Harvest index (HI)	PUF_Cd	PUF_Cu	PUF_Pb	PUF_Zn
Artichoke	0.85	0.79	0.49	0.24	0.23	0.01	0.11
Asparagus	0.93	0.26	0.49	0.77	0.14	0.03	0.28
Balm	0.76	1.90	0.49	0.48	0.03	0.03	0.10
Beet	0.87	2.84	1.00	0.12	0.51	0.00	0.64

Bell pepper	0.92	3.56	0.49	0.27	0.51	0.73	0.59
Black radish	0.94	2.84	1.00	0.35	0.24	0.01	0.25
Black salsify	0.77	1.50	0.49	0.25	0.21	0.01	0.17
Broad bean	0.77	0.96	0.49	0.12	0.32	0.01	0.19
Broccoli	0.89	1.36	0.49	0.69	0.82	0.14	0.52
Cabbage	0.92	2.20	0.49	0.34	0.09	0.02	0.20
Cardoon	0.94	5.00	0.49	0.24	0.23	0.01	0.11
Carrot	0.90	2.77	1.00	0.25	0.21	0.01	0.17
Cauliflower	0.93	1.59	0.49	0.41	0.73	0.20	0.45
Celeriac rave	0.89	2.70	1.00	0.91	0.31	0.07	0.27
Chard	0.95	3.10	0.49	1.09	0.15	0.12	0.21
Chervil	0.87	1.75	0.49	0.48	0.04	0.02	0.38
Chicory	0.91	2.11	0.49	1.40	0.23	0.02	0.35
Chili pepper	0.88	3.56	0.49	0.27	0.51	0.73	0.59
Chives	0.91	0.30	0.49	0.77	0.14	0.03	0.28
Cucumber	0.96	5.07	0.49	0.07	0.12	0.04	0.02
Eggplant	0.93	3.61	0.49	0.72	0.37	0.38	0.43
Escarole	0.93	2.30	0.49	1.40	0.23	0.02	0.35
Fennel	0.92	2.75	1.00	0.45	0.63	0.05	0.61
Garden cress	0.91	6.10	0.49	0.34	0.22	5.55	7.31
Garlic	0.90	0.79	0.49	0.77	0.14	0.03	0.28
Gherkin	0.90	1.05	0.49	0.07	0.12	0.04	0.02
Green bean	0.90	1.07	0.49	0.03	0.15	0.00	0.19
Lamb's lettuce	0.94	0.97	0.49	1.40	0.23	0.02	0.35
Leek	0.88	2.43	0.49	0.16	0.14	0.00	0.11
Lettuce	0.95	2.33	0.49	1.40	0.23	0.02	0.35
Baby lettuce	0.95	4.66	0.49	1.40	0.23	0.02	0.35
Onion	0.90	2.59	1.00	0.77	0.14	0.03	0.28
Parsnip	0.81	1.75	0.49	0.25	0.21	0.01	0.17
Pea	0.79	0.77	0.49	0.09	0.27	0.01	0.39
Portulaca oleracea	0.90	0.39	0.49	1.40	0.23	0.02	0.35
Potato	0.79	4.34	1.00	0.09	0.29	0.00	0.07
Pumpkin	0.92	2.55	0.49	0.07	0.12	0.04	0.02
Radish	0.96	1.54	1.00	0.35	0.24	0.01	0.25
Rheum	0.92	7.50	0.49	1.09	0.15	0.00	0.21
Salad burnet	0.87	1.75	0.49	0.48	0.04	0.02	0.38
Salsify	0.86	1.50	0.49	0.25	0.21	0.01	0.17
Shallot	0.80	1.43	1.00	0.47	0.14	0.01	0.19
Spinach	0.92	1.42	0.49	1.18	0.37	0.02	1.24
Squash	0.92	2.76	0.49	0.65	0.12	0.01	0.29
Strawberry	0.90	0.76	0.49	0.17	0.29	0.01	0.12
Tarragon	0.80	1.27	0.49	0.48	0.04	0.02	0.38
Tomato	0.94	3.15	0.49	0.17	0.29	0.00	0.12
Turnip	0.92	3.56	1.00	1.62	0.24	0.01	0.13

Zucchini	0.95	2.32	0.49	0.65	0.12	0.01	0.29
Medicinal plants	0.76	1.90	0.49	0.48	0.03	0.03	0.10

2.3.8 Metal leaching

Output of metals by leaching is estimated by

$$Q_{i,lea,n} = C_{i,solute,n-1} W_{percly,n} \quad (104)$$

$C_{i,solute,n}$ (mg L^{-1}) is the concentration of metals in soil solution of month *n*. $W_{percly,n}$ (mm) is the quantity of water percolating through the horizon (between 0 and *z* m), which was estimated by a hydrologic cycle model (Zhong et al., 2021). The climatological data was provided by Météo-France as normal values for the period 1981-2010, presented in Table 23. It was supposed the same since the creation of the KVG.

In the Great Square, gardeners always kept an eye on plant water deficit. They used the water from the central basin and intermediate tanks to water crops with watering cans. We estimated that garden soils were maintained to 70% of soil water content at field capacity if it fell below this value. The monthly average flows of percolating water in the Great Square are presented in the Figure A9. We simulated in average 159 mm/year percolating water in the ploughing soil horizon.

To estimate $C_{i,solute,n}$, we used the models from our previous study (Zhong et al., 2021), shown in Table 31. Soil organic carbon and pH are the dominant variables in these models. They could vary due to different agricultural inputs, such as organic amendment and fertilizers. The *RothC* model (Coleman and Jenkinson, 1996) was therefore used to simulate soil organic carbon dynamic, and the VSD^{+} model (Bonten et al., 2016; Posch and Reinds, 2009; Xu et al., 2020; Zeng et al., 2017; Zhu et al., 2018b, 2018a) to simulate the change in soil pH over time. More details of pH modelling can be found in the Chapter 3.

Table 31. Regression models for calculating the metal concentrations in solution concentration. Metal(S): concentration of dissolved metal (µg L^{-1}). Metal(T): total metal concentration (mg kg^{-1}). OM: Organic matter = 1.72*OC. OC: organic carbon.

Metal	Model equation	Based on data from
Cd	log Cd(S) = 3.62 - 0.50 pH + 0.96 log Cd(T) - 0.45 log OM ($g\ kg^{-1}$)	McBride et al. (1997)
Cu	log Cu(S) = 1.37 - 0.21 pH + 0.93 log Cu(T) – 0.21 log %OC	Sauve et al. (2000a)
Pb	log K_d = 1.32 + 0.40 pH + 0.50 log %OC	Degryse et al. (2009)
Zn	log K_d = 0.349 + 0.541 pH + 0.209 log %OM	Ivezic et al. (2012)

2.4 Modelling accuracy assessment

The model sensibility analysis of our previous study showed that variables relating to metal inputs are dominant factors of the evolution of these metals in garden soils (Zhong et al., 2021). To estimate the modelling uncertainty, different range values are deduced for these independent variables (Table A4). Each of them was randomly sampled using a uniform distribution in the range, to create a sample of 1,000 simulation cases. Model accuracy assessment is made by comparing the simulated metal contents and the measured metal contents.

The probabilities $P_{acc,\varphi}$ of difference between predicted and measured values within φ = ±10%, 25%, 50% and 100% are calculated by using the following equation:

$$E_{rel} = \frac{\left|[X]_{sim} - [X]_{mea}\right|}{[X]_{mea}} 100 \quad (105)$$

$$P_{acc,\varphi} = \frac{N_\varphi}{N_T} \quad (106)$$

Where,

$[X]_{sim}$ is the simulated soil content for metal X,

$[X]_{mea}$ is the measured soil content for metal X,

N_φ is the number of simulated scenarios for which $E_{rel} < \varphi$ with φ = 25%, 25%, 50% or 100%,

N_T is the total number of simulated scenarios, $N_T = 1000$.

2.5 Predicting future soil metal contents

The evolution of Cd, Cu, Pb and Zn contents in topsoil (0-20 cm) of the Great Square was simulated for the next 100 years from 2021, with the same mass balance model, basing on the current KVG's gardening practices. Only biowaste composts are currently used to maintain soil fertility. Home-made composts with on-site produced crop waste are more and more used for lasagna-beds in the KVG from 2013. The return of metals from home-made composts have therefore been considered in our model. Moreover, regular use of 8-10 cm layer of imported biowaste composts on the carrot, parsnip and mesclun beds can bring metals into soils.

3 Results and discussion

3.1 Impact of historical gardening practices on soil metals accumulation

Agricultural inputs caused the accumulation of P in the soil layer from 0-60 cm (Figure A13). Over the last 300 years, the highest soil P accumulation was observed in plots used for vegetable monoculture in the Great Square, followed by orchard/vegetable plots with two uses over time, then plots planted alternately with orchard and vegetable, and finally plots planted with fruit trees only. The values around 500 mg P_2O_5 kg^{-1} in Pit 3 (when it is in the order of 100 mg P_2O_5 kg^{-1} in cultivated soils) indicate that the soils of the Great Square were over-fertilized by intensive application of organic amendment, as those observed from other urban vegetable gardens in France (Joimel et al., 2016).

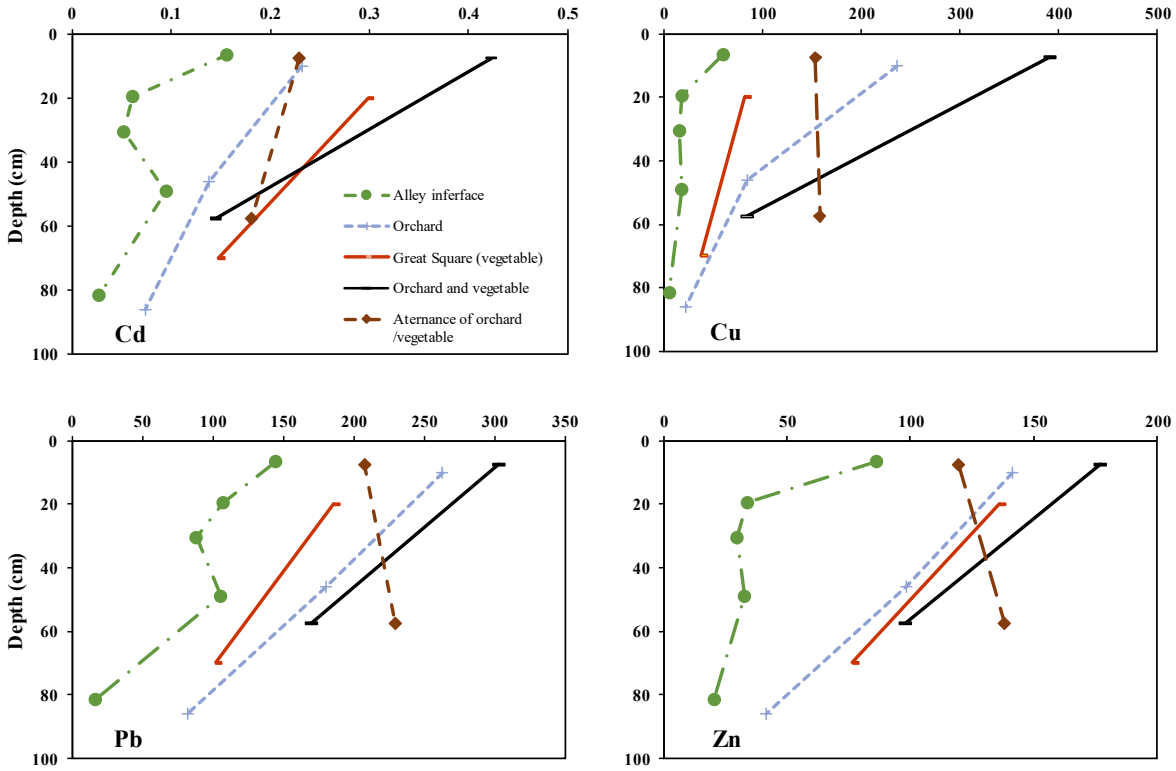

Figure 41. Concentrations of Cd, Cu, Pb and Zn in different pits of KVG: driveway border(Pit 1), orchard plot-one use over time (Pit 2), Great Square (Pit 3), orchard/vegetable plot-two use over time (Pit 4), alternance of orchard/vegetable (Pit 5)

Significant variations of metal concentrations were observed between topsoil and subsoil in the 5 pits located differently in KVG. Topsoil (0-20 cm) used for cultivation contain more metals than topsoil in driveway border, up to 2.7, 6.5, 2.1 and 2.1 times for Cd, Cu, Pb and Zn respectively (Figure 41). For Cd and Zn, higher soil concentrations were found in plots that

have been used for vegetable cultivation. For Cu and Pb, their concentrations in soils were significantly lower for plots used solely for vegetable growing than for other plots which had been used as orchard. The accumulation pattern of Cu and Pb was observed to be similar in the five soil profiles (Figure 41), and both principal component analysis (PCA) and Pearson correlation coefficient (PCC) reveal a strong correlation between Cu and Pb in the Great Square soils (Figure 42; Figure A10).

The mean concentrations (n =16) of Cd, Cu, Pb and Zn in the 0-20 cm of topsoil are 0.34, 55.4, 189 and 159 mg kg^{-1} measured in 2021, respectively (Table 26). Comparing initial metal concentrations estimated from Fe content, we found that topsoil of 0-20 cm has enrichment factors (current metal content/initial metal content), in average 4.4 for Cd, 7.5 for Cu, 18 for Pb and 5 for Zn. Enrichment with the four metals reaches 80 cm soil depth (Table A5). Soil Cd concentrations are still below both regional and international threshold values (Table 32). However, soil Cu concentrations are well above the regional threshold value, but still below the international threshold value. Soil Pb concentrations in the Great Square are well above both regional and international threshold values, close to the guideline value. Soil Zn concentrations are between the regional threshold and the international threshold.

In the current situation, the level of Cu, Pb and Zn in the Great Square soils is already in an anomalous state, and perhaps there is no need for soil remediation yet, but more precautions should be taken for reducing metal contamination and transfer to edible plant parts.

Table 32. Threshold and guideline values for metals in agricultural soils

Element	Regional Threshold value (mg kg^{-1})[a]	International Threshold value (mg kg^{-1})[b]	International Lower guideline value (mg kg^{-1}) [b]
Cadmium (Cd)	0.5	1	10
Copper (Cu)	28.0	100	150
Lead (Pb)	53.7	60	200
Zinc (Zn)	88.0	200	250

a. The regional threshold values were defined on the basis of 95th percentile of metal concentrations from more than 1000 agricultural soil samples in Paris region (Mathieu et al., 2008).

b. The international threshold and lower guideline value were defined based on either ecological risks and health risks (Ministry of the Environment, Finland, 2007)

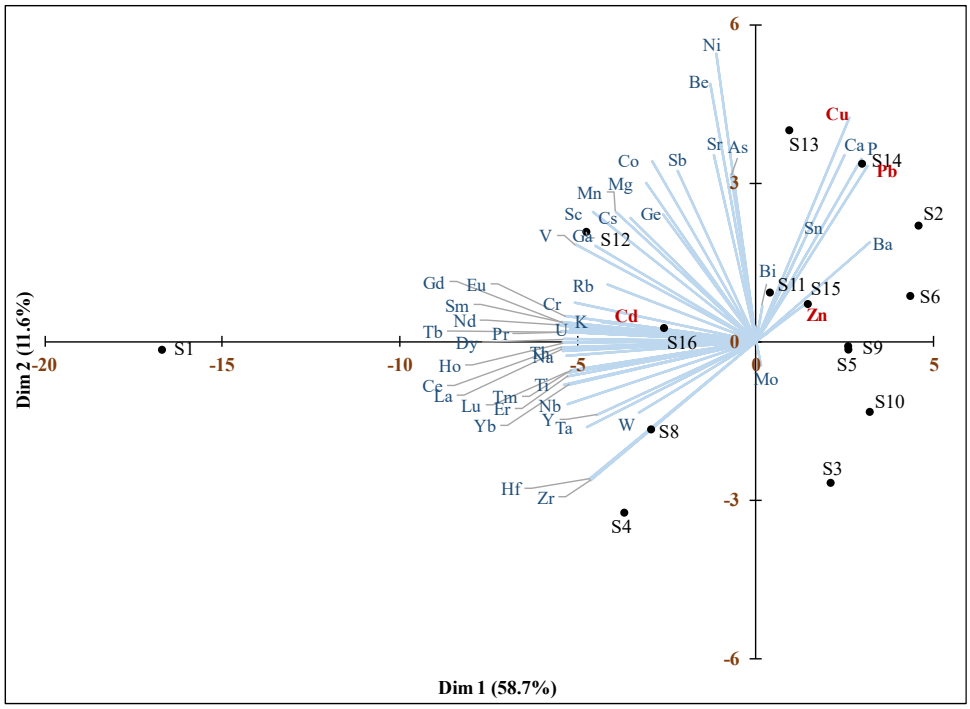

Figure 42. Principal component analysis of major and trace elements for Great Square soils. S1-S16: Soil samples of 0-20 cm layer collected from each of the 16 plots.

3.2 Historical trends of Cd, Cu, Pb and Zn contents in KVG

The historical trends of Cd, Cu, Pb and Zn contents in the Great Square topsoil (0-20 cm) were simulated with the mass balance model, basing on historical gardening practices (Figure 43; Table 33). *Terreau* has been extensively used as fertilizer during the first 200 years, where the recommended application rate of *terreau* in the past reached to 6.66 kg DW m^{-2} per seeding which is quite unrealistic considering long-term *terreau* availability. Therefore, we simulated the historical trends of Cd, Cu, Pb and Zn contents in the 0-20 cm of topsoil from 1683 to 2021 by using 25%, 50%, 75% and 100% of recommended application rate of *terreau*.

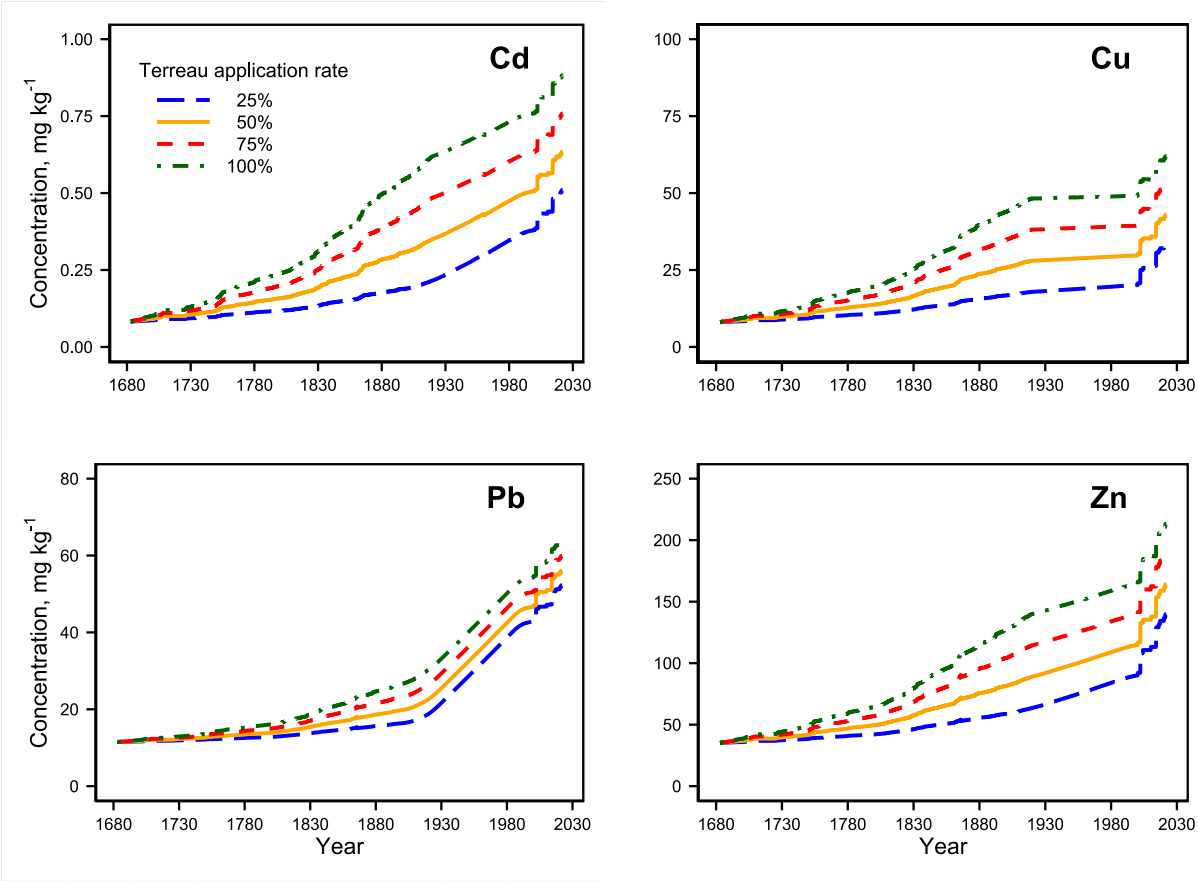

Figure 43. Evolution of the four metals soil concentration in the surface layer (0-20 cm) of the Great Square with different application rates of *terreau*

Table 33. Measured and simulated values of the four metals' soil content in the surface layer (0–20 cm) of the Great Square, according to different application rates of terreau. Differences (D) to measured values are expressed in %

Element	Measured mean value	Simulated values with different application rates							
		25%		50%		75%		100%	
	mg kg^{-1}	mg kg^{-1}	D, %	mg kg^{-1}	D, %	mg kg^{-1}	D, %	mg kg^{-1}	D, %
Cd	0.34	0.51	50	0.63	87	0.76	124	0.88	160
Cu	55	33	-40	43	-22	52	-5	62	12
Pb	189	52	-72	56	-70	60	-68	64	-66
Zn	159	140	-12	164	3	189	18	200	25
SOC, g kg^{-1}	38	36	-6	40	5	44	17	49	28

Different application rates of *terreau* led to differences in simulated current soil metal concentrations for Cd, Cu and Zn. All scenarios overestimated soil Cd concentrations with a range of variation from 50% to 160% comparing to mean measured value. For Zn, we obtained the best approximation of mean measured value in the 50% application rate scenario with

variations of 3%, following by the 25% application rate scenario with variation of -12%. Soil Cu concentrations were underestimated in the 25%, 50% and 75% application rate scenarios. All scenarios have failed to simulate soil Pb content, with a range of variation of -66% to -72%. We obtained an excellent estimation of topsoil organic carbon content with RothC model in both 25% and 50% application rate scenario, with variable variation of -6% and 5% respectively. *Terreau* with application rate of 20-50% of recommended dose seems to close to real average usage in the past, as referring to their good predictions of topsoil Zn and SOC contents.

The accumulation of Cd in the past was a nearly linear process, but appears quicker from 1900 to 2000 (Figure 43). In 25% application rate scenario, soil Cd concentration has increased from an initial value of 0.08 mg kg^{-1} to 0.19 mg kg^{-1} from 1683 to 1900 (in more than two centuries), followed by higher increase to 0.38 mg kg^{-1} from 1900 to 2000 (in only one century). Estimated accumulating flows of the four metals in the ploughing soil layer are shown in Table A8, for different periods during 1683-2021. The simulated Cd increase during 1900-2000 is dominantly due to atmospheric deposition (Figure 43), with annual input of 0.48 mg m^{-2} yr^{-1}. This value is very close to the amount reported (0.53 mg m^{-2} yr^{-1}) in a peri-urban vegetable farm located in Nanjing, China (Hu et al., 2013), but is far greater than the inputs before 1900 or after 2000 (Table 28). Moreover, literature shows that the amount of atmospheric deposition of pollution can vary dramatically depending on the proximity to the source. Heavy metal contents in atmospheric deposition strongly decreased in Paris region from the end of 20^{th} century (Azimi et al., 2005). The overestimation of topsoil Cd content may be partly caused by the error of estimated Cd inflow from atmospheric deposition. Thus, we made a simulation by reducing Cd bulk atmospheric deposition to half of the previous value. Nevertheless, we have still overestimated topsoil Cd contents by 24% (0.42 mg kg^{-1}) in the 25% *terreau* application rate scenario, and 61% (0.55 mg kg^{-1}) in the 50% *terreau* application rate scenario (Figure A12).

In our model, estimated Cd loss by leaching represents only 1.8% of total metal input (Table A8). Simulated Cd concentration in soil solution decreases with increasing organic matter content and pH of the soil (Table 31). Fang et al. (2016) found that repeated addition of compost can increase soil total OM content and dissolved organic matter (DOM) concentration, and DOM-bound Cd becomes the dominant specie in liquid phase at neutral to alkaline pH. The pH of the Great Square soils has been always maintained around 7.5 by organic amendment, as simulated by VSD^{+} model (Figure 32). At this pH, increasing dissolved organic matter from compost application would enhance Cd leaching (equivalently for Cu and Pb) (Fang et al., 2018). This dissolution enhancement could not be considered in our Cd partitioning model and

the loss of Cd by leaching might therefore be underestimated leading to an overestimation of current topsoil Cd content.

To understand the inaccuracy of the Cu and Pb mass balance simulations, we compared the simulated topsoil metal contents in the Great Square of KVG with measured topsoil metal contents in 104 French vegetable gardens located in Marseille, Nancy and Nantes respectively (Joimel. 2015; Zhong et al., 2021). Particularly, soils from Nantes have basically the same geological background contents for Cd, Cu, Pb and Zn as the KVG's soil (Table 26; Table A6). Vegetable gardens in Nantes city were generally constructed during the late 20th and early 21st centuries. In Nantes city, the average concentrations of Cu and Pb in vegetable garden soils were 49 mg kg^{-1} and 57 mg kg^{-1} (Table 2). In the Great Square, soil Pb accumulation accumulated mainly from atmospheric deposition in the past and, to a lesser extent from organic amendment (Figure 43). Assuming similar levels of atmospheric pollution in the past in Nantes and in Versailles, and neglecting the additional Pb input from use of *terreau* during 1683-1900 (which represents 15% of total Pb inflow over time), the simulated topsoil Pb contents (range of 52 to 64 mg kg^{-1}) have the same order of magnitude to measured average topsoil Pb concentration (57 mg kg^{-1}) in vegetable gardens of Nantes city. Therefore, the Pb concentration in the Great Square topsoil (189 mg kg^{-1}) cannot be explained by the simulated fluxes, although those are consistent with the Pb content found in vegetable gardens as those of Nantes. In the Great Square of KVG, an important part of the soil contamination with Pb should come from other sources, that were not considered in our mass balance.

Acid lead arsenate ($PbHAsO_4$) was the most extensively used inorganic insecticide from the end of 19th century to the end of 20th century (Shepard, 1951). Many orchard soils worldwide has elevated Pb and As due to the past use of lead arsenate insecticides (Leblanc et al., 2000; Paltseva et al., 2018; Peryea and Creger, 1994; Rocha et al., 2015). In France, lead arsenate was allowed to be used in orchard from 1916, but was forbidden to apply into vegetables (Delbard, 1947). It was banned from use on food crops in 1988. In the past, inappropriate use of insecticides has also caused heavy Pb and As contamination in vine soils (Rocha et al., 2015; Peryea and Creger, 1994). High volume of insecticides were incorrectly sprayed, leading to contamination of surrounding areas of treatment spot (Baharuddin et al., 2011; Nuyttens et al., 2009). In KVG, soil As enrichment has been found in the soils under different historical usages, and highest contamination level was observed for orchard plots (Figure A14).

Lead arsenate was usually mixed with copper chloride oxide in France for application on pear and apple trees (Delbard, 1947). Topsoil Cu content is significantly correlated with Pb content

(R^2 = 0.9, p = 2.76E-06) (Figure A10). This indicates that they might derive from the similar contamination source. This result agrees with previous studies (Hu et al., 2018; Wang et al., 2021b), while no coefficient was found between As and Pb (R^2 = 0.023) (Figure A10). This should be due to the different vertical mobility of As and Pb in soils. Soil As is more mobile than Pb, and it can be slowly leached to deeper soil layer. Repeated addition of compost was found to increase As concentration in leaching solution (Fang et al., 2017). Pb is mostly immobile and thus accumulate in the reception layer (Peryea and Creger, 1994). PCA shows that the topsoil contents of Pb, Cu and As could be explained by Component 2 (11.6%) (Figure 42). Therefore, we hypothesize that the large enrichment with Pb and Cu in the topsoil was caused by the application of mixed insecticides and fungicides (lead arsenate and copper chloride oxide) on the trees surrounding each of the 16 plots of the Great Square. That could also explain the underestimation of Cu in the mass balance simulation.

It seems difficult to consider in our mass balance model the inflows of Cu and Pb due to insecticide application during 20th century, as there is very limited information about historical usage of phytosanitary products in the KVG. Only two records were provided by a senior gardener of KVG. In 1987 and 1989, copper-based fungicide treatments were applied on tomato, lettuce, strawberry, cabbage (less than 10 treatments/year). However, it cannot be excluded that the unexplained contaminations, in particular with Cu and Pb would have been caused by other unknown sources. For instance, Pb lead could also have been introduced into the soil from all the lead equipment (e.g., gutters, greenhouse structures) that were on the site. Even earlier, there was a mass production of lead ammunition during the stay of the royal family in Versailles (Quenet, 2015). It indicates that overall, the simulation errors are mainly caused by the uncertainty of historical pollution data and gardening practices.

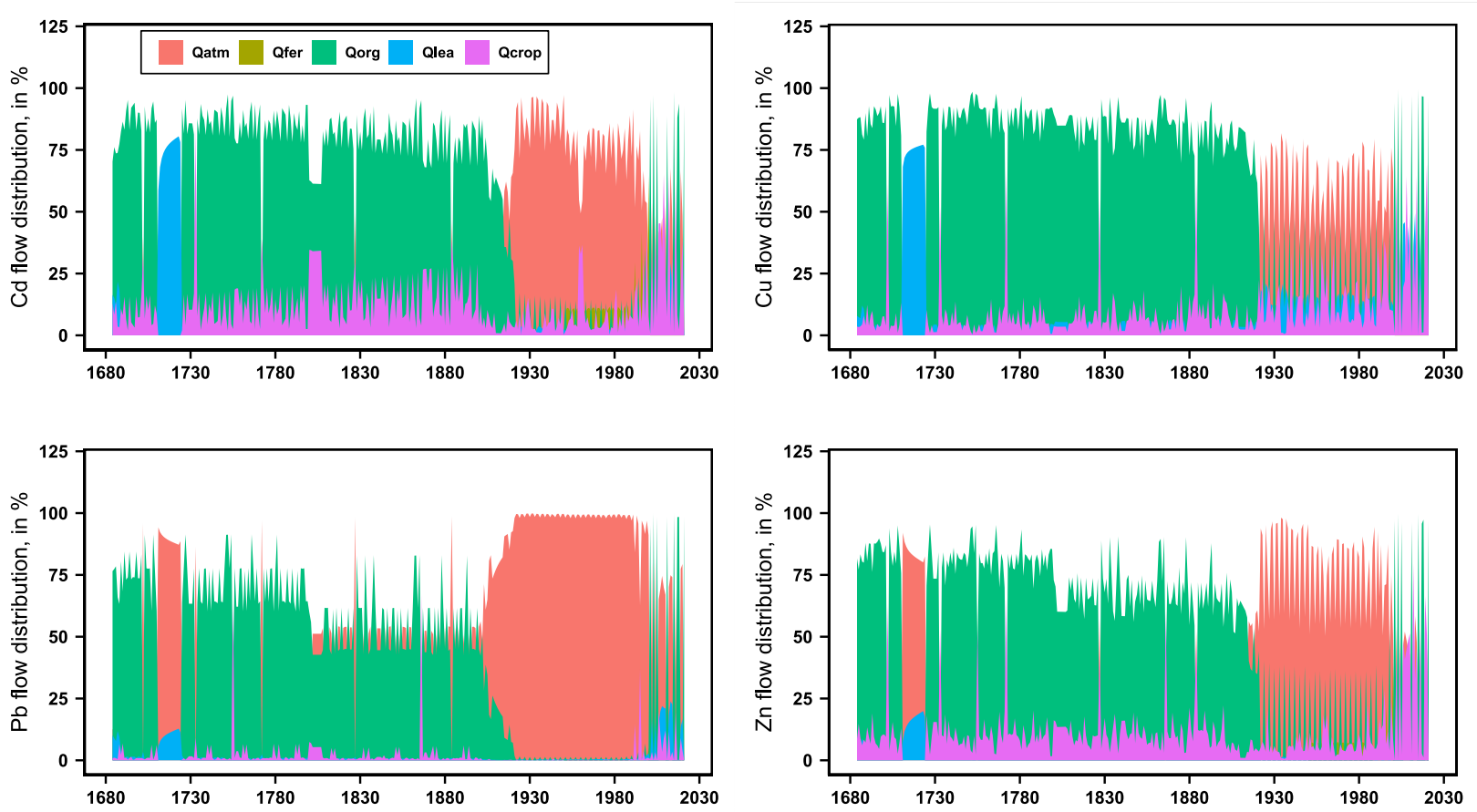

Figure 44. Annual distribution of input and output flows of the four metals during the period of 1683-2021, with 25% terreau application rate. In % of the sum of the absolute value of all flows. Qatm: atmospheric deposition; Qfer: NPK fertilizers; Qorg: organic amendments; Qlea: leaching; Qcrop: crop offtake

3.3 Modelling accuracy assessment

Atmospheric deposition, manure, green waste compost and NPK type fertilizer are the main contamination sources of the four metals for the Great Square soil. Their data errors, despite not as important as that of the historical *terreau* application rate, can also lead to simulation errors. We simulated the mass balance for 1000 scenarios consisting in random combinations of these variables within the ranges of possible values found in literature. The historical trends of metal contents for the 1000 scenarios are shown in Figure A16. N_{φ} the number of predicted values within ± x% difference of the average measured value, was shown in Table A9. The analysis indicates that our model has 22% and 70% chance to obtain simulated Cd value within ± 25-50% and 50-100% difference of the average measured value, and 7% chance to obtain simulated value with difference above 100% of the average measured value. For Zn, the model has 42%, 39% and 19% chance to obtain simulated value within ± 10%, 10-25% and 25-50% difference of the average measured value, respectively. For Cu, the model has 29%, 40% and 31% chance to obtain simulated results within ± 10%, 10-25% and 25-50% difference of the average measured, respectively. All scenarios underestimate topsoil Pb content with 50-100% difference of the average measured value.

3.4 Future trends of the Cd, Cu, Pb, Zn contents in the Great Square soils

Figure 45 shows the relative changes in soil metal content for the coming 20, 50 and 100 years while maintaining the current gardening practices in the Great Square. The distribution of the four metal flows after a century is shown in Figure 46. The proposition of each flow is presented in % of the sum of the absolute value of all flows. Today, the levels of pollutants in the atmosphere are much lower than they were in the industrial era of the 20th century. The future mode of gardening practices could be considered 100% organic farming without use of chemical fertilizers and phytosanitary products. Organic amendments are the dominant source resulting in soil metal accumulation (Figure 46).

As illustrated in Figure 46, soil Cd content should increase by 9% after 20 years, 22% after 50 years and 39% after 100 years. The distribution of the input flows follows the order: Qorg (70%) > Qatm (12%). For Cu, Pb, soil Cu content would increase by 4.5% after 20 years and 20% after 100 years. The distribution of the input flows follows the order: Qorg (72%) > Qatm (3.6%). Simulations showed a slight increase in soil Pb content, of around 5% after 100 years.

For Zn, the model predicts an increase of 7% after 20 years, 18% after 50 years and 32% after 100 years.

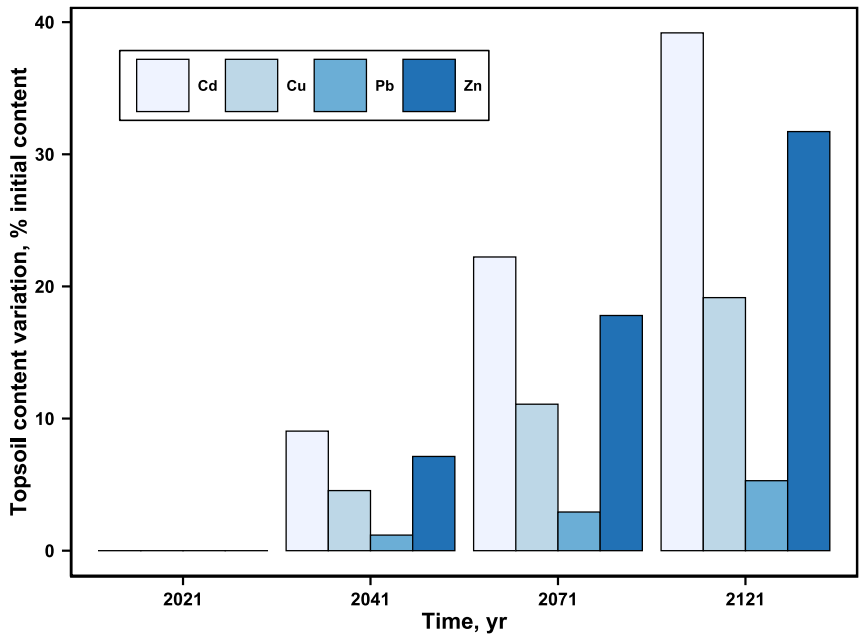

Figure 45. Relative variation of metal content in Great Square topsoil (0-20 cm) by decade

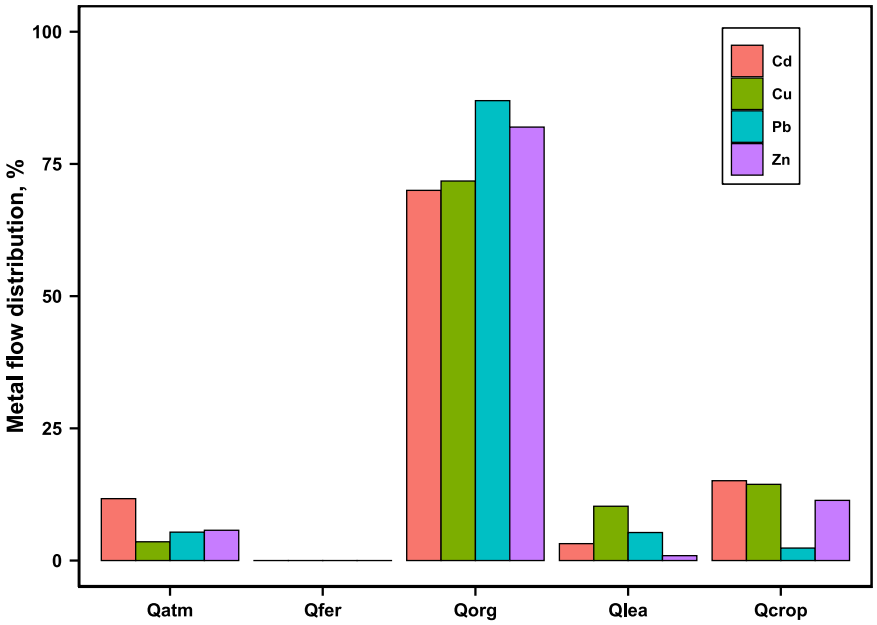

Figure 46. Mean distribution of input and output flows of the four metals during the period of 2021-2121 for Great Square topsoil (0-20 cm). In % of the sum of the absolute value of all the flows. Qatm: atmospheric deposition; Qfer: NPK fertilizers; Qorg: organic amendments; Qlea: leaching; Qcrop: crop offtake

Figure A20 shows the evolution of the four metal contents in topsoil for the next century. The predicted level of Cd in the soil will reach 0.47 mg kg^{-1} in 2121, which is nearly close to the regional threshold. Soil Cu concentrations are predicted to reach 66 mg kg^{-1} in 2121, which is between the regional and international thresholds. Soil Pb concentrations predicted to increase to 199 mg kg^{-1} in 2021. This concentration nearly reaches the international guideline value, indicating potential ecological and health risks causing by Pb contamination. Soil Zn concentrations are predicted to reach the international threshold (200 mg kg^{-1}) in 2102. Referring to Chinese soil quality standard, the concentrations of Cd, Cu, Pb and Zn in the soil should be less than 0.3, 50, 50, 200 mg kg^{-1} for farmland or greenhouse vegetable production (SEPAC, 2007). The concentrations of Cd and Pb in the Great Square soil already exceed these values and this situation will get worse in the future. More investigations are needed to evaluate the risk related to the KVG soil contamination.

3.5 Optimizing soil pH management by relating to soil metal availability

Accumulation of Cd, Cu, Pb and Zn in the Great Square soil should be occurred in the future. Metal concentration in soil solution can be used to assess the evolution of their ecotoxicity, since this drives the impact of metals on soil organisms and their transfer to cultivated plant (Lin et al., 2016; Liu et al., 2014; Slaveykova and Wilkinson, 2005).

Metal concentrations in soil solution were calculated by using total metal content in soil, pH and OM as input variables in our model (Table 31). The evolution of organic carbon was simulated in our model by RothC module (Figure A11). Results of simulated topsoil OC content showed a good agreement with measured SOC content in the scenarios of 25% and 50% application rate of *terreau* (Table 33). In our current model, coupling VSD^{+} model has successfully simulated the changes in soil pH value over time, as the simulated soil pH value was very close to the measured value in 2021 (Figure 32). Measured pH of the Great Square soils was essentially the same at different depths (Table 26). It is due to a large number of base cations added to topsoil through organic amendments, which surplus was leached into the subsoil. Since 2000, approximately 2 kg FW m^{-2} of green waste compost have been added to the soil each year, and it maintains a neutral soil pH, between 6.5 and 7.5. The simulated metal concentrations in soil solution decreases significantly with increasing soil pH (Figure A18). In a previous study of 104 vegetable gardens in France, we suggested that liming might be an effective way to lower soil metal availability and thus reduce the potential risk due to soil metal

accumulation (Zhong et al., 2021). Based on the results of the pH trend simulations in the Great Square of KVG, it appears that the current soil can be maintained at a near base saturation state by the addition of green waste compost. There is no much space to increase soil pH by liming, while soil pH is nearly close to 7 or higher.

Reducing the trace metal contents in organic fertilizers is practically unrealistic for the average garden owner. In addition, soils in urban gardens are often over-fertilized by the current application rate of organic fertilizers (Joimel, 2015; Joimel et al., 2021). Prospectively, the optimal idea should include minimizing the addition of organic fertilizers while meeting the plant's nutrient requirements, and maintaining a proper soil pH value via organic fertilizers and reducing BC^{2+} loss by plant removal. As the nutriment composition is not the same in different organic fertilizers, mixing different organic fertilizers maybe be also a possible way to reduce their total use still meeting plant’s nutrient requirements. For a better insight of organic farming in urban vegetable gardens, more studies would be needed in the future to fill this gap of knowledge.

4 Conclusions

Overall, long-term use of organic fertilizers in large quantities, improper use of insecticides, and atmospheric pollution in the past led to a high level of soil metal contamination in the King's Vegetable Garden. The accuracy of the model was evaluated. The availability and accuracy of historical data are of crucial importance for the relevance of the long-term simulations of the trace metal mass balance.

Mass balance modeling suggests that if current gardening practices continue, the soil metal contents will increase 39% for Cd, 20% for Cu, 5% for Pb, and 32% for Zn for the next century. The soil of the Great Square of KVG has reached a critical level for Cd, Cu and Pb. There is a risk of overexposure to Cd and Pb through inhalation of soil dust or direct ingestion if children have access to the site during educational visits, or directly through the consumption of vegetables grown in the KVG. In order to ensure the safety of vegetable products, more investigations on vegetable contamination and exposure pathways are needed.

Appropriate application rate of organic amendments should be deduced, depending on different plant requirements. Regular use of organic amendment can help to maintain soil pH at neutral or slightly alkaline state. More dissolved organic matters are added into soil through organic amendment. We need to consider the effect of DOM on metal leaching to further improve our metal leaching model. To provide useful information how to better manager urban vegetable gardens for decision-makers, that is necessary to effectively quantify transmission of metals from the soil to the food chain. The current simplified crop uptake model should be improved in the future by considering plant species, soil physicochemical properties and important mechanistic processes.

.

Chapitre 5 : Discussion générale sur la modélisation du bilan de masse des métaux traces dans les sols des jardins urbains français

Après avoir présenté le Green Deal de l'UE en 2019, la Commission européenne a élaboré en mai 2020 la stratégie de l'UE en faveur de la biodiversité à l'horizon 2030. Il s'agit d'un plan complet et ambitieux à long terme visant à protéger la nature et à inverser la dégradation des écosystèmes (https://ec.europa.eu/environment/strategy/soil-strategy_en).

L'utilisation raisonnée des boues d'épuration en agriculture et les nouvelles normes de teneurs en éléments nocifs dans les engrais commerciaux ont été redéfinies en 2019 (notamment pour réduire les niveaux de cadmium dans les sols). En outre, la Commission européenne a proposé, dans la stratégie de l'UE pour 2030, d'intensifier les efforts pour protéger la fertilité des sols et réduire l'érosion des sols et la surutilisation des nutriments, ainsi augmenter le teneur en matière organique dans les sols. Cet objectif devrait être atteint par l'adoption de pratiques durables pour les sols agricoles. Les sols des jardins potagers ont subi des pratiques culturales intenses et répétées. Il s'agit d'évaluer si les pratiques actuelles dans les jardins potagers urbains sont durables.

Dans cette thèse, nous nous sommes basés sur les niveaux élevés de contamination de sols supports d'agriculture urbaine par les métaux dans 104 jardins potagers localisés à Nancy, Nantes et Marseille tels que décrit par Joimel et al. (2016) et nous avons acquis des données supplémentaires que pour des sols du Potager du Roi à Versailles. Dans ces jardins, la matière organique et les niveaux de phosphore dans les sols étaient généralement plus élevés que dans les sols agricoles en raison de la sur-fertilisation. Des pratiques de jardinage intensives et inappropriées peuvent en effet entraîner l'accumulation de métaux dans le sol (Hu et al., 2018; Schwartz, 2013a). Dans la plupart de ces jardins potagers, les niveaux de la concentration de Cu, Pb et Zn dans le sol étaient supérieurs aux valeurs seuils et dépassaient même les valeurs guides (Table 32). Pour le Potager du Roi à Versailles, les niveaux de contamination de Cu, Pb et Zn dans les sols sont bien supérieurs aux valeurs du 95e percentile pour les sols agricoles de la région parisienne (Mathieu et al., 2008). Pour le Cd, ses concentrations dans les sols de ces jardins potagers étaient plus élevées que celles observées dans les différents systèmes selon un gradient d'anthropisation (forêt, prairie, agriculture conventionnelle, verger et vignoble) (Joimel et al., 2016). Dans Le Potager du Roi, des méthodes de jardinage courantes étaient appliquées pour chaque époque de son évolution (Anonymous, 1759; La Quintinie, 1690;

Moreau and Daverne, 1845). Il n'est donc pas difficile d'en déduire que d'autres sols de jardins ayant une longue histoire ont pu être le lieu d'une contamination similaire en métaux.

Dans le contexte actuel d’évaluation des risques de dissémination des polluants des sols et de préservation de la santé humaine et des écosystèmes, nous proposons un modèle de bilan de masse pour simuler l’évolution de la teneur en métaux du sol dans les jardins potagers français en fonction du temps et des pratiques de jardinage.

1 Valeur pratique du modèle de bilan de masse et comment l'adapter à d'autres études dans les sols agricoles

La Figure 47 présente les processus formalisés dans la modélisation du bilan de masse des métaux en traces dans un sol de jardin potager. D'après une enquête par questionnaire réalisée dans les 104 jardins potagers en France (Joimel 2015), nous pouvons connaître les principales pratiques de jardinage et les sources de contamination métallique des sols. Contrairement aux grandes cultures, les pratiques de jardinage dans les jardins potagers français n'ont pas de norme et ne font pas l'objet de recommandations formelles. Elles varient considérablement en fonction de la ville, du climat et des habitudes des jardiniers.

Lors de la construction du modèle, nous avons tenu compte du nombre de paramètres requis et de la facilité avec laquelle ces paramètres pouvaient être obtenus, et de la possibilité de l'intégrer à une simulation du bilan de masse des métaux dans le sol à long terme (de la décennie au siècle). Notre première question était de savoir si un modèle classique de bilan de masse pouvait être amélioré pour l'adaptation aux sols de jardins potagers en considérant notamment l'utilisation régulière et intensive d'amendements organiques. Par exemple, la lixiviation des métaux à travers les sols dépend de leur solubilité et de leur mobilité, qui sont influencées par le pH du sol et la matière organique. Par conséquent, nous avons incorporé, respectivement, les modèles RothC et VSD^+ pour simuler les changements du carbone et du pH dans les sols. Nous avons combiné le modèle RothC, le modèle VSD^+ et le modèle de partition des métaux avec un modèle de cycle hydrologique pour simuler la perte de métaux par lixiviation.

Pour la modélisation des teneurs en métaux dans les sols des 104 jardins français et du Potager du Roi à Versailles, outre l'analyse des propriétés physico-chimiques des sols et des informations sur les pratiques de jardinage, nous avons collecté les données nécessaires à l'exécution du modèle à partir de la littérature scientifique et d'un certain nombre de bases de données nationales et internationales, telles que les rendements annuels en légumes (Agreste, 2020b), les fongicides à base de cuivre (ITAB, 2020), le dépôt atmosphérique de métaux (EMEP database : https://www.emep.int/). Certaines de ces données sont détaillées au niveau de la ville, d'autres sont des moyennes pour une région.

En comparant le bilan de masse utilisé en grande culture (Sterckeman et al., 2019, 2018), notre modèle est également applicable à la grande culture. Les données nécessaires aux calculs de notre modèle sont disponibles à l'échelle nationale.

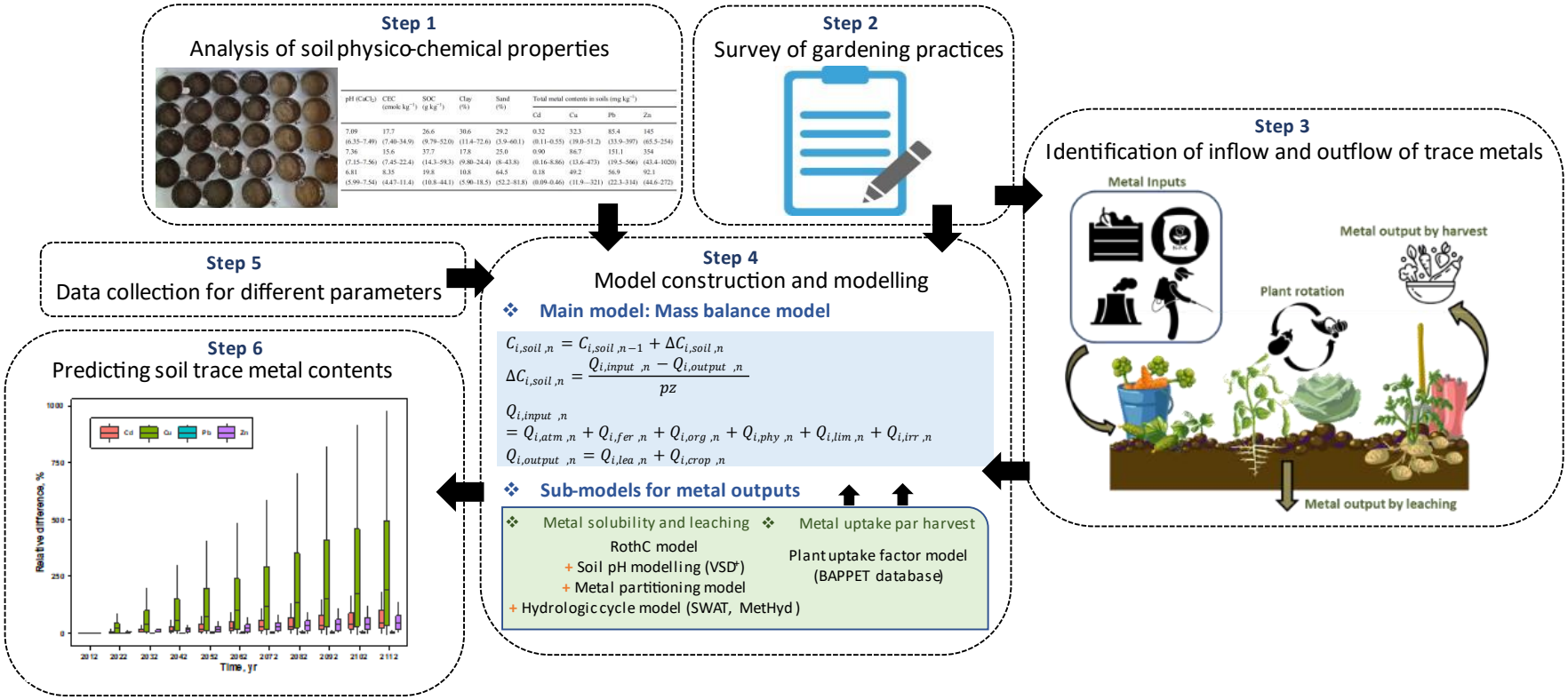

Figure 47. Processus formalisés dans la modélisation du bilan de masse des métaux en traces dans les sols de jardins potagers

2 Impact des pratiques de jardinage sur l'accumulation des métaux dans le sol

Sur la base de la modélisation du bilan de masse dans 104 jardins français, les teneurs des quatre métaux dans les sols vont augmenter de manière significative dans le futur. Cette augmentation est principalement due aux apports de fongicides dans le cas du Cu, et aux amendements organiques et secondairement aux engrais chimiques dans le cas de Cd, Pb et Zn. Nous avons ensuite fait l'hypothèse que l'utilisation à long terme d'amendements organiques en grandes quantités, l'application d'insecticides et la pollution atmosphérique passée ont conduit à un niveau élevé de contamination des sols par les métaux dans le Potager du Roi. Dans le scénario basé sur une poursuite des pratiques actuelles au Potager du Roi, en agriculture biologique, sans aucun apport de pesticide ni d'engrais chimique, le modèle a prédit des augmentations jusqu'à 40 % pour la teneur en Cd dans les sols, 20 % pour Cu, 5 % pour Pb, and 32 % pour Zn à la fin du prochain siècle. Les sols du Potager du Roi pourraient être contaminés par le Cd et le Pb à un point tel que cela pourrait entraîner une exposition excessive à ces deux métaux pour les consommateurs de fruits et légumes, si les produits du Potager du Roi constituaient leur principale source quotidienne de végétaux. D'après les simulations du bilan de masse, les pertes de métaux simulées par lixiviation ou par prélèvement par les plantes sont largement inférieures aux flux d'entrée par différentes pratiques de jardinage. Cela a également été constaté dans des travaux antérieurs (Cambier et al., 2014, 2014; Fang et al., 2018, 2017; Hu et al., 2013; Yang et al., 2021; Yang et al., 2018).

Pour les jardins potagers français, nous avons montré que l'application des amendement organiques avec les doses recommandées par l'ADEME (2019) constitue l'apport le plus important des métaux dans le sol. Le même résultat est observé dans le Potager du Roi avec l'application actuelle du compost de déchets verts. Comme mentionné précédemment, l'épandage des déchets organiques est encouragé en Europe pour maintenir la fertilité des sols. Nos résultats montrent que l'utilisation à long terme d'amendements organiques peut entraîner une forte contamination par les métaux des sols de jardins potagers, similaire aux résultats trouvés dans la littérature (Cagnarini et al., 2020; Hu et al., 2013; Michaud et al., 2020; Qian et al., 2018, 2020).

Les deux études suggèrent que les amendements organiques devraient contenir moins de métaux et être appliqués à des doses correspondant aux besoins du sol et des plantes. Par ailleurs,

l'utilisation de produits à base de cuivre comme fongicides est à remettre en question, eu égard à la contamination des sols par cet élément.

3 La performance du modèle et l'incertitude liée à la simulation

Il existe deux façons de vérifier la performance du modèle de bilan de masse : soit à partir de simulations de concentrations des métaux actuelles à partir des données antérieures (Oporto et al., 2012; Peng et al., 2017), soit à partir du suivi des teneurs dans les sols à l'avenir sur le moyen ou long terme, dans une logique d'observation (McDowell and Gray, 2022; Qian et al., 2018; Yang et al., 2021).

Nous avons évalué la précision des composants du modèle grâce à l'étude sur les tendances historiques des métaux dans le Potager du Roi. Le modèle RothC nous a servi à calibrer les apports d'amendements organiques. Le modèle VSD^{+} a prédit avec précision l'évolution du pH du sol. Le modèle a également été très précis dans la prédiction de la teneur en Zn des sols. Pour le Cd, le Cu et le Pb, le modèle est peu performant. Nous révélons que la disponibilité et la précision des données historiques sont essentielles pour la pertinence des simulations à long terme du bilan de masse des métaux dans les sols. Au chapitre 2, les résultats de l'analyse de sensibilité du modèle montrent que les paramètres associés aux apports des métaux ont une plus grande influence que les propriétés physico-chimiques du sol. Les incertitudes de la simulation sont dues aux simplifications du modèle et à l'incertitude des données sur les flux d'entrées (Peng et al., 2016).

Dans l'étude de Yang et al. (2021), la composition du modèle de bilan de masse qu'ils ont utilisé était très similaire à la nôtre. Ils ont extrapolé l'évolution historique du cadmium dans les sols rizicoles chinois sur la base d'enquêtes régionales à long terme sur les voies d'entrée et de sortie du cadmium à l'échelle du champ, et les résultats prédits étaient proches de ceux détectés. Cependant, c'est un vrai défi de collecter des données historiques pour le Potager du Roi sur ces 300 dernières années. La disponibilité et la précision des données historiques sont d'une importance cruciale pour la pertinence des simulations à long terme. C'est pour cela que nous avons besoin de plus de travaux à l'avenir pour la surveillance à long terme et l'évaluation des prédictions des modèles.

4 Principales avancées liées à la thèse

Dans cette thèse, nous avons établi un modèle de bilan de masse couplé avec des différent modules (*e.g.*, le modèle RothC, le modèle VSD^{+}), ce qui a permis de mieux prendre en compte l'effet des différents composants physico-chimiques du sol sur la dynamique du métal.

Grâce à ce modèle et à une vaste collecte de données qui ont été mises à notre disposition (thèse de S Joimel ; ANR JASSUR), nous avons mené la première étude sur l'évolution à long terme des métaux dans des sols de jardins potagers en France. Pour la première fois dans la littérature, des données historiques ont été utilisées pour simuler des effets de pratiques passées sur les teneurs en métaux du sol (Potager du Roi). En outre, c'est la première fois que la performance du modèle de bilan de masse des métaux à long terme a été évaluée.

Dans cette thèse, nous extrapolons l'impact des pratiques actuelles de jardinage dans les jardins potagers français sur la future contamination du sol par les métaux à l'aide la modélisation, qui apporte des informations significatives aux individus, aux décideurs ou aux responsables politiques pour prendre des contre-mesures, telles que par exemple la gestion rationnelle des amendement organiques et l'établissement de seuils pour les teneurs en métaux dans différents amendements organiques.

5 Limitations

Les prévisions actuelles souffrent encore de nombreuses incertitudes. Contrairement aux grandes cultures, les pratiques agricoles mises en œuvre dans les jardins potagers sont très individuelles. Il est donc plus difficile de collecter les données nécessaires pour alimenter le modèle du bilan de masse. La plupart des variables et paramètres du modèle proviennent d'une étude documentaire. Par exemple, les concentrations des quatre métaux dans les engrais chimiques, dans les différents amendements organiques, ou dans les retombées atmosphériques, de même que les données climatiques. Ces données peuvent être très variables d'un point de vue géographique. Par exemple, nous avons utilisé des quantités recommandées ou maximales (pesticides) pour estimer les doses appliqué (*e.g.*, engrais chimiques, amendements organiques, pesticides, eau d'irrigation). Ces valeurs peuvent être très différentes de celles utilisées localement par certains individus.

Au niveau de la modélisation, le modèle du prélèvement des métaux par les plantes est très simplifié. En fait, chaque légume a une capacité d'absorption différente pour un métal donné. Par exemple, certains légumes feuilles à croissance rapide, comme les salades, ont un taux de d'absorption des métaux beaucoup plus élevé que le légume moyen, tandis que d'autres présentent une capacité native élevée de sorption des métaux, comme les épinards (Bidar et al., 2020; Dala-Paula et al., 2018; Paltseva et al., 2018; Yang et al., 2018). En outre, le modèle PUF, exprimé comme le rapport entre la teneur totale en métaux du sol et la teneur en métaux de la fraction disponible des légumes, est un modèle basé sur des données. Les valeurs résumées par les auteurs pour un même légume peuvent varier considérablement d'une source à l'autre, ainsi qu'on peut le voir dans la base de données BAPPET. Cela est dû aux différences entre environnements dans lesquels ces légumes sont cultivés (*e.g.*, propriétés du sol, climat, cycle de croissance des végétaux, conditions expérimentales). En outre, le processus d'absorption, d'interception (foliaire) et de transfert des métaux vers les différentes parties de la plante est complexe et souvent lié à la forme du métal en solution aqueuse (Huang et al., 2020; Shahid et al., 2017; Sterckeman and Thomine, 2020; Uchimiya et al., 2020). Cependant, en raison de la grande variété de légumes cultivés dans un jardin, il est très difficile d'envisager un modèle aussi complexe pour chaque espèce végétale, voire pour chaque variété d'une même espèce.

Les concentrations des métaux en solution dans le sol ont été modélisées en tenant compte des changements dans la matière organique et le pH du sol. Cependant, de nombreux autres facteurs ne sont pas pris en compte dans le modèle, comme l'effet de l'ajout de différents engrais organiques et inorganiques sur la spéciation des métaux (Fang et al., 2018, 2017, 2016; Ren et al., 2015; Waterlot et al., 2017b, 2011) et l'effet du travail du sol sur les flux préférentiels (Kochem Mallmann et al., 2014). Ces facteurs peuvent entraîner des erreurs dans la simulation de la lixiviation des métaux. De plus, l'influence des organismes du sol sur la fixation/libération des métaux n'est pas non plus prise en compte dans le modèle, par exemple la stabilisation du métal par les résidus de vers de terre (Richardson et al., 2016). Des connaissances restent à acquérir pour être capable de construire des modèles pour ces processus dynamiques de métaux dans une situation réelle. En particulier, il faudra tenir compte de la disponibilité et de l'accessibilité des données requises pour alimenter le modèle.

6 Perspectives

Il existe encore de nombreuses lacunes dans les connaissances concernant la modélisation des métaux dans les sols de jardins potagers, des sols supports d'agricultures urbaines et général (et même dans les sols arables en milieu rural) qui méritent d'être abordées dans les études futures.

6.1 Proposition 1 :

Pour aller plus loin par rapport aux connaissances acquises dans la thèse, nous pourrions faire un suivi expérimental en mettant en place un groupe de contrôle avec différentes pratiques de jardinage. Par exemple, il serait possible de tester différents engrais organiques, en plantant les légumes fréquemment cultivés, avec ou sans travail du sol.

Il s'agirait alors de comparer et de quantifier les effets de différentes pratiques sur la dynamique des métaux dans le système sol-plante (*e.g.*, spéciation chimique, mobilité, biodisponibilité), la fixation des métaux par les organismes du sol, le transport des métaux du sol vers les eaux souterraines (*e.g.*, lixiviation, flux préférentiel), et l'absorption et la translocation des métaux dans différentes parties de plant (*e.g.*, parties résiduelles, comestibles (externe, interne)), et enfin d'améliorer et de valider notre modèle actuel.

De même, nous pourrions comparer les effets de modèles de différents niveaux de complexité sur la prédiction des changements des métaux dans les sols. Étant donné que les modèles complexes nécessitent plus de données, cela signifie qu'il faut tenir compte de l'accessibilité des données ainsi que des incertitudes associées aux données. Si un modèle simplifié ne nécessite pas autant de données et réduit donc les erreurs de données, il perd toutefois une partie des informations mécanistiques et conduit à des prédictions inexactes. Des études comparatives pourraient alors nous indiquer si nous devons améliorer le modèle et mieux comprendre les performances de différents modèles.

6.2 Proposition 2 : Comment transcrire les résultats de modélisation en recommandations de pratiques de jardinage ?

Dans le cadre de nos recherches, nous prévoyons les changements futurs des teneurs en métaux dans les sols de jardins potagers et nous quantifions également les effets de différentes pratiques

agricoles sur la pollution métallique des sols par ces métaux. Cependant, les résultats de notre modélisation ne répondent pas encore complètement à ces deux questions scientifiques :

- A partir de la modélisation, peut-on obtenir des scénarios optimaux des pratiques de jardinage pour réduire l'exposition aux métaux, en tenant compte à la fois des besoins des sols en nutriments et des enjeux environnementaux (*e.g.*, stockage du carbone, recyclage du phosphore) ?
- Peut-on construire un guide de recommandations, des bonnes pratiques de jardinage à utiliser (incluant le phyto-management) pour permettre une gestion durable des jardins et réduire la contamination métallique des sols ?

L'utilisation optimale des engrais organiques doit encore être explorée de manière plus approfondie dans les futures recherches. Pour ce faire, nous pourrions étudier et faire une synthèse des besoins en nutriments des différentes espèces végétales cultivées, ou encore les teneurs en nutriments et en substances nocives des différents amendements organiques. Nous pouvons élaborer différents scénarios en tenant compte des aspects environnementaux (*e.g..*, le stockage du carbone, recyclage du phosphore), des exigences de croissance des plantes et des avantages économiques. Ensuite, nous pourrions valoriser le modèle pour prédire les conséquences de ces scénarios sur la contamination en métaux des sols et donc trouver des solutions de gestion optimales. Ce type de résultat est plus susceptible d'être utilisé par des jardiniers des agriculteurs urbains, des décideurs ou des élus comme informations de référence.

Conclusion générale

Dans ce mémoire, nous démontrons que des données recueillies dans des publications peuvent être utilisées pour simuler les tendances des changements futurs des métaux dans les jardins potagers français à l'aide de modèles de bilan de masse. De même, nous démontrons la faisabilité de l'ajout des modèles liés à la dynamique des métaux au modèle de bilan de masse. Grâce à la simplicité du modèle et à l'accessibilité des données, il peut être facilement appliqué par les chercheurs à d'autres systèmes agricoles, ce qui renforce son applicabilité à des conditions locales contrastées.

Nous avons pu prédire les évolutions des teneurs en Cd, Cu, Pb et Zn dans les sols de jardins potagers situés sous des conditions climatiques et environnementales contrastées et ceci au cours du prochain siècle. L'agriculture biologique à 100 % pourrait légèrement diminuer le taux d'accumulation des métaux dans les sols. Une alternative à l'utilisation de produits à base de cuivre comme fongicides serait à envisager pour limiter la contamination des sols par cet élément.

Dans l'étude du Potager du Roi à Versailles, nous avons simulé les tendances historiques et futures des teneurs en métaux traces dans les sols grâce à une collecte des données historiques sur les pratiques de jardinage et les flux de métaux traces de 1683 à 2021. Nous avons confirmé que l'utilisation intensive à long terme d'amendements organiques, l'utilisation inappropriée de pesticides et la pollution atmosphérique passée ont conduit à des niveaux élevés de contamination des métaux dans les sols. Nous avons testé notre modèle en utilisant des flux historiques, par rapport aux teneurs actuelles en métaux traces mesurées. Le modèle a la meilleure performance pour simuler le Zn, suivis par les prédictions pour le Cd, le Cu et le Pb, respectivement. Une évaluation plus approfondie de la précision du modèle sera nécessaire dans les études futures.

La simulation de la tendance future de contamination des sols au Potager du Roi montre que le jardinage biologique privilégiée actuellement contribuera encore de manière significative à l'accumulation des quatre métaux dans les sols. Il existe alors un risque de surexposition au Cd et au Pb par inhalation de la poussière du sol ou par ingestion directe, ou par la consommation des légumes cultivés dans le Potager du Roi qui restera à confirmer. De plus, les résultats de notre étude montrent qu'il y a une très faible quantité de perte de métaux par lixiviation. Nous

devons cependant poursuivre les recherches pour savoir si cette faible quantité de métal pourrait contaminer les eaux souterraines.

En conclusion, afin de fournir aux décideurs des informations utiles sur la façon de mieux gérer les potagers urbains, il est nécessaire de valoriser ce travail pour élaborer un ensemble de recommandations pour les pratiques de jardinage en réponse aux problèmes de la santé du sol (*e.g.*, contamination par les métaux, fertilité du sol). En outre, il est également nécessaire de quantifier efficacement le transport des métaux du sol vers la chaîne alimentaire. D'autres études devraient être menées pour analyser la teneur en métaux dans les parties comestibles des légumes cultivés dans les jardins urbains français, en veillant à préserver la sécurité alimentaire.

Références

ADEME, 2019. Le compostage et le paillage.

ADEME, 2012. Base de données des teneurs en éléments traces métalliques de plantes potagères (BAPPET) : présentation et notice d'utilisation.

Agreste, 2020a. Utilisation du territoire|Agreste, la statistique agricole [WWW Document]. URL https://agreste.agriculture.gouv.fr/agreste-web/disaron/SAANR_1/detail/ (accessed 12.23.20).

Agreste, 2020b. Production mensuelle de légumes pour la France et ses bassins|Agreste, la statistique agricole [WWW Document]. URL https://agreste.agriculture.gouv.fr/agreste-web/disaron/D_0029/detail/ (accessed 4.3.20).

Allan, M., Roux, G.L., Vleeschouwer, F.D., Bindler, R., Blaauw, M., Piotrowska, N., Fagel, N., Sikorski, J., 2013. High-resolution reconstruction of atmospheric deposition of trace metals and metalloids since AD 1400 recorded by ombrotrophic peat cores in Hautes-Fagnes, Belgium. Environmental Pollution 178, 381–394. https://doi.org/10.1016/j.envpol.2013.03.018

Alloway, B.J., 2013a. Sources of Heavy Metals and Metalloids in Soils, in: Alloway, B.J. (Ed.), Heavy Metals in Soils: Trace Metals and Metalloids in Soils and Their Bioavailability, Environmental Pollution. Springer Netherlands, Dordrecht, pp. 11–50. https://doi.org/10.1007/978-94-007-4470-7_2

Alloway, B.J. (Ed.), 2013b. Heavy Metals in Soils: Trace Metals and Metalloids in Soils and their Bioavailability, 3rd ed, Environmental Pollution. Springer Netherlands.

Alloway, B.J., 2004. Contamination of soils in domestic gardens and allotments: a brief overview. Land Contamination & Reclamation 12, 179–187. https://doi.org/10.2462/09670513.658

Annette Piorr, 2011. Peri-urbanisation in Europe : towards European policies to sustain urban-rural futures : synthesis report. Frederiksberg : Forest & Landscape, University of Copenhagen.

Anonymous, 1759. Comparaison de différents types de culture en vue d'établir un budget pour le Potager.

Antoniadis, V., Levizou, E., Shaheen, S.M., Ok, Y.S., Sebastian, A., Baum, C., Prasad, M.N.V., Wenzel, W.W., Rinklebe, J., 2017a. Trace elements in the soil-plant interface: Phytoavailability, translocation, and phytoremediation–A review. Earth-Science Reviews 171, 621–645. https://doi.org/10.1016/j.earscirev.2017.06.005

Antoniadis, V., Shaheen, S.M., Boersch, J., Frohne, T., Du Laing, G., Rinklebe, J., 2017b. Bioavailability and risk assessment of potentially toxic elements in garden edible vegetables and soils around a highly contaminated former mining area in Germany. Journal of Environmental Management, Biogeochemistry of trace elements in the environment 186, 192–200. https://doi.org/10.1016/j.jenvman.2016.04.036

AROMIS, 2020. Heavy metals and nutrients in European cattle solid manure. Database AROMIS, assessment and reduction of heavy metal input into agro-ecosystems. [WWW Document]. URL https://daten.ktbl.de/aromis/heavyMetal.do (accessed 7.19.20).

Arora, M., Kiran, B., Rani, S., Rani, A., Kaur, B., Mittal, N., 2008. Heavy metal accumulation in vegetables irrigated with water from different sources. Food Chemistry 111, 811–815. https://doi.org/10.1016/j.foodchem.2008.04.049

Augustsson, A., Uddh-Soderberg, T., Filipsson, M., Helmfrid, I., Berglund, M., Karlsson, H., Hogmalm, J., Karlsson, A., Alriksson, S., 2018. Challenges in assessing the health risks of consuming vegetables in metal-contaminated environments. Environ. Int. 113, 269–280. https://doi.org/10.1016/j.envint.2017.10.002

AURAN, 2018. Nantes : 2 900 ha de couvert végétal - Les synthèses de l'Auran #36 [WWW Document]. URL https://www.auran.org/publications/nantes-2-900-ha-de-couvert-vegetal-les-syntheses-de-lauran-36 (accessed 6.28.19).

Azimi, S., Rocher, V., Garnaud, S., Varrault, G., THEVENOT, D.R., 2005. Decrease of atmospheric deposition of heavy metals in an urban area from 1994 to 2002 (Paris, France). Chemosphere 61, 645–651. https://doi.org/10.1016/j.chemosphere.2005.03.022

Baharuddin, M.R.B., Sahid, I.B., Noor, M.A.B.Mohd., Sulaiman, N., Othman, F., 2011. Pesticide risk assessment: A study on inhalation and dermal exposure to 2,4-D and paraquat among Malaysian paddy farmers. Journal of Environmental Science and Health, Part B 46, 600–607. https://doi.org/10.1080/03601234.2011.589309

Baize, D., Bourgeois, S., 2005. Estimation des apports agricoles et des retombées atmosphériques en éléments en traces et majeurs grâce à un essai de longue durée (dispositif Dehérain à Grignon).

Baize, D., Sterckeman, T., 2001. Of the necessity of knowledge of the natural pedo-geochemical background content in the evaluation of the contamination of soils by trace elements. Sci Total Environ 264, 127–139. https://doi.org/10.1016/s0048-9697(00)00615-x

Baveye, P., McBride, M.B., Bouldin, D., Hinesly, T.D., Dahdoh, M.S.A., Abdel-sabour, M.F., 1999. Mass balance and distribution of sludge-borne trace elements in a silt loam soil following long-term applications of sewage sludge. Science of The Total Environment 227, 13–28. https://doi.org/10.1016/S0048-9697(98)00396-9

Bechet, B., Joimel, S., Jean-Soro, L., Hursthouse, A., Agboola, A., Leitão, T.E., Costa, H., do Rosário Cameira, M., Le Guern, C., Schwartz, C., Lebeau, T., 2018. Spatial variability of trace elements in allotment gardens of four European cities: assessments at city, garden, and plot scale. Journal of Soils and Sediments 18, 391–406. https://doi.org/10.1007/s11368-016-1515-1

Bell, S., Fox-Kaemper, R., Keshavarz, N., Benson, M., Caputo, S., Noori, S., Voigt, A., 2016. Urban allotments gardens in Europe. Routledge.

Belon, E., Boisson, M., Deportes, I.Z., Eglin, T.K., Feix, I., Bispo, A.O., Galsomies, L., Leblond, S., Guellier, C.R., 2012. An inventory of trace elements inputs to French agricultural soils. Science of The Total Environment 439, 87–95. https://doi.org/10.1016/j.scitotenv.2012.09.011

Bengtsson, H., Alvenäs, G., Nilsson, S.I., Hultman, B., Öborn, I., 2006. Cadmium, copper and zinc leaching and surface run-off losses at the Öjebyn farm in Northern Sweden—Temporal and spatial variation. Agriculture, Ecosystems & Environment 113, 120–138. https://doi.org/10.1016/j.agee.2005.09.001

Bidar, G., Pelfrêne, A., Schwartz, C., Waterlot, C., Sahmer, K., Marot, F., Douay, F., 2020. Urban kitchen gardens: Effect of the soil contamination and parameters on the trace element accumulation in vegetables – A review. Science of The Total Environment 139569. https://doi.org/10.1016/j.scitotenv.2020.139569

Boekhold, A.E., Van der Zee, S.E.A.T.M., 1991. Long-term effects of soil heterogeneity on cadmium behaviour in soil. Journal of Contaminant Hydrology 7, 371–390. https://doi.org/10.1016/0169-7722(91)90003-J

Bonten, L.T.C., Reinds, G.J., Groenenberg, J.E., de Vries, W., Posch, M., Evans, C.D., Belyazid, S., Braun, S., Moldan, F., Sverdrup, H.U., Kurz, D., 2015. Dynamic Geochemical

Models to Assess Deposition Impacts and Target Loads of Acidity for Soils and Surface Waters, in: de Vries, W., Hettelingh, J.-P., Posch, M. (Eds.), Critical Loads and Dynamic Risk Assessments: Nitrogen, Acidity and Metals in Terrestrial and Aquatic Ecosystems, Environmental Pollution. Springer Netherlands, Dordrecht, pp. 225–251. https://doi.org/10.1007/978-94-017-9508-1_8

Bonten, L.T.C., Reinds, G.J., Posch, M., 2016. A model to calculate effects of atmospheric deposition on soil acidification, eutrophication and carbon sequestration. Environmental Modelling & Software 79, 75–84. https://doi.org/10.1016/j.envsoft.2016.01.009

Boulaine, J., 2006. Histoire de la fertilisation phosphatée 1762-1914. Etu Gestion Sols 129–137.

Boulaine, J., 1995a. Quatre siècles de fertilisation. Première partie. Etu Gestion Sols 201–208.

Boulaine, J., 1995b. Quatre siècles de fertilisation. Seconde partie. Etu Gestion Sols 219–226.

BRAMM, 2018. Surveillance des retombées atmosphériques en France par analyse de mousses, Campagne 2016 du dispositif BRAMM.

BRAMM, 2013. Surveillance des retombées atmosphériques en France par analyse de mousses, Campagne 2011 du dispositif BRAMM.

Bretzel, F., Calderisi, M., Scatena, M., Pini, R., 2016. Soil quality is key for planning and managing urban allotments intended for the sustainable production of home-consumption vegetables. Environ Sci Pollut Res 23, 17753–17760. https://doi.org/10.1007/s11356-016-6819-6

Bretzel, F., Caudai, C., Tassi, E., Rosellini, I., Scatena, M., Pini, R., 2018. Culture and horticulture: Protecting soil quality in urban gardening. Sci. Total Environ. 644, 45–51. https://doi.org/10.1016/j.scitotenv.2018.06.289

Broadley, M.R., White, P.J., Hammond, J.P., Zelko, I., Lux, A., 2007. Zinc in plants. New Phytologist 173, 677–702. https://doi.org/10.1111/j.1469-8137.2007.01996.x

Buchter, B., Davidoff, B., Amacher, M.C., Hinz, C., Iskandar, I.K., Selim, H.M., 1989. CORRELATION OF FREUNDLICH Kd AND n RETENTION PARAMETERS WITH SOILS AND ELEMENTS. Soil Science 148, 370.

Burghardt, W., Heintz, D., Hocke, N., 2018. Soil Fertility Characteristics and Organic Carbon Stock in Soils of Vegetable Gardens Compared with Surrounding Arable Land at the Center of the Urban and Industrial Area of Ruhr, Germany. Eurasian Soil Sc. 51, 1067–1079. https://doi.org/10.1134/S106422931809003X

Cagnarini, C., Lofts, S., D'Acqui, L.P., Mayer, J., Grüter, R., Tandy, S., Schulin, R., Costerousse, B., Orlandini, S., Renella, G., 2020. Modelling of long term Zn, Cu, Cd, Pb dynamics from soils fertilized with organic amendments. SOIL Discussions 1–43. https://doi.org/10.5194/soil-2020-21

Cambier, P., Michaud, A., Paradelo, R., Germain, M., Mercier, V., Guerin-Lebourg, A., Revallier, A., Houot, S., 2019. Trace metal availability in soil horizons amended with various urban waste composts during 17 years - Monitoring and modelling. Sci. Total Environ. 651, 2961–2974. https://doi.org/10.1016/j.scitotenv.2018.10.013

Cambier, P., Pot, V., Mercier, V., Michaud, A., Benoit, P., Revallier, A., Houot, S., 2014. Impact of long-term organic residue recycling in agriculture on soil solution composition and trace metal leaching in soils. Science of The Total Environment 499, 560–573. https://doi.org/10.1016/j.scitotenv.2014.06.105

Cameron, R.W.F., Blanuša, T., Taylor, J.E., Salisbury, A., Halstead, A.J., Henricot, B., Thompson, K., 2012. The domestic garden – Its contribution to urban green infrastructure. Urban Forestry & Urban Greening 11, 129–137. https://doi.org/10.1016/j.ufug.2012.01.002

Camia, A., Robert, N., Jonsson, R., Pilli, R., Garcia, S., Lopez-Lozano, R., Velde, M., Ronzon, T., Gurria, P., M'Barek, R., Tomosiunas, S., Fiore, G., Araujo, R., Hoepffner, N.,

Marelli, L., Giuntoli, J., 2018. Biomass production, supply, uses and flows in the European Union. First results from an integrated assessment.
Carlon, C., Marco, D., Frank, S., 2007. Derivation methods of soil screening values in Europe: a review of national procedures towards harmonisation. European Commission, Joint Research Centre, Ispra.
Chalmandrier, M., Canavese, M., Petit-Berghem, Y., Rémy, É., 2017. « L'agriculture urbaine », entre concept scientifique et modèle d'action. Une notion mise à l'épreuve par le jardinage et le sol urbains. Géographie et cultures 119–138. https://doi.org/10.4000/gc.5052
Chen, H., Teng, Y., Lu, S., Wang, Y., Wang, J., 2015. Contamination features and health risk of soil heavy metals in China. Sci. Total Environ. 512, 143–153. https://doi.org/10.1016/j.scitotenv.2015.01.025
Chen, S., Xu, M., Ma, Y., Yang, J., 2007. Evaluation of different phosphate amendments on availability of metals in contaminated soil. Ecotoxicol. Environ. Saf. 67, 278–285. https://doi.org/10.1016/j.ecoenv.2006.06.008
Chen, W., Chang, A.C., Wu, L., 2007. Assessing long-term environmental risks of trace elements in phosphate fertilizers. Ecotox. Environ. Safe. 67, 48–58. https://doi.org/10.1016/j.ecoenv.2006.12.013
Christensen, T.H., 1989. Cadmium soil sorption at low concentrations: VIII. correlation with soil parameters. Water Air Soil Pollut 44, 71–82. https://doi.org/10.1007/BF00228779
Coleman, K., Jenkinson, D.S., 1996. RothC-26.3 - A Model for the turnover of carbon in soil, in: Powlson, D.S., Smith, P., Smith, J.U. (Eds.), Evaluation of Soil Organic Matter Models. Springer Berlin Heidelberg, Berlin, Heidelberg, pp. 237–246. https://doi.org/10.1007/978-3-642-61094-3_17
COST, n.d. COST Project - Action Urban Agriculture Europe [WWW Document]. URL http://www.urban-agriculture-europe.org/online-atlas.html (accessed 6.28.19).
Cowan, I.R., 1965. Transport of Water in the Soil-Plant-Atmosphere System. Journal of Applied Ecology 2, 221–239. https://doi.org/10.2307/2401706
Dala-Paula, B.M., Custódio, F.B., Knupp, E.A.N., Palmieri, H.E.L., Silva, J.B.B., Glória, M.B.A., 2018. Cadmium, copper and lead levels in different cultivars of lettuce and soil from urban agriculture. Environmental Pollution 242, 383–389. https://doi.org/10.1016/j.envpol.2018.04.101
DAMAS, O., BRANCHU, P., DOUAY, F., SCHWARTZ, C., GRAND, C., MAROT, F., 2018. Présomption de pollution d'un sol : des clés pour comprendre et agir. Plante & Cité.
De Bon, H., Parrot, L., Moustier, P., 2010. Sustainable urban agriculture in developing countries. A review. Agron. Sustain. Dev. 30, 21–32. https://doi.org/10.1051/agro:2008062
de Meeûs, C., Eduljee, G.H., Hutton, M., 2002. Assessment and management of risks arising from exposure to cadmium in fertilisers. I. Science of The Total Environment 291, 167–187. https://doi.org/10.1016/S0048-9697(01)01098-1
de Vries, W., McLaughlin, M.J., 2013a. Modeling the cadmium balance in Australian agricultural systems in view of potential impacts on food and water quality. Science of The Total Environment 461–462, 240–257. https://doi.org/10.1016/j.scitotenv.2013.04.069
de Vries, W., McLaughlin, M.J., 2013b. Modeling the cadmium balance in Australian agricultural systems in view of potential impacts on food and water quality. Science of The Total Environment 461–462, 240–257. https://doi.org/10.1016/j.scitotenv.2013.04.069
Dechow, R., Franko, U., Kätterer, T., Kolbe, H., 2019. Evaluation of the RothC model as a prognostic tool for the prediction of SOC trends in response to management practices

on arable land. Geoderma 337, 463–478. https://doi.org/10.1016/j.geoderma.2018.10.001
Degryse, F., Smolders, E., Parker, D.R., 2009. Partitioning of metals (Cd, Co, Cu, Ni, Pb, Zn) in soils: concepts, methodologies, prediction and applications – a review. European Journal of Soil Science 60, 590–612. https://doi.org/10.1111/j.1365-2389.2009.01142.x
Delbard, G., 1947. Les beaux fruits de France, Les édtions Georges Delbard. ed.
Doabi, S.A., Karami, M., Afyuni, M., 2016. Regional-scale fluxes of zinc, copper, and nickel into and out of the agricultural soils of the Kermanshah province in western Iran. Environ. Monit. Assess. 188, UNSP 216. https://doi.org/10.1007/s10661-016-5225-3
Doligez, P., Leveau, J.M., 2007. Le compostage de fumier de cheval en élevage.
Douay, F., Pruvot, C., Roussel, H., Ciesielski, H., Fourrier, H., Proix, N., Waterlot, C., 2008a. Contamination of Urban Soils in an Area of Northern France Polluted by Dust Emissions of Two Smelters. Water Air Soil Pollut 188, 247–260. https://doi.org/10.1007/s11270-007-9541-7
Douay, F., Roussel, H., Pruvot, C., Loriette, A., Fourrier, H., 2008b. Assessment of a remediation technique using the replacement of contaminated soils in kitchen gardens nearby a former lead smelter in Northern France. Sci. Total Environ. 401, 29–38. https://doi.org/10.1016/j.scitotenv.2008.03.025
Duan, L., Hao, J., Xie, S., Zhou, Z., Ye, X., 2002. Determining weathering rates of soils in China. Geoderma 110, 205–225. https://doi.org/10.1016/S0016-7061(02)00231-8
Dube, A., Zbytniewski, R., Kowalkowski, T., Cukrowska, E., Buszewski, B., 2001. Adsorption and migration of heavy metals in soil. Pol. J. Environ. Stud. 10, 1–10.
Dziubanek, G., Piekut, A., Rusin, M., Baranowska, R., Hajok, I., 2015. Contamination of food crops grown on soils with elevated heavy metals content. Ecotox. Environ. Safe. 118, 183–189. https://doi.org/10.1016/j.ecoenv.2015.04.032
EFSA, 2015. Scientific Opinion on Dietary Reference Values for copper | EFSA.
EFSA, 2014. Scientific Opinion on Dietary Reference Values for zinc | EFSA.
EFSA, 2012a. Cadmium dietary exposure in the European population. EFSA Journal 10, 2551. https://doi.org/10.2903/j.efsa.2012.2551
EFSA, 2012b. Lead dietary exposure in the European population | EFSA.
EFSA, 2011. Statement on tolerable weekly intake for cadmium | EFSA.
Egendorf, S.P., Cheng, Z., Deeb, M., Flores, V., Paltseva, A., Walsh, D., Groffman, P., Mielke, H.W., 2018. Constructed soils for mitigating lead (Pb) exposure and promoting urban community gardening: The New York City Clean Soil Bank pilot study. Landsc. Urban Plan. 175, 184–194. https://doi.org/10.1016/j.landurbplan.2018.03.012
Elbaz-Poulichet, F., Guédron, S., Anne-Lise, D., Freydier, R., Perrot, V., Rossi, M., Piot, C., Delpoux, S., Sabatier, P., 2020. A 10,000-year record of trace metal and metalloid (Cu, Hg, Sb, Pb) deposition in a western Alpine lake (Lake Robert, France): Deciphering local and regional mining contamination. Quaternary Science Reviews 228, 106076. https://doi.org/10.1016/j.quascirev.2019.106076
Equiterre, 2009. Guide de gestion globale de la ferme maraîchère biologique et diversifiée.
European Union, 2021a. Commission Regulation (EU) 2021/1323 of 10 August 2021 amending Regulation (EC) No 1881/2006 as regards maximum levels of cadmium in certain foodstuffs (Text with EEA relevance).
European Union, 2021b. Commission Regulation (EU) 2021/1317 of 9 August 2021 amending Regulation (EC) No 1881/2006 as regards maximum levels of lead in certain foodstuffs (Text with EEA relevance), OJ L.
European Union, 2006. Commission Regulation (EC) No 1881/2006 of 19 December 2006 setting maximum levels for certain contaminants in foodstuffs (Text with EEA relevance)Text with EEA relevance.

Faivre, R., Bertrand Iooss, Stéphanie Mahévas, David Makowski, Hervé Monod, 2013. Analyse de sensibilité et exploration de modèles.

Fang, W., Delapp, R.C., Kosson, D.S., van der Sloot, H.A., Liu, J., 2017. Release of heavy metals during long-term land application of sewage sludge compost: Percolation leaching tests with repeated additions of compost. Chemosphere 169, 271–280. https://doi.org/10.1016/j.chemosphere.2016.11.086

Fang, W., Qi, G., Wei, Y., Kosson, D.S., van der Sloot, H.A., Liu, J., 2018. Leaching characteristic of toxic trace elements in soils amended by sewage sludge compost: A comparison of field and laboratory investigations. Environmental Pollution 237, 244–252. https://doi.org/10.1016/j.envpol.2018.02.032

Fang, W., Wei, Y., Liu, J., 2016. Comparative characterization of sewage sludge compost and soil: Heavy metal leaching characteristics. Journal of Hazardous Materials 310, 1–10. https://doi.org/10.1016/j.jhazmat.2016.02.025

FAO, 2019. The State of Food and Agriculture 2019. Online.

FAO, 1999. Questions relatives à l'agriculture urbaine [WWW Document]. URL http://www.fao.org/Ag/fr/magazine/9901sp2.htm (accessed 6.28.19).

fao.org, n.d. SOFI 2018 - The State of Food Security and Nutrition in the World [WWW Document]. www.fao.org. URL http://www.fao.org/state-of-food-security-nutrition/en/ (accessed 12.13.18).

Farina, R., Testani, E., Campanelli, G., Leteo, F., Napoli, R., Canali, S., Tittarelli, F., 2018. Potential carbon sequestration in a Mediterranean organic vegetable cropping system. A model approach for evaluating the effects of compost and Agro-ecological Service Crops (ASCs). Agricultural Systems 162, 239–248. https://doi.org/10.1016/j.agsy.2018.02.002

Feng, W., Guo, Z., Peng, C., Xiao, X., Shi, L., Han, X., Ran, H., 2018. Modelling mass balance of cadmium in paddy soils under long term control scenarios. Environ. Sci.-Process Impacts 20, 1158–1166. https://doi.org/10.1039/c8em00153g

Fernandes, J.C., Henriques, F.S., 1991. Biochemical, physiological, and structural effects of excess copper in plants. Bot. Rev 57, 246–273. https://doi.org/10.1007/BF02858564

Fest, E.P.M.J., Temminghoff, E.J.M., Comans, R. a. J., van Riemsdijk, W.H., 2008. Partitioning of organic matter and heavy metals in a sandy soil: Effects of extracting solution, solid to liquid ratio and pH. Geoderma 146, 66–74. https://doi.org/10.1016/j.geoderma.2008.05.005

Filipovic, V., Cambier, P., Filipovic, L., Coquet, Y., Pot, V., Bodineau, G., Jaulin, A., Mercier, V., Houot, S., Benoit, P., 2016. Modeling Copper and Cadmium Mobility in an Albeluvisol Amended with Urban Waste Composts. Vadose Zone J. 15. https://doi.org/10.2136/vzj2016.07.0056

Fillol, C., Oleko, A., Gane, J., Pecheux, M., Saoudi, A., Zeghnoun, A., 2021a. Imprégnation de la population française par les métaux urinaires. Programme national de biosurveillance. Esteban 2014-2016.

Fillol, C., Oleko, A., Gane, J., Pecheux, M., Saoudi, A., Zeghnoun, A., 2021b. Imprégnation de la population française par les métaux et métalloïdes. Programme national de biosurveillance. Esteban 2014-2016.

France Galop, FIVAl, Cheval Français, 2013. Valorisation du fumier de cheval.

France Urbaine, 2018. « Villes, agriculture et alimentation : expériences françaises », une nouvelle publication de France urbaine | France urbaine [WWW Document]. URL http://www.franceurbaine.org/villes-agriculture-alimentation-experiences-francaises-une-nouvelle-publication-france-urbaine (accessed 6.28.19).

Galhena, D.H., Freed, R., Maredia, K.M., 2013. Home gardens: a promising approach to enhance household food security and wellbeing. Agriculture & Food Security 2, 8. https://doi.org/10.1186/2048-7010-2-8

Genuchten, M.T. van, 1980. A Closed-form Equation for Predicting the Hydraulic Conductivity of Unsaturated Soils. Soil Science Society of America Journal 44, 892–898. https://doi.org/10.2136/sssaj1980.03615995004400050002x

Hansson, S.V., Bindler, R., De Vleeschouwer, F., 2015. Using Peat Records as Natural Archives of Past Atmospheric Metal Deposition, in: Blais, J.M., Rosen, M.R., Smol, J.P. (Eds.), Environmental Contaminants: Using Natural Archives to Track Sources and Long-Term Trends of Pollution, Developments in Paleoenvironmental Research. Springer Netherlands, Dordrecht, pp. 323–354. https://doi.org/10.1007/978-94-017-9541-8_12

Harned, H.S., Davis, R., 1943. The Ionization Constant of Carbonic Acid in Water and the Solubility of Carbon Dioxide in Water and Aqueous Salt Solutions from 0 to 50°. J. Am. Chem. Soc. 65, 2030–2037. https://doi.org/10.1021/ja01250a059

Harrison, L.P., 1963. Fundamental concepts and definitions relating to humidity. Reinhold Publishing Company, N.Y.

Hernandez, L., Probst, A., Probst, J.L., Ulrich, E., 2003. Heavy metal distribution in some French forest soils: evidence for atmospheric contamination. Sci. Total Environ. 312, 195–219. https://doi.org/10.1016/S0048-9697(03)00223-7

Houot, P., Brugère, H., Casellas, M., Dabert, P., Fuchs, J., Giamberini, L., Patureau, D., Pons, M.-N., Pourcher, A.-M., Topp, E., 2014. Caractéristiques physico-chimiques et biologiques des Mafor 249.

Houot, S., Pons, M.-N., Pradel, M., Savini, I., Tibi, A., 2014. Valorisation des matières fertilisantes d'origine résiduaire sur les sols à usage agricole ou forestier.

Hu, W., Huang, B., Shi, X., Chen, W., Zhao, Y., Jiao, W., 2013. Accumulation and health risk of heavy metals in a plot-scale vegetable production system in a pen-urban vegetable farm near Nanjing, China. Ecotox. Environ. Safe. 98, 303–309. https://doi.org/10.1016/j.ecoenv.2013.09.040

Hu, W., Wang, H., Dong, L., Huang, B., Borggaard, O.K., Bruun Hansen, H.C., He, Y., Holm, P.E., 2018. Source identification of heavy metals in peri-urban agricultural soils of southeast China: An integrated approach. Environmental Pollution 237, 650–661. https://doi.org/10.1016/j.envpol.2018.02.070

Huang, L., Wang, Q., Zhou, Q., Ma, L., Wu, Y., Liu, Q., Wang, S., Feng, Y., 2020. Cadmium uptake from soil and transport by leafy vegetables: A meta-analysis. Environmental Pollution 264, 114677. https://doi.org/10.1016/j.envpol.2020.114677

Imperato, M., Adamo, P., Naimo, D., Arienzo, M., Stanzione, D., Violante, P., 2003. Spatial distribution of heavy metals in urban soils of Naples city (Italy). Environmental Pollution 124, 247–256. https://doi.org/10.1016/S0269-7491(02)00478-5

ITAB, 2020. Guide des produits de protection des cultures utilisables en AB en France.

IUSS Working Group WRB, 2015. World reference base for soil resources 2014, Update 2015. FAO, Rome.

Ivezic, V., Almas, A.R., Singh, B.R., 2012. Predicting the solubility of Cd, Cu, Pb and Zn in uncontaminated Croatian soils under different land uses by applying established regression models. Geoderma 170, 89–95. https://doi.org/10.1016/j.geoderma.2011.11.024

Jalali, M., Latifi, Z., 2018. Measuring and simulating effect of organic residues on the transport of cadmium, nickel, and zinc in a calcareous soil. J. Geochem. Explor. 184, 372–380. https://doi.org/10.1016/j.gexplo.2017.05.001

Janssen, R.P.T., Posthuma, L., Baerselman, R., Hollander, H.A.D., Veen, R.P.M.V., Peijnenburg, W.J.G.M., 1997. Equilibrium partitioning of heavy metals in dutch field soils. II. Prediction of metal accumulation in earthworms. Environmental Toxicology and Chemistry 16, 2479–2488. https://doi.org/10.1002/etc.5620161207

Joimel, S., 2015. Biodiversité et caractéristiques physico-chimiques des sols de jardins associatifs urbains français (thesis). Université de Lorraine.

Joimel, S., Capiaux, H., Schwartz, C., Hedde, M., Lebeau, T., Le Guern, C., Nahmani, J., Pernin, C., Salmon, S., Santorufo, L., Bechet, B., Cortet, J., 2018. Effect of Geogenic Lead on Fungal and Collembolan Communities in Garden Topsoil. Pedosphere 28, 215–226. https://doi.org/10.1016/S1002-0160(18)60022-0

Joimel, S., Cortet, J., Consalès, J.N., Branchu, P., Haudin, C.-S., Morel, J.L., Schwartz, C., 2021. Contribution of chemical inputs on the trace elements concentrations of surface soils in urban allotment gardens. J Soils Sediments 21, 328–337. https://doi.org/10.1007/s11368-020-02784-z

Joimel, S., Cortet, J., Jolivet, C.C., Saby, N.P.A., Chenot, E.D., Branchu, P., Consalès, J.N., Lefort, C., Morel, J.L., Schwartz, C., 2016. Physico-chemical characteristics of topsoil for contrasted forest, agricultural, urban and industrial land uses in France. Science of The Total Environment 545–546, 40–47. https://doi.org/10.1016/j.scitotenv.2015.12.035

Juste, C., Tauzin, J., 1986. Evolution du contenu en metaux lourds d'un sol de limon maintenu en jachere nue apres 56 annees d'application continue de divers engrais et amendements. Comptes Rendus des Séances de l'Académie d'Agriculture de France 72, 739.

Kachenko, A.G., Singh, B., 2006. Heavy Metals Contamination in Vegetables Grown in Urban and Metal Smelter Contaminated Sites in Australia. Water Air Soil Pollut 169, 101–123. https://doi.org/10.1007/s11270-006-2027-1

Keller, A.N., Steiger, B. von, Zee, S.E.A.T.M. van der, Schulin, R., 2001. A stochastic empirical model for heavy-metal balnces in Agro-ecosystems. Journal of Environmental Quality 30, 1976–1989. https://doi.org/10.2134/jeq2001.1976

Khan, Z.I., Ahmad, K., Rehman, S., Siddique, S., Bashir, H., Zafar, A., Sohail, M., Ali, S.A., Cazzato, E., De Mastro, G., 2017. Health risk assessment of heavy metals in wheat using different water qualities: implication for human health. Environ Sci Pollut Res 24, 947–955. https://doi.org/10.1007/s11356-016-7865-9

Kochem Mallmann, F.J., Rheinheimer, D. dos S., Ceretta, C.A., Cella, C., Gomes Minella, J.P., Guma, R.L., Filipovic, V., van Oort, F., Simunek, J., 2014. Soil tillage to reduce surface metal contamination - model development and simulations of zinc and copper concentration profiles in a pig slurry-amended soil. Agric. Ecosyst. Environ. 196, 59–68. https://doi.org/10.1016/j.agee.2014.06.024

La Quintinie, J., 1690. Instruction pour les jardins fruitiers et potagers, Claude Barbin. ed.

La Rosa, D., Barbarossa, L., Privitera, R., Martinico, F., 2014. Agriculture and the city: A method for sustainable planning of new forms of agriculture in urban contexts. Land Use Policy 41, 290–303. https://doi.org/10.1016/j.landusepol.2014.06.014

Laidlaw, M.A.S., Alankarage, D.H., Reichman, S.M., Taylor, M.P., Ball, A.S., 2018. Assessment of soil metal concentrations in residential and community vegetable gardens in Melbourne, Australia. Chemosphere 199, 303–311. https://doi.org/10.1016/j.chemosphere.2018.02.044

Lamb, D.T., Kader, M., Ming, H., Wang, L., Abbasi, S., Megharaj, M., Naidu, R., 2016. Predicting plant uptake of cadmium: validated with long-term contaminated soils. Ecotoxicology 25, 1563–1574. https://doi.org/10.1007/s10646-016-1712-0

Le Gentil, F. (16-1726) A. du texte, 1705. Le Jardinier solitaire, ou Dialogues entre un curieux & un jardinier solitaire. Partie 1 / , contenant la méthode... de cultiver un jardin fruitier

et potager. 2e édition... augmentée de plusieurs réflexions nouvelles sur la culture des arbres.
Leblanc, J.C., Malmauret, L., Guérin, T., Bordet, F., Boursier, B., Verger, P., 2000. Estimation of the dietary intake of pesticide residues, lead, cadmium, arsenic and radionuclides in France. Food Addit Contam 17, 925–932. https://doi.org/10.1080/026520300750038108
Lee, S.-Z., Allen, H.E., Huang, C.P., Sparks, D.L., Sanders, P.F., Peijnenburg, W.J.G.M., 1996. Predicting Soil−Water Partition Coefficients for Cadmium. Environ. Sci. Technol. 30, 3418–3424. https://doi.org/10.1021/es9507933
Lee, S.-Z., Chang, L., Yang, H.-H., Chen, C.-M., Liu, M.-C., 1998. Adsorption characteristics of lead onto soils. Journal of Hazardous Materials 63, 37–49. https://doi.org/10.1016/S0304-3894(98)00203-9
Leitão, T.E., Cameira, M.R., Costa, H.D., Pacheco, J.M., Henriques, M.J., Martins, L.L., Mourato, M.P., 2018. Environmental Quality in Urban Allotment Gardens: Atmospheric Deposition, Soil, Water and Vegetable Assessment at LISBON City. Water, Air, & Soil Pollution 229. https://doi.org/10.1007/s11270-017-3681-1
Li, Shumin, Li, J., Li, C., Huang, S., Li, X., Li, Shengxiu, Ma, Y., 2016. Testing the RothC and DNDC models against long-term dynamics of soil organic carbon stock observed at cropping field soils in North China. Soil and Tillage Research 163, 290–297. https://doi.org/10.1016/j.still.2016.07.001
Li, X., Liu, L., Wang, Y., Luo, G., Chen, X., Yang, X., Hall, M.H.P., Guo, R., Wang, H., Cui, J., He, X., 2013. Heavy metal contamination of urban soil in an old industrial city (Shenyang) in Northeast China. Geoderma 192, 50–58. https://doi.org/10.1016/j.geoderma.2012.08.011
Li, X., Poon, C., Liu, P.S., 2001. Heavy metal contamination of urban soils and street dusts in Hong Kong. Applied Geochemistry 16, 1361–1368. https://doi.org/10.1016/S0883-2927(01)00045-2
Li, X.D., Poon, C.S., Liu, P.S., 2001. Heavy metal contamination of urban soils and street dusts in Hong Kong. Appl. Geochem. 16, 1361–1368. https://doi.org/10.1016/S0883-2927(01)00045-2
Lin, Z., Schneider, A., Sterckeman, T., Nguyen, C., 2016. Ranking of mechanisms governing the phytoavailability of cadmium in agricultural soils using a mechanistic model. Plant Soil 399, 89–107. https://doi.org/10.1007/s11104-015-2663-6
Liu, T., Li, F., Jin, Z., Yang, Y., 2018. Acidic leaching of potentially toxic metals cadmium, cobalt, chromium, copper, nickel, lead, and zinc from two Zn smelting slag materials incubated in an acidic soil. Environ. Pollut. 238, 359–368. https://doi.org/10.1016/j.envpol.2018.03.022
Liu, Y., Vijver, M.G., Peijnenburg, W.J.G.M., 2014. Comparing three approaches in extending biotic ligand models to predict the toxicity of binary metal mixtures (Cu–Ni, Cu–Zn and Cu–Ag) to lettuce (Lactuca sativa L.). Chemosphere 112, 282–288. https://doi.org/10.1016/j.chemosphere.2014.04.077
Liu, Y., Xiao, T., Baveye, P.C., Zhu, J., Ning, Z., Li, H., 2015. Potential health risk in areas with high naturally-occurring cadmium background in southwestern China. Ecotoxicology and Environmental Safety 112, 122–131. https://doi.org/10.1016/j.ecoenv.2014.10.022
Liu, Y., Xiao, T., Ning, Z., Li, H., Tang, J., Zhou, G., 2013. High cadmium concentration in soil in the Three Gorges region: Geogenic source and potential bioavailability. Applied Geochemistry 37, 149–156. https://doi.org/10.1016/j.apgeochem.2013.07.022

Loganathan, P., Vigneswaran, S., Kandasamy, J., Naidu, R., 2012. Cadmium Sorption and Desorption in Soils: A Review. Crit. Rev. Environ. Sci. Technol. 42, 489–533. https://doi.org/10.1080/10643389.2010.520234

López, R., Hallat, J., Castro, A., Miras, A., Burgos, P., 2019. Heavy metal pollution in soils and urban-grown organic vegetables in the province of Sevilla, Spain. Biological Agriculture & Horticulture 35, 219–237. https://doi.org/10.1080/01448765.2019.1590234

Luo, X.S., Zhou, D.M., Liu, X.H., Wang, Y.J., 2006. Solid/solution partitioning and speciation of heavy metals in the contaminated agricultural soils around a copper mine in eastern Nanjing city, China. J. Hazard. Mater. 131, 19–27. https://doi.org/10.1016/j.jhazmat.2005.09.033

Manrique, L.A., Jones, C.A., 1991. Bulk Density of Soils in Relation to Soil Physical and Chemical Properties. Soil Science Society of America Journal 55, 476–481. https://doi.org/10.2136/sssaj1991.03615995005500020030x

Marie, M., 2019. Estimation de la contribution de la production potagère domestique au système alimentaire local . Enseignements à partir de l'étude des cas de Rennes, Caen et Alençon. VertigO - la revue électronique en sciences de l'environnement. https://doi.org/10.4000/vertigo.26215

Mariet, A.-L., Monna, F., Gimbert, F., Bégeot, C., Cloquet, C., Belle, S., Millet, L., Rius, D., Walter-Simonnet, A.-V., 2018. Tracking past mining activity using trace metals, lead isotopes and compositional data analysis of a sediment core from Longemer Lake, Vosges Mountains, France. J Paleolimnol 60, 399–412. https://doi.org/10.1007/s10933-018-0029-9

Martellozzo, F., Landry, J.-S., Plouffe, D., Seufert, V., Rowhani, P., Ramankutty, N., 2014. Urban agriculture: a global analysis of the space constraint to meet urban vegetable demand. Environ. Res. Lett. 9, 064025. https://doi.org/10.1088/1748-9326/9/6/064025

Mathee, A., Kootbodien, T., Kapwata, T., Naicker, N., 2018. Concentrations of arsenic and lead in residential garden soil from four Johannesburg neighborhoods. Environ. Res. 167, 524–527. https://doi.org/10.1016/j.envres.2018.08.012

Mathieu, A., Baize, D., Raoul, C., Daniau, C., 2008. Proposition de référentiels régionaux en éléments traces métalliques dans les sols : leur utilisation dans les évaluations des risques sanitaires. Environnement, Risques & Santé 7, 111–122.

McBride, M.B. (Cornell U.), Richards, B.K., Steenhuis, T., Russo, J.J., Sauve, S., 1997. Mobility and solubility of toxic metals and nutrients in soil fifteen years after sludge application. Soil science (USA).

McDougall, R., Kristiansen, P., Rader, R., 2019. Small-scale urban agriculture results in high yields but requires judicious management of inputs to achieve sustainability. PNAS 116, 129–134. https://doi.org/10.1073/pnas.1809707115

McDowell, R.W., Gray, C.W., 2022. Do soil cadmium concentrations decline after phosphate fertiliser application is stopped: A comparison of long-term pasture trials in New Zealand? Science of The Total Environment 804, 150047. https://doi.org/10.1016/j.scitotenv.2021.150047

McEldowney, J., European Parliament, European Parliamentary Research Service, Members' Research Service, 2017. Urban agriculture in Europe: patterns, challenges and policies : in-depth analysis.

McLaughlin, M.J., Smolders, E., Degryse, F., Rietra, R., 2011. Uptake of Metals from Soil into Vegetables, in: Swartjes, F.A. (Ed.), Dealing with Contaminated Sites: From Theory towards Practical Application. Springer Netherlands, Dordrecht, pp. 325–367. https://doi.org/10.1007/978-90-481-9757-6_8

Miccoli, S., Finucci, F., Murro, R., 2016. Feeding the Cities Through Urban Agriculture The Community Esteem Value. Agriculture and Agricultural Science Procedia 8, 128–134. https://doi.org/10.1016/j.aaspro.2016.02.017

Michaud, A.M., Cambier, P., Sappin-Didier, V., Deltreil, V., Mercier, V., Rampon, J.-N., Houot, S., 2020. Mass balance and long-term soil accumulation of trace elements in arable crop systems amended with urban composts or cattle manure during 17 years. Environ Sci Pollut Res 27, 5367–5386. https://doi.org/10.1007/s11356-019-07166-8

Ministry of the Environment, Finland, 2007. Government Decree on the Assessment of Soil Contamination and Remediation Needs.

Molz, F.J., Remson, I., Fungaroli, A.A., Drake, R.L., 1968. Soil Moisture Availability for Transpiration. Water Resources Research 4, 1161–1169. https://doi.org/10.1029/WR004i006p01161

Mondini, C., Cayuela, M.L., Sinicco, T., Fornasier, F., Galvez, A., Sánchez-Monedero, M.A., 2017. Modification of the RothC model to simulate soil C mineralization of exogenous organic matter. Biogeosciences 14, 3253–3274. https://doi.org/10.5194/bg-14-3253-2017

Moolenaar, S.W., Lexmond, T.M., 1998. Heavy-metal balances of agro-ecosystems in the Netherlands. 1 46, 171–192.

Moolenaar, S.W., Temminghoff, E.J.M., De Haan, F.A.M., 1998. Modeling dynamic copper balances for a contaminated sandy soil following land use change from agriculture to forestry. Environmental Pollution 103, 117–125. https://doi.org/10.1016/S0269-7491(98)00103-1

Moreau, J.-G.A. du texte, Daverne, J.-J. (1799-1845) A. du texte, 1845. Manuel pratique de la culture maraîchère de Paris / par J. G. Moreau et J. J. Daverne,...

Morel, J.L., Schwartz, C., 1999. Qualité et gestion des sols des jardins familiaux. Comptes Rendus de l'Académie d'Agriculture de France 85, 107–123.

Mougeot, L.J.A., 2001. Urban Agriculture: Definition, Presence, Potentials and Risks, and Policy Challenges.

Moustier, P., Fall, A.S., 2004. Les dynamiques de l'agriculture urbaine : caractérisation et évaluation [WWW Document]. Développement durable de l'agriculture urbaine en Afrique francophone : enjeux, concepts et méthodes. URL http://agritrop.cirad.fr/518807/ (accessed 6.28.19).

Mu, T., Zhou, T., Li, Z., Hu, P., Luo, Y., Christie, P., Wu, L., 2020. Prediction models for rice cadmium accumulation in Chinese paddy fields and the implications in deducing soil thresholds based on food safety standards. Environmental Pollution 258, 113879. https://doi.org/10.1016/j.envpol.2019.113879

Nahmias, P., Le Caro, Y., 2012. Pour une définition de l'agriculture urbaine : réciprocité fonctionnelle et diversité des formes spatiales. Environnement Urbain / Urban Environment.

Neitsch, S.L., Arnold, J.G., Kiniry, J.R., Williams, J.R., 2011. Soil and Water Assessment Tool: Theoretical Documentation, Version 2009.

Nriagu, J.O., 1989. A global assessment of natural sources of atmospheric trace metals. Nature 338, 47. https://doi.org/10.1038/338047a0

Nuyttens, D., Braekman, P., Windey, S., Sonck, B., 2009. Potential dermal pesticide exposure affected by greenhouse spray application technique. Pest Management Science 65, 781–790. https://doi.org/10.1002/ps.1755

Oleko, A., Fillol, C., Saoudi, A., Zeghnoun, A., Bidondo, M.-L., Gane, J., Balicco, A., 2021. Imprégnation de la population française par le cadmium. Programme national de biosurveillance, Esteban 2014-2016 (No. 43). Santé publique France, Saint-Maurice.

Omrani, M., Ruban, V., Ruban, G., Lamprea, K., 2017. Assessment of atmospheric trace metal deposition in urban environments using direct and indirect measurement methodology and contributions from wet and dry depositions. Atmos. Environ. 168, 101–111. https://doi.org/10.1016/j.atmosenv.2017.08.064

Opitz, I., Berges, R., Piorr, A., Krikser, T., 2016. Contributing to food security in urban areas: differences between urban agriculture and peri-urban agriculture in the Global North. Agric Hum Values 33, 341–358. https://doi.org/10.1007/s10460-015-9610-2

Oporto, C., Smolders, E., Vandecasteele, C., 2012. Identifying the cause of soil cadmium contamination with Monte Carlo mass balance modelling: a case study from Potosi, Bolivia. Environ. Technol. 33, 555–561. https://doi.org/10.1080/09593330.2011.586054

Orsini, F., Gasperi, D., Marchetti, L., Piovene, C., Draghetti, S., Ramazzotti, S., Bazzocchi, G., Gianquinto, G., 2014. Exploring the production capacity of rooftop gardens (RTGs) in urban agriculture: the potential impact on food and nutrition security, biodiversity and other ecosystem services in the city of Bologna. Food Sec. 6, 781–792. https://doi.org/10.1007/s12571-014-0389-6

Orsini, F., Kahane, R., Nono-Womdim, R., Gianquinto, G., 2013. Urban agriculture in the developing world: a review. Agron. Sustain. Dev. 33, 695–720. https://doi.org/10.1007/s13593-013-0143-z

Ouimet, R., Duchesne, L., 2005. Base cation mineral weathering and total release rates from soils in three calibrated forest watersheds on the Canadian Boreal Shield. Can. J. Soil. Sci. 85, 245–260. https://doi.org/10.4141/S04-061

Paillat, J.-M., Hassouna, M., Robin, P., 2005. Abattements d'azote lors du compostage de fumier de vaches laitières : exemple de cinq élevages des Côtes d'Armor. INRA - Agrocampus, UMR Sol Agronomie Spatialisation, Rennes. 11.

Paltseva, A., Cheng, Z., Deeb, M., Groffman, P.M., Shaw, R.K., Maddaloni, M., 2018. Accumulation of arsenic and lead in garden-grown vegetables: Factors and mitigation strategies. Sci. Total Environ. 640, 273–283. https://doi.org/10.1016/j.scitotenv.2018.05.296

Pearson, L.J., Pearson, L., Pearson, C.J., 2010. Sustainable urban agriculture: stocktake and opportunities. International Journal of Agricultural Sustainability 8, 7–19. https://doi.org/10.3763/ijas.2009.0468

Pelfrene, A., Waterlot, C., Mazzuca, M., Nisse, C., Bidar, G., Douay, F., 2011. Assessing Cd, Pb, Zn human bioaccessibility in smelter-contaminated agricultural topsoils (northern France). Environ. Geochem. Health 33, 477–493. https://doi.org/10.1007/s10653-010-9365-z

Pelfrene, A., Waterlot, C., Mazzuca, M., Nisse, C., Cuny, D., Richard, A., Denys, S., Heyman, C., Roussel, H., Bidar, G., Douay, F., 2012. Bioaccessibility of trace elements as affected by soil parameters in smelter-contaminated agricultural soils: A statistical modeling approach. Environ. Pollut. 160, 130–138. https://doi.org/10.1016/j.envpol.2011.09.008

Peng, C., Wang, M., Chen, W., 2016. Modelling cadmium contamination in paddy soils under long-term remediation measures: Model development and stochastic simulations. Environ. Pollut. 216, 146–155. https://doi.org/10.1016/j.envpol.2016.05.038

Peng, C., Wang, M., Chen, W., Chang, A.C., Crittenden, J.C., 2017. Mass balance-based regression modeling of Cd and Zn accumulation in urban soils of Beijing. J. Environ. Sci. 53, 99–106. https://doi.org/10.1016/j.jes.2016.05.012

Peryea, F.J., Creger, T.L., 1994. Vertical distribution of lead and arsenic in soils contaminated with lead arsenate pesticide residues. Water Air Soil Pollut 78, 297–306. https://doi.org/10.1007/BF00483038

Posch, Hettelingh, Slootweg, 2005. Manual for Dynamic Modelling of Soil Response to Atmospheric Deposition.

Posch, M., Reinds, G.J., 2009. A very simple dynamic soil acidification model for scenario analyses and target load calculations. Environmental Modelling & Software 24, 329–340. https://doi.org/10.1016/j.envsoft.2008.09.007

POURIAS, J., Duchemin, E., Aubry, C., 2015. Products from urban collective gardens : food for thought or for consumption? The Journal of Agriculture, Food Systems, and Community Development 5, 175–199. https://doi.org/10.5304/jafscd.2015.052.005

Qian, X., Wang, Z., Shen, G., Chen, X., Tang, Z., Guo, C., Gu, H., Fu, K., 2018. Heavy metals accumulation in soil after 4 years of continuous land application of swine manure: A field-scale monitoring and modeling estimation. Chemosphere 210, 1029–1034. https://doi.org/10.1016/j.chemosphere.2018.07.107

Qian, X.-Y., Shen, G.-X., Wang, Z.-Q., Chen, X.-H., Zhao, Q.-J., Bai, Y.-J., Tang, Z.-Z., 2020. Application of dairy manure as fertilizer in dry land in East China: field monitoring and model estimation of heavy metal accumulation in surface soil. Environ. Sci. Pollut. Res. https://doi.org/10.1007/s11356-020-09786-x

Quenet, G., 2015. Versailles, une histoire naturelle, La Découverte. ed.

Rekolainen, S., Posch, M., 1993. Adapting the CREAMS Model for Finnish Conditions. Hydrology Research 24, 309–322. https://doi.org/10.2166/nh.1993.10

Ren, Z.-L., Tella, M., Bravin, M.N., Comans, R.N.J., Dai, J., Garnier, J.-M., Sivry, Y., Doelsch, E., Straathof, A., Benedetti, M.F., 2015. Effect of dissolved organic matter composition on metal speciation in soil solutions. Chem. Geol. 398, 61–69. https://doi.org/10.1016/j.chemgeo.2015.01.020

Richardson, J.B., Renock, D.J., Gorres, J.H., Jackson, B.P., Webb, S.M., Friedland, A.J., 2016. Nutrient and pollutant metals within earthworm residues are immobilized in soil during decomposition. Soil Biol. Biochem. 101, 217–225. https://doi.org/10.1016/j.soilbio.2016.07.020

Rocha, G.H.O., Lini, R.S., Barbosa, F., Batista, B.L., de Oliveira Souza, V.C., Nerilo, S.B., Bando, E., Mossini, S.A.G., Nishiyama, P., 2015. Exposure to heavy metals due to pesticide use by vineyard farmers. Int Arch Occup Environ Health 88, 875–880. https://doi.org/10.1007/s00420-014-1010-1

Römkens, P.F.A.M., Salomons, W., 1998. Cd, Cu AND Zn SOLUBILITY IN ARABLE AND FOREST SOILS: CONSEQUENCES OF LAND USE CHANGES FOR METAL MOBILITY AND RISK ASSESSMENT. Soil Science 163, 859.

Rosen, V., Chen, Y., 2018. Effects of compost application on soil vulnerability to heavy metal pollution. Environ Sci Pollut Res. https://doi.org/10.1007/s11356-018-3394-z

Rühling, Å., Tyler, G., 2001. Changes in Atmospheric Deposition Rates of Heavy Metals in Sweden A Summary of Nationwide Swedish Surveys in 1968/70 – 1995. Water, Air, & Soil Pollution: Focus 1, 311–323. https://doi.org/10.1023/A:1017584928458

Salmanzadeh, M., Hartland, A., Stirling, C.H., Balks, M.R., Schipper, L.A., Joshi, C., George, E., 2017. Isotope Tracing of Long-Term Cadmium Fluxes in an Agricultural Soil. Environ. Sci. Technol. 51, 7369–7377. https://doi.org/10.1021/acs.est.7b00858

Santo, R., Palmer, A., 2016. Vacant Lots to Vibrant Plots: A Review of the Benefits and Limitations of Urban Agriculture.

Sauvé, S., Hendershot, W., Allen, H.E., 2000. Solid-Solution Partitioning of Metals in Contaminated Soils: Dependence on pH, Total Metal Burden, and Organic Matter. Environmental Science & Technology 34, 1125–1131. https://doi.org/10.1021/es9907764

Sauve, S., Hendershot, W., Allen, H.E., 2000a. Solid-solution partitioning of metals in contaminated soils: Dependence on pH, total metal burden, and organic matter. Environ. Sci. Technol. 34, 1125–1131. https://doi.org/10.1021/es9907764

Sauve, S., Norvell, W.A., McBride, M., Hendershot, W., 2000b. Speciation and complexation of cadmium in extracted soil solutions. Environ. Sci. Technol. 34, 291–296. https://doi.org/10.1021/es990202z

Schwartz, C., 2013a. Les sols de jardins, supports d'une agriculture urbaine intensive. VertigO - la revue électronique en sciences de l'environnement. https://doi.org/10.4000/vertigo.12858

Schwartz, C., 2013b. Jardins potagers: terres inconnues. EDP Sciences.

SEPAC, 2007. Environmental quality evaluation standard for farmland of greenhouse vegetables production.

Shahid, M., Dumat, C., Khalid, S., Schreck, E., Xiong, T., Niazi, N.K., 2017. Foliar heavy metal uptake, toxicity and detoxification in plants: A comparison of foliar and root metal uptake. Journal of Hazardous Materials 325, 36–58. https://doi.org/10.1016/j.jhazmat.2016.11.063

Shepard, H.H., 1951. The chemistry and action of insecticides. The chemistry and action of insecticides.

Sheppard, S.C., 2011. Robust Prediction of Kd from Soil Properties for Environmental Assessment. Human and Ecological Risk Assessment: An International Journal 17, 263–279. https://doi.org/10.1080/10807039.2011.538641

Shi, T., Ma, J., Wu, F., Ju, T., Gong, Y., Zhang, Y., Wu, X., Hou, H., Zhao, L., Shi, H., 2019. Mass balance-based inventory of heavy metals inputs to and outputs from agricultural soils in Zhejiang Province, China. Sci. Total Environ. 649, 1269–1280. https://doi.org/10.1016/j.scitotenv.2018.08.414

Singh, S., Kumar, M., 2006. Heavy Metal Load Of Soil, Water And Vegetables In Peri-Urban Delhi. Environ Monit Assess 120, 79–91. https://doi.org/10.1007/s10661-005-9050-3

Six, L., Smolders, E., 2014. Future trends in soil cadmium concentration under current cadmium fluxes to European agricultural soils. Science of The Total Environment 485–486, 319–328. https://doi.org/10.1016/j.scitotenv.2014.03.109

Skjemstad, J.O., Spouncer, L.R., Cowie, B., Swift, R.S., 2004. Calibration of the Rothamsted organic carbon turnover model (RothC ver. 26.3), using measurable soil organic carbon pools. Soil Res. 42, 79–88. https://doi.org/10.1071/sr03013

Slaveykova, V.I., Wilkinson, K.J., 2005. Predicting the Bioavailability of Metals and Metal Complexes: Critical Review of the Biotic Ligand Model. Environ. Chem. 2, 9–24. https://doi.org/10.1071/EN04076

Smit, J., Nasr, J., 1992. Urban agriculture for sustainable cities: using wastes and idle land and water bodies as resources. Environment and Urbanization 4, 141–152. https://doi.org/10.1177/095624789200400214

Sterckeman, T., Douay, F., Baize, D., Fourrier, H., Proix, N., Schvartz, C., 2006a. Trace elements in soils developed in sedimentary materials from Northern France. Geoderma 136, 912–929. https://doi.org/10.1016/j.geoderma.2006.06.010

Sterckeman, T., Douay, F., Baize, D., Fourrier, H., Proix, N., Schvartz, C., Carignan, J., 2006b. Trace element distributions in soils developed in loess deposits from northern France. European Journal of Soil Science 57, 392–410. https://doi.org/10.1111/j.1365-2389.2005.00750.x

Sterckeman, T., Gossiaux, L., Guimont, S., Sirguey, C., Lin, Z., 2019. Corrigendum to "Cadmium mass balance in French soils under annual crops: Scenarios for the next century" [Sci. Total Environ. 639 (2018) 1440–1452]. Science of The Total Environment 650, 3180–3188. https://doi.org/10.1016/j.scitotenv.2018.09.179

Sterckeman, T., Gossiaux, L., Guimont, S., Sirguey, C., Lin, Z., 2018. Cadmium mass balance in French soils under annual crops: Scenarios for the next century. Science of The Total Environment 639, 1440–1452. https://doi.org/10.1016/j.scitotenv.2018.05.225

Sterckeman, T., Thomine, S., 2020. Mechanisms of Cadmium Accumulation in Plants. Critical Reviews in Plant Sciences 0, 1–38. https://doi.org/10.1080/07352689.2020.1792179

Sverdrup, H., Warfvinge, P., 1988. Weathering of primary silicate minerals in the natural soil environment in relation to a chemical weathering model. Water Air Soil Pollut 38, 387–408. https://doi.org/10.1007/BF00280768

Tack, F., 2010. Trace elements: general soil chemistry, principles and processes, in: Trace Elements in Soils. Wiley-Blackwell, pp. 9–37.

Tack, F.M.G., Verloo, M.G., 1995. Chemical Speciation and Fractionation in Soil and Sediment Heavy Metal Analysis: A Review. International Journal of Environmental Analytical Chemistry 59, 225–238. https://doi.org/10.1080/03067319508041330

Taylor, S.R., McLennan, S.M., 1995. The geochemical evolution of the continental crust. Reviews of Geophysics 33, 241–265. https://doi.org/10.1029/95RG00262

Tedesco, C., Petit, C., Billen, G., Garnier, J., Personne, E., 2017. Potential for recoupling production and consumption in peri-urban territories: The case-study of the Saclay plateau near Paris, France. Food Policy 69, 35–45. https://doi.org/10.1016/j.foodpol.2017.03.006

Torres, A.C., Prevot, A.-C., Nadot, S., 2018. Small but powerful: The importance of French community gardens for residents. Landsc. Urban Plan. 180, 5–14. https://doi.org/10.1016/j.landurbplan.2018.08.005

Tóth, G., Hermann, T., Da Silva, M.R., Montanarella, L., 2016. Heavy metals in agricultural soils of the European Union with implications for food safety. Environment International 88, 299–309. https://doi.org/10.1016/j.envint.2015.12.017

Tresch, S., Moretti, M., Le Bayon, R.-C., Mader, P., Zanetta, A., Frey, D., Fliessbach, A., 2018. A Gardener's Influence on Urban Soil Quality. Front. Environ. Sci. 6, 25. https://doi.org/10.3389/fenvs.2018.00025

Uchimiya, M., Bannon, D., Nakanishi, H., McBride, M.B., Williams, M.A., Yoshihara, T., 2020. Chemical Speciation, Plant Uptake, and Toxicity of Heavy Metals in Agricultural Soils. J. Agric. Food Chem. 68, 12856–12869. https://doi.org/10.1021/acs.jafc.0c00183

Unamuno, V.I.R., Meers, E., Du Laing, G., Tack, F.M.G., 2009. Effect of Physicochemical Soil Characteristics on Copper and Lead Solubility in Polluted and Unpolluted Soils. Soil Science 174, 601. https://doi.org/10.1097/SS.0b013e3181bf2f52

United Nations, 2019. World Population Prospects 2019 [WWW Document]. URL https://population.un.org/wpp/ (accessed 12.21.20).

United unions, 2018. L'édition 2018 des Perspectives de l'urbanisation mondiale [WWW Document]. Langlois. URL http://langlois.blog.lemonde.fr/2018/05/11/ledition-2018-des-perspectives-de-lurbanisation-mondiale/ (accessed 12.13.18).

Verbeeck, M., Salaets, P., Smolders, E., 2020. Trace element concentrations in mineral phosphate fertilizers used in Europe: A balanced survey. Science of The Total Environment.

Vries, W. de, Posch, M., 2003. Derivation of cation exchange constants for sand, loess, clay and peat soils on the basis of field measurements in the Netherlands.

Wang, Y., Guo, G., Zhang, D., Lei, M., 2021a. An integrated method for source apportionment of heavy metal(loid)s in agricultural soils and model uncertainty analysis. Environmental Pollution 276, 116666. https://doi.org/10.1016/j.envpol.2021.116666

Wang, Y., Guo, G., Zhang, D., Lei, M., 2021b. An integrated method for source apportionment of heavy metal(loid)s in agricultural soils and model uncertainty analysis. Environmental Pollution 276, 116666. https://doi.org/10.1016/j.envpol.2021.116666

Waterlot, C., Pruvot, C., Ciesielski, H., Douay, F., 2011. Effects of a phosphorus amendment and the pH of water used for watering on the mobility and phytoavailability of Cd, Pb and Zn in highly contaminated kitchen garden soils. Ecol. Eng. 37, 1081–1093. https://doi.org/10.1016/j.ecoleng.2010.09.001

Waterlot, C., Pruvot, C., Marot, F., Douay, F., 2017a. Impact of a Phosphate Amendment on the Environmental Availability and Phytoavailability of Cd and Pb in Moderately and Highly Carbonated Kitchen Garden Soils. Pedosphere 27, 588–605. https://doi.org/10.1016/S1002-0160(17)60354-0

Waterlot, C., Pruvot, C., Marot, F., Douay, F., 2017b. Impact of a Phosphate Amendment on the Environmental Availability and Phytoavailability of Cd and Pb in Moderately and Highly Carbonated Kitchen Garden Soils. Pedosphere 27, 588–605. https://doi.org/10.1016/S1002-0160(17)60354-0

Wei, B., Yang, L., 2010. A review of heavy metal contaminations in urban soils, urban road dusts and agricultural soils from China. Microchemical Journal 94, 99–107. https://doi.org/10.1016/j.microc.2009.09.014

Weissengruber, L., Möller, K., Puschenreiter, M., Friedel, J.K., 2018. Long-term soil accumulation of potentially toxic elements and selected organic pollutants through application of recycled phosphorus fertilizers for organic farming conditions. Nutr Cycl Agroecosyst 110, 427–449. https://doi.org/10.1007/s10705-018-9907-9

WHO, 2020. Food safety [WWW Document]. URL https://www.who.int/news-room/fact-sheets/detail/food-safety (accessed 12.18.20).

Wösten, J.H.M., Lilly, A., Nemes, A., Le Bas, C., 1999. Development and use of a database of hydraulic properties of European soils. Geoderma 90, 169–185. https://doi.org/10.1016/S0016-7061(98)00132-3

Xu, D., Carswell, A., Zhu, Q., Zhang, F., de Vries, W., 2020. Modelling long-term impacts of fertilization and liming on soil acidification at Rothamsted experimental station. Science of The Total Environment 713, 136249. https://doi.org/10.1016/j.scitotenv.2019.136249

Yang, K., Zhang, T., Shao, Y., Tian, C., Cattle, S.R., Zhu, Y., Song, J., 2018. Fractionation, Bioaccessibility, and Risk Assessment of Heavy Metals in the Soil of an Urban Recreational Area Amended with Composted Sewage Sludge. Int. J. Environ. Res. Public Health 15, 613. https://doi.org/10.3390/ijerph15040613

Yang, Y., Chang, A.C., Wang, M., Chen, W., Peng, C., 2018. Assessing cadmium exposure risks of vegetables with plant uptake factor and soil property. Environ. Pollut. 238, 263–269. https://doi.org/10.1016/j.envpol.2018.02.059

Yang, Y., Li, Y., Chen, W., Wang, M., Wang, T., Dai, Y., 2020. Dynamic interactions between soil cadmium and zinc affect cadmium phytoavailability to rice and wheat: Regional investigation and risk modeling. Environmental Pollution 267, 115613. https://doi.org/10.1016/j.envpol.2020.115613

Yang, Y., Li, Y., Dai, Y., Wang, M., Chen, W., Wang, T., 2021. Historical and future trends of cadmium in rice soils deduced from long-term regional investigation and probabilistic modeling. Journal of Hazardous Materials 415, 125746. https://doi.org/10.1016/j.jhazmat.2021.125746

Yruela, I., 2005. Copper in plants. Braz. J. Plant Physiol. 17, 145–156. https://doi.org/10.1590/S1677-04202005000100012

Zasada, I., 2011. Multifunctional peri-urban agriculture-A review of societal demands and the provision of goods and services by farming. Land Use Pol. 28, 639–648. https://doi.org/10.1016/j.landusepol.2011.01.008

Zeng, M., de Vries, W., Bonten, L.T.C., Zhu, Q., Hao, T., Liu, X., Xu, M., Shi, X., Zhang, F., Shen, J., 2017. Model-Based Analysis of the Long-Term Effects of Fertilization

Management on Cropland Soil Acidification. Environ. Sci. Technol. 51, 3843–3851. https://doi.org/10.1021/acs.est.6b05491

Zhong, X., Joimel, S., Schwartz, C., Sterckeman, T., 2021. Assessing the future trends of soil trace metal contents in French urban gardens. Environ Sci Pollut Res. https://doi.org/10.1007/s11356-021-15679-4

Zhu, Q., de Vries, W., Liu, X., Hao, T., Zeng, M., Shen, J., Zhang, F., 2018a. Enhanced acidification in Chinese croplands as derived from element budgets in the period 1980-2010. Sci Total Environ 618, 1497–1505. https://doi.org/10.1016/j.scitotenv.2017.09.289

Zhu, Q., Liu, X., Hao, T., Zeng, M., Shen, J., Zhang, F., De Vries, W., 2018b. Modeling soil acidification in typical Chinese cropping systems. Science of The Total Environment 613–614, 1339–1348. https://doi.org/10.1016/j.scitotenv.2017.06.257

Zimmermann, 2007. Measured soil organic matter fractions can be related to pools in the RothC model - Zimmermann - 2007 - European Journal of Soil Science - Wiley Online Library [WWW Document]. URL https://onlinelibrary.wiley.com/doi/abs/10.1111/j.1365-2389.2006.00855.x (accessed 11.3.19).

Annexe

A1 Solubility of the four metals

Table A1. Meta-data of investigated Kd models

Modèle	Méthode de mesure			Métaux étudiés	n	Référence
	Métal sur la phase solide	Métal en solution				
		Séparation/extraction	Dosage			
Isotherme de Freundlich (Paramètres Kd et n)	Calculé par diminution de la concentration en solution	Eau des pores (centrifugation)	ICP-AES	Cd, Zn, Pb, Cu	11	Bucher et al. (1989)
	Acide nitrique concentré	Eau des pores (centrifugation)	ICP-MS	Cd	41	Lamb et al. (2016)
Coefficient de partage (Kd)	Acide nitrique concentré	Extraction par 0,001 M CaCl2	GFAAS	Cd	78	Christensen. (1989)
	Calculé par diminution de la concentration en solution	Extraction par eau (S/L : 1:100) avec régularisation de pH (0,01 M NaNO3)	AAS	Cd, Pd	15	Lee et al. (1996,1998)
	Acide nitrique concentré	Eau des pores (Centrifugation) ; extraction par 0,01 M CaCl2	GFAAS, AAS, ICP-AES	Cd, Zn, Pb, Cu	20	Janssen et al. (1997)
	Digestion par HNO3 - H2SO4 - HClO4	Eau des pores (centrifugation)	GFAAS	Cd, Zn, Cu	100	Römkens and Salomons. (1998)
	Digestion par HF, HClO4 and HNO3 (3:1:1)	Extraction par 10 mM KNO3	AAS, GFAAS	Cd, Zn, Cu	40	Luo et al. (2006)
	Digestion par acides chaudes	Différentes méthodes	GFAAS, AAS, ICP-AES, ICP-MS, ASV	Cd, Zn, Pb, Cu	123, 143, 128, 78	Degryse et al. (2009)
	Eau régale	Extraction par 0,001 M CaCl2	ICP-OES	Cu, Pb	87	Unamuno et al. (2009)
	Eau régale	Eau des pores (centrifugation)	ICP-MS	Cd, Pb, Cu	150, 362, 205	Sheppard et al. (2011)
	Acide nitrique concentré	Extraction par eau ultra pure (S/L : 1:10)	ICP-MS ; ICP-OES	Cd, Zn, Pb, Cu	74	Ivezić et al. (2012)

Régression linéaire multiple	Acide nitrique concentré	Extraction par 0,01 M CaCl2	AAS	Cu	101	McBRIDE et al. (1997)
	Différentes méthodes	Différentes méthodes	Différentes méthodes	Cd, Zn, Pb, Cu	830, 302, 204, 452	Sauvé et al. (2000a)
	Digestion par acides chaudes	Extraction par 0,01 M KNO3	GFAAS	Cd	64	Sauvé et al. (2000b)
	0,43 M HNO3	Eau des pores (centrifugation) ; extraction par 0,01 M CaCl2 ; extraction par 0,002 M $Ca(NO3)_2$	ICP-MS, ICP-AES	Cd, Zn, Pb, Cu	203	Groenenberg et al. (2012)

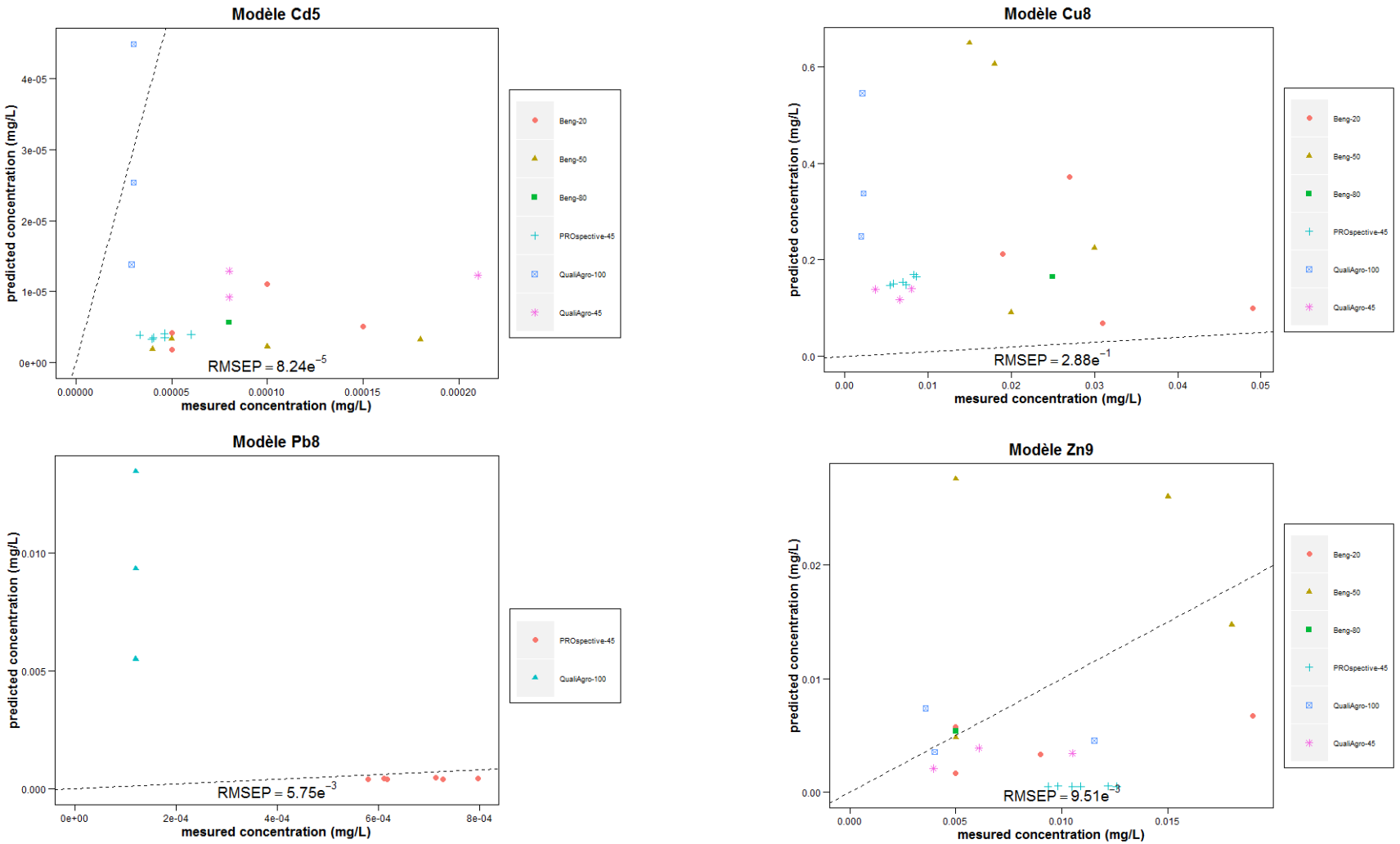

Figure A1. Comparison of measured values of metals concentrations in soil solution with predicted values from the selected regression models

A2 Benchmarking of RothC model

Table A2 presents input variables used in all RothC models for benchmarking. Figure A3 and

Figure A3 show a comparison of the simulated results between the three versions of RothC. We obtained the coincident curves for the three model versions. A test on the relative differences (in %) between the R version and the other two versions was done.

The results obtained by the Roth-R version and the RothC-Excel version are slightly different (Figure A4). The observed relative differences vary against different compartments (on average: 0.0461% for DPM; 0.0134% for RPM; 0.0017% for BIO; -0.0010% for HUM; 0.0043% for SOC). Checking the simulated values, this difference is mainly due to the approximation of the mathematical calculations in the RothC software. Despite this difference, the simulation results for SOC only differ by 0.0043%, so the RothC-R model can be considered validated.

Table A2. Input variables in RothC models

Land management			**Climate and soil parameters**				
Plant input (t/ha)	Amendment (t/ha)	Plant cover	T_air (°C)	Rain (mm)	Evaporation (mm)	Clay (%)	Depth (cm)
0	0	0	2.3	54.9	32	20	31
0	0	0	2.5	50.8	33.8	20	31
0	0	0	6.2	52.3	73.7	20	31
0.2	0	1	10.7	36.8	146.2	20	31
0.2	0	1	13.9	70	184.1	20	31
0.2	0	1	17	61.8	201.9	20	31
0.2	0	1	18.9	70.7	228.6	20	31
0.2	0	1	18.1	66	209.4	20	31
0.2	0	1	14.7	71.4	143.5	20	31
0.2	0	1	10.5	78.3	91.8	20	31
0	0	0	6.8	72.6	46.8	20	31
0	0	0	3	88.7	29.8	20	31

Initial values for each compartiments					
DPM	RPM	BIO	HUM	IOM	Total C
3.2687	73.971	2.2172	40.312	33.258	153.0269

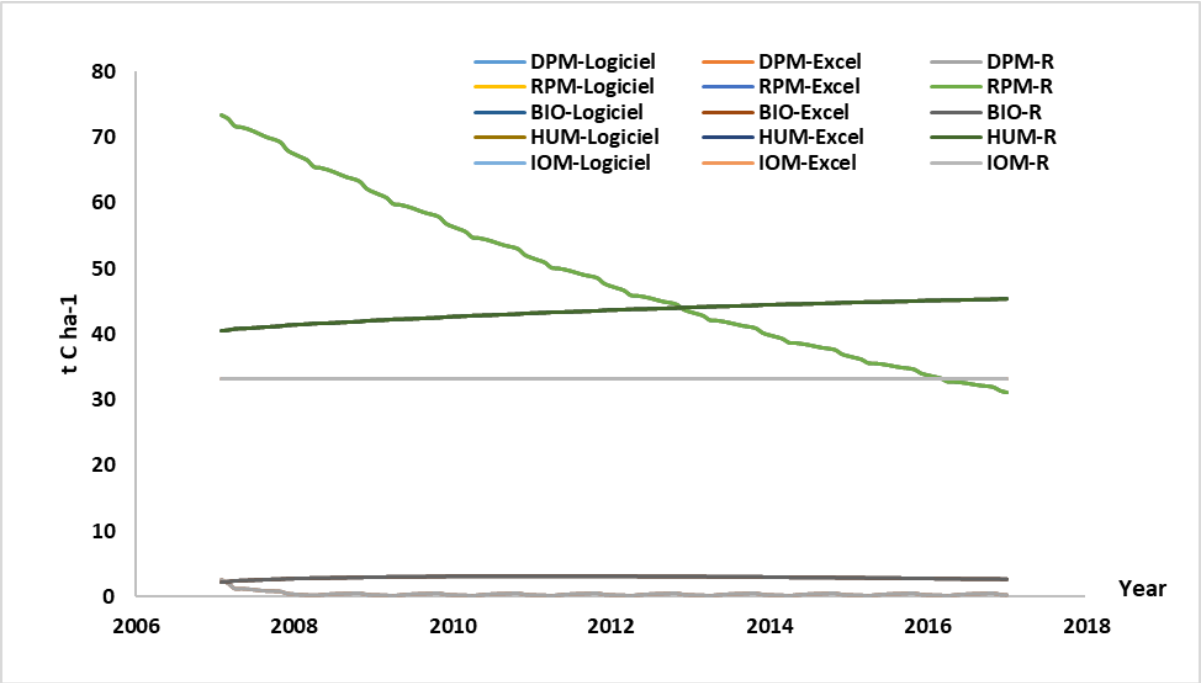

Figure A2. Organic carbon content in the 5 compartments for the 3 versions of RothC during 2007-2016

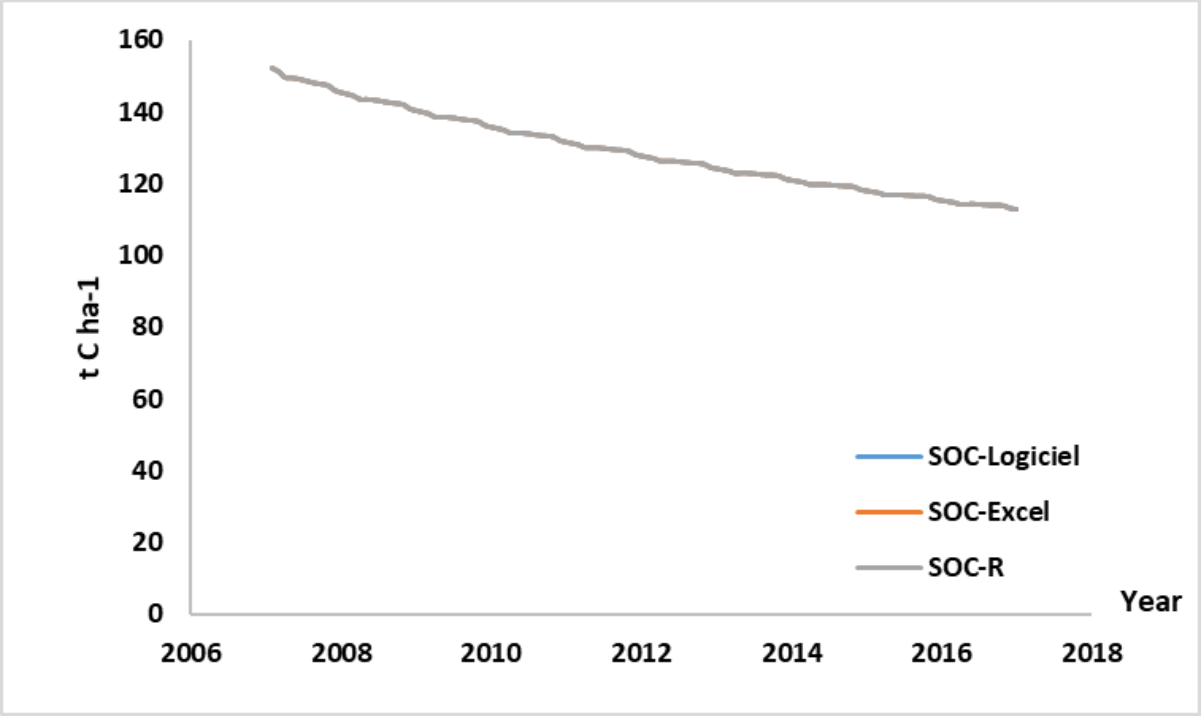

Figure A3. Total organic carbon content in soil for the 3 versions of RothC during 2007-2016

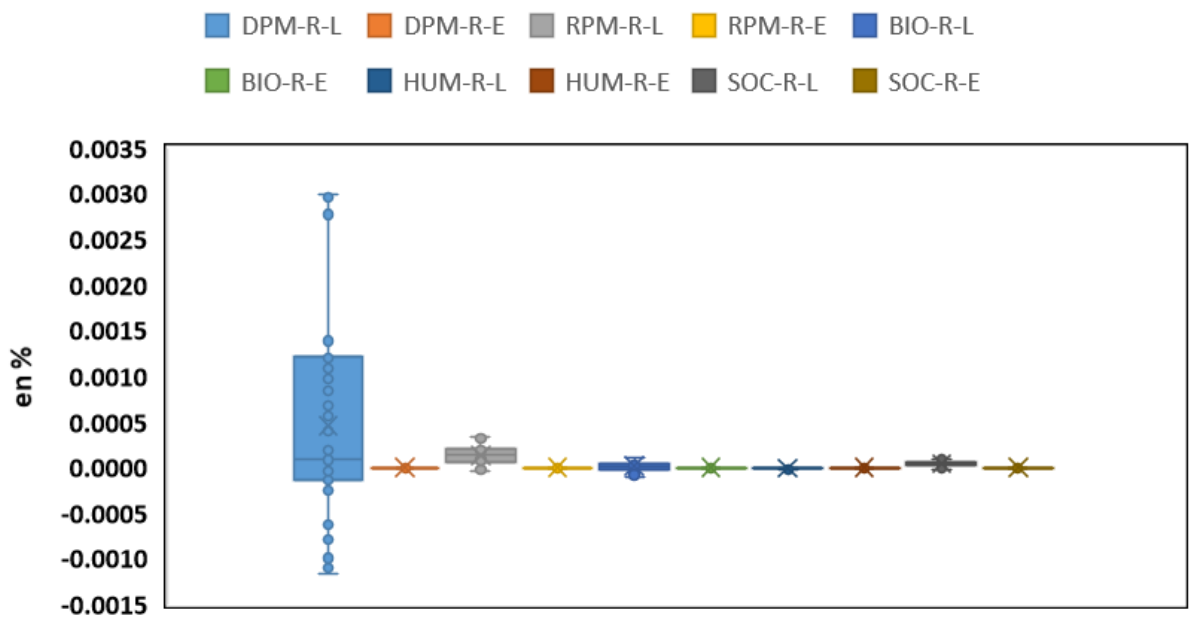

Figure A4. Relative difference in simulated results between RothC-R and the other two versions

A3 Assessing the future trends of soil trace metal contents in French urban gardens

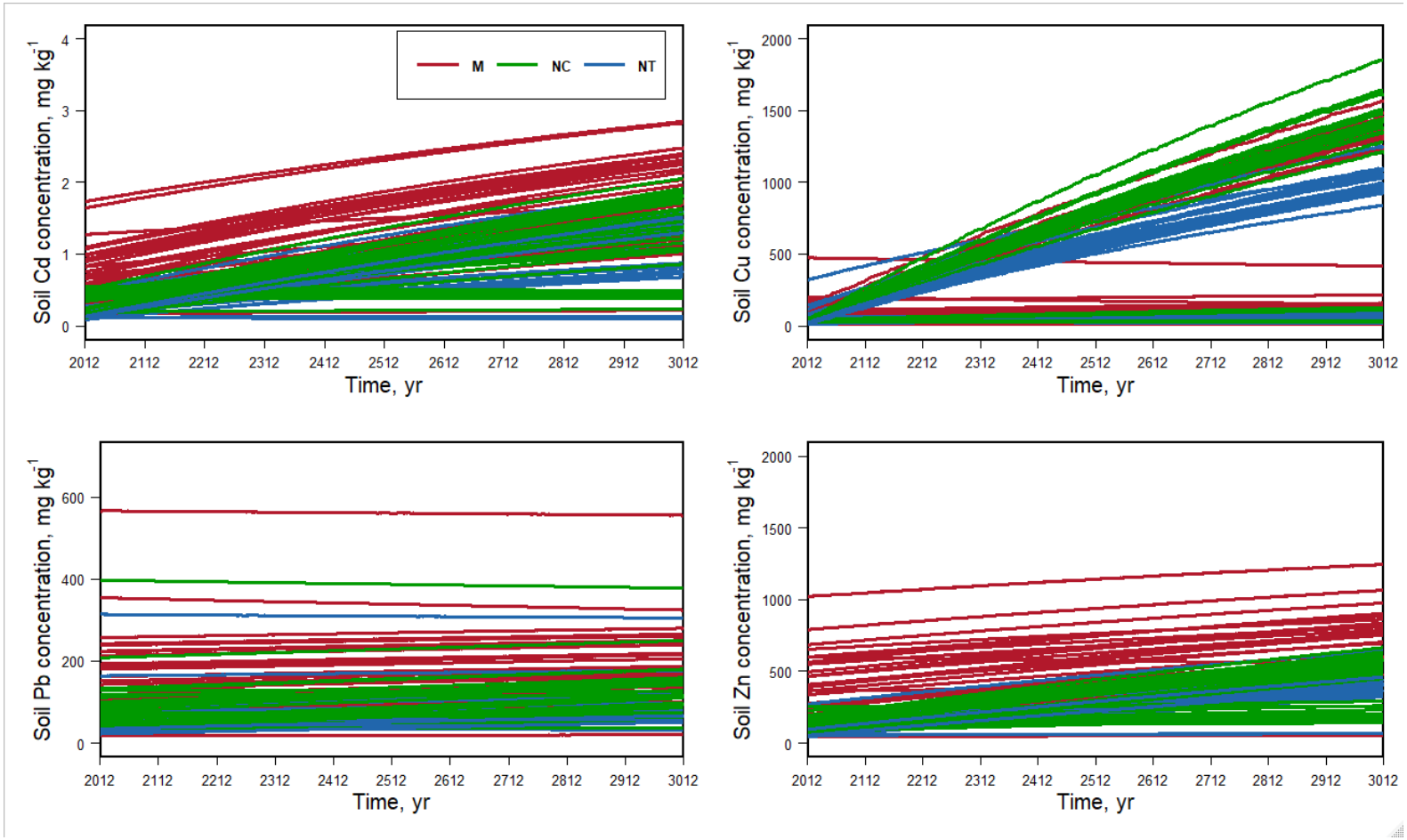

Figure A5. Evolution of the four metals soil concentration of in the dug layer (20 cm) of 104 gardens, under the CP scenario for 1000 years. M: Marseille; NC: Nancy; NT: Nantes

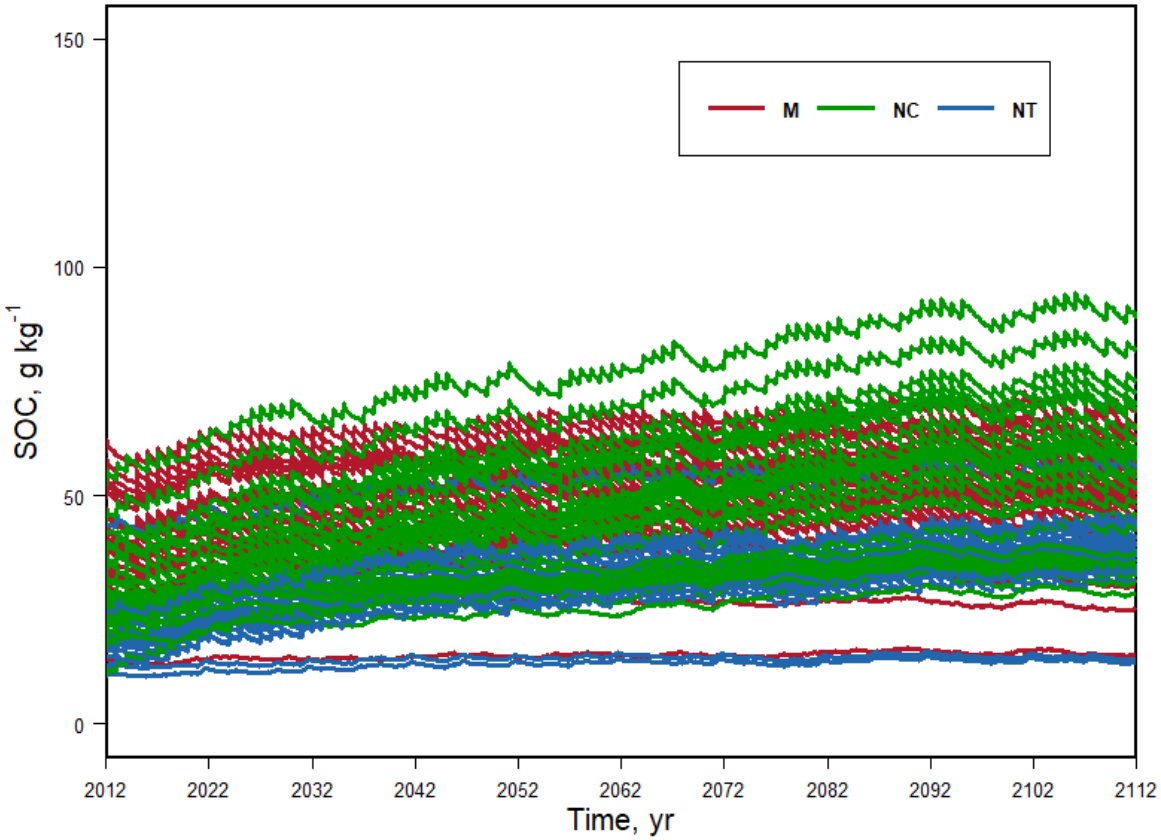

Figure A6. Evolution of soil organic carbon content of in the dug layer (20 cm) of 104 gardens, under the CP scenario. M: Marseille; NC: Nancy; NT: Nantes

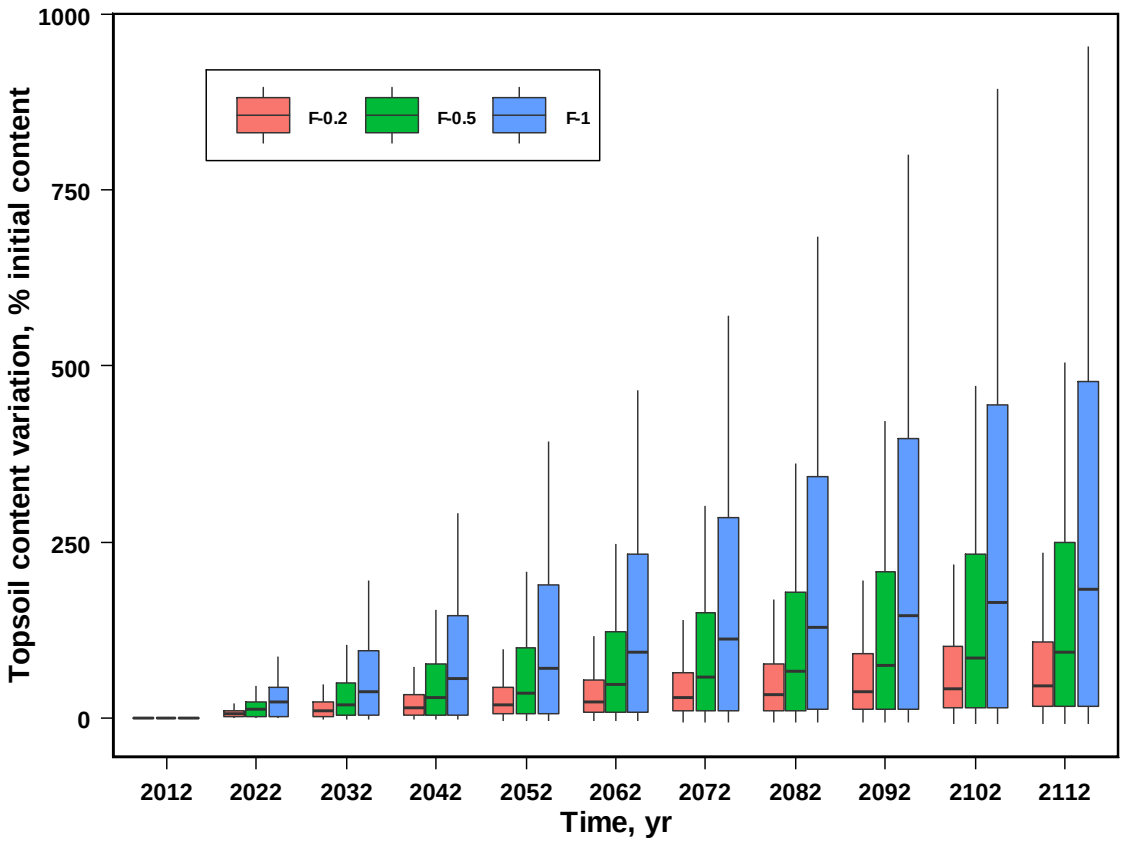

Figure A7. Relative variation of soil Cu content presented as boxplots by decade, for three fungicide application doses (F-0.2: 20% of recommended dose; F-0.5: 50% of recommended dose; F-1: recommended dose)

A4 Historical and future trends of soil trace metal contents in King's Vegetable Garden (Versailles, France)

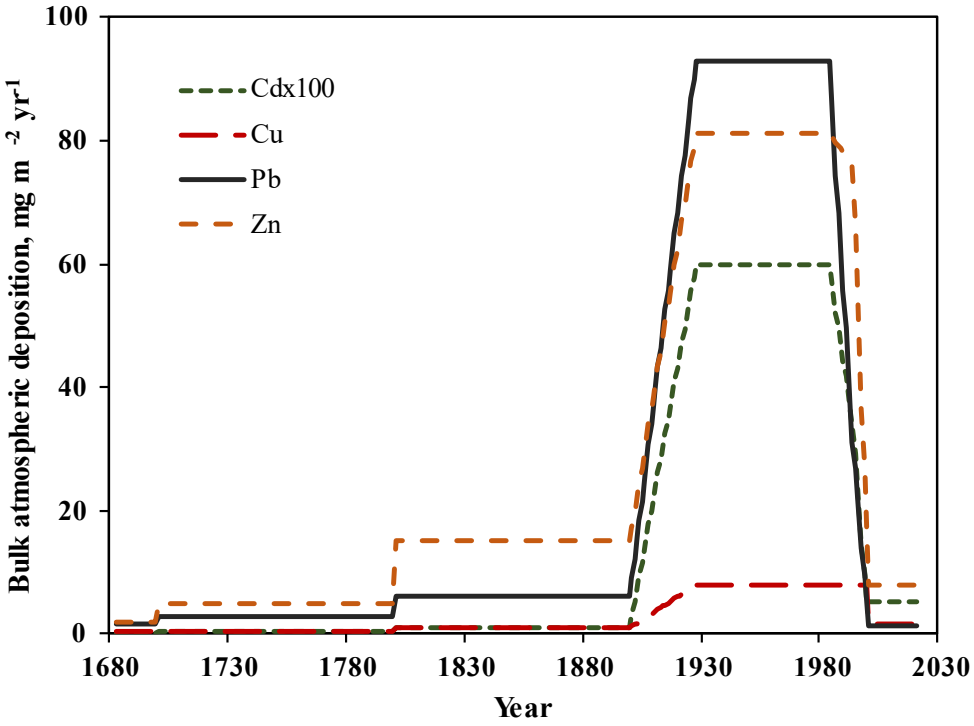

Figure A8. Reconstructed bulk atmospheric deposition of the four metals during 1683-2021 in Versailles

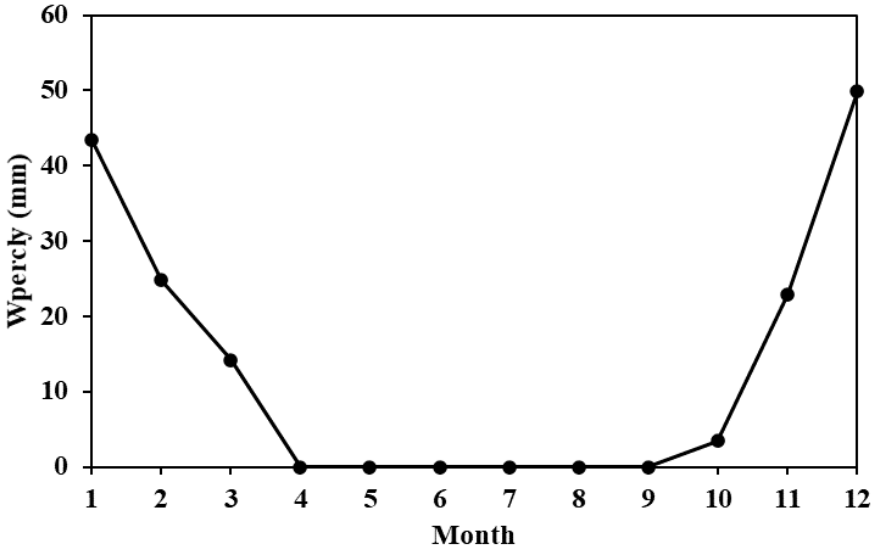

Figure A9. Monthly average percolating water in mm simulated by model for the Great Square of soi

Table A3. Crop rotation and ploughing depth in King's Vegetable Garden from 1683 to 2021

Year	Ploughing depth	Spring/summer	Autumn/winter	Year	Ploughing depth	Spring/summer	Autumn/winter
1683	65cm	Lettuce	Chicory	1853	32.5cm	Lettuce	Chicory
1684	65cm	Onion	Spinach	1854	32.5cm	Leek	Uncultivated
1685	65cm	Lettuce	Chicory	1855	32.5cm	Salsify	Uncultivated
1686	65cm	Salsify	Uncultivated	1856	32.5cm	Cabbage	Uncultivated
1687	65cm	Cauliflower	Uncultivated	1857	32.5cm	Lettuce	Chicory
1688	65cm	Lettuce	Celeriac rave	1858	32.5cm	Carrot	Uncultivated
1689	65cm	Broccoli	Uncultivated	1859	32.5cm	Parsnip	Uncultivated
1690	65cm	Lettuce	Chicory	1860	32.5cm	Lettuce	Chicory
1691	65cm	Cardoon	Uncultivated	1861	32.5cm	Multiple cultures	Uncultivated
1692	65cm	Beet	Uncultivated	1862	32.5cm	Chervil	Uncultivated
1693	65cm	Lettuce	Chicory	1863	32.5cm	Lettuce	Chicory
1694	65cm	Cabbage	Uncultivated	1864	32.5cm	Chicory	Uncultivated
1695	65cm	Leek	Uncultivated	1865	32.5cm	Garden cress	Uncultivated
1696	65cm	Carrot	Uncultivated	1866	32.5cm	Lettuce	Chicory
1697	65cm	Lettuce	Chicory	1867	32.5cm	Balm	Uncultivated
1698	65cm	Parsnip	Uncultivated	1868	32.5cm	Balm	Uncultivated
1699	65cm	Black salsify	Uncultivated	1869	32.5cm	Onion	Spinach
1700	65cm	Lettuce	Chicory	1870	32.5cm	Lettuce	Chicory
1701	65cm	Beet	Uncultivated	1871	32.5cm	Medicinal plants	Uncultivated
1702	65cm	Multiple cultures	Uncultivated	1872	32.5cm	Cauliflower	Uncultivated
1703	65cm	Lettuce	Chicory	1873	32.5cm	Lettuce	Uncultivated
1704	65cm	Onion	Spinach	1874	32.5cm	Broccoli	Uncultivated
1705	65cm	Lettuce	Chicory	1875	32.5cm	Lettuce	Chicory
1706	65cm	Cauliflower	Uncultivated	1876	32.5cm	Portulaca oleracea	Uncultivated

1707	65cm	Baby lettuce	Uncultivated	1877	32.5cm	Chicory	Uncultivated
1708	65cm	Lettuce	Celeriac rave	1878	32.5cm	Lettuce	Chicory
1709	65cm	Broccoli	Uncultivated	1879	32.5cm	Beet	Uncultivated
1710	65cm	Uncultivated	Uncultivated	1880	32.5cm	Lettuce	Chicory
1711	65cm	Uncultivated	Uncultivated	1881	32.5cm	Cardoon	Uncultivated
1712	65cm	Uncultivated	Uncultivated	1882	32.5cm	Beet	Uncultivated
1713	65cm	Uncultivated	Uncultivated	1883	32.5cm	Beet	Uncultivated
1714	65cm	Uncultivated	Uncultivated	1884	32.5cm	Lettuce	Chicory
1715	65cm	Uncultivated	Uncultivated	1885	32.5cm	Black salsify	Uncultivated
1716	65cm	Uncultivated	Uncultivated	1886	32.5cm	Lettuce	Chicory
1717	65cm	Uncultivated	Uncultivated	1887	32.5cm	Parsnip	Uncultivated
1718	65cm	Uncultivated	Uncultivated	1888	32.5cm	Onion	Spinach
1719	65cm	Uncultivated	Uncultivated	1889	32.5cm	Lettuce	Chicory
1720	65cm	Uncultivated	Uncultivated	1890	32.5cm	Cauliflower	Uncultivated
1721	65cm	Uncultivated	Uncultivated	1891	32.5cm	Lettuce	Uncultivated
1722	65cm	Uncultivated	Uncultivated	1892	32.5cm	Multiple cultures	Uncultivated
1723	65cm	Uncultivated	Uncultivated	1893	32.5cm	Broccoli	Uncultivated
1724	65cm	Beet	Uncultivated	1894	32.5cm	Lettuce	Chicory
1725	65cm	Lettuce	Chicory	1895	32.5cm	Carrot	Uncultivated
1726	65cm	Chicory	Uncultivated	1896	32.5cm	Leek	Uncultivated
1727	65cm	Lettuce	Chicory	1897	32.5cm	Cabbage	Uncultivated
1728	65cm	Tarragon	Uncultivated	1898	32.5cm	Lettuce	Chicory
1729	65cm	Tarragon	Uncultivated	1899	32.5cm	Beet	Uncultivated
1730	65cm	Tarragon	Uncultivated	1900	32.5cm	Cardoon	Uncultivated
1731	65cm	Lettuce	Chicory	1901	32.5cm	Potato	Uncultivated
1732	65cm	Lettuce	Celeriac rave	1902	32.5cm	Leek	Uncultivated
1733	65cm	Black salsify	Uncultivated	1903	32.5cm	Tomato	Uncultivated
1734	65cm	Lettuce	Chicory	1904	32.5cm	Squash	Uncultivated
1735	65cm	Beet	Uncultivated	1905	32.5cm	Cabbage	Uncultivated

1736	65cm	Cardoon	Uncultivated	1906	32.5cm	Carrot	Uncultivated
1737	65cm	Onion	Spinach	1907	32.5cm	Potato	Uncultivated
1738	65cm	Lettuce	Chicory	1908	32.5cm	Squash	Uncultivated
1739	65cm	Cauliflower	Uncultivated	1909	32.5cm	Strawberry	Uncultivated
1740	65cm	Lettuce	Celeriac rave	1910	32.5cm	Strawberry	Uncultivated
1741	65cm	Broccoli	Uncultivated	1911	32.5cm	Strawberry	Uncultivated
1742	65cm	Lettuce	Chicory	1912	32.5cm	Strawberry	Uncultivated
1743	65cm	Leek	Uncultivated	1913	32.5cm	Potato	Uncultivated
1744	65cm	Salsify	Uncultivated	1914	32.5cm	Garlic	Uncultivated
1745	65cm	Cabbage	Uncultivated	1915	32.5cm	Pea	Uncultivated
1746	65cm	Lettuce	Chicory	1916	32.5cm	Squash	Uncultivated
1747	65cm	Carrot	Uncultivated	1917	32.5cm	Onion	Uncultivated
1748	65cm	Parsnip	Uncultivated	1918	32.5cm	Cabbage	Uncultivated
1749	65cm	Lettuce	Chicory	1919	32.5cm	Leek	Uncultivated
1750	65cm	Multiple cultures	Uncultivated	1920	32.5cm	Potato	Uncultivated
1751	65cm	Chervil	Uncultivated	1921	25cm	Shallot	Uncultivated
1752	65cm	Lettuce	Chicory	1922	25cm	Broad bean	Uncultivated
1753	65cm	Chicory	Uncultivated	1923	25cm	Squash	Uncultivated
1754	65cm	Garden cress	Uncultivated	1924	25cm	Green bean	Uncultivated
1755	65cm	Lettuce	Chicory	1925	25cm	Spinach	Uncultivated
1756	65cm	Balm	Uncultivated	1926	25cm	Potato	Uncultivated
1757	65cm	Balm	Uncultivated	1927	25cm	Lettuce	Uncultivated
1758	65cm	Onion	Spinach	1928	25cm	Turnip	Uncultivated
1759	65cm	Lettuce	Chicory	1929	25cm	Squash	Uncultivated
1760	65cm	Cauliflower	Uncultivated	1930	25cm	Carrot	Uncultivated
1761	65cm	Lettuce	Celeriac rave	1931	25cm	Tomato	Uncultivated
1762	65cm	Broccoli	Uncultivated	1932	25cm	Potato	Uncultivated
1763	65cm	Lettuce	Chicory	1933	25cm	Asparagus	Uncultivated

1764	65cm	Portulaca oleracea	Uncultivated	1934	25cm	Asparagus	Uncultivated
1765	65cm	Chicory	Uncultivated	1935	25cm	Asparagus	Uncultivated
1766	65cm	Lettuce	Chicory	1936	25cm	Asparagus	Uncultivated
1767	65cm	Beet	Uncultivated	1937	25cm	Leek	Uncultivated
1768	65cm	Lettuce	Chicory	1938	25cm	Squash	Uncultivated
1769	65cm	Cardoon	Uncultivated	1939	25cm	Potato	Uncultivated
1770	65cm	Beet	Uncultivated	1940	25cm	Cabbage	Uncultivated
1771	65cm	Beet	Uncultivated	1941	25cm	Zucchini	Uncultivated
1772	65cm	Lettuce	Chicory	1942	25cm	Squash	Uncultivated
1773	65cm	Black salsify	Uncultivated	1943	25cm	Celeriac rave	Uncultivated
1774	65cm	Lettuce	Chicory	1944	25cm	Beet	Uncultivated
1775	65cm	Parsnip	Uncultivated	1945	25cm	Potato	Uncultivated
1776	65cm	Onion	Spinach	1946	25cm	Lamb's lettuce	Uncultivated
1777	65cm	Lettuce	Chicory	1947	25cm	Cabbage	Uncultivated
1778	65cm	Cauliflower	Uncultivated	1948	25cm	Squash	Uncultivated
1779	65cm	Lettuce	Celeriac rave	1949	25cm	Green bean	Uncultivated
1780	65cm	Multiple cultures	Uncultivated	1950	25cm	Beet	Uncultivated
1781	65cm	Broccoli	Uncultivated	1951	25cm	Potato	Uncultivated
1782	65cm	Lettuce	Chicory	1952	25cm	Cardoon	Uncultivated
1783	65cm	Carrot	Uncultivated	1953	25cm	Onion	Uncultivated
1784	65cm	Leek	Uncultivated	1954	25cm	Squash	Uncultivated
1785	65cm	Cabbage	Uncultivated	1955	25cm	Leek	Uncultivated
1786	65cm	Lettuce	Chicory	1956	25cm	Cabbage	Uncultivated
1787	65cm	Beet	Uncultivated	1957	25cm	Potato	Uncultivated
1788	65cm	Cardoon	Uncultivated	1958	25cm	Rheum	Uncultivated
1789	65cm	Lettuce	Chicory	1959	25cm	Rheum	Uncultivated
1790	65cm	Salsify	Uncultivated	1960	25cm	Rheum	Uncultivated
1791	65cm	Broccoli	Uncultivated	1961	25cm	Squash	Uncultivated

1792	65cm	Lettuce	Celeriac rave	1962	25cm	Shallot	Uncultivated
1793	65cm	Cauliflower	Uncultivated	1963	25cm	Parsnip	Uncultivated
1794	65cm	Lettuce	Chicory	1964	25cm	Potato	Uncultivated
1795	65cm	Onion	Spinach	1965	25cm	Artichoke	Uncultivated
1796	65cm	Lettuce	Chicory	1966	25cm	Artichoke	Uncultivated
1797	65cm	Chives	Uncultivated	1967	25cm	Artichoke	Uncultivated
1798	65cm	Chives	Uncultivated	1968	25cm	Squash	Uncultivated
1799	65cm	Medicinal plants	Medicinal plants	1969	25cm	Carrot	Uncultivated
1800	65cm	Medicinal plants	Medicinal plants	1970	25cm	Tomato	Uncultivated
1801	32.5cm	Medicinal plants	Medicinal plants	1971	25cm	Potato	Uncultivated
1802	32.5cm	Medicinal plants	Medicinal plants	1972	25cm	Leek	Uncultivated
1803	32.5cm	Medicinal plants	Medicinal plants	1973	25cm	Cabbage	Uncultivated
1804	32.5cm	Medicinal plants	Medicinal plants	1974	25cm	Squash	Uncultivated
1805	32.5cm	Medicinal plants	Medicinal plants	1975	25cm	Onion	Uncultivated
1806	32.5cm	Medicinal plants	Medicinal plants	1976	25cm	Green bean	Uncultivated
1807	32.5cm	Salad burnet	Uncultivated	1977	25cm	Potato	Uncultivated
1808	32.5cm	Lettuce	Chicory	1978	25cm	Broad bean	Uncultivated
1809	32.5cm	Onion	Spinach	1979	25cm	Squash	Uncultivated
1810	32.5cm	Lettuce	Chicory	1980	25cm	Chicory	Uncultivated
1811	32.5cm	Salsify	Uncultivated	1981	25cm	Radish	Uncultivated
1812	32.5cm	Cauliflower	Uncultivated	1982	25cm	Zucchini	Uncultivated
1813	32.5cm	Lettuce	Celeriac rave	1983	25cm	Potato	Uncultivated
1814	32.5cm	Broccoli	Uncultivated	1984	25cm	Spinach	Uncultivated
1815	32.5cm	Lettuce	Chicory	1985	25cm	Pea	Uncultivated

1816	32.5cm	Cardoon	Uncultivated	1986	25cm	Squash	Uncultivated
1817	32.5cm	Beet	Uncultivated	1987	25cm	Leek	Uncultivated
1818	32.5cm	Lettuce	Chicory	1988	25cm	Garlic	Uncultivated
1819	32.5cm	Cabbage	Uncultivated	1989	25cm	Cabbage	Uncultivated
1820	32.5cm	Leek	Uncultivated	1990	25cm	Potato	Uncultivated
1821	32.5cm	Carrot	Uncultivated	1991	25cm	Eggplant	Uncultivated
1822	32.5cm	Lettuce	Chicory	1992	25cm	Squash	Uncultivated
1823	32.5cm	Parsnip	Uncultivated	1993	25cm	Beet	Uncultivated
1824	32.5cm	Black salsify	Uncultivated	1994	25cm	Bell pepper	Uncultivated
1825	32.5cm	Lettuce	Chicory	1995	25cm	Potato	Uncultivated
1826	32.5cm	Beet	Uncultivated	1996	25cm	Celeriac rave	Uncultivated
1827	32.5cm	Multiple cultures	Uncultivated	1997	25cm	Tomato	Uncultivated
1828	32.5cm	Lettuce	Chicory	1998	25cm	Squash	Uncultivated
1829	32.5cm	Onion	Spinach	1999	25cm	Carrot	Uncultivated
1830	32.5cm	Lettuce	Chicory	2000	20cm	Cucumber	Uncultivated
1831	32.5cm	Cauliflower	Uncultivated	2001	20cm	Potato	Uncultivated
1832	32.5cm	Baby lettuce	Uncultivated	2002	20cm	Turnip	Uncultivated
1833	32.5cm	Lettuce	Celeriac rave	2003	20cm	Leek	Uncultivated
1834	32.5cm	Broccoli	Uncultivated	2004	20cm	Squash	Uncultivated
1835	32.5cm	Beet	Uncultivated	2005	20cm	Cabbage	Uncultivated
1836	32.5cm	Lettuce	Chicory	2006	20cm	Shallot	Uncultivated
1837	32.5cm	Chicory	Uncultivated	2007	20cm	Potato	Uncultivated
1838	32.5cm	Lettuce	Chicory	2008	20cm	Lettuce	Uncultivated
1839	32.5cm	Tarragon	Uncultivated	2009	20cm	Broad bean	Uncultivated
1840	32.5cm	Tarragon	Uncultivated	2010	20cm	Squash	Uncultivated
1841	32.5cm	Tarragon	Uncultivated	2011	20cm	Spinach	Uncultivated
1842	32.5cm	Lettuce	Chicory	2012	20cm	Green bean	Uncultivated
1843	32.5cm	Lettuce	Celeriac rave	2013	20cm	Potato	Uncultivated
1844	32.5cm	Black salsify	Uncultivated	2014	20cm	Lamb's lettuce	Uncultivated

1845	32.5cm	Lettuce	Chicory	2015	20cm	Onion	Uncultivated
1846	32.5cm	Beet	Uncultivated	2016	20cm	Squash	Uncultivated
1847	32.5cm	Cardoon	Uncultivated	2017	20cm	Carrot	Uncultivated
1848	32.5cm	Onion	Spinach	2018	20cm	Pea	Uncultivated
1849	32.5cm	Lettuce	Chicory	2019	20cm	Potato	Uncultivated
1850	32.5cm	Cauliflower	Uncultivated	2020	20cm	Leek	Uncultivated
1851	32.5cm	Lettuce	Celeriac rave	2021	20cm	Tomato	Uncultivated
1852	32.5cm	Broccoli	Uncultivated				

Table A4. Independent variables tested for modelling uncertainty analysis. *lack of data, minimum and maximum values estimated from ±25% of average values

Parameter	Description	Unit	Min	Max	Reference
	Parameters related to applied practices				
Catm	**Metal content in bulk sampling precipitation**				
	Cd	ug L^{-1}	fixed	fixed	(Allan et al., 2013; Azimi et al., 2005; Baize and
	Cu	ug L^{-1}	fixed	fixed	Bourgeois, 2005; BRAMM, 2018, 2013; Elbaz-
	Pb	ug L^{-1}	fixed	fixed	Poulichet et al., 2020; Hansson et al., 2015;
	Zn	ug L^{-1}	fixed	fixed	Juste and Tauzin, 1986; Mariet et al., 2018)
Cfer	**Metal content in chemical fertilizer**				
	Cd	mg kg^{-1}	0.72	4.86	(Verbeeck et al., 2020)
	Cu	mg kg^{-1}	2.27	51.7	(Verbeeck et al., 2020)
	Pb	mg kg^{-1}	2.27	24.3	(Verbeeck et al., 2020)
	Zn	mg kg^{-1}	29.2	602	(Verbeeck et al., 2020)
Mfer	**Quantity of chemical fertilizer application**	kg m^{-2}	0.028	0.046	(Joimel, 2015; Zhong et al., 2021)
Cmanu*	**Metal content in manure**				
	Cd	mg (kg DW)$^{-1}$	0.225	0.375	(AROMIS, 2020; Houot et al., 2014)

	Cu	mg (kg DW)$^{-1}$	17.3	28.8	(AROMIS, 2020; Houot et al., 2014)
	Pb	mg (kg DW)$^{-1}$	2.25	3.75	(AROMIS, 2020; Houot et al., 2014)
	Zn	mg (kg DW)$^{-1}$	99.8	166	(AROMIS, 2020; Houot et al., 2014)
Mmanu	**Quantity of manure application**	kg FW m^{-2}	1	3	Estimated dosage based on KVG's gardening practices record
Cbiow*	**Metal content in bio-waste compost**				
	Cd	mg (kg DW)$^{-1}$	0.3	0.5	(Weissengruber et al., 2018)
	Cu	mg (kg DW)$^{-1}$	30.8	51.3	(Weissengruber et al., 2018)
	Pb	mg (kg DW)$^{-1}$	21	35	(Weissengruber et al., 2018)
	Zn	mg (kg DW)$^{-1}$	113	188	(Weissengruber et al., 2018)
Mbiow	**Quantity of bio-waste compost application**	kg FW m^{-2}	fixed	fixed	Recorded in KVG's gardening practices
Cterreau*	**Metal content in terreau**				
	Cd	mg (kg DW)$^{-1}$	0.05	0.08	(France Galop et al., 2013)
	Cu	mg (kg DW)$^{-1}$	6.11	10.2	(France Galop et al., 2013)
	Pb	mg (kg DW)$^{-1}$	1.14	1.89	(France Galop et al., 2013)
	Zn	mg (kg DW)$^{-1}$	15.6	26.0	(France Galop et al., 2013)
Mterreau	**Quantity of terreau par each application**	kg DW m^{-2}	1.67	6.66	Estimated dosage based on KVG's gardening practices record

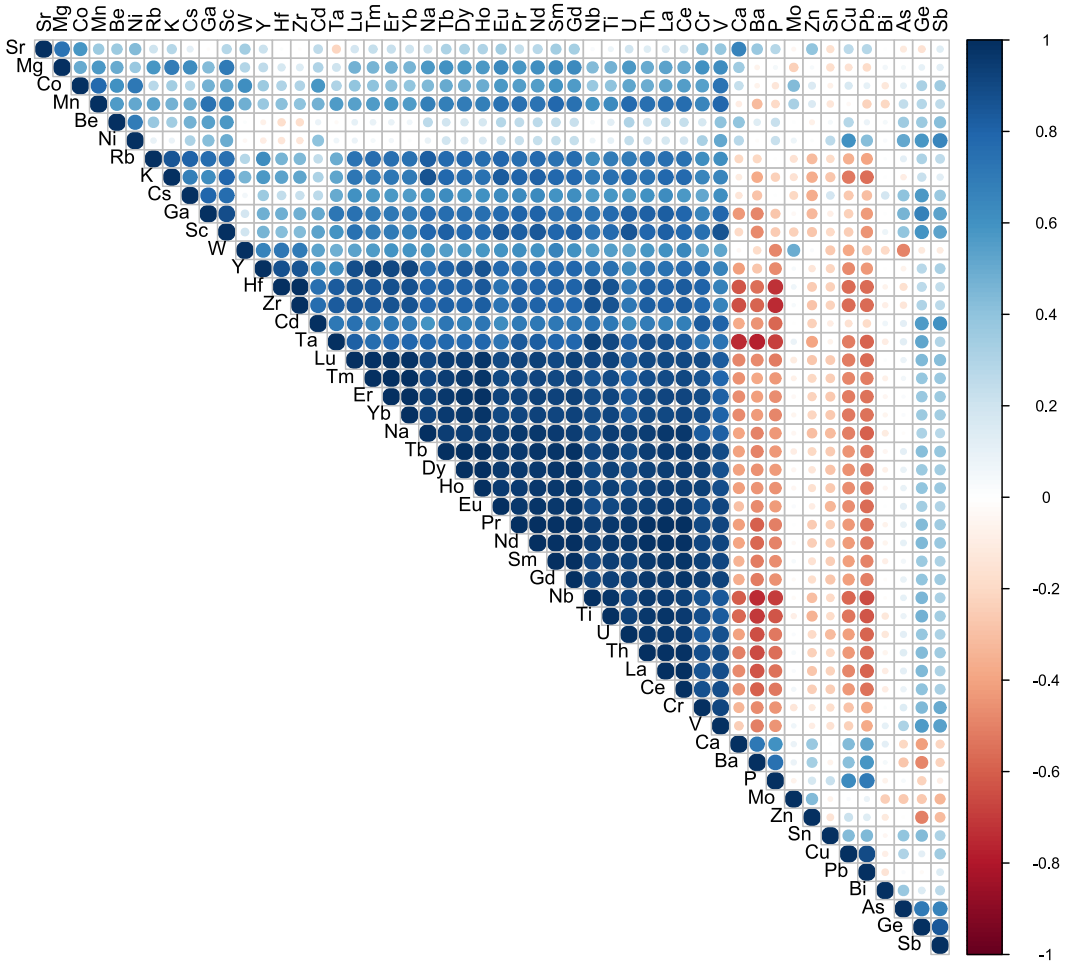

Figure A10. Pearson correlation coefficient among major and trace elements of KVG's topsoil

Table A5. Measured soil metal concentrations and initial metal concentrations estimated by pedo-transfer functions from soil Fe content. S1-S16: Soil samples of the first 20 cm collected from 16 vegetable plots; Symbol "C" indicates soil composites of deeper layers for the 16 vegetable plots (20-40 cm, 40-60 cm, 70-80 cm and 80-120 cm)

Sample	Cd, mg kg^{-1}		Cu, mg kg^{-1}		Pb, mg kg^{-1}		Zn, mg kg^{-1}	
	Measured	Initial	Measured	Initial	Measured	Initial	Measured	Initial
S1	0.42	0.08	41.9	7.3	109	10.4	147	31.9
S2	0.34	0.08	70.7	7.5	274	10.7	184	32.8
S3	0.33	0.07	53.0	6.8	210	9.7	148	29.5
S4	0.38	0.09	46.7	8.2	149	11.6	119	35.6
S5	0.32	0.08	60.7	7.4	177	10.6	301	32.4
S6	0.33	0.08	62.7	7.3	246	10.4	147	31.9
S7	0.32	0.07	46.6	6.6	141	9.4	140	28.7
S8	0.32	0.08	48.3	7.2	149	10.3	141	31.4
S9	0.31	0.07	49.0	7.0	204	9.9	186	30.4
S10	0.32	0.07	49.2	6.8	170	9.8	151	29.8
S11	0.35	0.08	51.5	7.7	194	10.9	183	33.4
S12	0.33	0.09	51.2	8.4	157	12.0	132	36.6
S13	0.34	0.08	66.2	8.0	199	11.3	147	34.7
S14	0.35	0.08	82.5	7.4	332	10.5	148	32.3
S15	0.34	0.08	51.1	7.3	156	10.4	143	31.8
S16	0.32	0.08	54.7	7.4	153	10.6	134	32.3
C20-40	0.28	0.09	48.0	8.5	223	12.1	114	37.0
C40-60	0.19	0.10	34.8	10.0	74	14.3	75	43.8
C70-80	0.16	0.11	22.4	10.1	50	14.4	57	43.9
C80-120	0.15	0.14	18.2	13.4	24	19.1	57	58.4

Table A6. Initial metal concentrations estimated by pedo-transfer functions from soil Fe content for garden soils (surface horizons: 0.2 m; n = 104) in the three metropolises: Marseille, Nancy and Nantes

Metropolis	Number of gardens	Mean initial metal content (mg $kg^{-1)}$			
		Cd	Cu	Pb	Zn
Marseille	33	0.11	10	15	45
Nancy	36	0.20	19	27	82
Nantes	35	0.08	8	11	35

Table A7. Total metal contents of the garden soils (surface horizons: 0.2 m; n = 104) in the three metropolises: Marseille, Nancy and Nantes

	Total metal contents in soils (mg kg^{-1})			
	Cd	Cu	Pb	Zn
mean	0.48	57	99	200
S.D.	0.89	60	85	182
median	0.34	39	75	133
min	0.09	12	20	43
max	8.9	473	566	1020

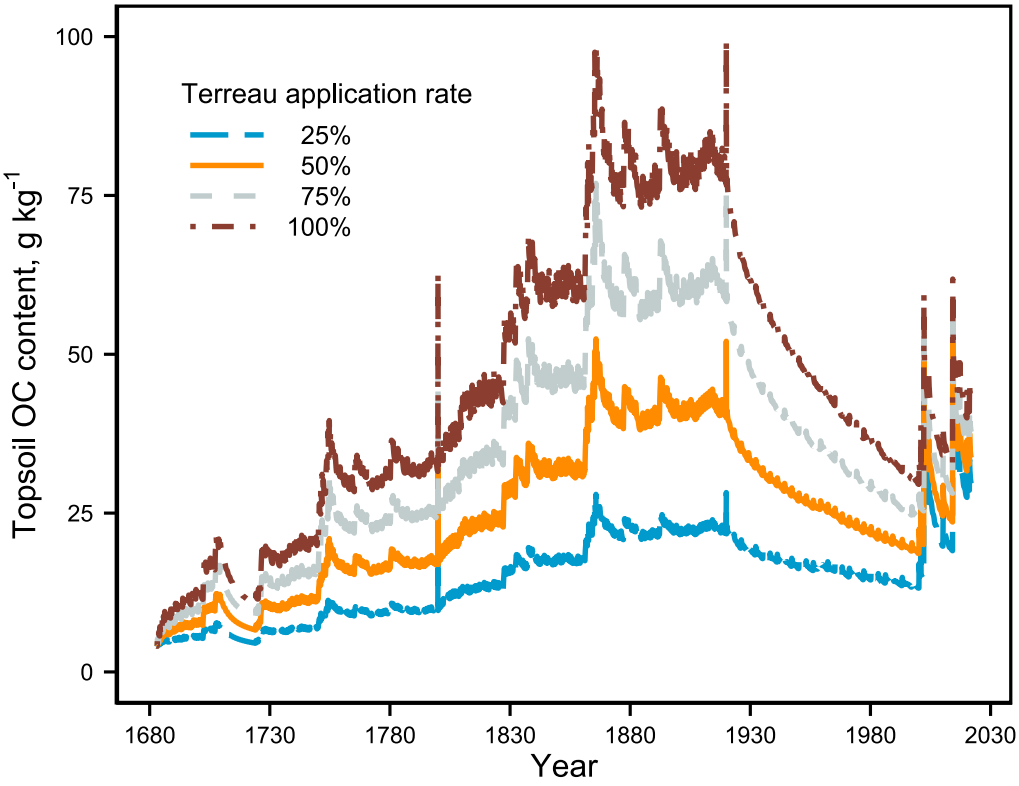

Figure A11. Evolution of topsoil organic carbon content in the surface layer (0-20 cm) of KVG with different application rates of terreau, simulated by RothC model during 1683-2021

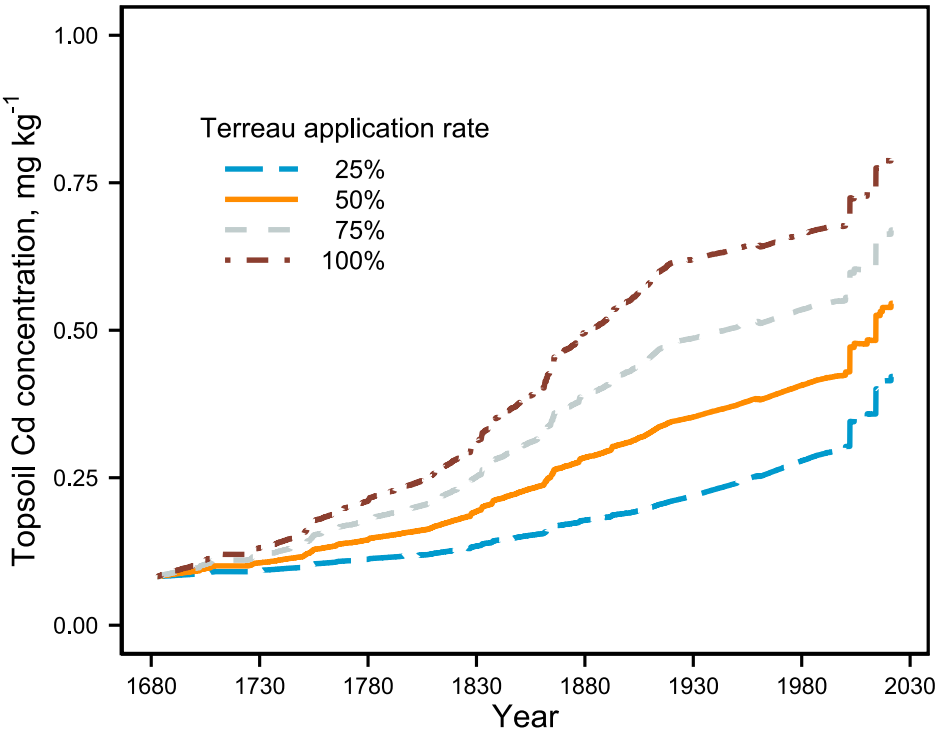

Figure A12. Evolution of topsoil Cd content in the surface layer (0-20 cm) of KVG with different application rates of terreau and reducing 50% of atmospheric deposition (during 1900-2000)

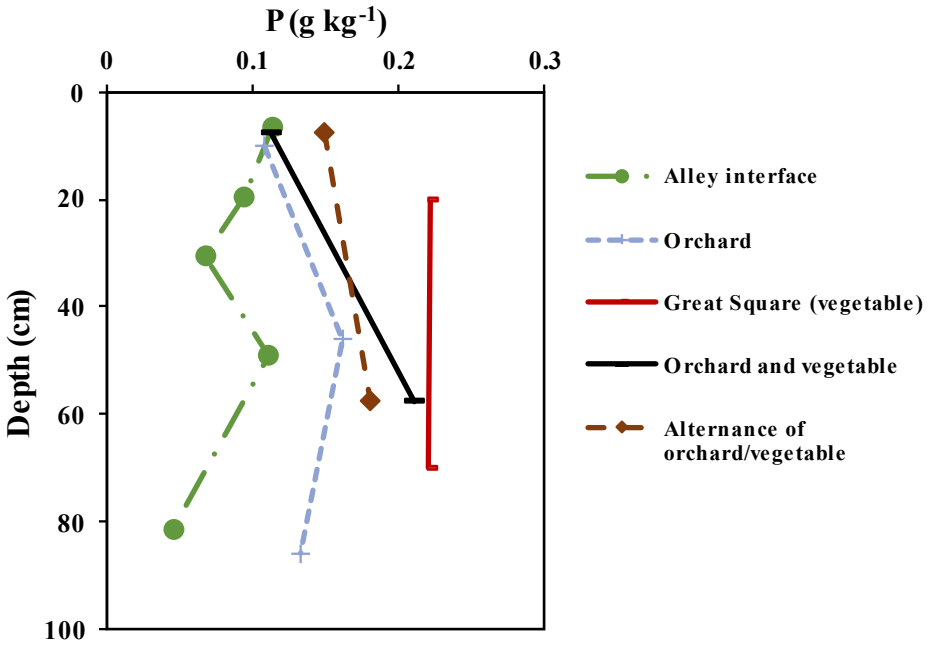

Figure A13. Concentrations of phosphorus in different pits of KVG: alley interface (Pit 1), orchard plot-one use over time (Pit 2), vegetable plot-one use over time (Pit 3), orchard/vegetable plot-two use over time (Pit 4), alternance of orchard/vegetable (Pit 5)

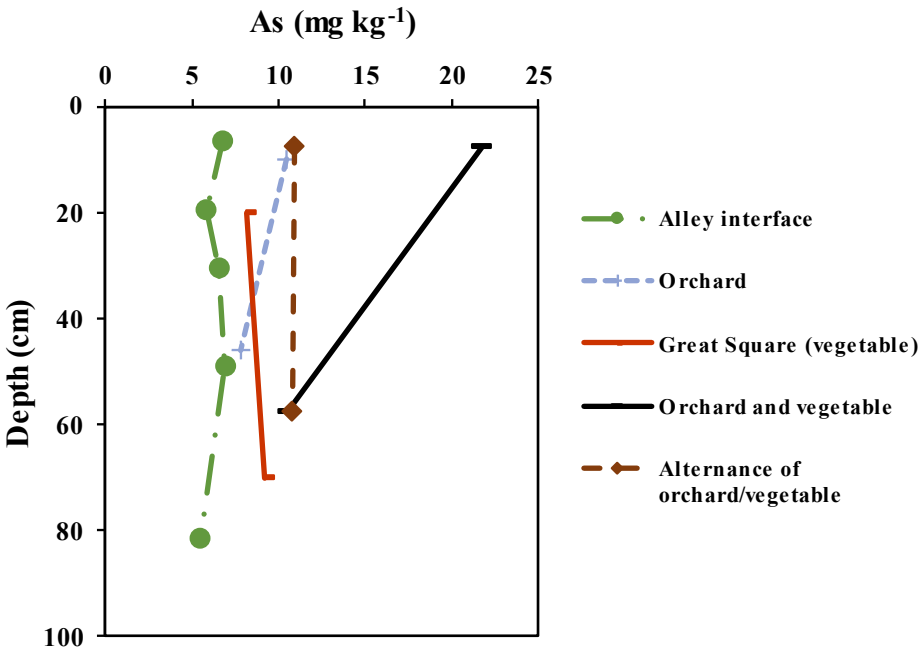

Figure A14. Concentrations of As in different pits of KVG: alley interface (Pit 1), orchard plot-one use over time (Pit 2), vegetable plot-one use over time (Pit 3), orchard/vegetable plot-two use over time (Pit 4), alternance of orchard/vegetable (Pit 5)

Table A8. Cumulated flows of the four metals in the ploughing soil layer of Great Square soil for different periods during 1683-2021.

Period	Input flow			Output flow	
	Qatm	Qfer	Qorg	Qlea	Qpla
			Accumulated Cd flow (mg kg^{-1})		
1683-1900	1.5	0	70	1.4	12
1900-2000	48	3.8	9	1.3	5.1
2000-2021	1.1	0	27	0.3	1.5
			Accumulated Cu flow (mg kg^{-1})		
1683-1900	146	0	5043	187	296
1900-2000	700	23	659	155	195
2000-2021	38	0	2745	42	57
			Accumulated Pb flow (mg kg^{-1})		
1683-1900	899	0	1876	27	208
1900-2000	7323	8	190	24	36
2000-2021	31	0	1875	6	4
			Accumulated Zn flow (mg kg^{-1})		
1683-1900	2023	0	12901	84	2285
1900-2000	6966	311	2458	65	687
2000-2021	175	0	10044	17	206

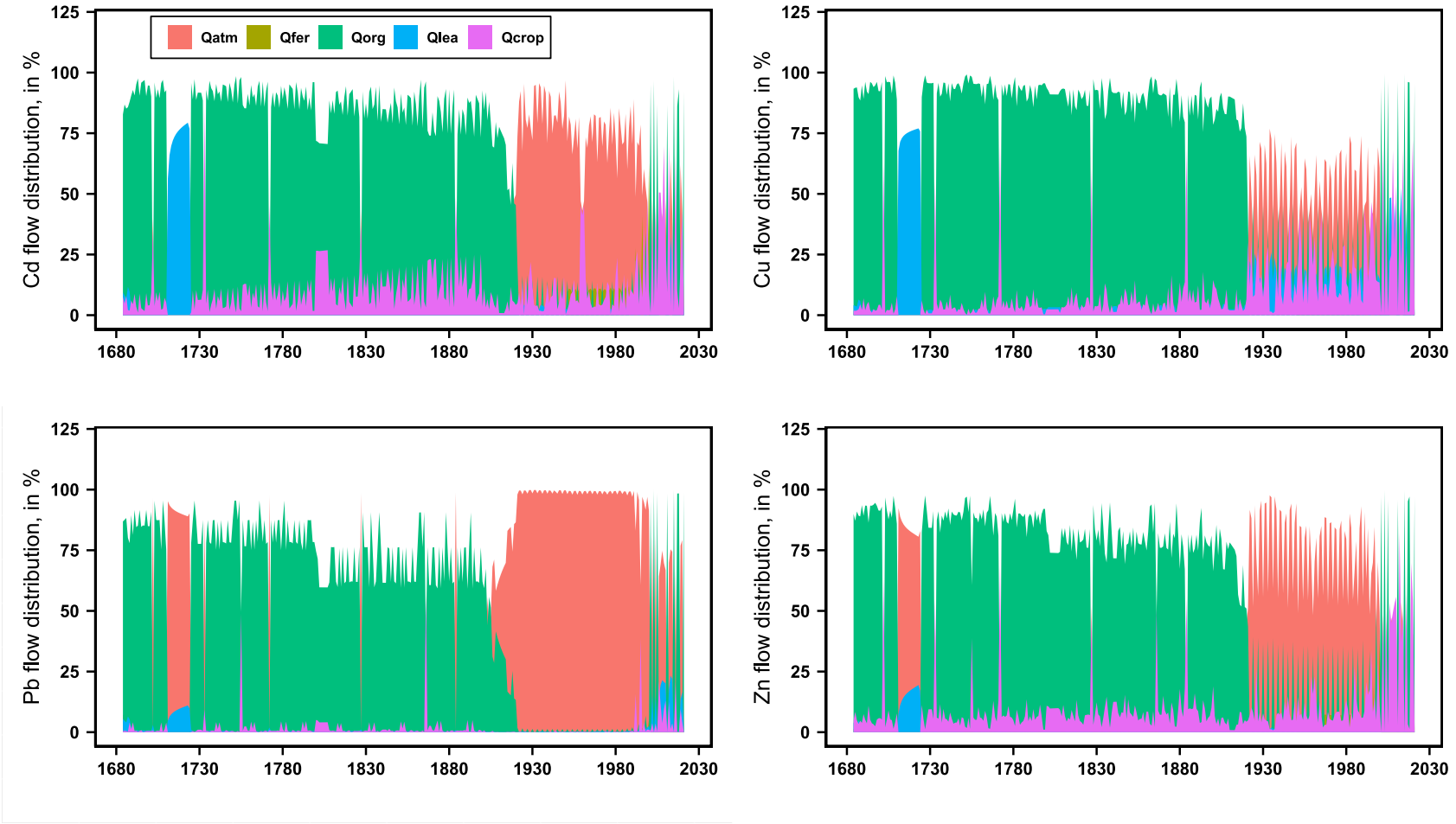

Figure A15. Annual distribution of input and output flows of the four metals during the period of 1683-2021 with 50% terreau application rate. In % of the sum of the absolute value of all flows. Qatm: atmospheric deposition; Qfer: NPK fertilizers; Qorg: organic amendments; Qlea: leaching; Qcrop: crop offtake

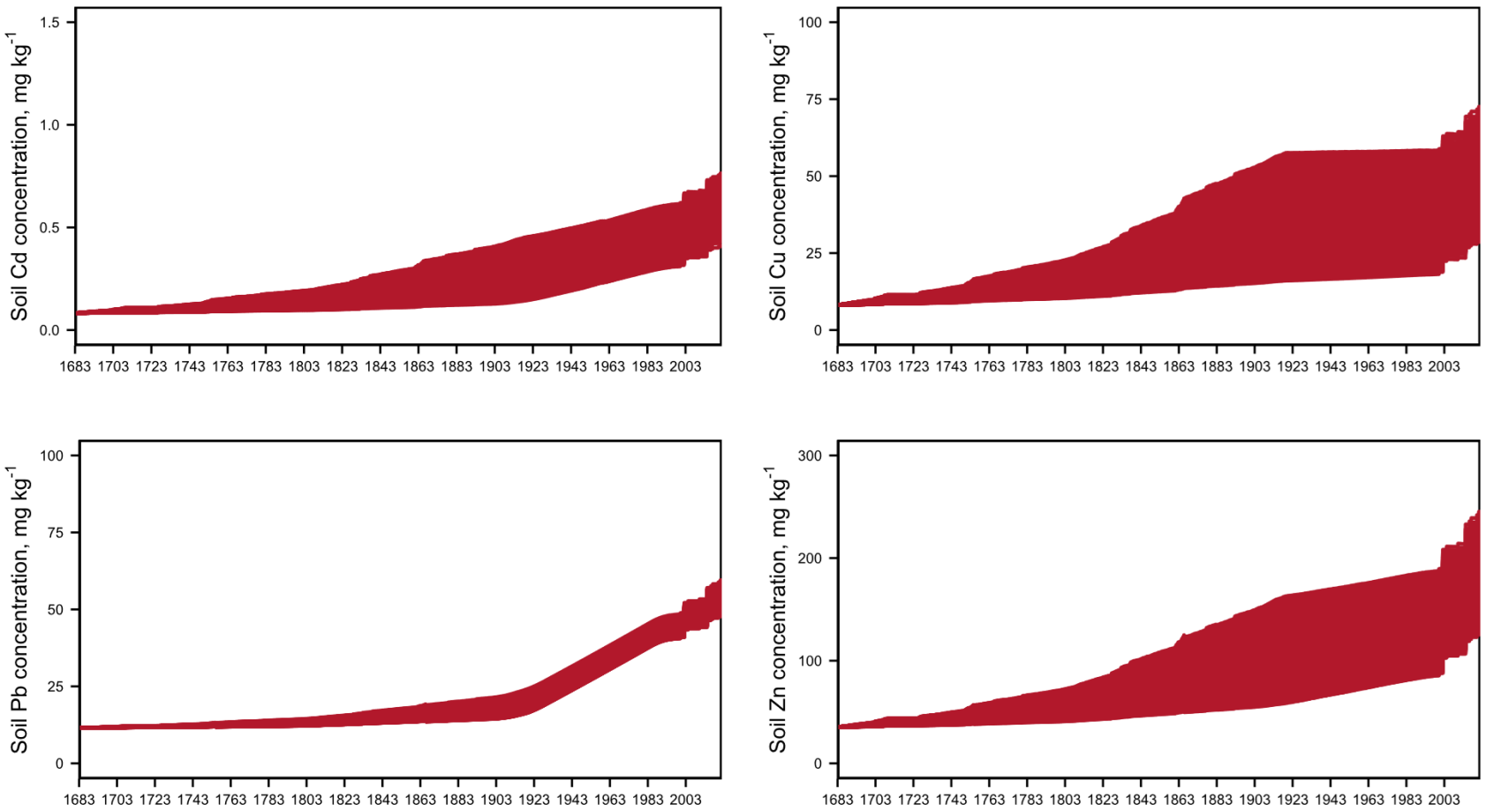

Figure A16. Evolution of the four metals soil concentration in the surface layer (0-20 cm) of the Great Square under the 1000 scenarios

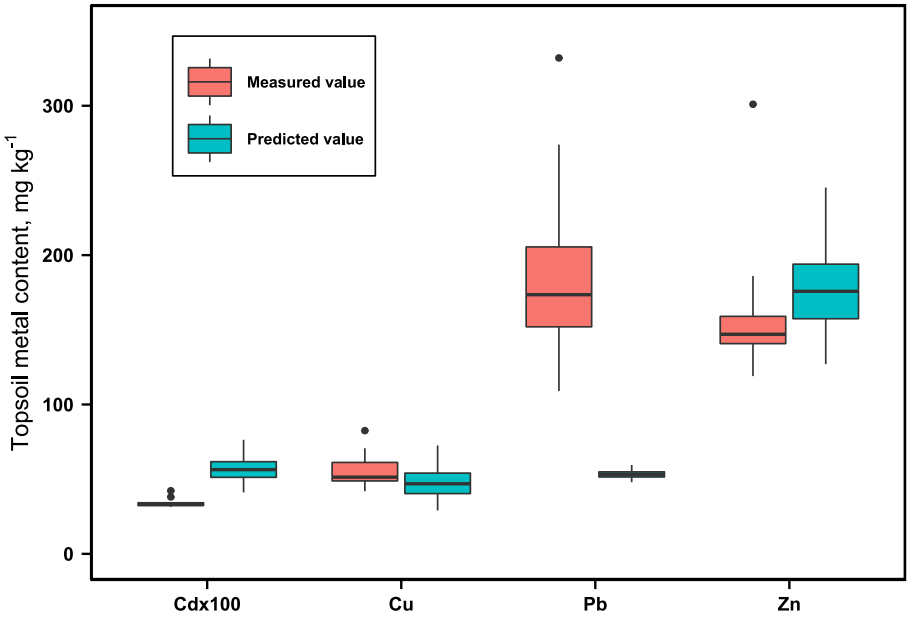

Figure A17. Measured (n = 16) and predicted (n = 1000) values of topsoil metal contents in the Great Square, in the left plot; frequency density of relative difference between predicted values and the average measured value, in the right plot

Table A9. Number of predicted values within ± x% difference of the average measured value. Range: the range of absolute relative differences, in %

Metal	Mean predicted value	N_φ									
		<10%	Range	10-25%	Range	25-50%	Range	50-100%	Range	>100%	Range
Cd	0.57	0	-	1	-	223	(28.0-50.0)	706	(50.1-99.9)	70	(100-125)
Cu	48	292	(0.18-9.99)	396	(10.0-25.0)	312	(25.0-47.5)	0	-	0	-
Pb	53	0	-	0	-	0	-	1000	(68.5-74.6)	0	-
Zn	177	420	(0.02-9.98)	391	(10.0-25.0)	186	(25.0-49.1)	3	(50.0-53.8)	0	-

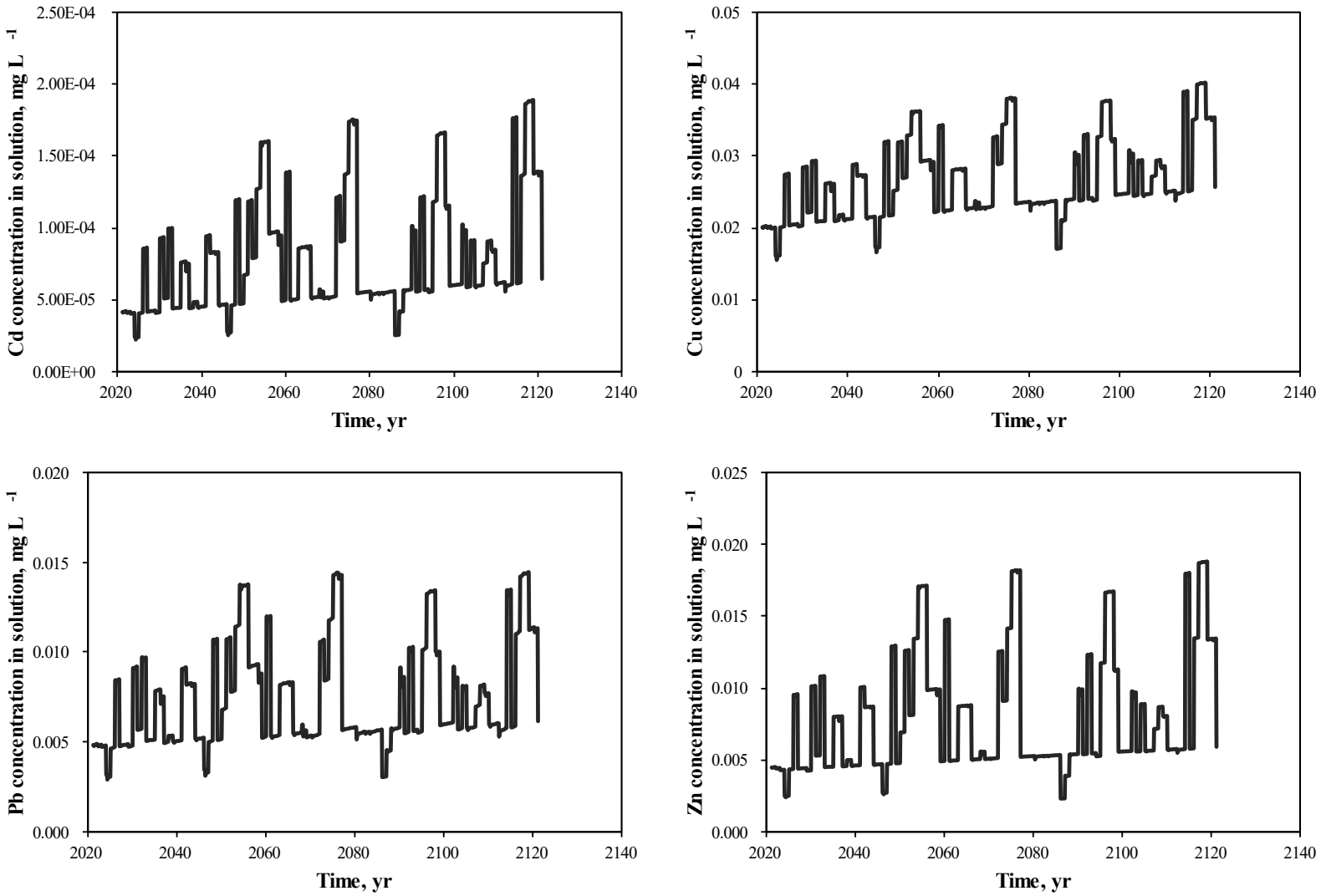

Figure A18. Evolution of the four metals concentration in soil solution in the surface layer (0-20 cm) of the Great Square for the next century

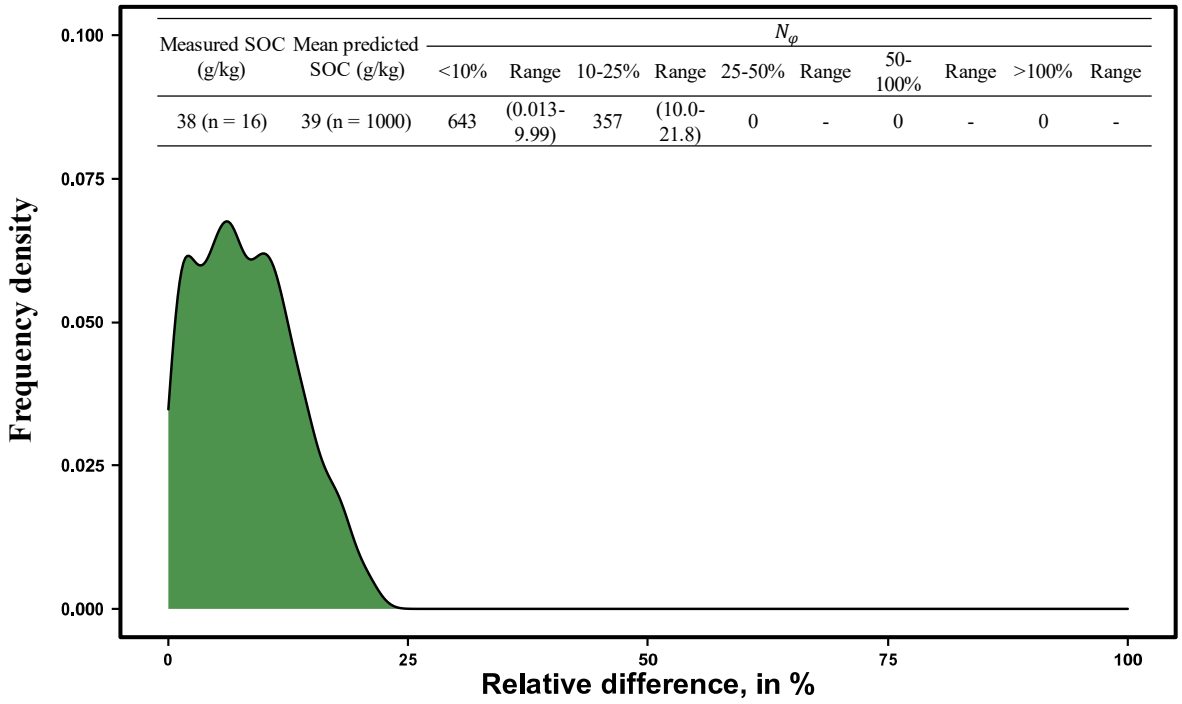

Figure A19. Frequency density of relative difference between predicted values and the average measured value of SOC

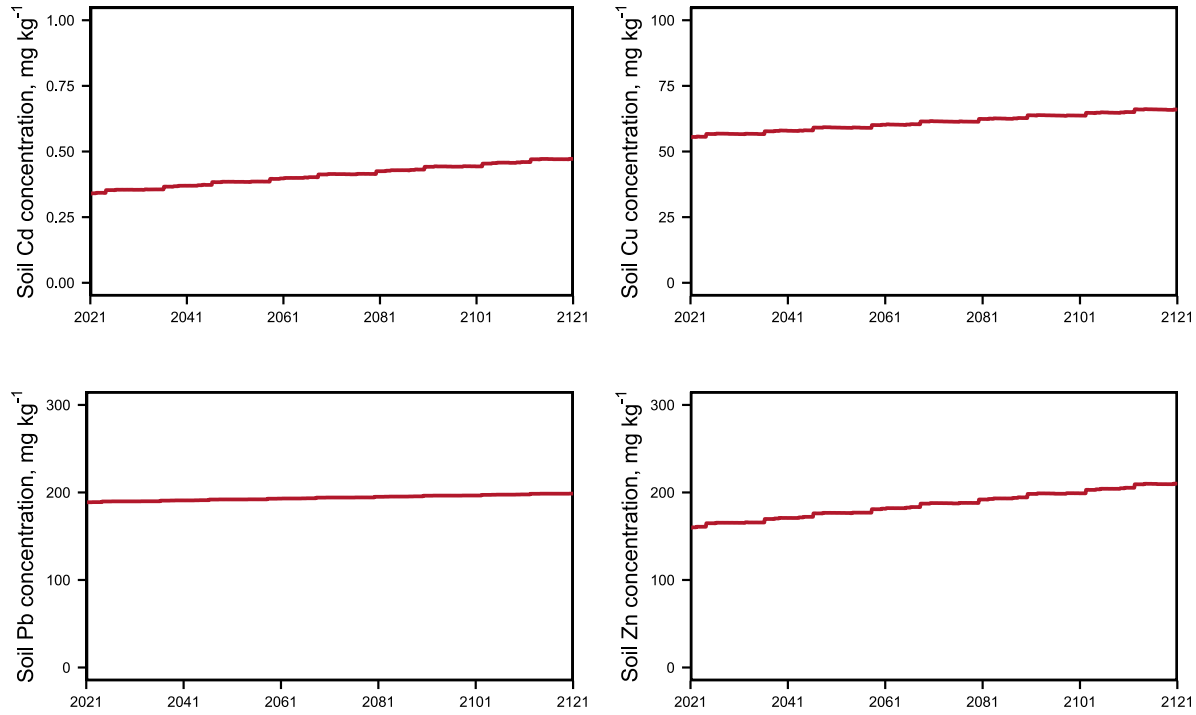

Figure A20. Evolution of the four metals soil concentration in the surface layer (0-20 cm) of the Great Square for the next century